PROBABILISTIC OPTIMAL SCHEDULING OF MULTI-ENERGY SYSTEMS USING HYBRID PARTICLE SWARM OPTIMIZATION AND LINEAR PROGRAMMING

SUTTIPONG DECHJINDA

A Thesis Submitted in Partial Fulfillment of the Requirements for
the Degree of Master of Engineering in Electrical Engineering
Suranaree University of Technology
Academic Year 2024

การจัดตารางการทำงานที่เหมาะที่สุดแบบความน่าจะเป็นของระบบพลังงานหลายรูปแบบด้วยวิธีผสมผสานการเคลื่อนตัวของอนุภาคที่เหมาะที่สุดและโปรแกรมเชิงเส้น

นายสุทธิพงษ์ เดชจินดา

วิทยานิพนธ์นี้เป็นส่วนหนึ่งของการศึกษาตามหลักสูตรปริญญาวิศวกรรมศาสตรมหาบัณฑิต
สาขาวิชาวิศวกรรมไฟฟ้า
มหาวิทยาลัยเทคโนโลยีสุรนารี
ปีการศึกษา 2567

PROBABILISTIC OPTIMAL SCHEDULING OF MULTI-ENERGY SYSTEMS USING HYBRID PARTICLE SWARM OPTIMIZATION AND LINEAR PROGRAMMING

Suranaree University of Technology has approved this thesis submitted in partial fulfillment of the requirements for a Master's Degree.

Thesis Examining Committee

.....

(Asst. Prof. Dr. Chai Chompoo-Inwai)
Chairperson

.....

(Assoc. Prof. Dr. Keerati Chayakulkheeree)
Member (Thesis Advisor)

.....

(Prof. Dr. Thanatchai Kulworawanichpong)
Member

Tosaphol Ratniyomchai

(Asst. Prof. Dr. Tosaphol Ratniyomchai)
Member

.....

(Assoc. Prof. Dr. Yupaporn Ruksakulpiwat)
Vice Rector for Academic Affairs and Quality Assurance

.....

(Assoc. Prof. Dr. Pornsiri Jongkol)
Dean of Institute of Engineering

สุทธิพงษ์ เดชจินดา : การจัดตารางการทำงานที่เหมาะที่สุดแบบความน่าจะเป็นของระบบพลังงานหลายรูปแบบด้วยวิธีผสมผสานการเคลื่อนตัวของอนุภาคที่เหมาะที่สุดและโปรแกรมเชิงเส้น.
อาจารย์ที่ปรึกษา : รองศาสตราจารย์ ดร. กีรติ ชยะกุลคีรี, 183 หน้า.

คำสำคัญ : ระบบพลังงานหลายรูปแบบ / การจัดตารางเวลาที่เหมาะที่สุด / การกักเก็บไฮโดรเจน / พลังงานหมุนเวียน / การเพิ่มประสิทธิภาพแบบหลายวัตถุประสงค์ / การวิเคราะห์เชิงความน่าจะเป็น

วิทยานิพนธ์ฉบับนี้นำเสนอกรอบการเพิ่มประสิทธิภาพสำหรับการจัดตารางเวลาในระบบพลังงานหลายรูปแบบที่เชื่อมต่อกับโครงข่ายไฟฟ้า ซึ่งรวมแหล่งพลังงานลมและแสงอาทิตย์ การผลิตไฟฟ้าแบบดั้งเดิม และเทคโนโลยีการกักเก็บไฮโดรเจน ระบบนี้สามารถแปลงพลังงานไฟฟ้าและก๊าซธรรมชาติให้เป็นทั้งไฟฟ้าและความร้อน พร้อมทั้งใช้พลังงานหมุนเวียนและการกักเก็บไฮโดรเจนเพื่อเพิ่มความยืดหยุ่น เป้าหมายของวิธีการนี้ส่งผลให้บรรลุการใช้พลังงานลมและแสงอาทิตย์ส่วนเกินให้เกิดประโยชน์สูงสุด พร้อมกับการเพิ่มประสิทธิภาพของการกักเก็บไฮโดรเจน กรอบการเพิ่มประสิทธิภาพที่นำเสนอใช้การผสมผสานระหว่างการเขียนโปรแกรมเชิงเส้น (Linear Programming, LP) และอัลกอริธึมฝูงอนุภาค (Particle Swarm Optimization, PSO) เพื่อลดต้นทุนการดำเนินงานทั้งหมด (Total Operating Costs, TOC) การปล่อยก๊าซคาร์บอน (Total Carbon Emissions, TCE) และภาระพลังงานไฟฟ้าสูงสุดที่จัดหาโดยโครงข่ายไฟฟ้า (Electricity Peak from the Grid, EP) ภายใต้โครงสร้างอัตราค่าไฟฟ้าตามช่วงเวลา (Time-of-Use, TOU) และราคาจริงตามเวลา (Real-Time Pricing, RTP) นอกจากนี้ยังใช้แนวทางการเพิ่มประสิทธิภาพแบบหลายวัตถุประสงค์เชิงฟัซซี (Fuzzy Multi-Objective Optimization, FMOO) เพื่อสร้างสมดุลระหว่างต้นทุน ความยั่งยืนด้านสิ่งแวดล้อม และการจัดการภาระโหลดสูงสุดจากโครงข่ายไฟฟ้า พร้อมผสานการวิเคราะห์เชิงสุ่ม หรือความน่าจะเป็น ด้วยวิธีการจำลองแบบมอนติคาร์โล (Monte Carlo Simulation, MCS) เพื่อรับมือกับความไม่แน่นอนของพลังงานหมุนเวียนและความผันผวนของอุปสงค์

ผลการจำลองแสดงให้เห็นว่าการเพิ่มประสิทธิภาพแบบวัตถุประสงค์เดียวสามารถลดต้นทุนการปล่อยก๊าซคาร์บอนไดออกไซด์ หรือภาระพลังงานไฟฟ้าสูงสุดที่จัดหาโดยโครงข่ายไฟฟ้าได้อย่างมีประสิทธิภาพเมื่อทำการเพิ่มประสิทธิภาพทีละปัจจัย การวิเคราะห์การประสานงานของพลังงานหลายรูปแบบชี้ให้เห็นว่าการประสานงานอย่างเต็มรูปแบบส่งผลให้เกิดการลดต้นทุนการดำเนินงาน

มากขึ้น ซึ่งเน้นถึงประโยชน์ของการบูรณาการแหล่งพลังงานที่หลากหลาย ในทางกลับกัน การเพิ่มประสิทธิภาพแบบหลายวัตถุประสงค์ ช่วยให้สามารถหาทางออกที่สมดุลระหว่างวัตถุประสงค์ที่ขัดแย้งกัน ทำให้ได้โซลูชันที่มีความเป็นไปได้และสามารถนำไปใช้งานได้จริง นอกจากนี้ การวิเคราะห์เชิงสุ่ม หรือความน่าจะเป็นช่วยเพิ่มความน่าเชื่อถือโดยรวมของระบบพลังงานหลายรูปแบบ ด้วยการให้โซลูชันที่เหมาะสมที่สุดภายใต้เงื่อนไขความไม่แน่นอน โดยสรุปกรอบการเพิ่มประสิทธิภาพที่นำเสนอช่วยให้การจัดการพลังงานมีประสิทธิภาพมากขึ้นโดยลดต้นทุนการดำเนินงาน ลดการปล่อยก๊าซคาร์บอนไดออกไซด์ และลดภาระพลังงานไฟฟ้าสูงสุดที่จัดหาโดยโครงข่ายไฟฟ้า ผลลัพธ์ของการศึกษานี้มีส่วนช่วยในการพัฒนาเทคโนโลยีพลังงานที่ยั่งยืน โดยปรับปรุงการบูรณาการพลังงานหมุนเวียนและเพิ่มประสิทธิภาพการใช้พลังงานในระบบพลังงานหลายรูปแบบ

สาขาวิชาวิศวกรรมไฟฟ้า ลายมือชื่อนักศึกษา .....สุทธินาง์.....

ปีการศึกษา 2567 ลายมือชื่ออาจารย์ที่ปรึกษา .....

SUTTIPONG DECHJINDA : PROBABILISTIC OPTIMAL SCHEDULING OF MULTI-ENERGY SYSTEMS USING HYBRID PARTICLE SWARM OPTIMIZATION AND LINEAR PROGRAMMING.
THESIS ADVISOR : Assoc. Prof. Keerati Chayakulkheeree, D.Eng., 183 PP.

Keyword : MULTI-ENERGY SYSTEM / OPTIMAL SCHEDULING / HYDROGEN STORAGE / RENEWABLE ENERGY / MULTI-OBJECTIVE OPTIMIZATION / PROBABILISTIC ANALYSIS

This thesis presents an optimization framework for scheduling in multi-energy systems connected to the electrical grid. The system integrates wind and solar renewable energy sources, conventional electricity generation, and hydrogen storage technologies. It is capable of converting electricity and natural gas into both electricity and heat, enhancing flexibility with renewable energy and hydrogen storage. The proposed approach aims to maximize the utilization of surplus wind and solar energy while optimizing hydrogen storage to improve the overall efficiency of the energy system. The optimization framework combines Linear Programming (LP) and Particle Swarm Optimization (PSO) to minimize Total Operating Costs (TOC), Total Carbon Emissions (TCE), and the Electricity Peak from the Grid (EP), under Time-of-Use (TOU) and Real-Time Pricing (RTP) scheme. Furthermore, a Fuzzy Multi-Objective Optimization (FMOO) approach is employed to balance cost, environmental sustainability, and peak load management. Monte Carlo Simulation (MCS) is incorporated to address the uncertainty of renewable energy and demand fluctuations, adding a probabilistic dimension to the optimization process.

Simulation results indicate that single-objective optimization is effective in reducing either costs, carbon emissions, or peak grid electricity demand when optimized individually. The analysis of multi-energy coordination reveals that full integration leads to greater reductions in operating costs, highlighting the benefits of multi-source energy integration. In contrast, multi-objective optimization provides a balanced trade-off among conflicting objectives, resulting in feasible and practical

solutions. Additionally, stochastic or probability analysis enhances the overall reliability of the multi-energy system by delivering robust solutions under uncertainty. In conclusion, the proposed optimization framework facilitates more efficient energy management by reducing operating costs, carbon emissions, and peak grid electricity demand. The findings contribute to the advancement of sustainable energy technologies by improving renewable energy integration and optimizing energy utilization in multi-energy systems.

School of Electrical Engineering
Academic Year 2024

Student's Signature .....
Advisor's Signature .....

ACKNOWLEDGEMENT

The authors deeply appreciate the financial support provided by the Kittibandit Scholarship at Suranaree University of Technology. This thesis would not have been possible without the guidance, support, and encouragement from numerous individuals who significantly contributed to its success.

First and foremost, I extend my heartfelt gratitude to my parents, who have been my constant source of support. Their unwavering encouragement, inspiration, and financial assistance have been invaluable throughout this journey.

I am especially thankful to Assoc. Prof. Dr. Keerati Chayakulkheeree, my thesis advisor, for his invaluable guidance and continuous support during this research. I also wish to express my sincere appreciation to the committee members: Asst. Prof. Dr. Chai Chompoo-Inwai, Prof. Dr. Thanatchai Kulworawanichpong, and Asst. Prof. Dr. Tosaphol Ratniyomchai, for their valuable advice and assistance.

Lastly, I would like to acknowledge my lecturers for consistently providing knowledge and guidance throughout my studies. I am equally grateful to my seniors and peers for their motivation and support during challenging times. Special thanks are also extended to all the faculty members and staff at the school of Electrical Engineering, Suranaree University of Technology, for their advice and assistance. Additionally, I would like to express my sincere gratitude to the members of the Energy and Power Engineering Research Group (EPERG) for their invaluable support, encouragement, and collaboration throughout this journey.

Suttipong Dechjinda

TABLE OF CONTENTS

Page

TABLE OF CONTENTS (Continued)

Page

TABLE OF CONTENTS (Continued)

Page

TABLE OF CONTENTS (Continued)

Page

TABLE OF CONTENTS (Continued)

Page

LIST OF TABLES

Table **Page**

LIST OF TABLES (Continued)

Table **Page**

LIST OF FIGURES

Figure **Page**

LIST OF FIGURES (Continued)

Figure **Page**

LIST OF FIGURES (Continued)

Figure **Page**

LIST OF FIGURES (Continued)

Figure **Page**

LIST OF FIGURES (Continued)

Figure **Page**

LIST OF ABBREVIATIONS

MES	= multi-energy system
RE	= renewable energy
PDP	= power development plans
HS	= hydrogen storage
AEDP	= alternative energy development plan
EH	= energy hub
TOC	= total operating costs
EP	= electricity peak from the grid
TCE	= total carbon emissions
OMES-WSPHS	= optimal scheduling of multi-energy systems with wind-solar power and hydrogen storage
NG	= natural gas
PSO	= particle swarm optimization
LP	= linear programming
PSO-LP	= hybrid particle swarm optimization and linear programming
MES-WSPHS	= multi-energy system with wind-solar power and hydrogen storage
MES-WSP	= multi-energy system with wind-solar power
FMOO	= fuzzy muti-objective optimization
MCS	= Monte Carlo simulation
WTs	= wind turbines
PVPs	= photovoltaic panels
PDF	= probabilistic density function
GA	= genetic algorithm
MIP	= mixed integer programming
GAMS	= general algebraic modeling system
EA	= evolutionary algorithm
CPLEX	= C programming language for mathematical programming execution

LIST OF ABBREVIATIONS (Continued)

MINLP	= mixed-integer non-linear programming
GA-PSO	= hybrid genetic algorithm and par
PtG	= power-to-gas
WSMO	= weight sum multi-objective optimization
CHP	= combined heat and power
MOPSO	= multi-objective particle swarm optimization
TOU	= time of use
SAUGMECON	= stepwise augmented ε-constraint method
VIKOR	= VIseKriterijumska Optimizacija i Kompromisno Resenje
RO	= robust optimization
BESS	= battery energy storage system
ESS	= energy storage system
PV	= photovoltaic
EL	= electrolyzer
FC	= fuel cell
RTP	= real-time pricing
TR	= transformer
GB	= gas boiler
MT	= micro-turbine
DC	= direct current
AC	= alternative current
SOT	= state of the tank
FSMF	= fuzzy-satisfaction membership function
TGO	= Thailand greenhouse gas management organization
OBJ	= objective function
SD	= standard deviation
THB	= Thai baht

LIST OF NOMENCLATURE

Variable

$\mathbf{P}$ = The matrix contains a scheduling variable.

η = Efficiency (%).

P = The power inputs or the power flow through the device (kW).

L = The power outputs or power demands (kW).

NT = The total number of wind turbines.

v = The velocity (m/s).

Y = The parameter indicates the operation state.

C = The cost of the energy input (THB/kWh).

PNF = The penalty functions.

ρ = The penalty factor.

LHV = The low heat value (MJ/kmol).

$\Re$ = The gas constant (J/mol·K).

T = The mean temperature (K).

V = The volume (m^3).

p = The pressure (bar).

n = The molar flow (mol/s).

h = The times (hour).

z = The height (m).

α = The power law exponent.

A = Area of PVPs installed (m^3).

β = PVPs efficiency (%).

SI = Solar irradiance (W/m^2).

w = Inertia weight.

c = Learning factor.

LIST OF NOMENCLATURE (Continued)

$rand$ = A random number between 0 and 1.

$pbest$ = personal best.

$gbest$ = global best.

$initial$ = initial setting value.

μ = The satisfactory membership function.

a = Shape.

b = Scale.

f = The probability density function.

σ = The standard deviation of the normal distribution.

M = The mean value of the normal distribution.

SOT = The state of the tank (%).

TOC = The total operating costs (THB).

TCE = The total carbon emissions (kg/CO_2).

EP = The electricity peak from the grid (kW).

Subscript and Superscript

1 = The number which indicates the order.

2 = The number which indicates the order.

E = Electricity.

H = Heat.

NG = Natural gas.

H_2 = Hydrogen.

EL = Electrolyzer.

FC = Fuel cell.

MT = Micro-turbine.

TR = Transformer.

LIST OF NOMENCLATURE (Continued)

GB	= Gas boiler.
L	= The power outputs or power demands.
WSP	= Wind-solar power.
AC/DC	= AC-to-DC converter.
DC/AC	= DC-to-AC converter.
r	= Reference.
WTs	= Wind turbines.
SI	= Solar irradiance.
i	= Power injected into the grid.
ex	= The excess power.
$PVPs$	= Photovoltaic panels.
tank	= The storage of hydrogen.
$rated$	= The maximum limit.
min	= The minimum limit.
T	= Total.

CHAPTER I

INTRODUCTION

1.1 General Introduction

The increasing global demand for clean and sustainable energy solutions has propelled significant interest in the multi-energy system (MES). MES integrates various energy carriers, such as electricity, heat, and gas, to optimize the production, conversion, storage, and consumption of energy across sectors. These systems represent a process shift from infrastructure single-source energy models by incorporating flexibility, efficiency, and sustainability. One of the key factors propelling MES forward is the high penetration of renewable energy (RE), such as wind and solar power, which significantly contributes to reducing greenhouse gas emissions and mitigating climate change impacts. However, the inherent variability and intermittent RE sources present challenges in ensuring grid reliability and stability. Thus, energy storage, which stores energy for later use, when necessary, is a common approach aimed at efficiently mitigating the volatility of RE sources. Moreover, Thailand's power development plans (PDP) of 2018 and the 2024 draft hearing, referred to as PDP2018 and PDP2024-hearing, respectively, outline the country's strategies for transitioning to a more sustainable energy mix by increasing the share of renewable energy and reducing dependence on fossil fuels (Ministry of Energy, 2019). A key challenge in achieving this transition is the intermittency of RE sources. To address this issue, energy storage solutions, such as hydrogen storage (HS), are essential for ensuring a reliable energy supply and able to energy arbitrage. This study aligns with the objectives of PDP2018 and PDP2024-hearing by proposing an optimal scheduling framework for MES that integrates HS with RE sources, thereby improving energy efficiency, reducing carbon emissions, and supporting Thailand’s long-term sustainability goals.

1.2 Problem Statement

According to PDP2018 to PDP2024-hearing, it has mentioned minimizing carbon dioxide emissions from electricity generation by increasing the proportion of electricity generation from RE and reducing the proportion of electricity generation from coal-fired power plants. The Alternative Energy Development Plan (AEDP) for 2018 and 2024 draft hearing, referred to as AEDP2018 and AEDP2024-hearing, respectively, emphasizes the necessity of developing alternative energy sources to minimize dependence on fossil fuels, enhance energy security, and reduce environmental impacts (Ministry of Energy, 2020). The primary goals of AEDP2018 to 2024-hearing are to increase the share of RE in the overall energy mix, enhance energy efficiency, and promote sustainable energy practices. Additionally, it aims to support technological advancements and foster innovation in RE sectors.

Energy from renewable sources is currently encountering a major obstacle due to its variability. The intermittent nature of these resources presents a significant limitation, due to the inability of many to provide a consistent energy supply. For example, wind power is subject to changes in wind speed and solar power generation fluctuates due to variations in solar irradiance, which leads to fluctuations in electricity generation (Shatnawi et al., 2018). HS is a new trend for energy storage. This solution will solve the challenges of RE, that face intermittent nature. Consequently, integrating HS into the system has generated significant interest in this research topic. In power systems, HS can be utilized to minimize daily energy loss by implementing a scheduling strategy based on peak shaving (Dechjinda & Chayakulkheeree, 2024). However, the efficiency of HS is quite lower than battery storage. To enhance efficiency, many researchers employ the energy hub (EH) model. This model is designed to optimize the supply of energy across various sectors by integrating multiple types of energy sources. The goal is to coordinate these sources effectively to reduce operational costs and advance carbon neutrality. The EH infrastructure was initially introduced by Geidl et al. (2007), with the fundamental concept of an energy hub. This concept aims to achieve the primary objectives for industrial, commercial, and residential consumers

by focusing on minimizing total operating costs (TOC) and reducing electricity peak from the grid (EP). Additionally, minimizing total carbon emissions (TCE) has become a critical concern in the modern era, driven by the global push toward sustainability and reducing environmental impacts. The implementation of EH facilitates a more coordinated cost-effective and carbon neutrality approach to energy management, addressing the diverse needs of different sectors while promoting sustainability (Zidan & Gabbar, 2016). In this thesis, recognize the challenges of optimal scheduling of multi-energy systems with wind-solar power and hydrogen storage (OMES-WSPHS) to minimize TOC, TCE, and EP when considering multiple energy sources such as electricity and natural gas (NG). The proposed method is expected to be highly beneficial in helping achieve the main objectives of minimizing costs, emissions, and electricity peak from the grid, while also enhancing the overall performance of MES that integrate renewable and conventional energy sources. This work contributes to the growing body of research focused on creating more sustainable and efficient energy systems in the face of increasing environmental concerns and the global transition toward low-carbon energy solutions.

1.3 Research Objectives

The main objective of this research is to explore how integrating HS can help achieve optimal solutions in different scenarios. It employs particle swarm optimization (PSO) for daily HS scheduling and linear programming (LP) for hourly electricity and NG operations. To enhance efficiency, a hybrid PSO-LP approach is proposed for optimal MES-WSPHS scheduling. For multi-objective solutions, fuzzy multi-objective optimization (FMOO) is used to balance TOC, TCE, and EP, while Monte Carlo Simulation (MCS) handles probabilistic scheduling uncertainties.

The specific main objectives are

1) To analyze the optimal operation of MES-WSPHS.

2) To minimize TOC, TCE, and EP in MES-WSPHS.

3) To apply FMOO for trading-offs among the solution of TOC, TCE, and EP.

4) To analyze the stochastic model while considering the uncertainty of the multi-energy load and RE profile, using MCS.

1.4 Scope and Limitation

The scope and limitations of this thesis are outlined as follows:

1.4.1 Optimization parameter validation and performance analysis between PSO and PSO-LP for MES-WSPHS integration is proposed. The objective is to validate the PSO parameters and select the optimal ones for solving the daily scheduling problem. The data acquisition process and assumptions are also presented. Additionally, a comparison between the PSO and PSO-LP algorithms is conducted. For a fair comparison, the same PSO parameters are used in both algorithms.

1.4.2 Optimal scheduling of MES-WSPHS integration is conducted under TOC minimization using scenario-based case analysis. Each scenario evaluates the impact of HS or the cooperation between electricity and NG on the system's performance, leading to improved economic operation.

1.4.3 The multi-objective optimization using fuzzy is proposed in this study that aims to achieve a balanced solution among multiple conflicting objectives. This approach is employed to handle the trade-offs among the solution of TOC, TCE, and EP and ensures that the final scheduling solution reflects a fair compromise, addressing the priorities of TOC, TCE, and EP reduction effectively.

1.4.4 The uncertainties in load demand due to user behavior and renewable energy generation fluctuations caused by weather conditions are considered in this study. These uncertainties can impact the scheduling performance, leading to variations in system operations. The study incorporates scenario-based and probabilistic analysis by using MCS to address these variations, ensuring the robustness of the proposed scheduling approach.

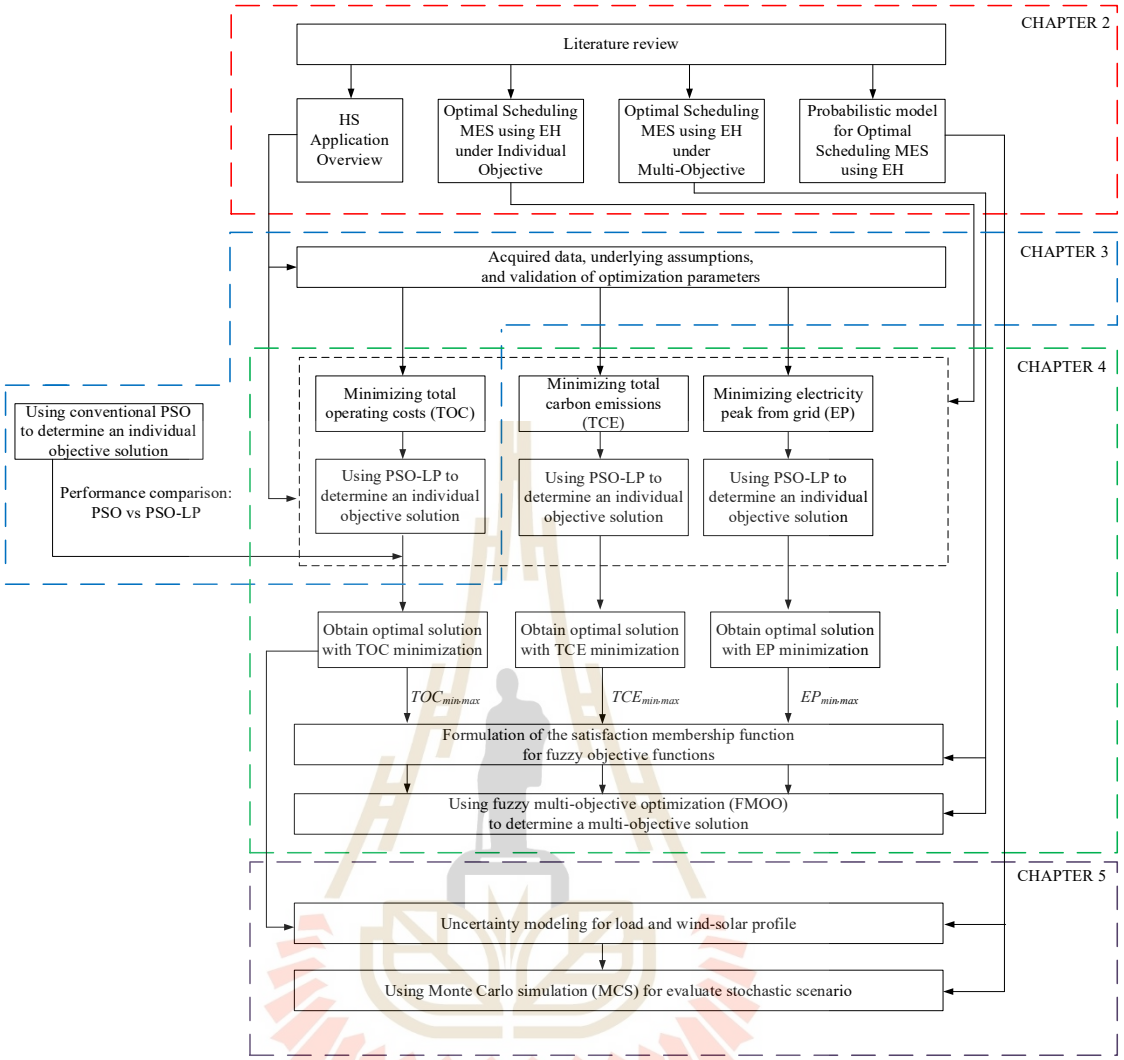

Figure 1.1 Framework of thesis

The limitations of this work are neglect of both the natural gas flow computation and the power flow analysis in the bulk system. The energy management framework presented primarily focuses on the end-use level, targeting energy consumers such as residential and industrial loads, rather than large-scale, system-wide operations.

1.5 Conception

The overall idea of this thesis is to solve the problem of energy management strategy to minimize TOC, TCE, and EP. This concept considers the load profile as a

typical summer day in the northeastern region of Thailand. The wind and solar profile are derived from data collected on a summer day in Pakchong, Thailand, with the wind turbines (WTs) and photovoltaic panels (PVPs), respectively. However, the probabilistic model is proposed for evaluating the fluctuation conditions by using MCS and represents the results through a probability density function (PDF). The objective needs to handle constraints such as device limitations and power balance. This study is conducted using MATLAB, where the TOC, TCE and EP are simulated using a hybrid of PSO-LP. The optimization integrates hourly scheduling for multi-energy dispatch and daily scheduling for HS to determine the optimal scheduling solution. This study focuses on integrating green hydrogen into the system to mitigate RE curtailment when WTs and PVPs generate excessive power while ensuring optimal operation across energy sectors. Finally, a multi-objective approach is considered, employing FMOO to find the optimal balance among TOC, TCE, and EP.

1.6 Research Benefits

Technological advancements now enable better coordination of multiple energy sources. This research, aligned with the PDP2018 to PDP2024 plan, focuses on integrating HS with wind-solar power and coordinating electricity and NG systems. By optimizing scheduling and enhancing algorithms to address scheduling challenges, this proposed procedure advances the energy scheduling problem in the field of MES-based EH research. Ultimately, this work contributes to sustainable energy solutions for the future.

1.7 Thesis Outline

The rest of the thesis is organized as follows: Chapter 2 presents a literature review covering key aspects of HS applications, optimal scheduling of MES using EH under both individual and multi-objective frameworks, and the probabilistic modeling approach for optimal MES scheduling. Chapter 3 details the validation of the PSO algorithm and compares PSO-LP with PSO for optimizing scheduling. The focus is on

minimizing TOC under the pricing mechanism while analyzing the impact of HS integration and the cooperation between electricity and NG on system performance. Chapter 4 presents the FMOO techniques for determining the optimal scheduling by balancing all objective functions simultaneously. The results aim to achieve a compromise among the three discussed objectives. Chapter 5 presents uncertainty modeling and stochastic analysis for optimal scheduling of MES-WSPHS integration. It addresses the impact of load and renewable energy fluctuations using probabilistic modeling and MCS to enhance the robustness of the scheduling strategy. Finally, Chapter 6 provides a comprehensive summary of the key findings, highlighting the most significant insights drawn from the analysis.

1.8 Chapter Summary

Chapter 1 introduces research on optimizing MES-WSPHS integration to address the challenges arising from the variability of RE. The study is contextualized within the national energy development plans, particularly from PDP2018 to PDP2024, highlighting its relevance to sustainable and resilient energy solutions. The chapter outlines the problem statement, defines the scope and limitations, and clarifies the main objectives and expected benefits of the research. Additionally, it provides an overview of the thesis structure, explaining the organization of content and analysis across the subsequent chapters.

CHAPTER II

LITERATURE REVIEW

2.1 General Introduction

The integration of HS and high penetration RE into MES with EH has gained significant attention due to the demand for sustainable and efficient energy systems. EHs coordinate multiple energy carriers such as electricity, heat, and fuel with RE to improve overall system efficiency. The directionality and variability of RE are key factors for effective HS integration in both current and future applications. As MES grows in complexity, energy scheduling plays a vital role in optimizing RE and HS operations. Effective energy scheduling is critical not only for balancing supply and demand in real-time, but also for achieving objective function optimization. This literature review examines the current state of research on HS integration, EH models, and optimal MES scheduling, highlighting technological advancements, benefits, challenges, and case studies that demonstrate how HS improves MES performance and sustainability.

2.2 Conventional Electrical Energy Scheduling Problems

According to Power Generation, Operation, and Control (Wood et al., 2013), energy scheduling plays a crucial role in managing the generation and consumption of energy across various sources, aiming to optimize the objective function. In the past, hydroelectric systems involved the complex task of scheduling water releases while satisfying hydraulic and energy demand constraints. When thermal generation was not present, the challenge centered on reservoir management to maximize stored energy through simulation-based scheduling. However, in hydrothermal systems where both hydro and thermal resources are present, the scheduling strategy depended on the

dominance and balance of each source. Pseudo-fuel costs could be assigned to hydro units to facilitate cost-based optimization similar to conventional systems. A key aspect of traditional scheduling involves determining when to start up each generating unit, known as unit commitment, and how much power each unit should produce at a given time, known as economic dispatch. These problems were typically solved over a defined planning horizon, such as daily, weekly, or seasonally, to achieve minimum operating cost while maintaining system reliability.

As energy systems have evolved, the concept of optimal scheduling has expanded beyond hydrothermal coordination into more complex MES. MES involves the integration of multiple energy carriers which requires coordinated scheduling across these interdependent subsystems. The focus of MES scheduling shifts toward optimizing several objectives at once, while managing the dynamic interactions among the system components. In this context, the principles of hydrothermal scheduling provide a foundational basis. However, the increasing complexity of MES necessitates the adoption of more advanced methods, including multi-objective optimization techniques, the integration of RE resources, the use of modern energy storage technologies, and probabilistic approaches for planning under uncertainty.

2.3 Trend in Renewable Energy Integration with Hydrogen Storage

In the era of clean energy transition, the integration of RE sources with HS systems has emerged as a promising strategy to address the intermittency of RE and enhance energy system flexibility. Among various RE options, solar and wind energy are particularly well-suited for coupling with HS due to their decreasing costs and technological maturity. In Thailand, the cost of electricity generation from solar energy has significantly dropped, averaging around 2.16 baht/kWh, while wind energy costs average approximately 3.10 baht/kWh. These competitive price points make both solar and wind energy attractive candidates for integration with HS systems. By storing excess energy during periods of high generation and releasing it during low-output periods, HS not only offsets the variability of these sources but also contributes to grid stability

and the decarbonization. This synergy supports Thailand's broader commitment to a sustainable and low-carbon energy future (Energy Policy and Planning Office, 2023). Additionally, wind and solar technologies have seen substantial technological advancements, resulting in greater efficiency and reduced costs. Their scalability and adaptability across diverse geographic regions further increase their practicality for widespread HS integration (D'Silva, 2024). Continued improvements in electrolyzer (EL) technologies and energy storage systems (ESS) also enhance the technical and economic viability of using wind and solar energy for hydrogen production (Ikuerowo et al., 2024).

2.4 Literature Overview

This section explores key research areas, including HS application overview, optimal scheduling of MES using EH models under individual objective, and optimal scheduling of MES using EH models under multi-objective. Table 2.1 outlines the HS application overview from existing literature, while Table 2.2 presents studies that address optimal scheduling of MES using EH models focusing on individual objectives. Table 2.3 highlights studies focusing on the optimal scheduling of MES using EH models under multi-objective. Additionally, Table 2.4 elaborates the probabilistic model for optimal scheduling MES using EH. Finally, Table 2.5 shows the research gap between the existing and this study. This review identifies research gaps and suggests future study directions.

Table 2.1 HS application overview

Author and publication year	Topic	Key findings
Cau et al. (2014)	Energy management strategy based on short-term generation scheduling for a renewable microgrid using a hydrogen storage system	The demonstration of modeling a hydrogen storage system, which operates via electrolyzer and fuel cell with Faraday's law. The relationship between the hydrogen pressure in the tank and the amount of stored hydrogen is based on the ideal gas law.
Qadrdan et al. (2015)	Role of power-to-gas in an integrated gas and electricity system in Great Britain	These findings demonstrate that power-to-gas systems can play a key role in balancing energy systems, integrating renewable sources, and reducing operational costs in real-world systems.
Ould Amrouche et al. (2016)	Overview of energy storage in renewable energy systems.	This review highlights the use of existing energy storage technologies, including HS. HS involves the use of electrolyzers to convert surplus electricity into hydrogen, which can then be stored and later converted back into electricity through fuel cells.

Table 2.1 HS application overview (Continued)

Author and publication year	Topic	Key findings
X. Chen et al. (2019)	Optimal Control for a Wind-Hydrogen-Fuel Cell Multi-Vector Energy System	The research shows how the integration of hydrogen storage enhances the stability of the energy supply, compensating for the intermittent nature of wind power. This approach, which coordinates multiple energy vectors, has the potential to improve the efficiency of RE systems in wind-rich areas and encourage broader adoption of renewable technologies.
Osman et al. (2022)	Hydrogen production, storage, utilisation and environmental impacts: a review	This review provides a hydrogen production is defined in various color codes depending on the manufacturing process and cleanliness. It can be categorized into five colors: grey, brown, blue, turquoise, and green hydrogen.
Dash et al. (2023)	A Brief Review of Hydrogen Production Methods and Their Challenges	The review highlights the production of purple hydrogen, which is derived from nuclear energy. Nuclear fission generates heat, which is utilized to produce electricity and subsequently fuel hydrogen production.

Table 2.1 HS application overview (Continued)

Author and publication year	Topic	Key findings
Xiangping Chen et al. (2019)	GA Optimization Method for a Multi-Vector Energy System Incorporating Wind, Hydrogen, and Fuel Cells for Rural Village Applications	This paper presents a genetic algorithm (GA)-based optimization method for a power generation system with hydrogen storage. The method balances fluctuating demand and intermittent wind power, optimizing RE use by converting wind energy into hydrogen and electricity.
Dechjinda and Chayakulkheeree (2024)	Optimal Daily Scheduling of Hybrid Wind-Hydrogen Storage using Particle Swarm Optimization	This study proposes a power system that integrates HS and wind power to minimize daily power losses. The system's performance is evaluated using a PSO-based scheduling algorithm on a modified IEEE 33-bus test system. The results demonstrate that excess wind energy can be effectively utilized for peak shaving, reducing peak load and leading to more efficient loss minimization.

Table 2.2 Optimal scheduling of MES using EH under individual objectives

Author and publication year	Topic	Objective function	Method	Key findings
Geidl et al. (2007)	The Energy Hub – A Powerful Concept for Future Energy Systems.	-	-	The research introduces a concept of MES using an EH, where multiple energy carriers convert and store energy for various applications like electricity, heating, cooling, or compressed air. The main challenge is managing the multi-energy flow to utility demand.
Thanh-tung et al. (2016)	Energy Hub Modeling for Minimal Energy Usage Cost in Residential Areas.	Minimize the energy usage cost	Mixed integer programming (MIP)-based general algebraic modeling system (GAMS)	This work demonstrates MES using the EH model, integrating electricity and NG resources and addressing electricity, heating, and cooling load demands, resulting in significant cost reduction.

Table 2.2 Optimal scheduling of MES using EH under individual objectives (Continued)

Author and publication year	Topic	Objective function	Method	Key findings
Ha et al. (2017)	Energy hub modeling to minimize residential energy costs considering solar energy and BESS.	Minimize the residential energy costs	Mixed integer programming (MIP)-based general algebraic modeling system (GAMS)	This study integrates solar energy and battery energy storage (BESS) with electricity and NG to meet electricity, heating, and cooling demands. Full integration of RE and BESS results in the lowest residential energy costs.
Timothée et al. (2017)	Optimum dispatch of a multi-storage and multi-energy hub with demand response and restricted grid interactions.	Minimize the operating cost for a time horizon	Evolutionary algorithm (EA) and PSO	This study compares evolutionary algorithms (EA) and PSO for optimizing a MES with grid, fuel, solar, wind, and thermal demands. Results show dispatch fluctuations, which can be reduced by increasing battery storage capacity.

Table 2.2 Optimal scheduling of MES using EH under individual objectives (Continued)

Author and publication year	Topic	Objective function	Method	Key findings
Zhang et al. (2017)	Optimal Operation of Wind-Solar-Hydrogen Storage System Based on Energy Hub.	Maximize the total operational profits	CPLEX Optimization	This paper provides a model incorporating hydrogen energy, electricity-gas heat loads, TOU scheme, and distributed generation, achieving higher RE penetration and profitability compared to traditional methods.
Javadi et al. (2017)	Optimal scheduling of a multi-carrier energy hub supplemented by battery energy storage systems	Minimize the operating cost	Mixed integer nonlinear programming (MINLP)	This study highlights the critical role of BESS integration in optimizing a MES with electricity and NG, enhancing efficiency, reducing costs, and improving system reliability across electricity, heating, and cooling demands.

Table 2.2 Optimal scheduling of MES using EH under individual objectives (Continued)

Author and publication year	Topic	Objective function	Method	Key findings
Geng and Jia (2020)	Hybrid Genetic Particle Swarm Optimization Based Economical Operation of Energy Hub	Minimize the daily electricity and NG purchasing cost	Hybrid genetic particle swarm optimization (GA-PSO)	This study proposes a hybrid GA-PSO approach to optimize the operation of an EH model involving electricity, NG, and both heat and electricity storage. This enables efficient use of gas turbines, gas boilers, electric chillers, and absorption chillers. The GA-PSO method improves optimizes EH operations, leading to enhances economic performance and system efficiency.

Table 2.2 Optimal scheduling of MES using EH under individual objectives (Continued)

Author and publication year	Topic	Objective function	Method	Key findings
Liu et al. (2021)	Optimal Scheduling Considering Different Energy Hub Model of Integrated Energy System	Minimize the operating costs	LP	This study evaluates three types of EH models based on case-specific scenarios, including power-to-gas (PtG) technology and ESS to meet electricity, heating, and cooling demands from electricity and NG. The optimal configuration lowers energy costs by coupling electricity, gas, and heat networks, and optimizing equipment such as combined heat and power CHP and heat pumps.

Table 2.2 Optimal scheduling of MES using EH under individual objectives (Continued)

Author and publication year	Topic	Objective function	Method	Key findings
Wang (2023)	Optimal Scheduling Strategy for Multi-Energy Microgrid Considering Integrated Demand Response	Minimize operating expenses	Mixed integer linear programming (MILP)	The study investigates the optimal scheduling of MES for microgrids using electricity and thermal energy sources. Three energy dispatch schemes are tested, with the third incorporating a demand response strategy showing the best results.

Table 2.3 Optimal scheduling of MES using EH under multi-objective

Author and publication year	Topic	Objective function	Method	Key findings
Zidan and Gabbar (2016)	Optimal Scheduling of Energy Hubs in Interconnected Multi Energy Systems	Minimize operation costs and emissions	Weight-sum multi-objective optimization (WSMO)	The paper presents an EH model integrating CHP and gas furnaces to maintain steady-state efficiency, demonstrating that WSMO effectively balances costs and emissions for optimal compromise solutions.
Ma et al. (2017)	Improved Particle Swarm Optimization Algorithm to Multi-objective Optimization Energy Hub Model with P2G and Energy Storage	Minimize the fuel cost of the EH and interaction cost with the main network	Improved multi-objective PSO (MOPSO)	The paper proposes an improved MOPSO with a search variable in velocity updates, enhancing efficiency and selecting compromise solutions from the Pareto front.

Table 2.3 Optimal scheduling of MES using EH under multi-objective (Continued)

Author and publication year	Topic	Objective function	Method	Key findings
Kholardi et al. (2018)	Optimal Management of Energy Hub with Considering Hydrogen Network	Minimize the energy hub operating costs and emissions	WSMO	This study focuses on the hydrogen network management strategy. The electricity-wind power and NG dispatch to meet various demands. It reveals that a weighting strategy of 0.8 and 0.2 results in lower operating costs.
Farah et al. (2020)	Optimal Scheduling of Hybrid Multi-Carrier System Feeding Electrical/Thermal Load Based on Particle Swarm Algorithm	Minimize the energy hub operating costs and emissions	WSMO	This paper studies an integrated RE to assist the dispatch of electricity demand and wood chips to convert to heat demand via biomass. The combination of NG turbine, biomass unit, boiler, and RE is an optimized configuration for an EH, resulting in lower operational costs and reduced emissions.

Table 2.3 Optimal scheduling of MES using EH under multi-objective (Continued)

Author and publication year	Topic	Objective function	Method	Key findings
Mousavi et al. (2022)	Multi-objective Scheduling of an Energy Hub in a Multi-energy System Using Genetic Algorithm	Minimize the operating costs and emissions	WSMO	The study optimizes EH, including CHP and gas furnaces, by using a 0.5 weighting factor in emissions and pricing mechanisms. The results show CHP starts operating when high demand is needed, resulting in lower costs and emissions.
Imeni and Ghazizadeh (2023)	Pave the Way for Hydrogen-Ready Smart Energy Hubs in Deep Renewable Energy System	Minimize the operating costs and emissions	WSMO	This work simulates three scenarios of EH model with HS integration, each with varying weights for operation costs and emissions. The results showed that using hydrogen as the primary energy carrier improved performance, particularly in reducing pollution emissions while TOU tariffs further reduced operation costs.

Table 2.3 Optimal scheduling of MES using EH under multi-objective (Continued)

Author and publication year	Topic	Objective function	Method	Key findings
Imeni et al. (2023)	Optimal scheduling of a Hydrogen-Based energy hub considering a stochastic Multi-Attribute Decision-Making approach	Minimize operation costs and emissions	SAUGMECON	This research enhances multi-objective optimization by integrating photovoltaic (PV) and BESS, achieving a better trade-off between economic performance and environmental impact, effectively reducing costs and emissions.
Hassan et al. (2023)	Optimal Day-ahead Management of a Hydrogen-based Energy Hub Considering Different Electrolyzer Technologies	Minimize operation costs and emissions	WSMO	This research optimizes EH management by minimizing day-ahead operating costs and emissions while meeting hydrogen, electricity, and heat demands. Using the WSMO method, results show how different electrolyzers impact costs and emissions.

Table 2.3 Optimal scheduling of MES using EH under multi-objective (Continued)

Author and publication year	Topic	Objective function	Method	Key findings
Xu et al. (2024)	A multi-objective operation optimization model for the electro-thermal integrated energy systems considering power to gas and multi-type demand response	Minimize the operation costs, carbon emissions, and energy curtailment rate	MOPSO and VIKOR	This study develops a multi-objective optimization model for electro-thermal integrated energy systems using PtG technology and demand response strategies. The results show PtG technology significantly improves system performance, leading to significant reductions in costs, emissions, and energy curtailment rates.

Table 2.4 Probabilistic model for optimal scheduling MES using EH

Author and publication year	Topic	Uncertainty variables	Method	Key findings
Mohammadi et al. (2017)	Optimal scheduling of energy hubs in the presence of uncertainty-A Review	Demand / the price of energy / solar irradiance etc.	MCS, fuzzy approach, robust optimization, and interval analysis	This review illustrates the recent research about uncertainty methods for MES using EH. This study reflects the uncertainty of modeling, stochastic methods, hybrid techniques, and demand response programs that improve operational costs, system resilience, energy scheduling accuracy, and economic and environmental benefits.

Table 2.4 Probabilistic model for optimal scheduling MES using EH (Continued)

Author and publication year	Topic	Uncertainty variables	Method	Key findings
Honarmand et al. (2021)	A robust optimization framework for energy hub operation considering different time resolutions: A real case study	Electrical, heat, and cooling demand / Photovoltaic (PV) output power	Robust optimization (RO)	This paper presents an optimization framework for real-world energy supply management in an EH. It shows that uncertainties increase total operation costs by 6.41%, mainly due to additional energy procurement and system adjustments. However, including energy storage system (ESS) can reduce costs by 0.87%, demonstrating their effectiveness in improving system flexibility.

Table 2.4 Probabilistic model for optimal scheduling MES using EH (Continued)

Author and publication year	Topic	Uncertainty variables	Method	Key findings
Thang et al. (2022)	Stochastic optimization in multi-energy hub system operation considering solar energy resource and demand response	Electrical, heat, and cooling demand / electrical prices / output power of RE	A scenario reduction technique	The study uses PDF to model uncertain parameters such as solar energy resources, energy demand, and electricity prices. It uses clustering and scenario reduction techniques to reduce uncertainties. Incorporating uncertainties improves system robustness and reduces total operational costs by 2.0-14.5% compared to deterministic approaches.

Table 2.4 Probabilistic model for optimal scheduling MES using EH (Continued)

Author and publication year	Topic	Uncertainty variables	Method	Key findings
Ranjbarzadeh et al. (2022)	A probabilistic model for minimization of solar energy operation costs as well as CO_2 emissions in a multi-carrier microgrid (MCMG)	Cost of electricity / the load for AC electricity / the power sourced from PVPs	2m+1 point estimate	This work models uncertainties in solar generation and power prices using the 2m+1 point estimation method to minimize costs and emissions. Incorporating uncertainty raises operational costs but enhances system resilience, leading to adjusted energy storage scheduling and demand response for a more conservative operation strategy.

2.5 HS Application Overview

In the modern era, ESS are widely utilized in electric power systems, particularly with the integration of high levels of RE penetration. The primary function of ESS is to enhance the flexibility of the electrical grid. Notably, ESS can efficiently mitigate power fluctuations caused by the variable nature of RE sources (Ould Amrouche et al., 2016). ESS are increasingly adopting HS technologies due to the clean energy production from RE sources and the ability to store energy in various forms. Ould Amrouche et al. (2016) highlighted the mechanisms of HS, categorizing it into gaseous, liquid, and chemical forms. In HS operations, RE can be converted into hydrogen gas through an EL. When excess energy is generated, it can be stored as hydrogen or later converted back to electricity via a fuel cell (FC). Additionally, hydrogen production is mentioned in Osman et al. (2022) research. They are defined in various color codes depending on the manufacturing process and cleanliness. It can be categorized into five colors: grey, brown, blue, turquoise, and green hydrogen. Grey hydrogen is produced from fossil fuels such as NG through steam reforming, emitting around 10 tons of CO_2 during the process. It's commonly used in petroleum-based chemicals and ammonia production. Brown hydrogen, derived from coal gasification, also releases significant CO_2. Blue hydrogen mitigates these emissions by employing carbon capture and storage. Turquoise hydrogen, generated via methane pyrolysis, produces solid carbon soot instead of CO2. Green hydrogen, the cleanest form of hydrogen, is produced from RE sources like wind and solar, offering significant environmental benefits without greenhouse gas emissions. However, its production faces challenges related to system efficiency and the intermittent nature of RE sources. Integrating HS can mitigate these issues by storing excess energy during peak production, ensuring a stable hydrogen supply during low-generation periods. HS also enhances the efficiency of RE systems by capturing surplus energy that would otherwise be wasted, converting it into hydrogen for various applications. Then, Dash et al. (2023) proposed the production of purple hydrogen, which is derived from nuclear energy. By utilizing the high temperatures generated from uranium fission, nuclear power plants can produce

steam that drives turbines for electricity generation without direct greenhouse gas emissions. This thermal energy can also support various hydrogen production methods, making purple hydrogen a promising option for sustainable energy transition. Different types of hydrogen production are displayed in Fig. 2.1 (Dash et al., 2023; Osman et al., 2022).

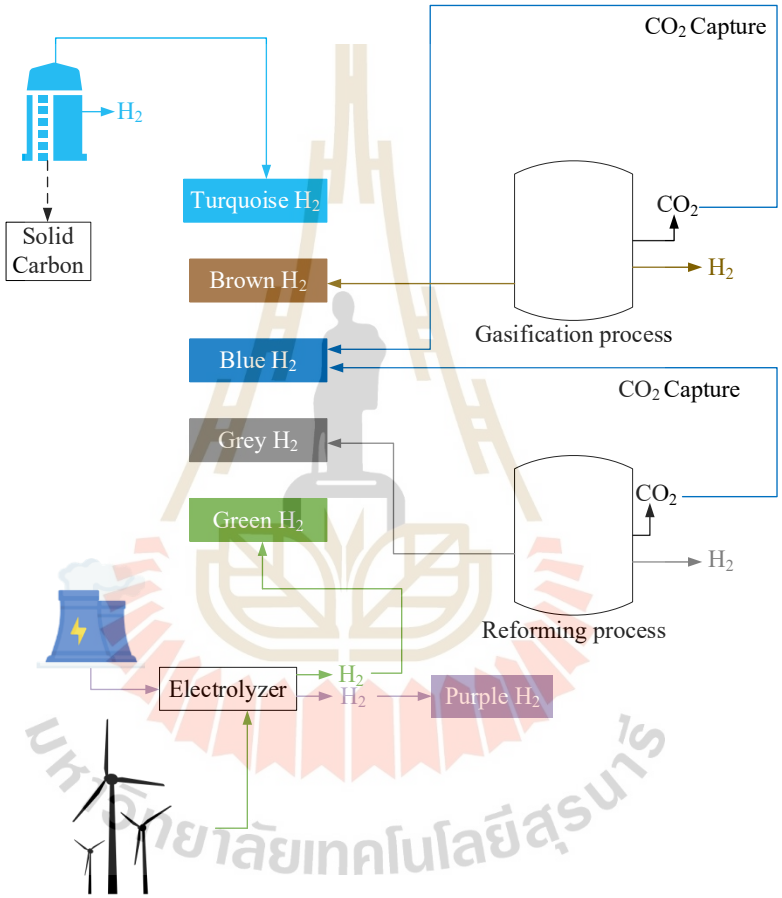

Figure 2.1 Different types of hydrogen production

In applying HS in an electricity system, Cau et al. (2014) proposed the scheduling for a renewable microgrid using a HS system. With HS integration, the model of HS utilizes Faraday's law to determine the molar flow and can convert back to power. The hydrogen pressure in the tank can be modeled based on the ideal gas law. To identify the amount of hydrogen in the tank, the pressure in the tank plays a role in telling how much hydrogen is left. In the following year, the work of Qadrdan et al.

(2015) proposed a power-to-gas (PtG) concept, which is converting electricity to hydrogen using an electrolysis process. The model of Great Britain assessed the HS within an integrated gas and electricity system. According to the findings, generating hydrogen from electricity can lower wind curtailment in high wind scenarios and lower the total cost of running the Great Britain gas and electricity network. After that, X. Chen et al. (2019) and Xiangping Chen et al. (2019) studied a power generation system incorporating HS and wind energy, initially wind energy is converted into electrical energy, with a portion of this electricity used for water electrolysis to produce hydrogen for energy storage. This hydrogen can then be converted back into electricity using FC during peak electrical demand. An analytical model has been developed to coordinate energy conversion among mechanical, electrical, and chemical forms. The proposed system is designed to meet the electrical needs of a rural village in the UK, helping to balance intermittent RE supplies with fluctuating demand and improving overall system efficiency. A genetic algorithm (GA) is employed as the optimization strategy to determine the operational scheme for this multi-vector energy system. Four case studies are conducted using real-world measurement data. The novelty of this study lies in its GA-based optimization methods aimed at maximizing wind energy utilization. In recent years, Dechjinda and Chayakulkheeree (2024) introduced a modified IEEE-33 bus test system, a distribution power system that incorporates hybrid wind and HS integration using load and wind profiles specific to Thailand. The primary objective of this research is to minimize daily energy loss through optimal daily scheduling based on PSO. The study is divided into two cases: the conventional IEEE-33 bus test system and the modified version. A comparison of the two systems reveals that the modified IEEE-33 bus test system, with its hybrid wind-HS integration, effectively reduces daily energy losses through the proposed approach.

2.6 Optimal Scheduling MES using EH under Individual Objectives

Recently, with modern technology, the incorporation of several different energy systems that are composed of many energy carriers is paving the way for a

more sustainable future (Imeni et al., 2023). One of the most significant characteristics of MES is that it has multiple energy carriers, not only electricity. Synergies among different types of energy are seen to provide a substantial capability for system development (Geidl et al., 2007). The MES is the solution to decrease the operating cost and promote carbon neutrality. EH concept is used to consider efficiently supplying energy in each section using many kinds of energy. Geidl et al. (2007) demonstrated the EH is a system where multiple energy carriers, such as electricity and NG, are converted, conditioned, and stored to provide services like electricity, heating, cooling, or compressed air. It acts as an interface between various energy infrastructures and consumer loads. EH utilizes technologies like combined heat and power (CHP), transformers, and heat exchangers. Examples of EHs include industrial plants, large buildings, urban districts, and island energy systems. Figure 2.2 shows an example of an energy hub and outlines this modeling concept. A coupling matrix represents the conversion of power from input to output in an energy hub, based on the converter's structure and efficiency. Storage devices require time and energy as key variables. Different flow models, ranging from general to detailed, can be used for hydraulic and electric networks, depending on the level of analysis. Interconnectors can also be modeled like energy hubs, using coupling matrices to describe energy flow. However, this work does not optimize objective function rather, it is a discovery and raises questions about EH design, operation, energy storage, and impact on the system.

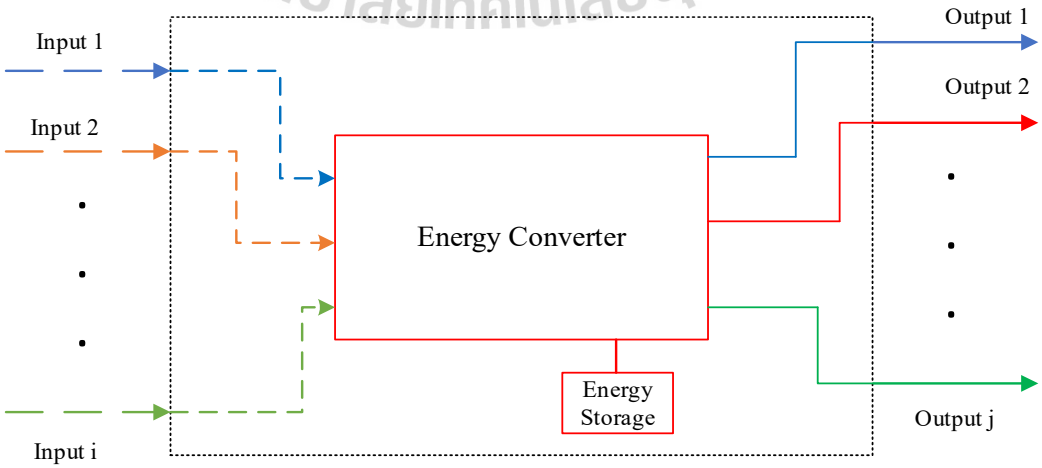

Figure 2.2 The example of an energy hub and outlines this modeling concept

Thanh-tung et al. (2016) proposed a model of residential area load including electricity and heat from dispatching a multi-energy source (electricity and NG). Using mixed integer programming (MIP) based-general algebraic modeling system (GAMS) software to minimize the energy usage cost. The optimal results show that off-peak energy demand is primarily supplied by the grid, while normal and peak-hour demand is partially met by converting heat energy to electricity, reducing system peaks, and lowering customer costs. The integration of multiple energy types improves electricity supply reliability. In the next year, Ha et al. (2017) presented an integrating battery energy storage systems (BESS), photovoltaic panels (PVP), and solar energy to residential areas model. The case study is divided into four scenarios, each comprising variations such as with or without BESS and PV systems. The energy usage cost minimization using MIP-GAMS illustrates that the result in each case is decreasing. When PV and BESS are integrated, the total energy costs are lowest. Also, Zhang et al. (2017) delve into a model that takes into account hydrogen energy, electricity-gas heat load, time-of-use electricity pricing, and distributed generation. They also employ electrolytic bath, FC, and energy storage technologies to provide a multi-energy joint optimization model based on an energy hub. The objective function is maximizing the total operational profits through adjusting the distribution coefficient of energy conversion in the scheduling period. CPLEX optimization is used to obtain optimal solutions. The outcome demonstrates that the suggested model outperforms the conventional operating mode without using hydrogen in terms of RE penetration and profitability. Furthermore, Javadi et al. (2017) focused on BESS integration to enhance the operational efficiency of a multi-carrier EH through optimal scheduling. The EH consists of various components, including micro-combined heat (mCHP), electric heat pumps (EHP), boilers, absorption chillers, and battery storage with the energy management problem modeled using mixed-integer nonlinear programming (MINLP). The optimization aims to reduce costs and improve battery life by considering energy prices and battery state of charge. Simulation results highlight the importance of optimizing energy storage, leading to lower operational costs, better load

management, and improved system reliability. Moreover, Timothée et al. (2017) investigated the optimal dispatch of a multi-storage and multi-energy hub, integrating solar PV panels, WTs, boilers, internal combustion generators (ICG), and cogeneration plants, alongside both heat and electricity storage systems. The study employed an evolutionary algorithm (EA) for optimization and compared the results with PSO. Results highlighted the volatility in dispatch strategies, which could be mitigated by increasing battery storage capacity. The results indicate that both the battery and ICG are utilized to meet peak power demand and export electricity to the grid when prices are elevated. In terms of heat demand, the boiler operates at full capacity, with the cogeneration plants unit contributing a smaller portion of the heat supply compared to the boiler. The research emphasizes the importance of optimizing energy hubs to manage demand, renewable variability, and grid interactions, ensuring cost-effective and efficient energy distribution. In the next three years, Geng and Jia (2020) proposed a hybrid genetic algorithm and particle swarm optimization (GA-PSO) strategy, which combines PSO with GA to solve the optimal operation of EH. The EH model is comprised of electricity storage and heat storage coordinated with a gas turbine, gas boiler, electric chiller, and absorption chiller to dispatch electricity, heat, and cooling demand. When comparing a proposed algorithm GA-PSO with the conventional PSO, the results emphasize that GA-PSO significantly enhances convergence capability while also demonstrating a better economy in optimizing EH operations. In the next year, Liu et al. (2021) studied an EH model in different energy integrated. The study separated three kinds of EH cases to assess how different combinations of energy equipment. The components of EH include a boiler, cogeneration unit, chiller boiler, electric heat pump, and ESS to dispatch electricity, heat, and cooling demand from electricity and NG as a source. The optimization process aims to minimize the total operating cost of the energy system, ensuring efficient energy utilization and balancing between different energy sources. The result shows that the optimal EH configuration is the most collaborative of energy. It can significantly reduce energy costs by coupling electricity, gas, and heat networks while optimizing the use of equipment like CHPs and heat

pumps. In the previous year, Wang (2023) proposed the strategy of optimal scheduling for multi-energy microgrids that integrates electricity and thermal energy sources, considering demand response and ESS integration. Using a mixed-integer linear programming model solved by CPLEX, the study simulates the operation of a grid-connected microgrid consisting of FC, WTs, solar panels, and thermal storage. Three different energy dispatch schemes are tested, with the third scheme incorporating demand responses showing the best results. This scheme not only reduces operational costs but also turns grid interactions into profit opportunities by smoothing energy demand and optimizing the use of RE and storage. The research demonstrates how integrating IDR can enhance system flexibility, lower costs, and promote sustainable energy use.

2.7 Optimal Scheduling MES using EH under Multi-Objective

In the research that focuses on multi-objective, Zidan and Gabbar (2016) presented an EH scheduling during different seasons of the year to minimize the costs and CO_2 emissions. The EH model proposed CHP and gas furnace as a steady state efficiency conversation, to coordinate with electricity to dispatch load. GA optimization is utilized for an individual objective function, including the costs and CO_2 emissions considered. The study is separated into three main cases, which are scheduling EH in each objective only and scheduling EH with two objective functions. The result shows each case has a different schedule for the best individual solution. When using the WSMO technique to balance between two objectives, the compromise solution is found to be an intermediate result between the optimal solutions of each objective. Then, Ma et al. (2017) proposed the improved PSO to multi-objective optimize EH model. The model of this work focuses on PtG operation, to schedule in each component is obtained from optimize variable by PSO. The main goal of this operation is to minimize the fuel cost of EH and to minimize the cost of interaction with the main power grid. To find the optimal solution for the two objectives considered, the improved MOPSO is used for balancing the two objectives by selecting from the Pareto

front. The result focuses on the efficiency of improved MOPSO when compared with traditional MOPSO, the improved MOPSO has more optimization than MOPSO. Additionally, Kholardi et al. (2018) focus on the hydrogen network as one of the main networks that are connected to the EH. With the management strategy, the wind power from a WT is connected to electricity to dispatch several demands and NG is the power source to dispatch heat load and assist the electricity demand. Under the pricing mechanism, the operating costs are used to find the optimal managed energy in each sector. Also, the emissions factor is considered as the second objective. By MILP optimization, the two objectives are solved completely separately. The WSMO is the easiest to balance two objectives and is used to find the optimal solution between two objectives. This study is separated into three cases which define a different weighting coefficient for both objectives. In the third scenario, where the weighting coefficients are set to 0.8 and 0.2 respectively, the EH's management results in a lower operating cost compared to the other scenarios due to the defined weighting strategy. Furthermore, Farah et al. (2020) studied a traditional EH that integrated RE to assist the dispatch of electricity demand and wood chips to convert to heat demand via biomass generator. Each objective function consists of the energy hub operating cost and emissions. Utilizing PSO is an effort to solve individual objective functions and using WSMO to balance the optimal solution of two objectives. The case study of EH serves five local sites, including campus restaurants, an office building, 100 residential, a school campus, and a hotel with different scenarios such as with or without RE. The results indicate that the optimal configuration for the EH combines a natural gas turbine, biomass unit, boiler, and RE. This setup achieves both lower operational costs and reduced emissions. The carbon emissions in this model are primarily influenced by using biomass and RE. Moreover, Mousavi et al. (2022) proposed a GA algorithm that aims to solve the optimization problem in EH which includes CHP and gas furnaces to coordinate dispatch heat and electricity demand. The objective function consists of the operating cost and emissions. To assess the multi-objective problem in this work is utilized the simplest method is WSMO, the weighting factor is 0.5 in each objective.

Under the emissions factor and pricing mechanism, the result shows CHP starts operating when high demand is needed, resulting in lower costs and emissions. In the previous year, Imeni and Ghazizadeh (2023) explored how to optimally and efficiently manage a hydrogen-ready sustainable EH model that incorporates hydrogen. They framed the issue as a multi-objective optimization problem with two key objectives: minimizing the operating costs of the EH and reducing CO_2 emissions. These objectives are combined using the WSMO method. The study examined three different scenarios (Case A, B, and C), each with varying weights assigned to operation costs and emissions. The findings indicated that using hydrogen as the primary energy carrier in a MES significantly improved performance, particularly in lowering pollution emissions. Additionally, the implementation of an integrated demand response program (IDRP), which uses time-of-use (TOU) tariffs to manage electrical and heat loads, further contributed to reducing the operation costs of the hydrogen-ready smart energy hub. However, the WSMO method still faces challenges in determining the optimal weights for each objective. Then, Imeni et al. (2023) extended their previous work by incorporating photovoltaic (PV) and BESS into the system and enhancing the solution efficiency of the multi-objective optimization problem by employing the Simple Augmented e-Constraint (SAUGMECON) method. Moreover, the HS is modeled using molar flow calculations, and the ideal gas law is applied to determine the hydrogen quantity in the storage tank, resulting in a more complex formulation. The result demonstrates that it is possible to find an optimal trade-off between these objectives, providing a range of solutions based on different weightings. This study significantly improves both economic performance (by reducing operational costs) and environmental impact (by minimizing emissions), while effectively handling the inherent in RE generation. Additionally, Hassan et al. (2023) presented the EH model, including RE, grid interconnection, BESS, NG, CHP, furnace, and HS. The main study aims to examine to assess their impact on EH performance between two technologies of EL that as a component of HS include solid oxide (SOEC) and proton exchange membrane (PEM). the EH operation that serves hydrogen fuel-cell vehicles, battery

electric vehicles, and heat demands. MILP is used to optimize management problems which comprise minimizing the EH day-ahead operating cost and minimizing the emissions that are produced inside the EH while meeting the hydrogen, electricity, and heat demands. This study utilizes WSMO to balance between two objectives. The results indicate that SOEC EL has lower operating costs and emissions compared to PEM EL. However, SOEC consumes more NG to offset internal heat losses, while the PEM EL requires more electricity due to its lower efficiency. At present, Xu et al. (2024) proposed a multi-objective operation optimization model for electro-thermal integrated energy systems (IES) that incorporates PtG technology and demand response (DR) strategies. The model categorizes electro-thermal loads into various types, including fixed, reducible, transferable, translational, and heating loads, and establishes corresponding DR strategies. The optimization model aims to minimize total cost, carbon emissions, and energy curtailment rates. In a case study, after 500 iterations, 20 non-dominated solutions are generated, with the best solution identified using the VIKOR approach. The optimal values achieved included total cost, carbon emissions, and energy curtailment rates, demonstrating that PtG technology significantly enhances system performance. This led to notable reductions in total costs, carbon emissions, and energy curtailment rates. Additionally, the implementation of DR strategies contributed to further improvements in each respective objective.

2.8 Probabilistic model for optimal scheduling MES using EH

The uncertainties in EH optimization arise from various sources, including variable renewable generation (wind and solar), market fluctuations, consumer behavior, and environmental changes. Ignoring these uncertainties can lead to inaccurate scheduling, increased operational costs, and suboptimal decision-making. To address these challenges, different uncertainty modeling approaches have been explored. Mohammadi et al. (2017) reviewed the literature on methods for dealing

with uncertainty in the optimal scheduling of EH. Probabilistic methods rely on PDF to model uncertainties, with MCS being a widely used but computationally intensive technique. Alternatively, scenario-based stochastic optimization improves computational efficiency by reducing the number of uncertainty scenarios. Another approach involves fuzzy logic, this method enables more realistic energy scheduling by addressing vague or imprecise system parameters. In contrast, robust optimization (RO) provides different strategies for handling uncertainty. RO ensures optimal performance in worst-case scenarios by defining uncertainty sets, making it a conservative yet reliable approach. Honarmand et al. (2021) The study developed an optimization framework to address uncertainties in the operation of an energy hub for a hospital in Hamedan, Iran. It considered variations in electrical, cooling, and heating loads, as well as PVPs output power. The results showed a 6.41% increase in total operation costs due to uncertainties, primarily due to additional energy procurement and system adjustments. The study also examined the role of energy storage systems in mitigating uncertainty impacts, finding that when storage systems are excluded, operation costs increased by 0.87%. The study also examined the effects of different time resolutions and contingency analysis. Thang et al. (2022) developed a stochastic optimization framework to address uncertainties in MES, focusing on solar energy generation, energy demand, and electricity prices. They used Beta PDF for solar energy generation and normal PDF for electricity prices and demand fluctuations. The study used a clustering technique to classify distributions into distinct states, forming a scenario matrix. The SCENRED tool in GAMS is used to reduce scenarios to 10. The results showed that incorporating uncertainties in the framework improved system robustness and reduced total operational costs by 2.0-14.5% compared to deterministic approaches. Ranjbarzadeh et al. (2022) studied a probabilistic optimization approach to address uncertainties in solar energy production and electricity market prices within a multi-carrier microgrid. The 2m+1 point estimation method is used to model uncertainties efficiently while minimizing computational complexity. This method estimates the statistical properties of uncertain variables,

such as solar power output and electricity prices, by focusing on a limited number of evaluation points. Compared to traditional MCS, which require many samples, the 2m+1 approach significantly reduces computational burden while maintaining a high level of accuracy in uncertainty modeling. The study shows that incorporating uncertainty into the optimization framework increases operational costs but improves resilience to renewable energy fluctuations and market conditions. The model adjusts energy storage system scheduling and demand response strategies to mitigate price volatility and intermittent solar generation. This results in a more conservative strategy, increasing costs but improving system robustness.

This study addresses a research gap by proposing an EH model that fully integrates green hydrogen production from HS. Previous works used a mix of RE and grid power, making hydrogen not fully green. Additionally, past research primarily used the WSMO method for solving multi-objective problems. To enhance this, the study introduces FMOO, a novel approach in EH research. Furthermore, the uncertainties of RE and load are considered. To analyze these uncertainties more effectively, a probabilistic approach is incorporated, leading to a more accurate and optimized model.

Table 2.5 The research gap between the existing and this study

Works	*Interconnect multi-energy*					*Objectives*				*Type of hydrogen*		*Method*
	Electricity	NG	WTs	PVPs	H_2	TOC	TCE	EP	Others	Grey	Green	
Thanh-tung et al. (2016)	✓	✓				✓						MIP

Table 2.5 The research gap between the existing and this study (Continued)

Works	*Interconnect multi-energy*					*Objectives*				*Type of hydrogen*		*Method*
	Electricity	NG	WTs	PVPs	H_2	TOC	TCE	EP	Others	Grey	Green	
Javadi et al. (2017)	✓	✓				✓						MINLP
Geng and Jia (2020)	✓	✓				✓						GA-PSO
Liu et al. (2021)	✓	✓				✓						LP
Ha et al. (2017)	✓	✓		✓		✓						MIP
Wang (2023)	✓	✓	✓	✓		✓						MILP
Zhang et al. (2017)	✓		✓	✓	✓				✓		✓	CPLEX
Zidan and Gabbar (2016)	✓	✓	✓	✓		✓	✓					- GA WSMO
Ma et al. (2017)	✓	✓	✓			✓			✓			- Improved MOPSO
Kholardi et al. (2018)	✓	✓	✓		✓	✓	✓			✓		- MILP WSMO
Farah et al. (2020)	✓	✓	✓	✓		✓	✓					- PSO WSMO

Table 2.5 The research gap between the existing and this study (Continued)

Works	*Interconnect multi-energy*					*Objectives*				*Type of hydrogen*		*Method*
	Electricity	NG	WTs	PVPs	H_2	TOC	TCE	EP	Others	Grey	Green	
Mousavi et al. (2022)	✓	✓				✓	✓					- GA WSMO
Hassan et al. (2023)	✓	✓	✓			✓	✓					- MINLP WSMO
Imeni and Ghazizadeh (2023)	✓	✓	✓		✓	✓	✓			✓		- MINLP WSMO
Imeni et al. (2023)	✓	✓	✓		✓	✓	✓			✓		- MINLP - SAUGMECON
Xu et al. (2024)	✓	✓	✓	✓		✓	✓		✓			- MOPSO VIKOR
Honarmand et al. (2021)	✓	✓		✓		✓						- MINLP RO
Thang et al. (2022)	✓	✓		✓		✓						- MINLP A scenario reduction
Ranjbarzadeh et al. (2022)	✓	✓		✓		✓	✓					- MILP - WSMO and FMOO 2m+1 point estimation
This work (Proposed)	✓	✓	✓	✓	✓	✓	✓	✓			✓	- PSO-LP - FMOO MCS

2.9 Chapter Summary

The concept of MES has gained significant attention due to the increasing integration of RE resources and energy storage technologies. Section 2.2 introduces the conventional approach to electrical energy scheduling problems, highlighting its importance in managing the supply-demand balance and enhancing system performance. Building on this, Section 2.3 outlines the trends in RE resources, emphasizing investments in wind and solar power as well as technological advancements, which directly influence the selection of appropriate RE types for HS integration. Consequently, Section 2.5 of this chapter contains a comprehensive literature review that focuses on HS application overview. Section 2.6 investigates optimal scheduling of MES using EH models that focus on individual objectives such as minimizing operating costs or carbon emissions. Meanwhile, Section 2.7 delves into studies on optimal scheduling of MES using EH models under multi-objective optimization, emphasizing the need for compromise solutions to balance multiple objectives effectively. Then, Section 2.8 demonstrates a probabilistic model, which describes an uncertainty scenario, leading to determining an optimal scheduling solution to handle uncertainty. Lastly, by combining the knowledge from these reviews, Table 2.5 provides a summary of the identified research gaps, highlighting areas that require further exploration.

CHAPTER III

OMES-WSPHS INTEGRATION CONSIDERING PRICING MECHANISM UNDER TOC MINIMIZATION

3.1 General Introduction

This chapter focuses on the integration of OMES-WSPHS under a pricing mechanism to minimize the TOC. The study aims to enhance the efficiency of energy dispatch by coordinating multiple energy sources, including the electricity grid, NG, WTs, PVPs, and HS. The proposed system integrates hydrogen storage as a key element to optimize energy utilization by converting excess RE into hydrogen, which can later be used for electricity generation. To achieve the optimal scheduling of the system, the PSO-LP method is employed. This optimization technique enables effective coordination between multiple energy sources while considering the TOU tariff and real-time pricing (RTP). The study explores various case studies to evaluate the impact of different operational scenarios, including the presence or absence of HS, coordinated and uncoordinated operations between electricity and NG, as well as cases with and without solar power integration. The results provide insights into how integrating HS and optimizing energy dispatch strategies can contribute to cost reduction and improved energy management.

3.2 Problem Formulation

3.2.1 System Modeling

For system modeling, the components of MES-WSPHS are shown in Fig. 3.1. The input part consists of an electricity grid and NG to dispatch energy to the output which is electricity and heat demands. Conversion technology, which is the center of EH includes a transformer (TR), gas boiler (GB), micro-turbine (MT), WTs, and

PVPs. With HS, the excessive RE can be converted to hydrogen and stored for utilization at the proper period. As a result, the resources can be coordinately utilized, leading to higher overall efficiency. Electricity (P_E) and NG (P_{NG}) serve as the primary input power for the system and must supply the required electricity demand (L_E) and heat demand (L_H), respectively (Zidan & Gabbar, 2016). Conversion efficiency is considered and can be mathematically expressed as shown in Eq. (3.1).

$$\begin{bmatrix} L_E \\ L_H \end{bmatrix} = \begin{bmatrix} \eta_{TR} & \eta_{MT}^{E} & 0 \\ 0 & \eta_{MT}^{H} & \eta_{GB} \end{bmatrix} \begin{bmatrix} P_E \\ P_{NG}^{1} \\ P_{NG}^{2} \end{bmatrix} + \begin{bmatrix} P_{WPS}^{i} + P_{FC} \\ 0 \end{bmatrix}. \tag{3.1}$$

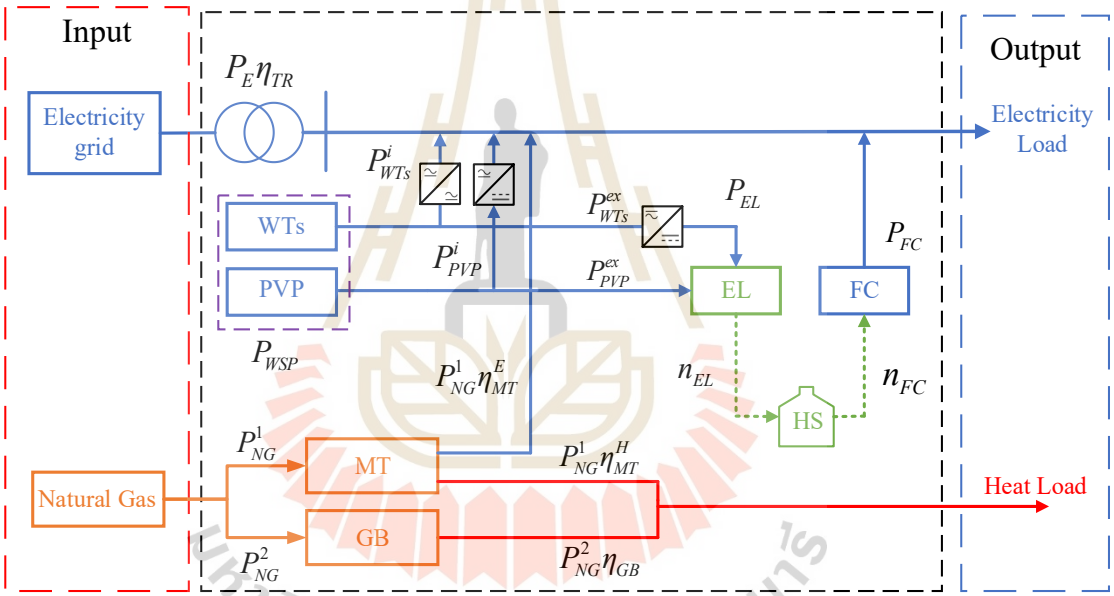

Figure 3.1 The components of MES with EH model

In part of WTs and PVPs modeling, the wind speed profile must be evaluated at a height corresponding to the turbine's cross-sectional area. Therefore, Eq. (3.2) illustrates a calculation for estimating wind speed at this altitude based on the power law theory (Manwell et al., 2002).

$$\frac{v_{WT}(h)}{v_{WT,r}(h)} = \left(\frac{z}{z_r}\right)^{\alpha}. \tag{3.2}$$

A wind turbine generates electricity when the wind speed is above the cut-in speed or below the cut-off speed, otherwise the turbine produces no power.

The power output increases with the cube of the wind speed divided by the rated wind speed when the wind speed is between the cut-in speed and the rated wind speed. Once the wind speed reaches the rated level, the turbine generates a constant rated power until the cut-off speed is reached. Above the cut-off speed condition, it is shut down to prevent damage. A wind turbine power output can be expressed Eq. (3.3) (Dechjinda & Chayakulkheeree, 2024):

$$P_{WT}(h)=\begin{cases} 0 \quad \text{for} \quad 0<v_{WT}(h)\le v_{cut-in}, \\ P_{WT,rated}\times\left(\dfrac{v_{WT}(h)}{v_{wt,rated}}\right)^3 \text{ for } v_{cut-in}<v_{WT}(h)\le v_{WT,rated}, \\ P_{WT,rated} \quad \text{for} \quad v_{WT,rated}<v_{WT}(h)\le v_{cut-off}, \\ 0 \quad \text{for} \quad v_{WT}(h)>v_{cut-off}. \end{cases} \tag{3.3}$$

The total wind power per hour from Eq. (3.3) can be defined as the sum of individual wind turbines, defined as WTs can be modeled in Eq. (3.4). The PVPs can be modeled as Eq. (3.5) which considers solar energy converted into electrical energy. The output is DC power and needs to be converted into AC power through an inverter (Yammani et al., 2012).

$$P_{WTs}(h)=\sum_{k=1}^{NT}P_{WT,k}(h), \tag{3.4}$$

$$P_{PVPs}(h)=A\times\beta\times SI(h). \tag{3.5}$$

When the wind and solar power are excessed, it can be stored in the form of hydrogen. Therefore, the grid-injected wind and solar power at time *h* can be shown in Eq. (3.6) - (3.11).

$$P_{WTs}(h)=P^{i}_{WTs}(h)+P^{ex}_{WTs}(h), \tag{3.6}$$

$$P_{PVPs}(h)=P^{i}_{PVPs}(h)+P^{ex}_{PVPs}(h), \tag{3.7}$$

$$P_{WSP}(h)=P_{WTs}(h)+P_{PVPs}(h), \tag{3.8}$$

$$P^{ex}_{WSP}(h)=\begin{cases} 0 & if\ P^{i}_{WTs}(h)+(P^{i}_{PVPs}(h)\times\eta_{DC/AC})\le L_E(h) \\ (P^{i}_{WTs}(h)+(P^{i}_{PVPs}(h)\times\eta_{DC/AC}))-L_E(h) & if\ P^{i}_{WTs}(h)+(P^{i}_{PVPs}(h)\times\eta_{DC/AC})>L_E(h) \end{cases}, \tag{3.9}$$

$$P^{i}_{WSP}(h)=\begin{cases} (P^{i}_{WTs}(h)+(P^{i}_{PVPs}(h)\times\eta_{DC/AC})) & if\ P^{i}_{WTs}(h)+(P^{i}_{PVPs}(h)\times\eta_{DC/AC})\le L_E(h) \\ L_E(h) & if\ P^{i}_{WTs}(h)+(P^{i}_{PVPs}(h)\times\eta_{DC/AC})>L_E(h) \end{cases}, \tag{3.10}$$

$$P_{EL}(h)=(P^{ex}_{WTs}(h)\times\eta_{AC/DC})+P^{ex}_{PVPs}(h). \tag{3.11}$$

The conversion devices are TR, GB, and MT. In the electrical energy sector, TR is used to convert the grid voltage to the load. The TR efficiency model can

be expressed as Eq. (3.12) when electricity flows through the TR to supply loads. In the NG energy sector, GB and MT are employed to convert NG to power (Ha et al., 2017; Thanh-tung et al., 2016). The efficiencies of the GB and MT are utilized to determine the load supply from NG formed as in Eq. (3.13) and (3.14). When considering NG cost, the power from NG can be defined as Eq. (3.15).

$$P_{TR} = P_E \eta_{TR}. \tag{3.12}$$

$$P_{GB} = P_{NG}^2 \eta_{GB}, \tag{3.13}$$

$$P_{MT}^{E,H} = \begin{cases} P_{NG}^1 \eta_{MT}^E; \text{ for electricity output} \\ P_{NG}^1 \eta_{MT}^H; \text{ for heat output} \end{cases}, \tag{3.14}$$

$$P_{NG} = P_{NG}^1 + P_{NG}^2. \tag{3.15}$$

HS has gained considerable attention in recent studies and research efforts. In these systems, hydrogen is produced by EL when the power generated by WTs and PVPs exceeds the power demand and is stored as a chemical substance. This stored hydrogen can later be used in the FC, where it reacts with oxygen from the air to generate electricity in its gaseous state. HS enables long-term energy retention, as highlighted in (Ould Amrouche et al., 2016). By applying Faraday's law, the molar flow rate of hydrogen is produced by the EL. The FC turns hydrogen into electricity, and hydrogen consumption is directly proportional to its power output (Cau et al., 2014; Imeni et al., 2023). The molar flow of EL and FC can be described as a function in Eq. (3.16) and (3.17), respectively. When HS is operating, the FC and EL cannot be operated simultaneously. Therefore, Y_{EL} and Y_{FC}, representing binary numbers (0,1), are introduced for FC and EL operating conditions as shown in Eq. (3.18) (Cau et al., 2014; Imeni et al., 2023). A key control variable in the HS system is the hydrogen tank pressure at each hour. The tank pressure reflects the amount of hydrogen contained in the storage vessels and molar flow from Eq. (3.16) and (3.17) are used to calculate the pressure at each hour. The pressure calculation for the hour *h* is dependent on the previous time step, as shown in Eq. (3.19) and can calculate the state of the tank (SOT) as shown in Eq (3.20) (Cau et al., 2014; Imeni et al., 2023).

$$n_{H_2,EL} = \frac{\eta_{EL} P_{EL}}{LHV_{H_2}}, \tag{3.16}$$

$$n_{H_2,FC} = \frac{P_{FC}}{\eta_{FC} LHV_{H_2}}. \tag{3.17}$$

$$Y_{EL} = \begin{cases} 1 \text{ when } Y_{FC} = 0 \\ 0 \text{ when } Y_{FC} = 1 \end{cases}. \tag{3.18}$$

$$p_{\text{tank}}(h) = p_{\text{tank}}(h-1) + (\frac{\Re T_{H_2}}{V_{H_2}} n_{H_2,EL}(h) - n_{H_2,FC}(h)), \tag{3.19}$$

$$SOT(h) = \frac{p_{\text{tank}}(h) - p_{\text{tank,min}}}{p_{\text{tank,rated}} - p_{\text{tank,min}}} \times 100\%. \tag{3.20}$$

3.2.2 Objective Function

The proposed method uses the PSO-LP technique to find the optimal scheduling of MES-WSPHS. The multiple energy deliveries are formed as variables on an hourly basis, to find the optimal solution for the system that makes it the minimum operating cost. The analysis considers the TOU tariff and RTP as separate factors throughout the day. Therefore, the objective function is to minimize TOC while accounting for the TOU tariff and RTP independently, with a penalty function incorporated to address any constraints violations, as shown in Eq. (3.21). The operation of this work procedure, which involves calculating the objective function while handling constraints, follows the workflow depicted in Fig. 3.2.

$$Minimize\ TOC = \sum_{h=1}^{24} (C_E(h) P_E(h) + C_{NG}(h) P_{NG}(h)) + PNF. \tag{3.21}$$

Subjected to the power balance constraints in Eq. (3.22) - (3.23),

$$L_E(h) - P_{FC}(h) - P_{WSP}^{i}(h) = P_{TR}(h) + P_{MT}^{E}(h), \tag{3.22}$$

$$L_H(h) = P_{GB}(h) + P_{MT}^{H}(h), \tag{3.23}$$

and the limit constraints of each conversion device as demonstrated by Eq. (3.24) - (3.29).

$$0 \le P_{TR}(h) \le P_{TR,rated}, \tag{3.24}$$

$$0 \le P_{MT}^{E,H}(h) \le P_{MT,rated}^{E,H}, \tag{3.25}$$

$$0 \le P_{GB}(h) \le P_{GB,rated}, \tag{3.26}$$

$$0 \le Y_{EL} P_{EL}(h) \le P_{EL,rated}, \tag{3.27}$$

$$0 \le Y_{FC} P_{FC}(h) \le P_{FC,rated}, \text{ and} \tag{3.28}$$

$$p_{\text{tank,min}} \le p_{\text{tank}}(h) \le p_{\text{tank,rated}}. \tag{3.29}$$

The initial pressure which is indicated in the content of the HS tank is set to the final pressure when the day is over, as shown in Eq. (3.29). Additionally, penalty function terms can handle some constraints, which can't define a lower and upper boundary such as Eq. (3.29) and (3.30). The penalty function can be defined in Eq. (3.31)

$$p_{\text{tank}}(h = initial) = p_{\text{tank}}(h = 24). \tag{3.30}$$

$$PNF = \rho[(p_{\text{tank}}(t) - p_{\text{tank,min}})^2 + (p_{\text{tank}}(t) - p_{\text{tank,max}})^2 + (p_{\text{tank}}(24) - p_{\text{tank}}(\text{initial}))^2] \tag{3.31}$$

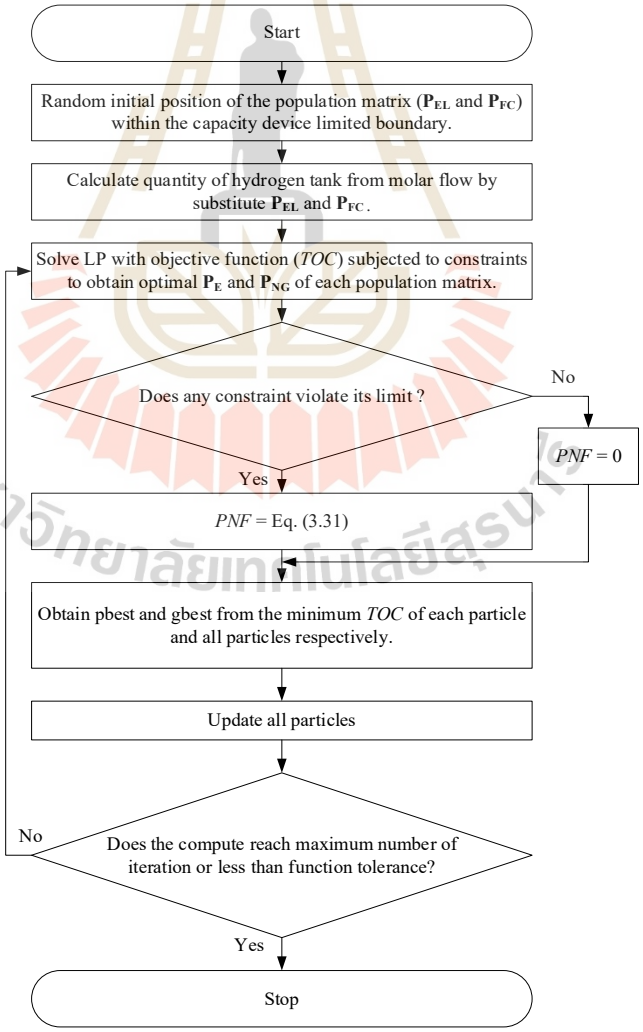

Figure 3.2 Flowchart of the PSO-LP technique under TOC procedure

3.2.3 PSO-LP Technique

The HS scheduling is a continuous variable (P_{EL} and P_{FC}), while the relation of power from the grid and NG (P_E and P_{NG}) can be formed as a linear problem. Therefore, we modify the mathematical formulation of the problem to account for utilizing a heuristic algorithm in the main loop and utilizing a deterministic algorithm in the subroutines. LP will optimize the problem in subroutines. Then, the main loop will be optimized by PSO. The overview concept of hybrid PSO-LP is shown in Fig. 3.3.

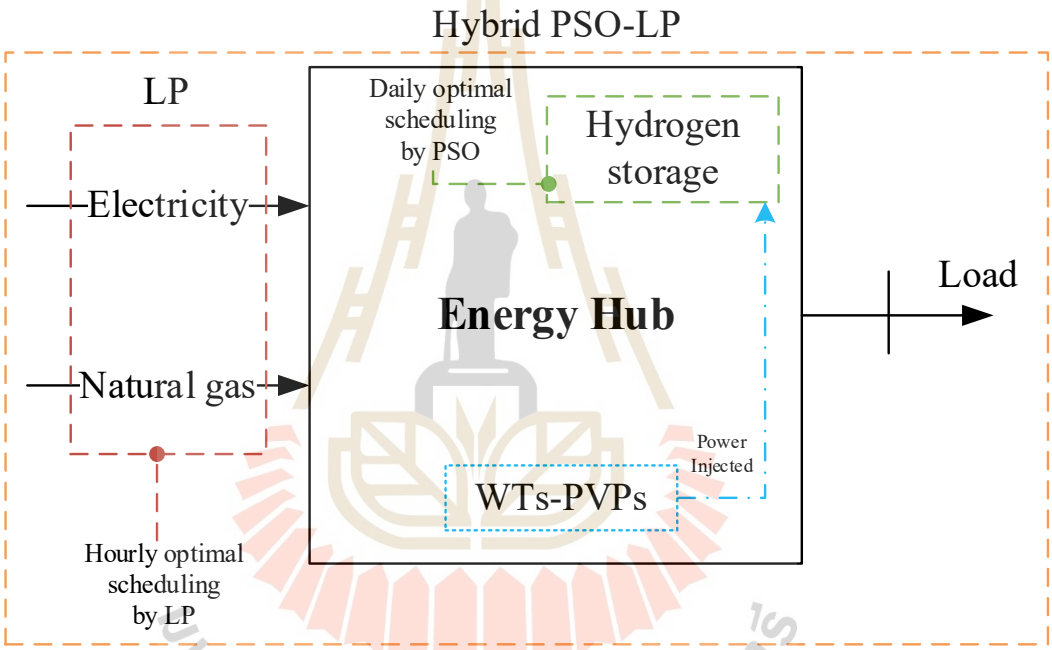

Figure 3.3 The overview of hybrid PSO-LP

The hybrid PSO-LP technique is an enhanced model of the traditional PSO algorithm, designed to be more efficient. The PSO is used for searching for optimal HS scheduling incorporating the optimal condition of electricity from the power grid and NG, under wind and solar power, electricity load, and heating load conditions. As a stochastic optimization technique, the PSO algorithm is a stochastic optimization technique inspired by the collective behavior of bird flocks and their emergent dynamics. In PSO, a population of potential solutions, referred to as particles, is used to search for the optimal result. This population is called a swarm, and each particle

represents a possible solution. The algorithm begins by randomly assigning positions to the particles within the search space. These particles then update their positions in successive iterations, adjusting based on their velocities. Each particle keeps track of its best position, referred to as *pbest(i,h)*, and updates its velocity based on that. Particles also communicate with one another to adjust their movement. If a particle finds a solution better than its previous *pbest*, the value is replaced. Among the entire population, the best solution found is called the global best (*gbest*). In this work, the population is formulated as follows Eq. (3.32) and the matrix in Eq. (3.32) will solve the individual objective function simultaneously. Then this matrix is used to update each particle's velocity as displayed in Eq. (3.33), and the next step of the matrix is updated by velocity as shown in Eq. (3.34) (Kennedy & Eberhart, 1995).

$$\mathbf{P_{EL,FC}} = [P_{EL,FC}(1), P_{EL,FC}(2), ..., P_{EL,FC}(h), ..., P_{EL,FC}(24)]. \tag{3.32}$$

$$v(i,h+1) = wv(i,h) + c_1 rand_1(pbest(i,h) - \mathbf{P_{EL,FC}}(i,h)) + c_2 rand_2(gbest(i,h) - \mathbf{P_{EL,FC}}(i,h)), \tag{3.33}$$

$$\mathbf{P_{EL,FC}}(i,h+1) = \mathbf{P_{EL,FC}}(i,h) + v(i,h+1). \tag{3.34}$$

In this work, Eq. (3.32) defines the upper and lower boundaries based on the operational range of energy converter components in Table 3.1, specifically from 0 to $P_{EL,rated}$ and 0 to $P_{FC,rated}$. In cases where the excess power from RE is less than the rated capacity of the EL, the upper boundary is redefined by Eq. (3.11).

Although PSO is effective in exploring global search spaces, it often encounters challenges in fine-tuning solutions within constrained environments due to its stochastic nature. To overcome this limitation, the LP algorithm is incorporated into the proposed PSO-LP framework. After PSO generates an initial HS scheduling solution, LP is employed to further refine and optimize the solution under a set of linear constraints and objective functions. By combining the global exploration capability of PSO with the local optimization precision of LP, the hybrid approach aims to achieve faster convergence, improved solution accuracy, and enhanced feasibility for multi-energy system scheduling problems. The mathematical formulation of the LP optimization stage is established as follows and can be expressed by Eqs. (3.35)–(3.41).

$$\text{minimize } TOC = \mathbf{C}^{\mathbf{T}}\mathbf{x} \tag{3.35}$$

$$\mathbf{C} = [C_{E_{(24\times1)}}; C_{NG_{(24\times1)}}; C_{NG_{(24\times1)}}] \in \mathbb{R}^{72\times1} \tag{3.36}$$

$$\mathbf{x} = [P_{E_{(24\times1)}}; P^{1}_{NG_{(24\times1)}}; P^{2}_{NG_{(24\times1)}}] \in \mathbb{R}^{72\times1} \tag{3.37}$$

Subject to $\mathbf{A_{eq}x} = \mathbf{b_{eq}}$ (3.38)

$$lb \le \mathbf{x} \le ub \tag{3.39}$$

$$\mathbf{A_{eq}} = \begin{bmatrix} \mathbf{A}_{11} & \mathbf{A}_{12} & \mathbf{0}_{(24\times24)} \\ \mathbf{0}_{(24\times24)} & \mathbf{A}_{22} & \mathbf{A}_{23} \end{bmatrix} \in \mathbb{R}^{48\times72} \tag{3.40}$$

$$\mathbf{b_{eq}} = \left[L_E(h)_{(1\times24)}, L_H(h)_{(1\times24)} \right]^T \tag{3.41}$$

Where

$$\mathbf{A_{11}} = diag(\eta_{TR}) \in \mathbb{R}^{24\times24}$$

$$\mathbf{A_{12}} = diag(\eta^{E}_{MT}) \in \mathbb{R}^{24\times24}$$

$$\mathbf{A_{22}} = diag(\eta^{H}_{MT}) \in \mathbb{R}^{24\times24}$$

$$\mathbf{A_{23}} = diag(\eta_{GB}) \in \mathbb{R}^{24\times24}$$

$\mathbf{0}_{(24\times24)}$ = zero matrix (no coupling)

The matrices denoted as *diag(·)* represent diagonal matrices, where all off-diagonal elements are equal to zero. Each diagonal entry corresponds to a parameter specific to a given time step or energy source. Furthermore, the optimization problem is subject to lower and upper bounds, denoted as *lb* and *ub*, respectively. The lower bound is always set to zero, while the upper bound is defined based on the energy flow pathways through the system. Specifically, the upper bound is assigned according to the rated capacity of each device along its respective energy flow path, as detailed in Table 3.1.

3.3 Data Acquired and Assumptions

To evaluate the performance and feasibility of the MES-WSPHS configuration, it is essential to analyze the efficiency and capabilities of its individual components as shown in Table 3.1 (Ha et al., 2022; Son et al., 2021). The electricity load profile utilized in this study is obtained from a typical summer day in the northeastern region of Thailand, with a peak load defined at 2 MW (Dechjinda & Chayakulkheeree, 2024) as shown in Fig. 3.4(a). The heat load profile is adapted from Anna Sandhaas as illustrated

in Fig. 3.4(b). The wind and solar profile are derived from data collected on a summer day in Pakchong, Thailand (Dechjinda & Chayakulkheeree, 2024). Finally, additional details of the entire energy profile are provided in Appendix A.

Table 3.1 The efficiency and rated device of each component

List	No.1	No.2	No.3	No.4	No.5	No.6	No.7
Component	TR	EL	FC	MT	GB	Converter	Pressure tank
Efficiency	98%	70%	60%	40%, 50%	88%	95%	-
Rated	2500 kVA	500 kW	500 kW	500 kW	1600 kW	-	100 bar

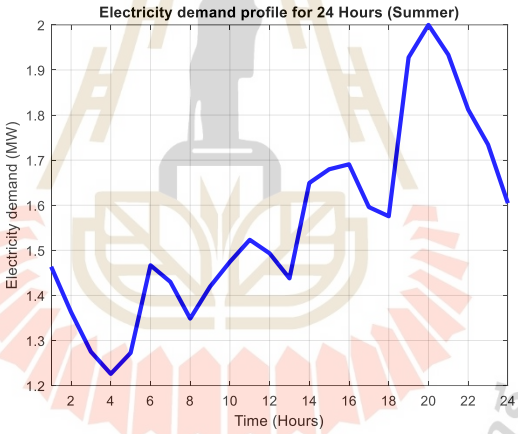

(a)

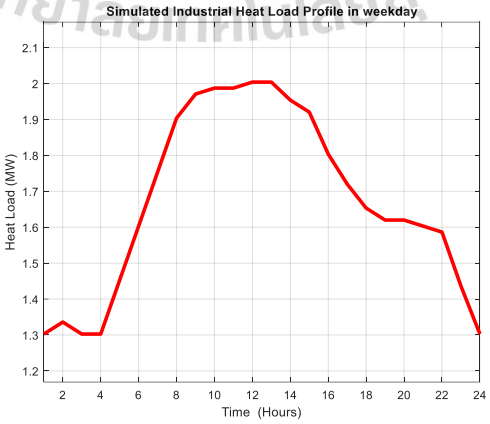

(b)

Figure 3.4 The load profile (a) electricity (b) heat

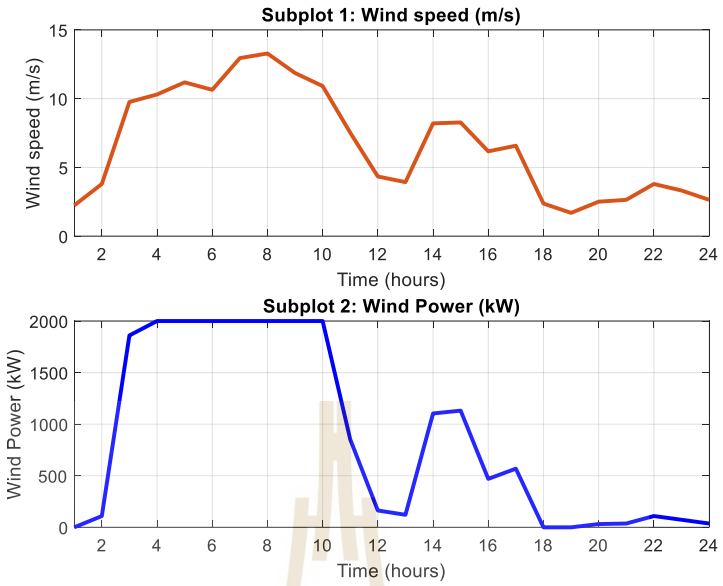

Figure 3.5 The wind profile

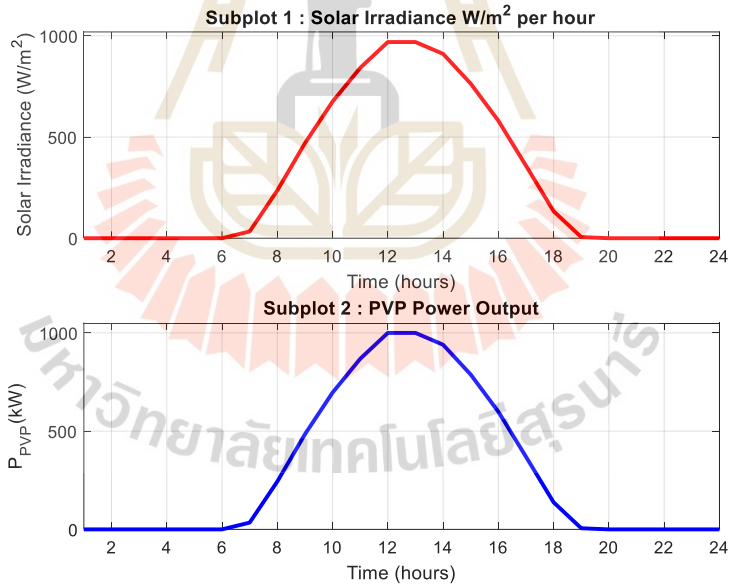

Figure 3.6 The solar profile

This study examines a wind power system with four turbines rated at 500 kW each (NT = 4), as shown in Fig. 3.5. Subplots 1 and 2 in Fig. 3.5 illustrate wind speed conversion to power. Hourly solar irradiance and PVPs output are shown in Fig. 3.6, subplots 1 and 2, respectively. Fig. 3.7 highlights excess wind and solar power over

demand. Electricity costs follow TOU tariff (Piawises & Chayakulkheeree, 2024), while NG prices remain constant. Furthermore, RTP, which reflects dynamic price adjustments, both are described in Fig. 3.8.

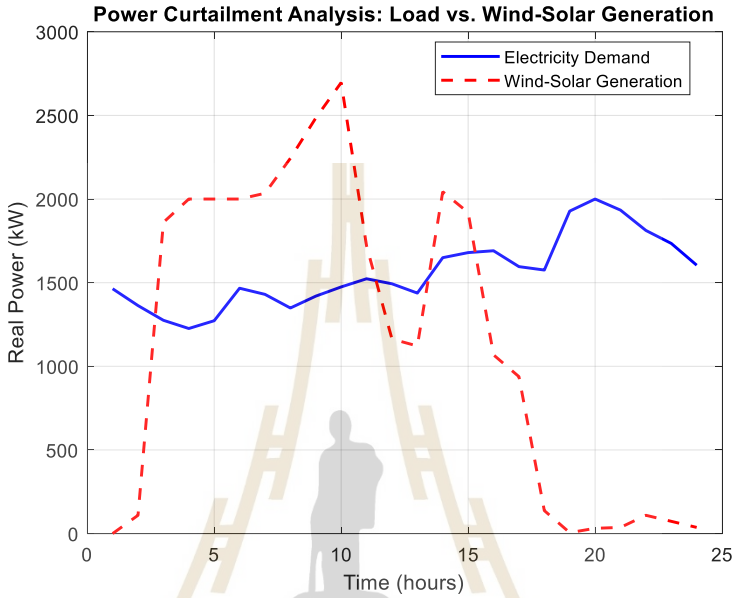

Figure 3.7 The excess wind-solar generation

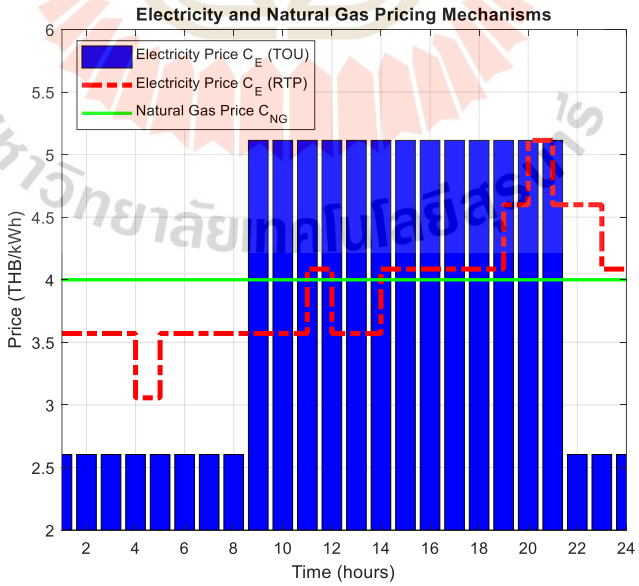

Figure 3.8 The electricity and natural gas pricing mechanism

3.4 Simulation Results

The case studies presented in Fig. 3.9 are analyzed under five distinct scenarios, each with specific operational conditions:

Case I: MES-WSP operates without HS and lacks coordination between electricity and NG (Base Case).

Case II: MES-WSP includes HS with no coordination between electricity and NG.

Case III: MES-WSP operates with coordinated electricity and NG but without HS.

Case IV: MES-WSP (excluding solar power) operates with HS and coordinated electricity and NG operations.

Case V: MES-WSP operates with HS and coordinated electricity and NG operations.

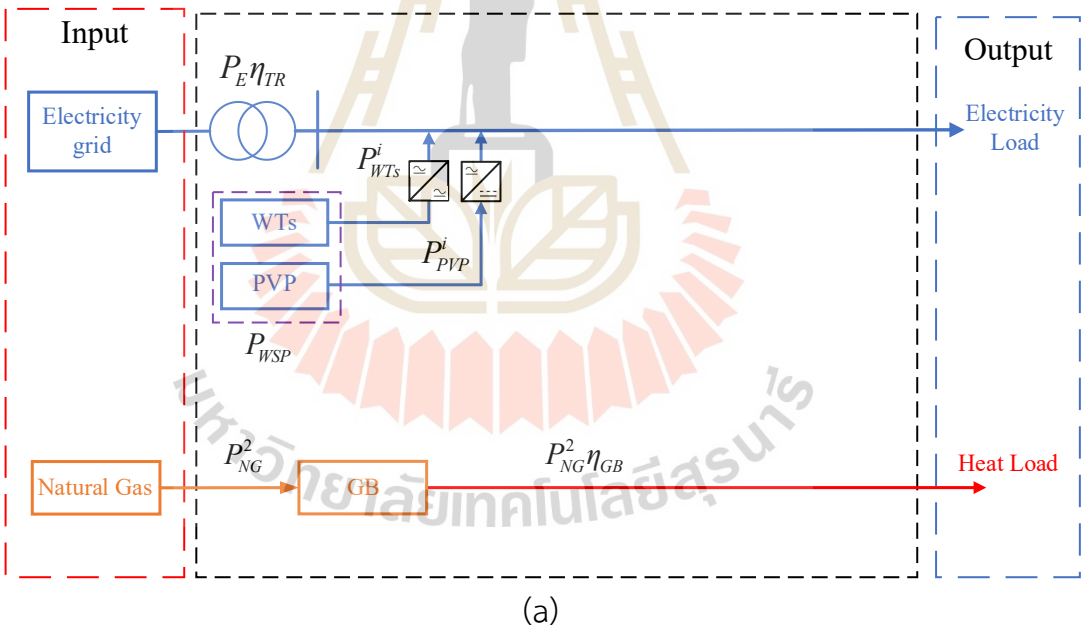

(a)

Figure 3.9 Configuration of the MES-WSP under different case studies

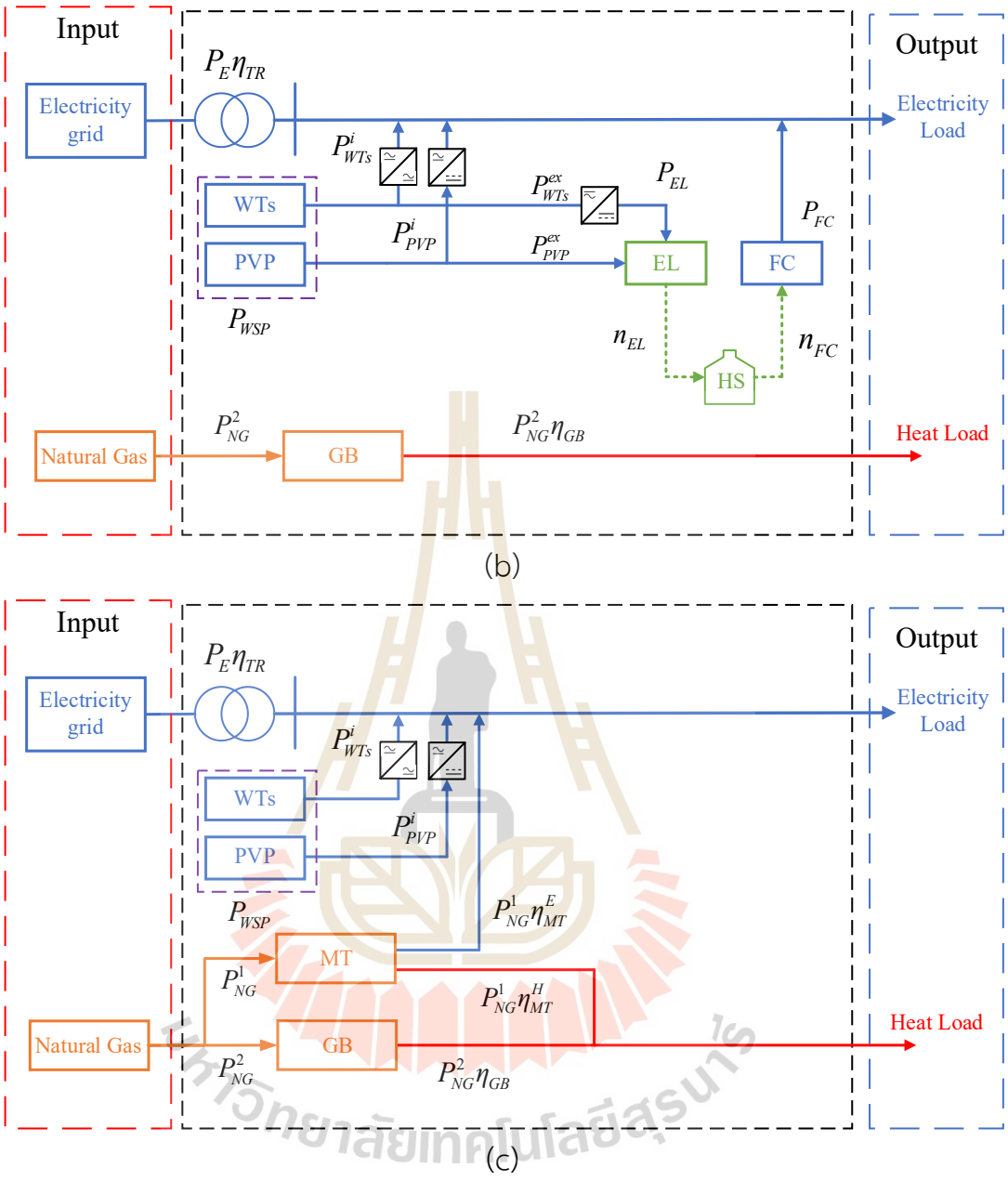

Figure 3.9 Configuration of the MES-WSP under different case studies (Continued)

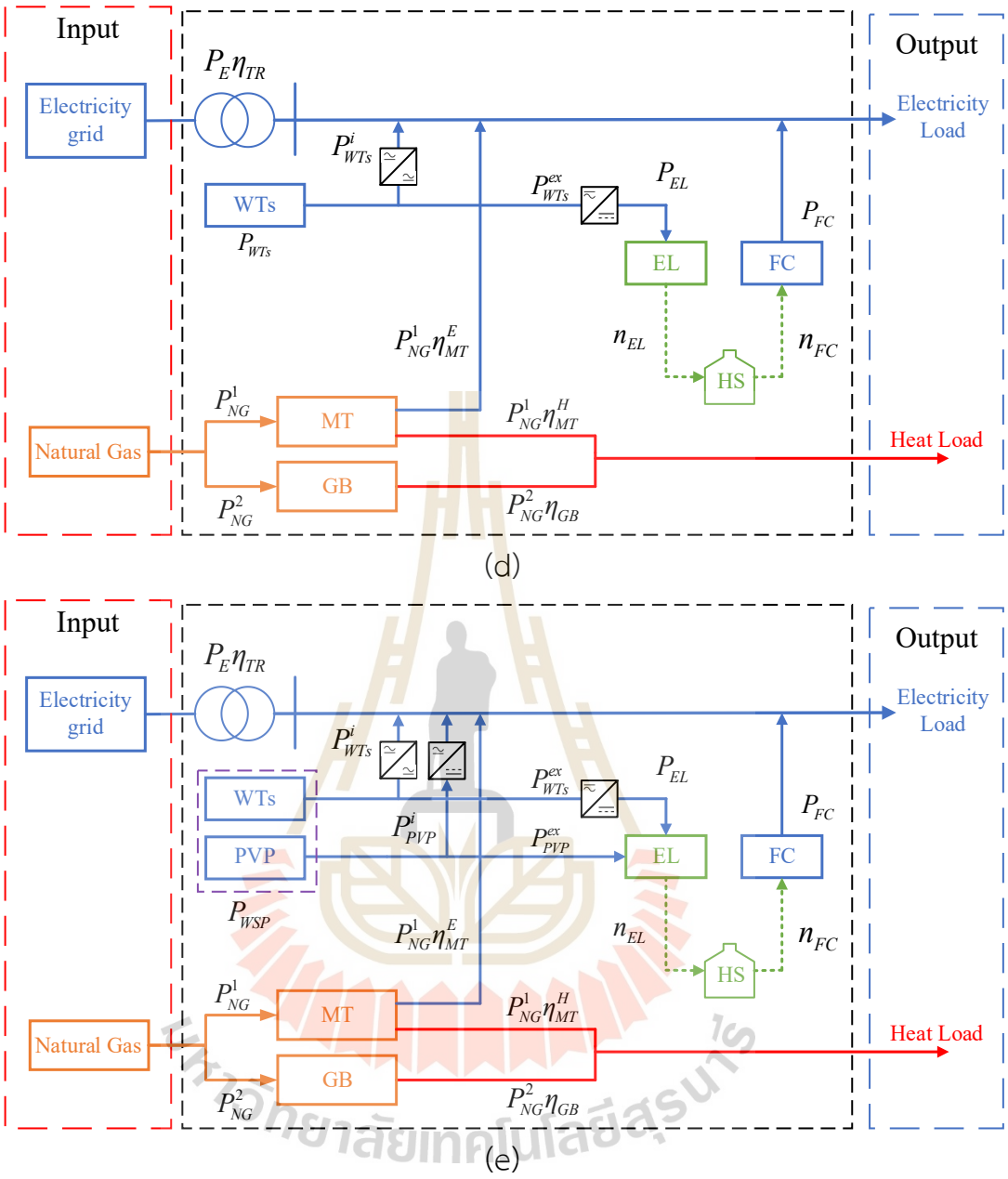

Figure 3.9 Configuration of the MES-WSP under different case studies (Continued)

However, the case studies will be analyzed under the TOU scheme for all given cases, while under the RTP scheme, only the case with the lowest TOC will be considered and presented. This analysis aims to determine which scenario achieves the greatest reduction in operating costs throughout the day.

3.4.1 Optimization Parameter Validation

To determine the optimal solution for minimizing the TOC considering Case IV, a sensitivity analysis is conducted on the PSO-LP method. The analysis involved varying key PSO parameters, specifically the inertia weight (w) and cognitive and learning factors (c_1, c_2), to assess their impact on optimization performance. Specifically, an adaptive inertia weight is used while varying the cognitive and learning factors. Conversely, the cognitive and learning factors are kept at their default values while varying inertia weight. These parameters can be modeled as shown in Table 3.2.

Table 3.2 Vary the parameters w, c1, and c2 of the PSO-LP settings

Variable	Settings							
	Varies w			*Varies* c_1 *and* c_2				
w	0.1	0.6	1.1	[0.1,1.1]				
c_1	1.49			1.49	1	2	1	2
c_2	1.49			1.49	2	1	1	2
Random values ($rand_1$,$rand_2$)	[0,1]							

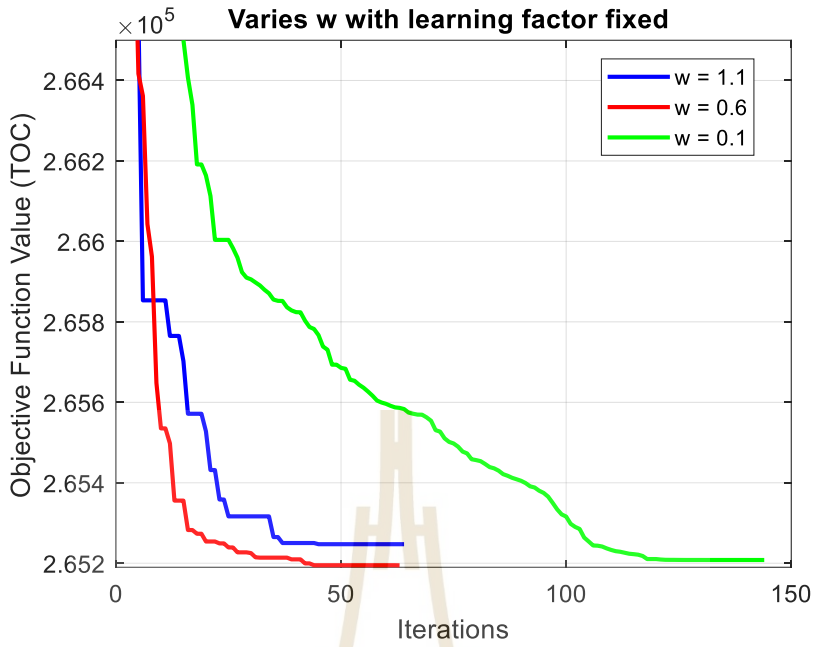

Figure 3.10 Convergence of TOC optimization with different inertia weights

The inertia weight (w) is tested at three different levels while keeping the learning factors (c_1 and c_2) constant:

- Low (w = 0.1): The best objective function value obtained is 265,208 THB.
- Medium (w = 0.6): The best objective function value obtained is 265,195 THB.
- High (w = 1.1): The best objective function value obtained is 265,247 THB.

These results suggest that an intermediate inertia weight (w = 0.6) provides better convergence performance compared to lower or higher values. The convergence plot of the variation of the inertia weight is illustrated in Fig. 3.10.

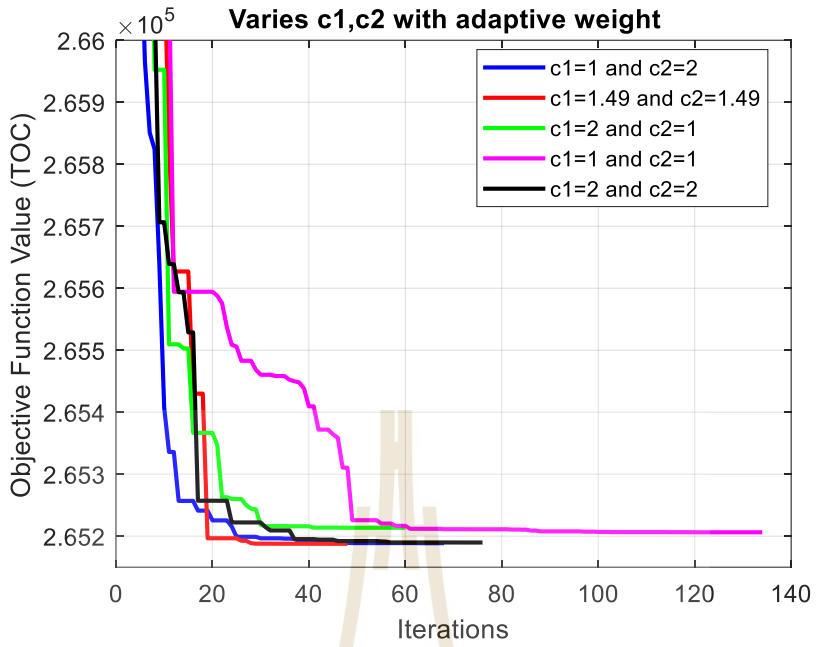

Figure 3.11 Convergence of TOC optimization with different learning factors

The cognitive and social learning factors are tested under different configurations while maintaining a fixed range of inertia weight.

- $c_1 < c_2$ ($c_1 = 1$, $c_2 = 2$):

  The best objective function value obtained is 265,189 THB.

- $c_1 = c_2$:
  - ($c_1 = 1.49$, $c_2 = 1.49$):

    The best objective function value obtained is 265,188 THB.
  - ($c_1 = 1$, $c_2 = 1$):

    The best objective function value obtained is 265,190 THB.
  - ($c_1 = 2$, $c_2 = 2$):

    The best objective function value obtained is 265,767 THB.

- $c_1 > c_2$ ($c_1 = 2$, $c_2 = 1$):

  The best objective function value obtained is 265,214 THB.

Among these settings, the combination of $c_1 = 1.49$, $c_2 = 1.49$ demonstrated the best optimization performance, yielding the lowest TOC. The

convergence plot of the variation of cognitive and social learning factors is illustrated in Fig. 3.11.

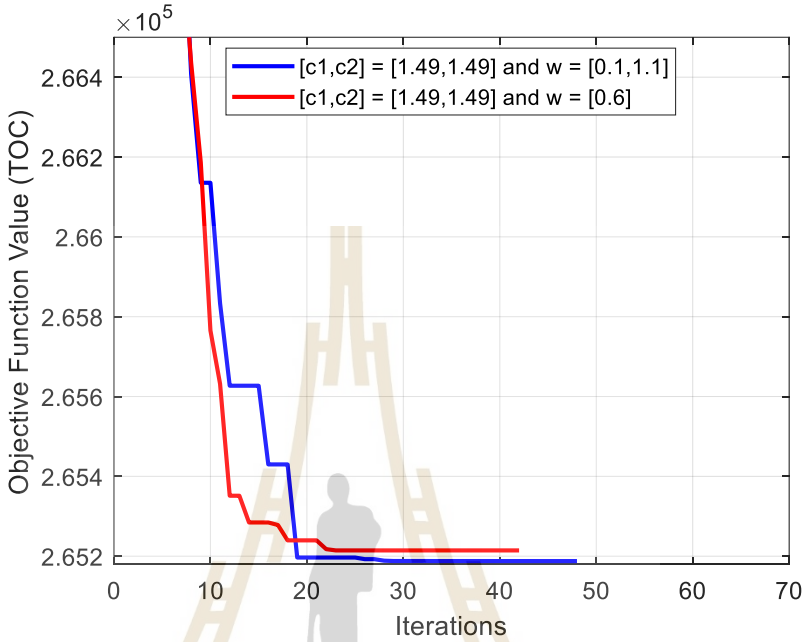

Figure 3.12 Convergence of TOC optimization with selected PSO parameters

To further refining the parameter selection, two configurations are compared from selection PSO parameters by Fig. 3.10 and Fig. 3.11 The convergence plot of the selection PSO parameters is illustrated in Fig. 3.12:

- (c_1, c_2) = (1.49, 1.49) and w = 0.6:
  The best objective function value obtained is 265,195 THB.
- (c_1, c_2) = (1.49, 1.49) and w = [0.1,1.1]:
  The best objective function value obtained is 265,188 THB.

3.4.2 TOU Tariffs Considerations

In each case, the scheduling of energy proportions varies depending on the scenario. For cases without HS, only LP is employed to find the solution since there are no variables for the FC and EL. However, in scenarios incorporating HS, a hybrid PSO-LP method is utilized. This approach first optimizes the operation of the

fuel cell and EL using PSO, and the results are subsequently processed using LP. The scheduled energy output for each component, as well as the costs associated with each energy sector, are summarized in Table 3.3. Furthermore, since HS is considered in Cases II, Case IV, and Case V, with PSO-LP employed to derive the solutions, Figs. 3.13 to 3.18 provide detailed insights into the power balance, optimization algorithm, and the impact of HS on the proposed system. The figures are organized based on case studies: (a) Case II, (b) Case IV, and (c) Case V, illustrating the effectiveness of the proposed optimization approach in achieving optimal solutions. These cases highlight the role of HS integration, both with and without the coordinated operation of NG-electricity, in balancing multiple energy types with energy demand. Notably, Case IV excludes solar power to analyze the influence of wind power injections exclusively. Furthermore, when the MT is integrated, additional power losses occur due to operational efficiency limitations. However, despite these losses, MT integration significantly contributes to reducing the TOC.

Various energy sources are utilized to meet output demands through multiple energy scheduling in the EH. In Table 3.3, Case I represents no cooperation between electricity and NG systems, where each sector operates independently, focusing solely on its efficiency. Conversely, Case III involves coordinated operation between electricity and NG, with NG being used to dispatch the electricity load via MT to reduce electricity consumption. Excess wind and solar power, as shown in Fig. 3.7, are not utilized, resulting in no additional energy savings.

Case II integrates HS without coordination with the electricity and NG systems, whereas Cases IV and Case V incorporate both HS and coordinated operation. This significantly enhances energy management strategy since HS stores only excess wind in Case IV and excess wind and solar energy in Case II and V, which is then discharged at other times. The power balance in each energy sector is depicted in Fig. 3.13(a), 3.13(b), and 3.13(c) for electricity and in Fig. 3.14(a), 3.14(b), and 3.14(c) for heat. Both Figs 3.13 and 3.14 focus exclusively on cases involving HS integration.

Table 3.3 Summary of power scheduling and energy costs for each sector

Case	Energy scheduling (kWh)										Operation costs (THB)		
	Energy through components						Demand-side				Electricity	NG	Total
	TR	MT	WTs	PVPs	FC	GB	Gen	Used	Loss	Curtailed			
I	16,956	-	20,669	7,166	-	40,130	90,382	77,530	5,818	7,034	68,887	182,410	251,297
II	15,024	-			1,933		84,996		5,779	1,687	61,711	182,410	244,121
III	15,356	3,600			-	38,130	90,679		5,913	7,236	60,538	189,319	249,857
IV	17,798	4,950		-	1,680	37,380	84,242		6,011	701	73,278	191,910	265,188
V	13,424	3,600		12,113	1,933	38,130	85,090		5,873	1,687	50,453	189,319	239,772

The energy flow through the MT, which operates in Cases III and V, produces both electricity and heat. In these cases, the MT is scheduled to run from 12 a.m. to 9 p.m., as NG costs during this period are lower than the peak electricity costs in TOU tariffs. However, when energy generation is sufficient to meet demand, the MT remains inactive, as shown in Figs. 3.13(c) and 3.14(c), where it does not operate at 2 p.m. and 3 p.m. In Case IV, where only excess wind power is utilized, the MT operates for an extended period of 11 hours from 11 a.m. to 10 p.m., resulting in the highest power loss among all cases, as indicated in Table 3.3 and shown in Figs. 3.13(b) and 3.14(b).

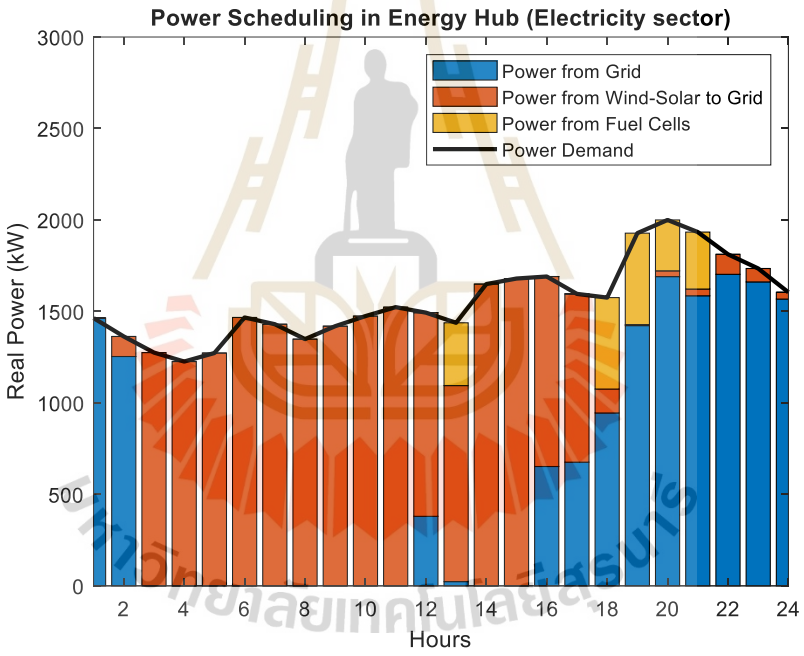

(a)

Figure 3.13 Power scheduling in EH for (a) Case II, (b) Case IV, and (c) Case V (electricity sector)

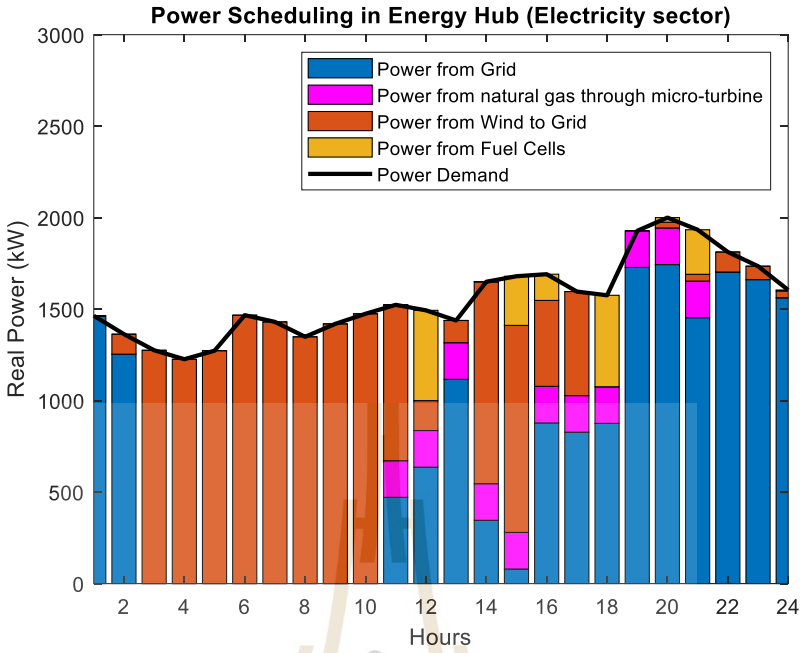

(b)

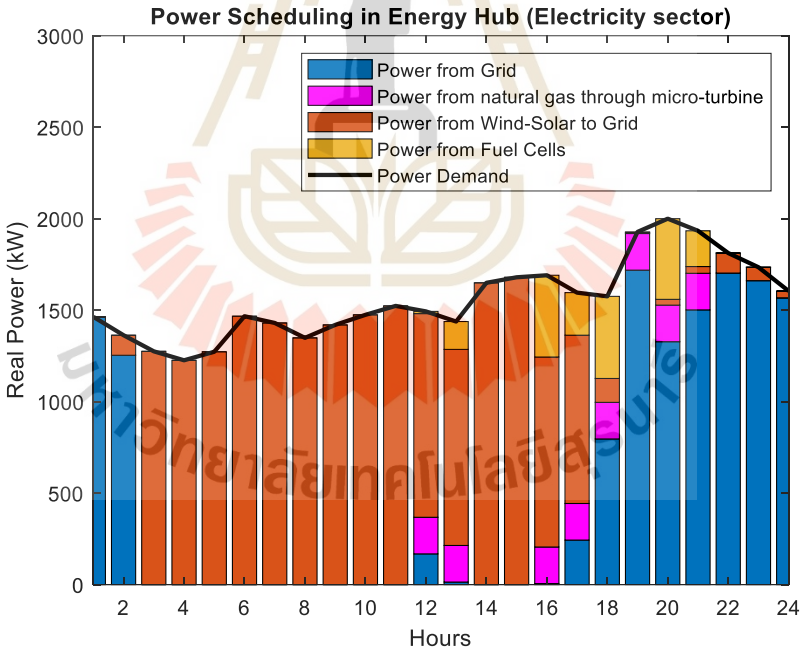

(c)

Figure 3.13 Power scheduling in EH for (a) Case II, (b) Case IV, and (c) Case V (electricity sector) (Continued)

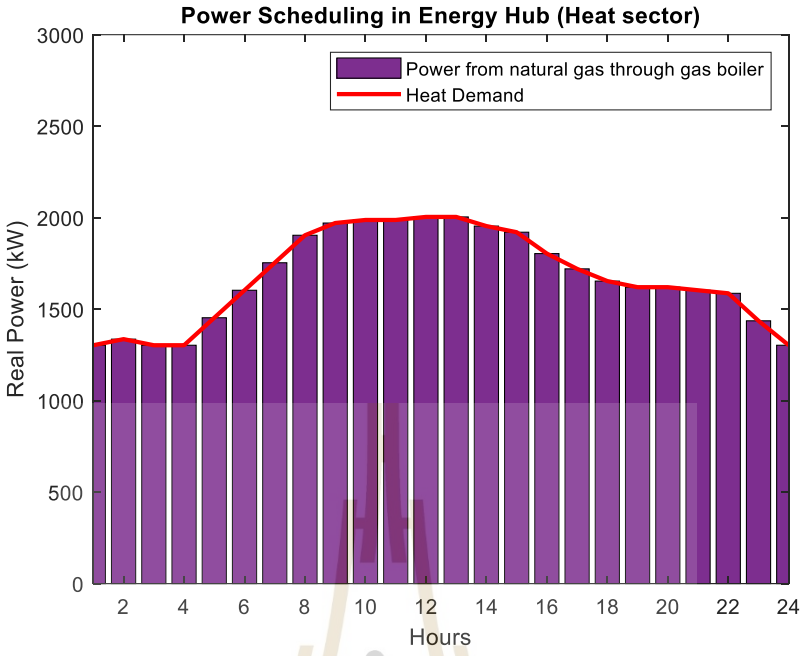

(a)

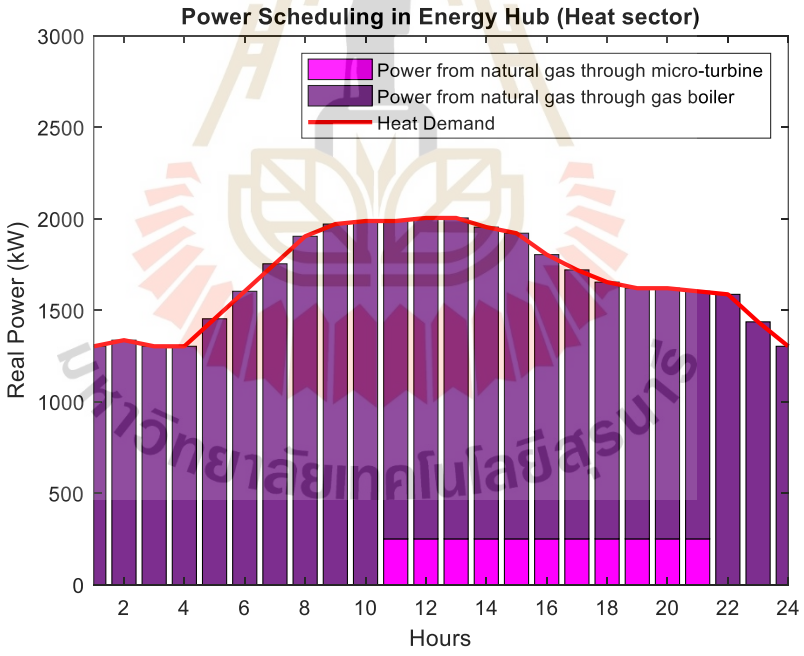

(b)

Figure 3.14 Power scheduling in EH for (a) Case II, (b) Case IV, and (c) Case V (heat sector)

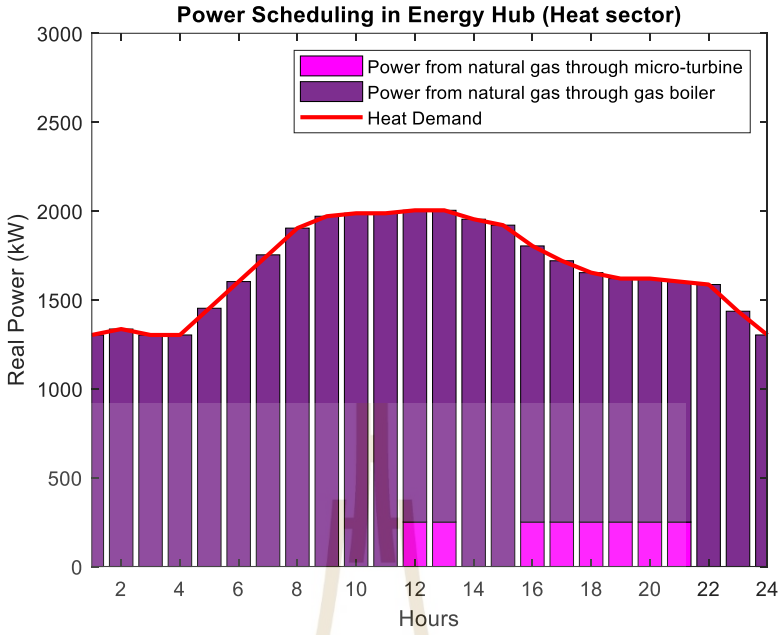

(c)

Figure 3.14 Power scheduling in EH for (a) Case II, (b) Case IV, and (c) Case V (heat sector) (Continued)

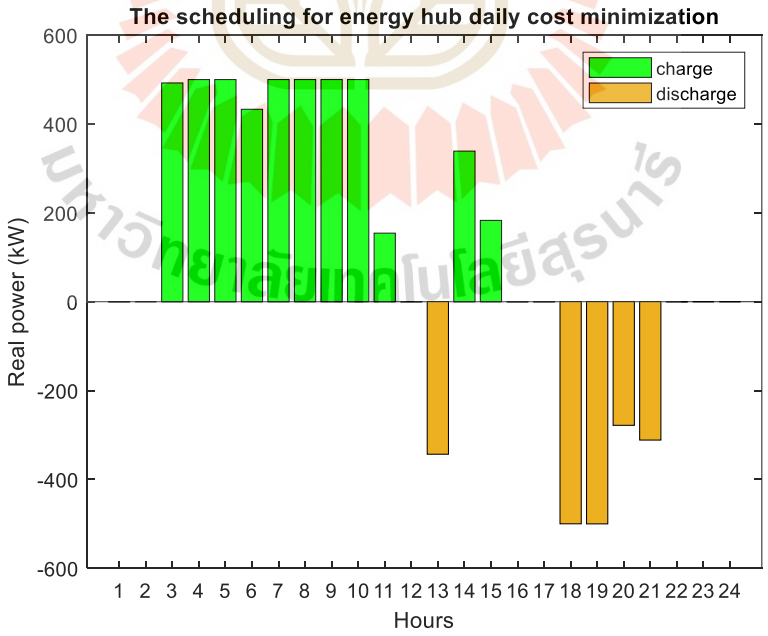

(a)

Figure 3.15 HS scheduling for 24 hours (a) Case II, (b) Case IV, and (c) Case V

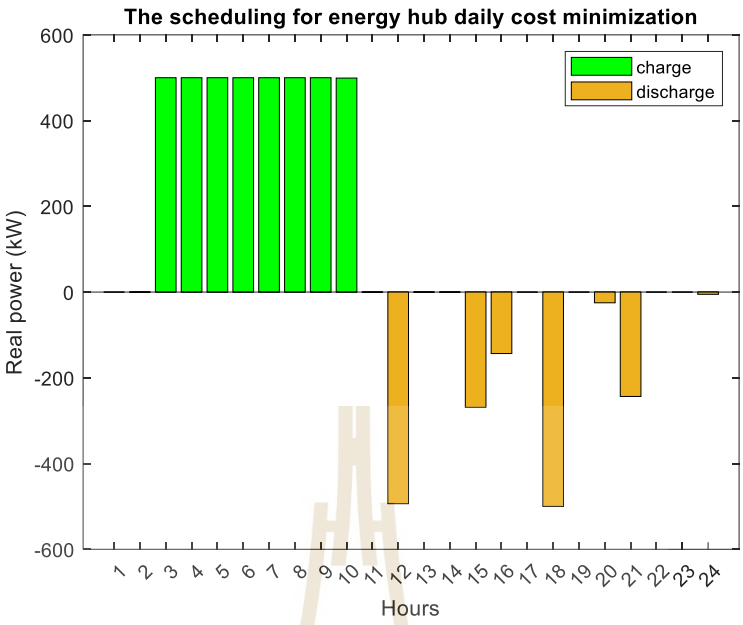

(b)

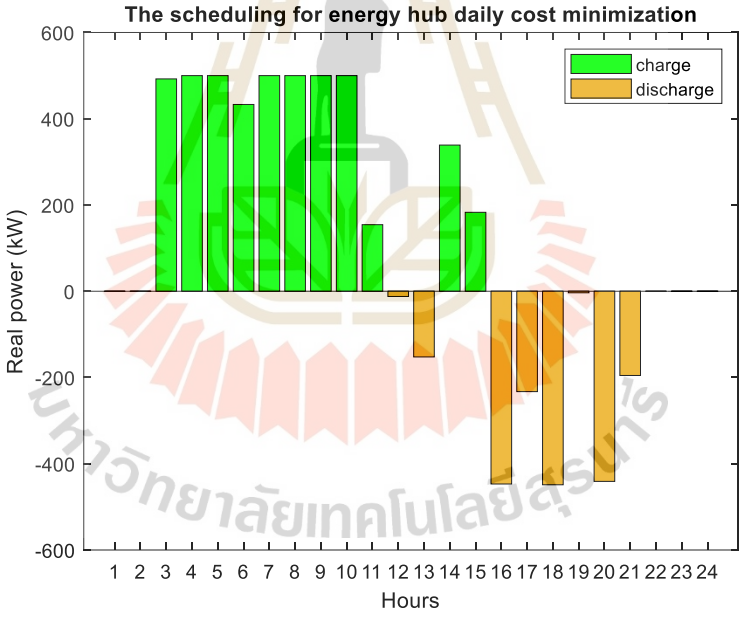

(c)

Figure 3.15 HS scheduling for 24 hours (a) Case II, (b) Case IV, and (c) Case V (Continued)

In Case II and Case V, with HS integration, EL converts excess wind and solar power into HS from 3 a.m. to 11 a.m. and 2 p.m. to 3 p.m. However, in Case IV,

due to the absence of solar energy, the EL only utilizes excess wind power for HS from 3 a.m. to 11 a.m. In all cases, FC converts stored hydrogen into electricity to reduce grid dependency, with the HS operation schedule varying across cases. Additionally, the FC scheduling patterns differ among Case II, Case IV, and Case V. However, the power from FC operated is performing in the peak electricity costs period to reduce energy from the grid, resulting in a lower TOC and energy curtailment. The TOU tariff is utilized to define the objective, resulting in the FC operating as illustrated in Fig. 3.15 (a) Case II, (b) Case IV, and (c) Case V. In the study, the initial hydrogen tank pressure is set at 20 bar. During HS scheduling, the tank pressure is maintained within a range of no more than 100 bar and no less than 10 bar, which is defined in SOT is 100% and 0%, respectively. With the pressure at the final hour of the day equal to that of the initial hour. As shown in Fig. 3.16 (a) Case II, (b) Case IV, and (c) Case V, SOT is displayed as a percentage, representing the HS model. However, further initial settings of pressure are studied in Appendix C

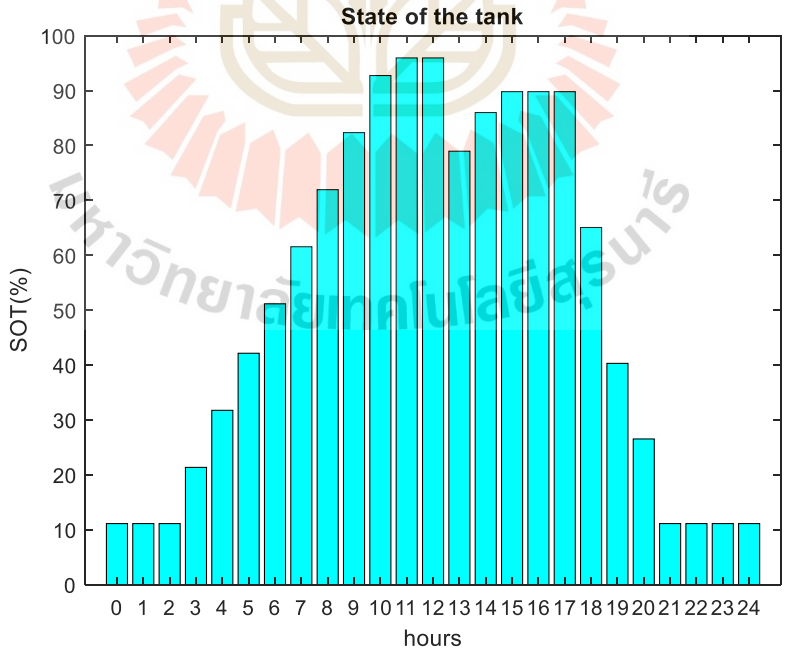

(a)

Figure 3.16 State of the tank (%SOT) in HS (a) Case II, (b) Case IV, and (c) Case V

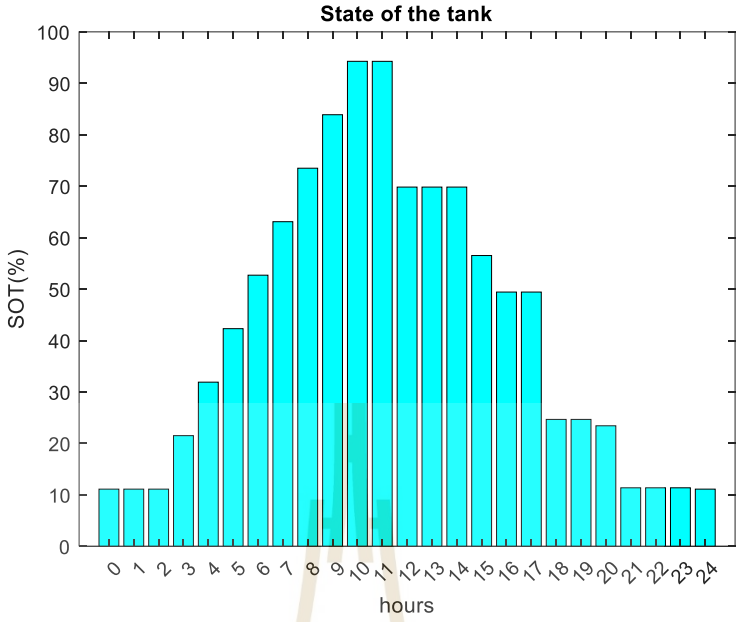

(b)

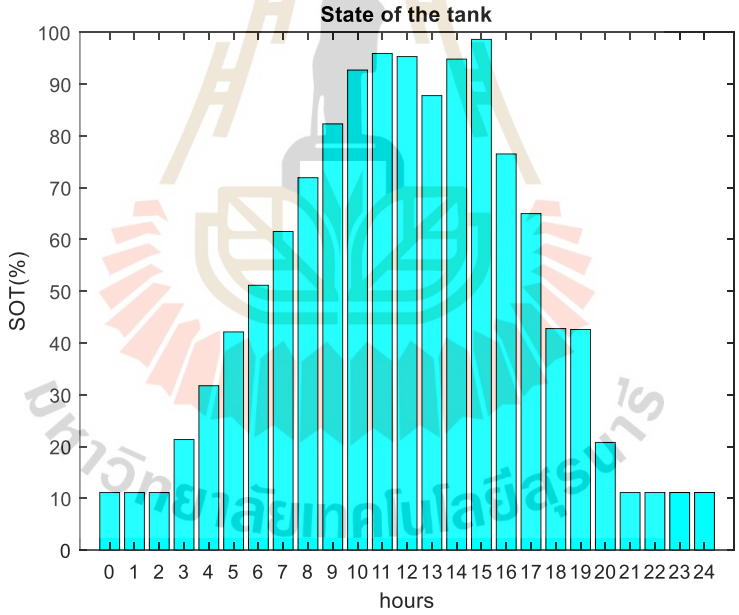

(c)

Figure 3.16 State of the tank (%SOT) in HS (a) Case II, (b) Case IV, and (c) Case V (Continued)

Figure 3.17 (a), (b) and (c) show the convergent PSO-LP solutions of Case II, Case IV, and Case V respectively. The best function value is TOC in all three cases.

Case II begins converging around 20 iterations and stops finding the optimal solution in 128 iterations. Case IV starts converging around 20 iterations and stops finding the optimal solution in 48 iterations. Case V also begins converging around 30 iterations and stops finding the optimal solution in 285 iterations. However, all cases can converge before the maximum iteration setting because the final solution is less than the function tolerance. Notably, Case IV exhibits a significant reduction in the number of iterations required to find a solution due to the stable wind speed profile during exceed hours, which operates at the rated power. As a result, Case IV is the fastest to converge.

Figure 3.18 (a) and (b) demonstrate the results from 30 trials of Case II, Case IV, and Case V which show the best, worst, and average lines of solutions, indicate that the fitness results of PSO-LP are clustered, with the standard derivations (SD) of 4.30, 3.9, and 5.11, respectively. Therefore, the proposed method is demonstrated to be reliable and has the potential to find the optimal solutions

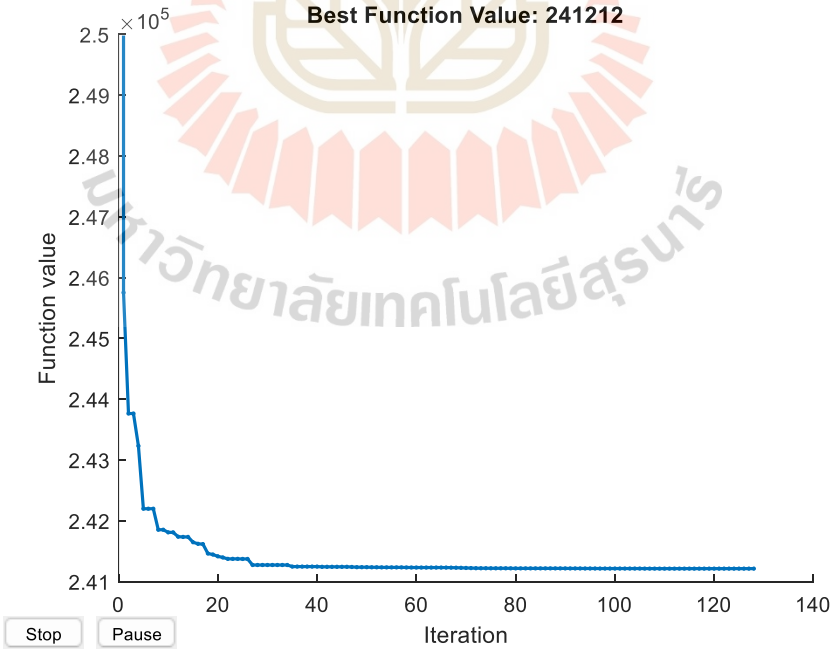

(a)

Figure 3.17 The PSO-LP convergence plot (a) Case II, (b) Case IV, and (c) Case V

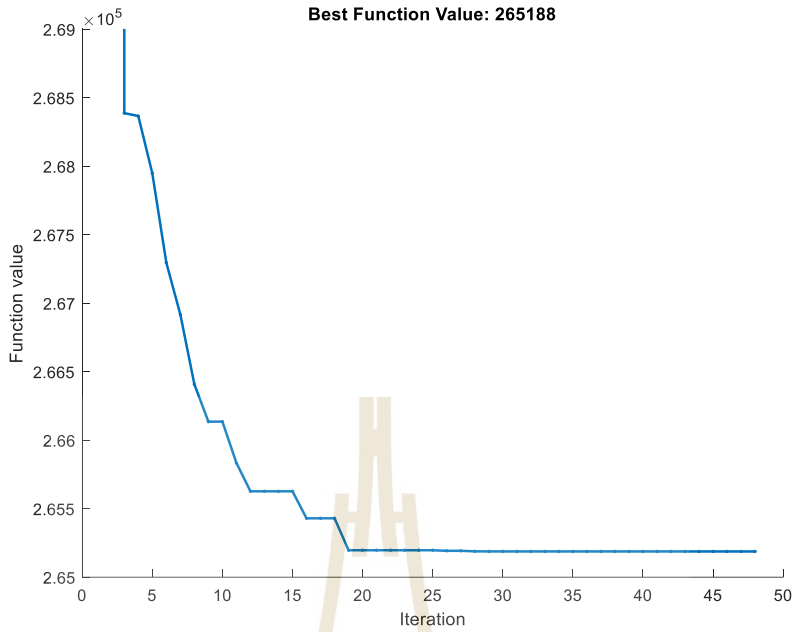

(b)

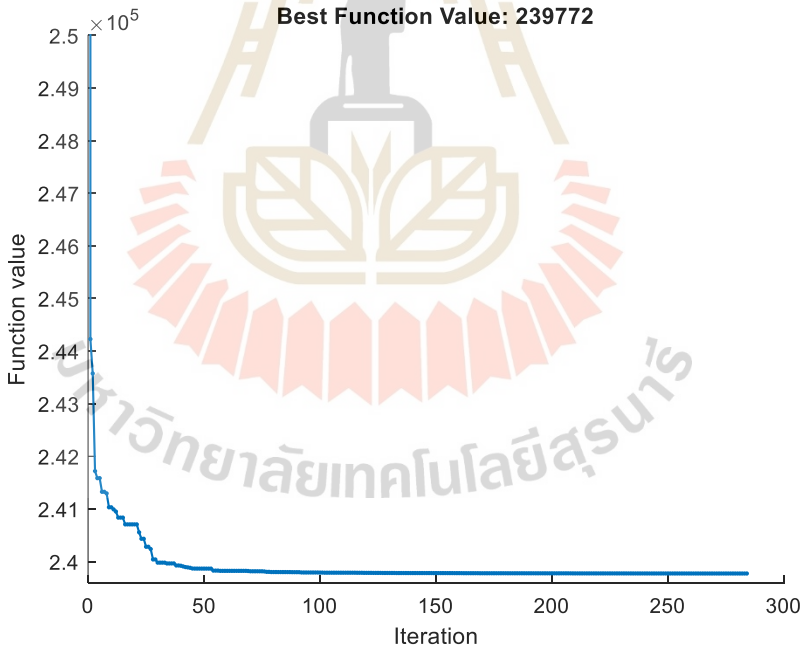

(c)

Figure 3.17 The PSO-LP convergence plot (a) Case II, (b) Case IV, and (c) Case V (Continued)

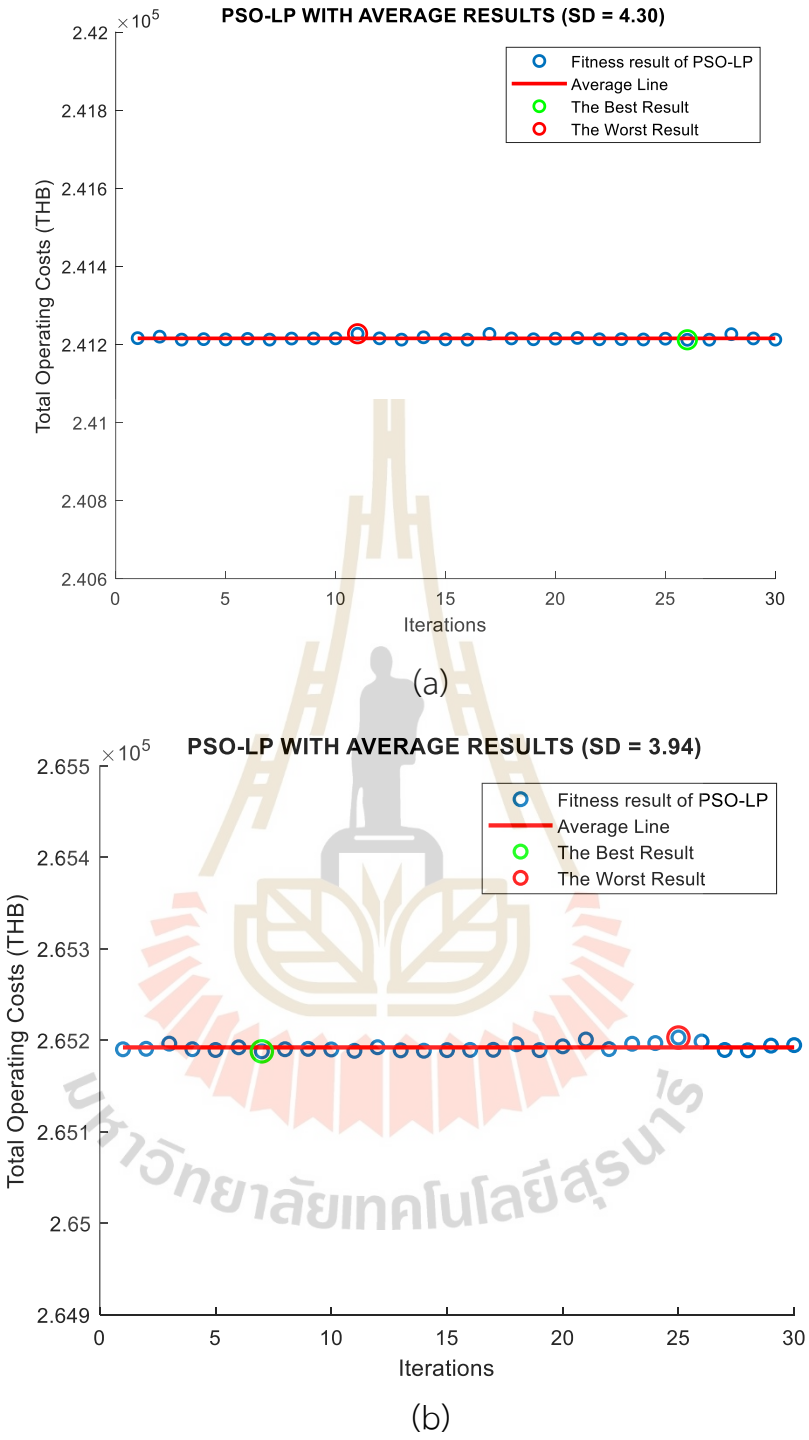

Figure 3.18 The PSO-LP fitness results with 30 iterations (a) Case II, (b) Case IV, and (c) Case V

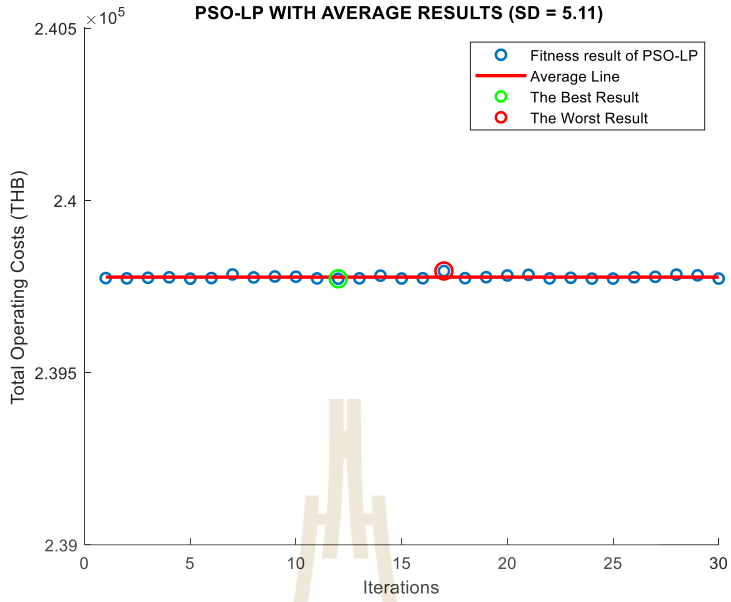

(c)

Figure 3.18 The PSO-LP fitness results with 30 iterations (a) Case II, (b) Case IV, and (c) Case V (Continued)

When comparing the results across the five case studies, TOC shows a significant reduction in all optimized scenarios compared to the base case (Case I), except for Case IV. The higher TOC in Case IV is primarily due to the limited RE profile, which excludes solar power and consequently reduces the utilization of HS. This emphasizes the effectiveness of incorporating multi-energy scheduling and single-objective optimization strategies in enhancing system cost reduction. Table 3.4 presents the TOC values for each case along with the corresponding percentage reduction relative to the base case.

Table 3.4 TOC percentage comparison across all case studies

Case study	Case I	Case II	Case III	Case IV	Case V
TOC	251,297	244,121	249,857	265,188	239,772
% Reduction from Case I	-	2.86%	0.57%	–5.53%	4.58%

3.4.3 RTP Considerations

In this section, the impact of RTP on the operation of the MES-WSPHS, which is on Case V, is analyzed. The study investigates how dynamic electricity pricing influences the scheduling of various energy resources, ensuring cost-effective and efficient energy management. Fig. 3.19 and Fig. 3.20 illustrate the power scheduling for each energy sector. In the electricity sector, MT and HS are scheduled to operate between 7 p.m. and 10 p.m., that reflects the RTP scheme indicates higher electricity prices during this period. Therefore, the power from NG through MT is occurring in both energy sectors.

The integration of HS further enhances system flexibility, as depicted in Fig. 3.21(a), which illustrates the charge and discharge patterns of the HS system. It can be observed that hydrogen is primarily stored during low electricity price periods and discharged during peak price hours, aligning with the cost-minimization strategy. SOT is displayed in Fig. 3.21(b). The quantity of hydrogen in tank shows hydrogen reserves gradually increasing during the daytime and depleting as energy is discharged in the evening.

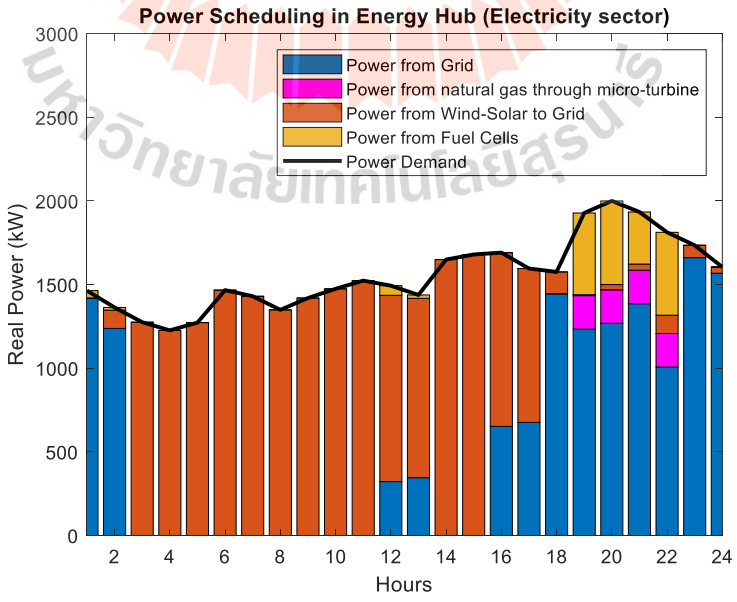

Figure 3.19 Power scheduling in EH under RTP scheme (electricity sector)

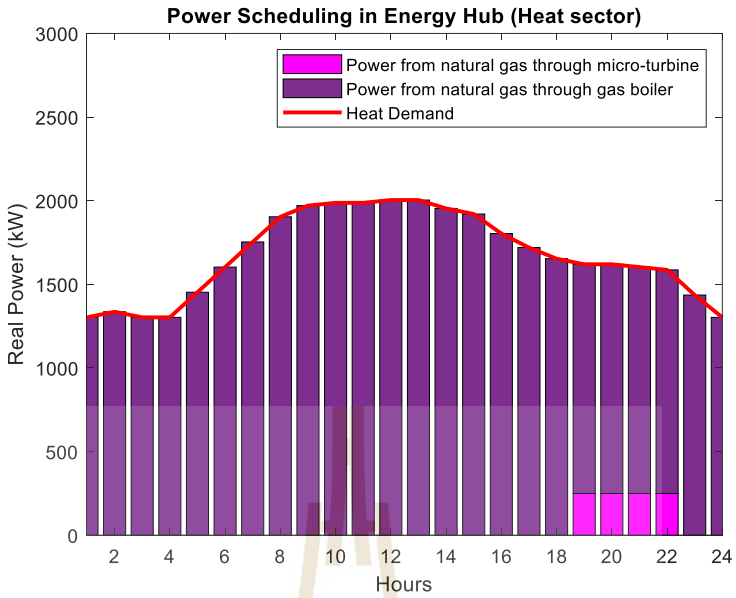

Figure 3.20 Power scheduling in EH under RTP scheme (heat sector)

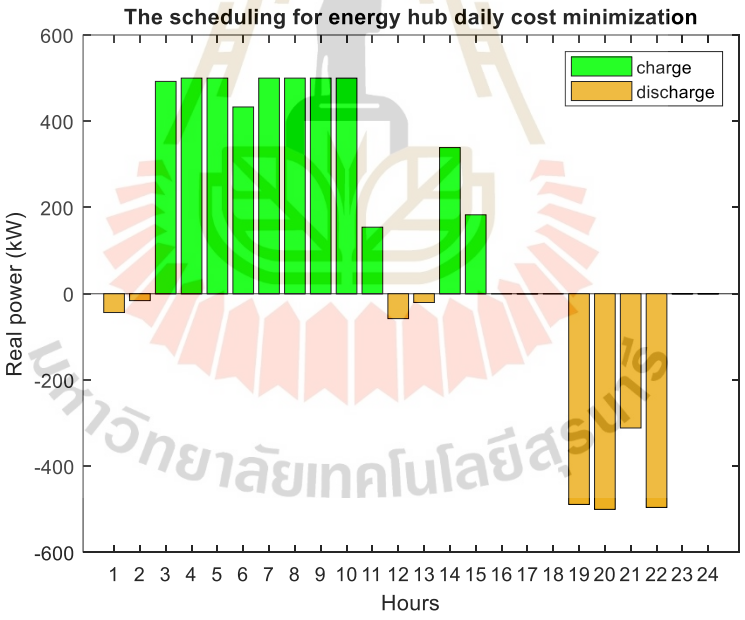

(a)

Figure 3.21 (a) HS scheduling for 24 hours and (b) State of the tank (%SOT) under RTP scheme

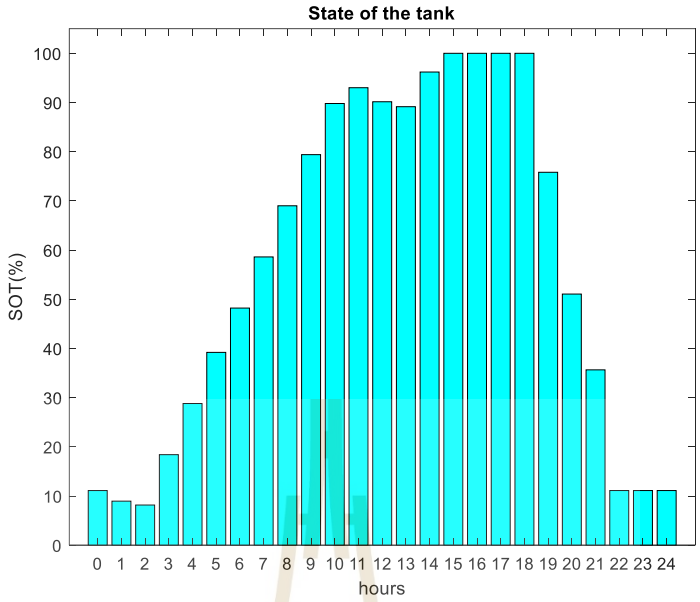

(b)

Figure 3.21 (a) HS scheduling for 24 hours and (b) State of the tank (%SOT) under RTP scheme (Continued)

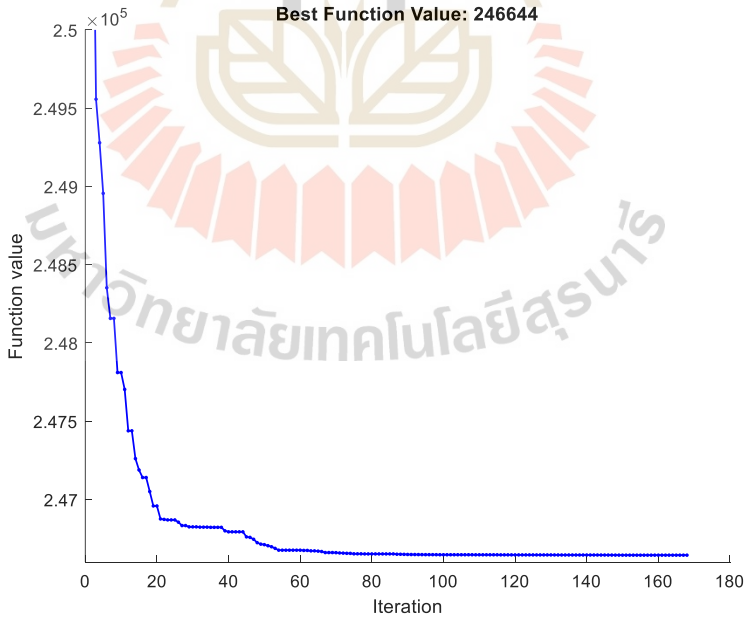

(a)

Figure 3.22 The PSO-LP (a) convergence plot and (b) fitness results with 30 iterations under RTP scheme

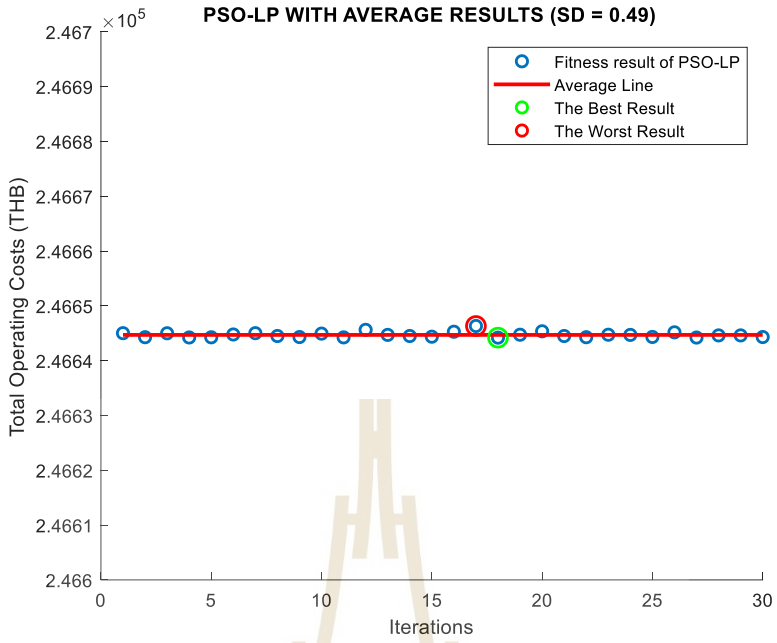

(b)

Figure 3.22 The PSO-LP (a) convergence plot and (b) fitness results with 30 iterations under RTP scheme (Continued)

Figure 3.22 (a) and (b) demonstrate the results from 30 trials of MES-WSPHS under RTP which show the best, worst, and average lines of solutions, indicate that the fitness results of PSO-LP are clustered, with the SD of 0.49. This study is reliable and has the potential to find optimal solutions more than TOU tariff.

3.4.4 The Comparison Between PSO and PSO-LP

This section illustrates a different solution between the PSO and PSO-LP technique under the TOC as an objective function and demonstrated in Case V. The aim is to highlight the performance of each approach that can minimize TOC effectively. To ensure a fair comparison between algorithms, the study established consistent parameters, as outlined in Table 3.5.

Table 3.5 The parameters of the PSO and PSO-LP settings

Variable	Settings
Swarm sizes	100
Iterations	500
Function Tolerance	$<10^{-6}$
w	[0.1,1.1]
c_1	1.49
c_2	1.49
$rand_1, rand_2$	[0,1]

Figure 3.23 presents a comparison between PSO and PSO-LP, illustrating that both algorithms demonstrate similar convergence behavior. However, the proposed PSO-LP terminates the optimization process at 285 iterations, due to the predefined convergence criteria based on the tolerance between the current particle swarm and the previous swarm, with a function tolerance of less than 10^{-6}. This enables PSO-LP to achieve a near-optimal global solution. In contrast, PSO requires 291 iterations to terminate, taking slightly longer and failing to reach a near-optimal solution. On the other hand, PSO-LP requires significant computational resources due to its two-step process: running PSO in the main loop and executing LP as a subroutine. This results in a longer runtime for PSO-LP compared to conventional PSO. Nevertheless, both algorithms are suitable for this problem, as the scheduling process must be completed within a day. The runtime details for this study are provided in Table 3.6.

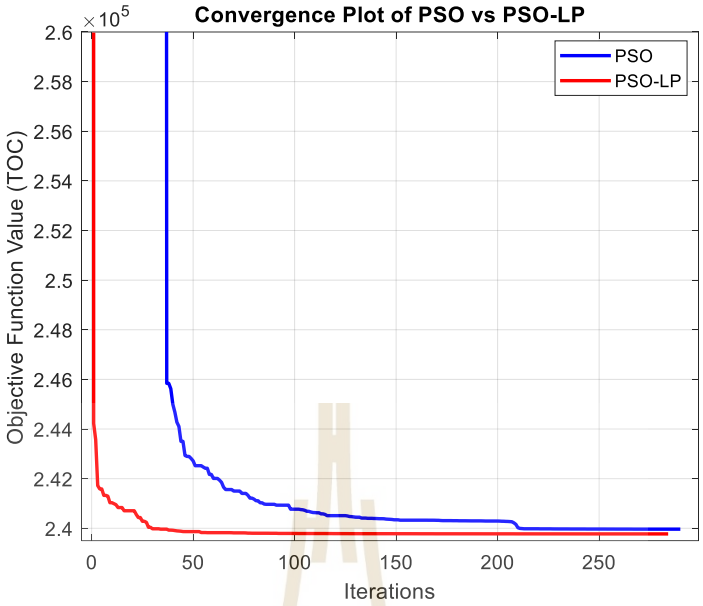

Figure 3.23 Convergence comparison between PSO and PSO-LP

Table 3.6 The runtime of the PSO and PSO-LP

Algorithm	PSO	PSO-LP
Runtime (s)	611	3,000

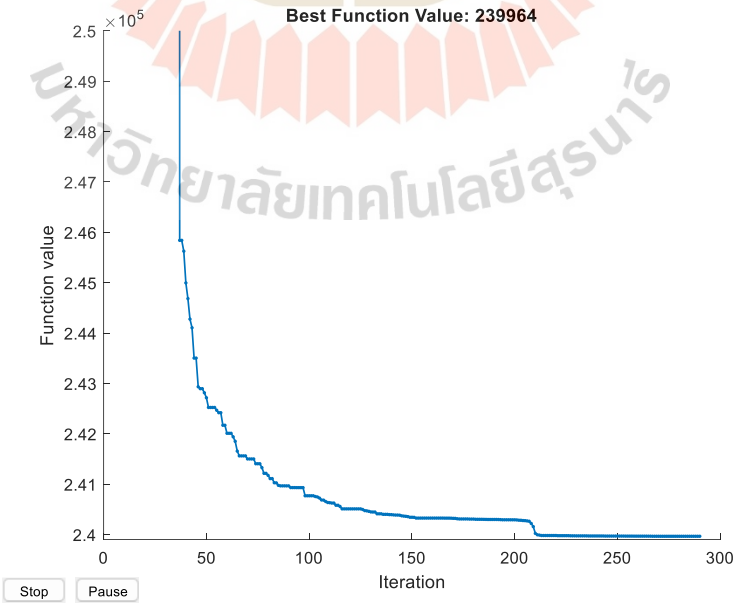

Figure 3.24 The PSO convergence plot

The PSO convergence plot in Fig. 3.24 indicates a final TOC value of 239,964 THB, whereas the PSO-LP convergence plot in Fig. 3.17 (c) shows a final TOC value of 239,772 THB. This comparison highlights that PSO-LP achieves a more optimal solution than the conventional PSO algorithm.

3.4.5 The Percentage of Multi-Energy Usage

This section presents the proportion of energy consumption from various sources within MES, which typically includes electricity from the grid, RE (wind and solar energy), and NG. Understanding the percentage contribution of each energy source offers valuable insights into the system's operational efficiency, sustainability, and its reliance on non-renewable energy sources. The results reflect that energy usage aligns with PDP2018, which emphasizes electricity and NG as the primary energy sources, while RE serves as an alternative to reduce carbon emissions. To further enhance the clarity of energy distribution, a pie chart is presented to visually illustrate the total energy consumption by source during the simulation, providing an intuitive understanding of each source's role within the system as shown in Fig. 3.25.

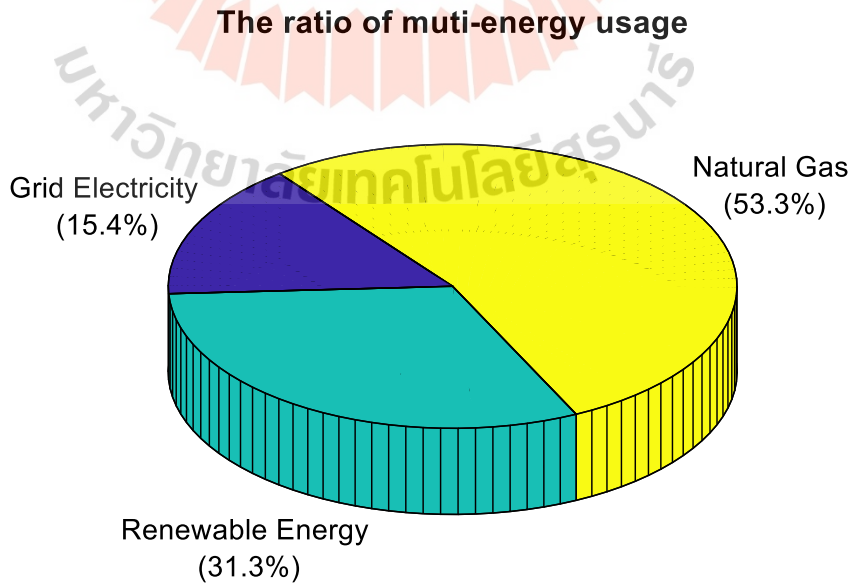

Figure 3.25 The energy consumption distribution among different sources for Case V

Based on the results, Case V is selected for this analysis as it demonstrates the most integrated operation among all the tested scenarios, showcasing the synergistic contribution of all available energy sources grid electricity, RE, NG, and hydrogen. The energy consumption ratio illustrates a diverse mix of sources, with a relatively modest contribution from RE. While fossil-based sources such as grid electricity and NG remain dominant, increasing the share of renewable energy is strongly recommended. A higher penetration of renewables can lead to significant long-term cost savings by reducing dependency on fuel-based sources, while simultaneously decreasing carbon dioxide emissions. Moreover, with effective energy scheduling and integration of storage systems like hydrogen, the variability of renewables can be managed efficiently. Therefore, future energy planning should prioritize renewable expansion to enhance sustainability, economic performance, and environmental benefits.

3.5 Chapter Summary

This chapter presented an optimized scheduling approach for OMES-WSPHS under a pricing mechanism aimed at minimizing the TOC. The study introduced a hybrid PSO-LP optimization method to enhance system efficiency by optimizing energy dispatch while considering TOU tariffs and RTP schemes. The simulation results demonstrated that integrating HS significantly enhances energy flexibility, particularly in balancing excess renewable including solar and wind power generation and peak demand periods. Comparing different operational scenarios, it is revealed that coordinated electricity and NG operations, along with HS, provide the lowest operating costs. Among the tested cases, Case V, which included both HS and coordinated energy dispatch, achieved the best determination of the objective function as TOC under the TOU scheme. When comparison between every case study, TOC decreased to a maximum of 4.58% compared to Case I (base case). Additionally, Under the RTP scheme, the coordination between energies is rescheduled to respond to dynamic

pricing scheme, leading to flexible operation with economic consideration. Moreover, the comparison between conventional PSO and the proposed PSO-LP method highlighted the advantages of incorporating linear programming in refining the optimization process. Although PSO-LP required higher computational resources, it converged to a more optimal solution with lower TOC compared to conventional PSO. Overall, the findings confirm that the proposed optimization framework effectively reduces operational costs while improving energy utilization and system flexibility.

CHAPTER IV

MULTI-OBJECTIVE OPTIMIZATION USING FMOO FOR OMES-WSPHS INTEGRATION

4.1 General Introduction

This chapter presents a comprehensive multi-objective optimization framework for OMES-WSPHS integration. The proposed optimization methodology employs fuzzy techniques to address multiple objectives, including the minimization of TOC, TCE, and EP. The optimization approach utilizes PSO-LP to achieve an optimal single objective, followed by the construction of a fuzzy-satisfaction membership function (FSMF). PSO is then used to maximize FSMF, ensuring a balanced trade-off among these conflicting objectives. By integrating fuzzy decision-making techniques into the optimization framework, the proposed method ensures a balanced and efficient operation of the MES-WSPHS system, considering cost-effectiveness, environmental sustainability, and energy demand management. Furthermore, the performance of the proposed FMOO technique is benchmarked against WSMO.

4.2 Problem Formulation

4.2.1 TOC Minimization

The proposed method uses the PSO-LP technique to find the optimal scheduling of MES-WSPHS. The multiple energy deliveries are formed as variables on an hourly basis, to find the optimal solution for the system that makes it the minimum operating cost. The analysis considers the TOU tariff throughout the day. Therefore, the objective function is to minimize TOC while accounting for the TOU tariff, with a

penalty function incorporated to address any constraints violations, as shown in Eq. (4.1).

$$Minimize\ TOC = \sum_{h=1}^{24}(C_E(h)P_E(h) + C_{NG}(h)P_{NG}(h)) + PNF. \tag{4.1}$$

Subjected to the power balance constraints in (4.2) - (4.3),

$$L_E(h) - P_{FC}(h) - P_{WSP}^{i}(h) = P_{TR}(h) + P_{MT}^{E}(h), \tag{4.2}$$

$$L_H(h) = P_{GB}(h) + P_{MT}^{H}(h), \tag{4.3}$$

and the limit constraints of each conversion device as demonstrated by Eq. (4.4) - (4.9). The initial pressure which is indicated in the content of the HS tank is set to the final pressure when the day is over, as shown in Eq. (4.10). Additionally, penalty function terms can handle some constraints, which can't define a lower and upper boundary such as Eq. (4.9) and (4.10). The penalty function can be defined in Eq. (4.11)

$$0 \le P_{TR}(h) \le P_{TR,rated}, \tag{4.4}$$

$$0 \le P_{MT}^{E,H}(h) \le P_{MT,rated}^{E,H}, \tag{4.5}$$

$$0 \le P_{GB}(h) \le P_{GB,rated}, \tag{4.6}$$

$$0 \le Y_{EL}P_{EL}(h) \le P_{EL,rated}, \tag{4.7}$$

$$0 \le Y_{FC}P_{FC}(h) \le P_{FC,rated}, \text{ and} \tag{4.8}$$

$$p_{\text{tank,min}} \le p_{\text{tank}}(h) \le p_{\text{tank,rated}}. \tag{4.9}$$

$$p_{\text{tank}}(h = initial) = p_{\text{tank}}(h = 24). \tag{4.10}$$

$$PNF = \rho[(p_{\text{tank}}(t) - p_{\text{tank,min}})^2 + (p_{\text{tank}}(t) - p_{\text{tank,max}})^2 + (p_{\text{tank}}(24) - p_{\text{tank}}(\text{initial}))^2] \tag{4.11}$$

The operation of this work procedure, which involves calculating the objective function while handling constraints. This process follows a structured workflow, as depicted in Chapter 3, specifically in Fig. 3.2.

4.2.2 TCE Minimization

The proposed method uses the PSO-LP technique to find the optimal scheduling of MES-WSPHS. The multiple energy deliveries are formed as variables on

an hourly basis, to find the optimal solution of the system that makes it the minimum carbon emissions, under the emission factor depending on the generation source. The operation of this work procedure, which involves calculating the objective function while handling constraints, follows the workflow depicted in Fig. 4.1.

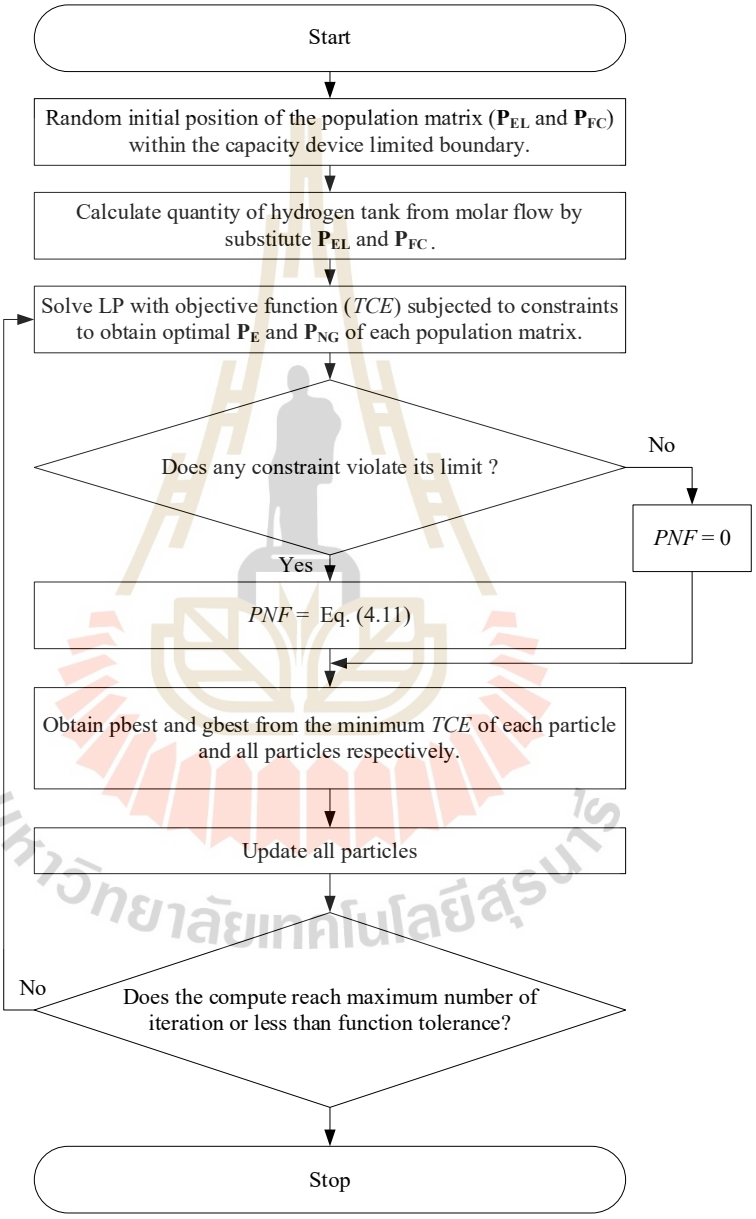

Figure 4.1 The workflow of the PSO-LP technique under TCE

In this model, carbon emissions do not appear in WSP and green HS operations. Therefore, the objective function is to minimize total carbon emissions considering the energy mix from the grid and NG, obtained by Thailand greenhouse gas management organization (TGO), and handle a penalty function for a constraints violation as shown in Eq. (4.12).

$$\text{Minimize } TCE = \sum_{h=1}^{24} [k_{TR}P_{TR}(h) + k_{GB}P_{GB}(h) + k_{MT}^{H}P_{MT}^{H}(h) + k_{MT}^{E}P_{MT}^{E}(h)] + PNF. \quad (4.12)$$

Subjected to the power balance, the limit constraints of each conversion device, and the pressure of the HS tank constraints in Eq. (4.4) – (4.11).

The carbon emissions factor is reported by Thailand Greenhouse Gas Management Organization (Public Organization) (2022). TGO is a public organization under the Ministry of Natural Resources and Environment of Thailand. Its main role is to promote and coordinate efforts to reduce greenhouse gas emissions in Thailand. Therefore, Table 4.1 represents the value of carbon emissions in each energy generation. This work considers two main sources of emission factors including electricity from the grid which is an energy mix and NG which is fueling power to electricity and heat.

Table 4.1 A value of carbon emissions in each energy generation (Thailand Greenhouse Gas Management Organization (Public Organization), 2022)

Source	Variable	Value
Electricity grid to TR	k_{TR}	0.6116
NG to MT produces heat	k_{MT}^{H}	0.3910
NG to MT produces electricity	k_{MT}^{E}	0.4888
NG to GB produces heat	k_{GB}	0.2222

4.2.3 EP Minimization

The proposed method uses the PSO-LP technique to find the optimal scheduling of MES-WSPHS. To find the optimal solution of the system that makes it the minimum EP, under the cooperation multiple energy. The operation of this work procedure, which involves calculating the objective function while handling constraints, follows the workflow depicted in Fig. 4.2.

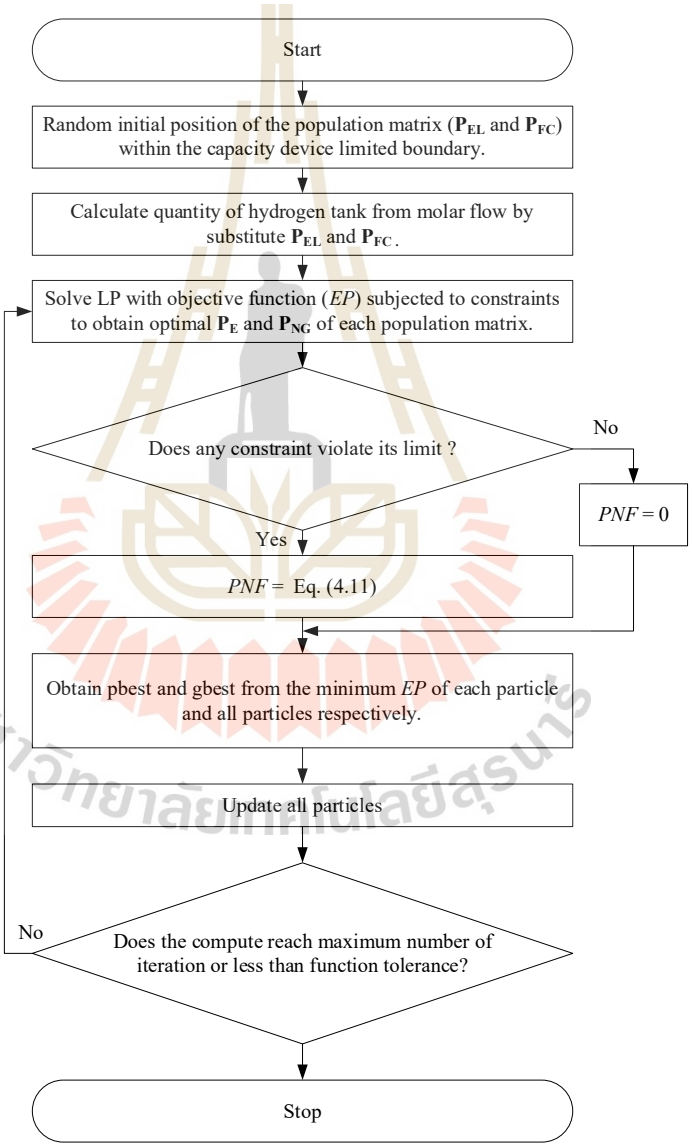

Figure 4.2 The workflow of the PSO-LP technique under EP

Therefore, the objective function is to minimize EP from the grid considering electricity dispatch all day and handle a penalty function for a constraints violation as shown in Eq. (4.13).

$$\text{Minimize } EP = \max([P_E(1), P_E(2), ...P_E(h), ..., P_E(24)]) + PNF. \quad (4.13)$$

Subjected to the power balance, the limit constraints of each conversion device, and the pressure of the HS tank constraints in Eq. (4.4) – (4.11).

4.3 FMOO-based OMES-WSPHS

The optimization of multi-objective functions is carried out to achieve a balanced compromise solution. FMOO-based OMES-WSPHS is employed to solve the optimal scheduling problem. The proposed OMES-WSPHS addresses the following objectives, which can be modeled as a FSMF as displayed in shown in Figs. 4.3, 4.4 and 4.5.

1. Total operating costs (TOC) minimization in Eq. (4.14)

$$\mu_{TOC} = \frac{-1}{TOC_{\max} - TOC_{\min}} TOC + \frac{TOC_{\max}}{TOC_{\max} - TOC_{\min}}. \quad (4.14)$$

2. Total carbon emissions (TCE) minimization in Eq. (4.15)

$$\mu_{TCE} = \frac{-1}{TCE_{\max} - TCE_{\min}} TCE + \frac{TCE_{\max}}{TCE_{\max} - TCE_{\min}}. \quad (4.15)$$

3. Electricity peak from the grid (EP) minimization in Eq. (4.16)

$$\mu_{EP} = \frac{-1}{EP_{\max} - EP_{\min}} EP + \frac{EP_{\max}}{EP_{\max} - EP_{\min}}. \quad (4.16)$$

For decision-making, the multi-objective problem in Eq. (4.14) – (4.16) aim to maximize the total membership function value, which encompasses the membership functions for objectives 1, 2, and 3 respectively. The fuzzy maximization can be represented as Eq. (4.17). The computation concept of the fuzzy decision procedure overview can be illustrated in Fig. 4.3.

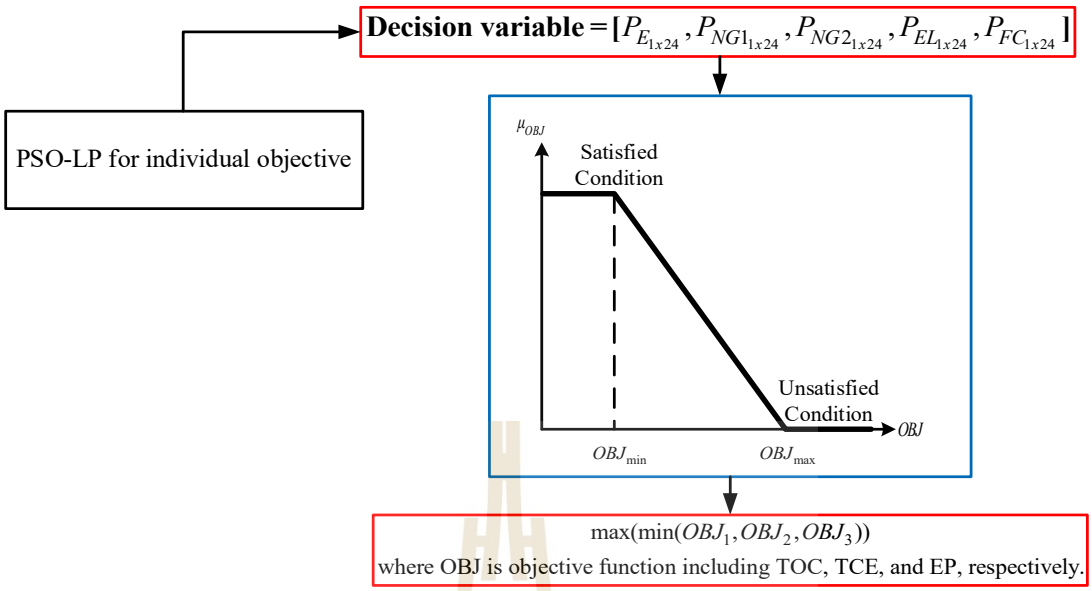

Figure 4.3 The computation concept of the fuzzy decision procedure overview

$$\text{Maximize } \mu_T = \min\{\mu_{TOC}, \mu_{TCE}, \mu_{EP}\} + PNF. \tag{4.17}$$

Subjected to the power balance, the limit constraints of each conversion device, and the pressure of the HS tank constraints in Eq. (4.4) – (4.11).

Where,

$$\mu_{TOC} = \begin{cases} 1 & , \text{for } TOC \le TOC_{\min} \\ \text{Eq. (4.14)} & , \text{for } TOC_{\min} \le TOC \le TOC_{\max} \\ 0 & , \text{for } TOC \ge TOC_{\max} \end{cases} \tag{4.18}$$

$$\mu_{TCE} = \begin{cases} 1 & , \text{for } TCE \le TCE_{\min} \\ \text{Eq. (4.15)} & , \text{for } TCE_{\min} \le TCE \le TCE_{\max} \\ 0 & , \text{for } TCE \ge TCE_{\max} \end{cases} \tag{4.19}$$

$$\mu_{EP} = \begin{cases} 1 & , \text{for } EP \le EP_{\min} \\ \text{Eq. (4.16)} & , \text{for } EP_{\min} \le EP \le EP_{\max} \\ 0 & , \text{for } EP \ge EP_{\max} \end{cases} \tag{4.20}$$

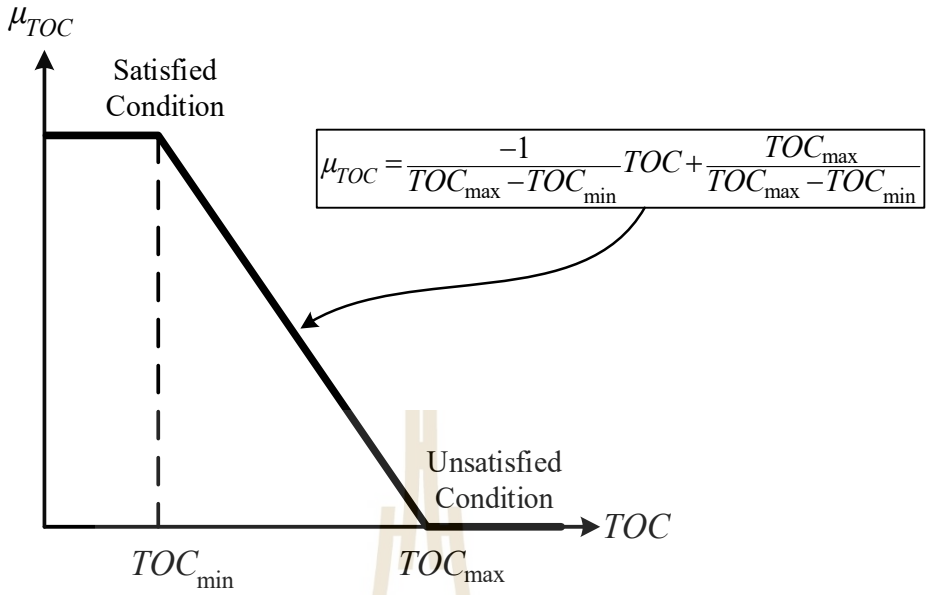

Figure 4.4 FSMF of total operating costs

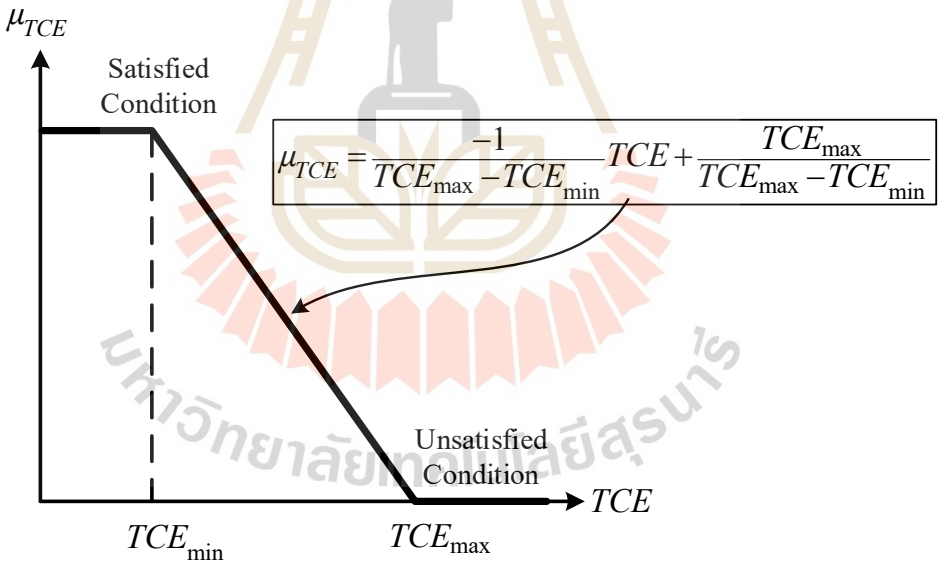

Figure 4.5 FSMF of total carbon emissions

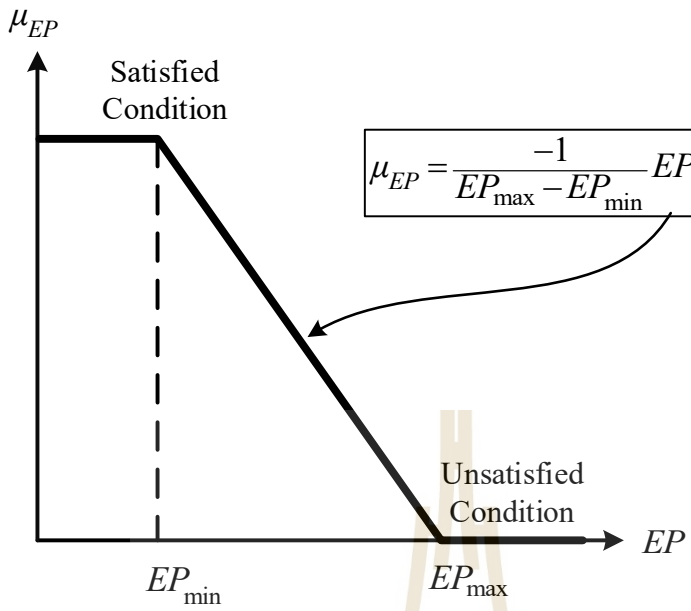

Figure 4.6 FSMF of electricity peak from the grid

4.4 WSMO-based OMES-WSPHS

In this study, WSMO method is applied to solve OMES-WSPHS. The WSMO approach transforms the original multi-objective problem comprising TOC, TCE, and EP into a single-objective function by assigning appropriate weights to each objective based on their relative importance. To enable comparison with the proposed FMOO approach, all three objectives are transformed into equivalent monetary costs. This conversion, as defined in Eq. (4.21), allows the integration of both economic and environmental factors into a unified cost-based objective function, thereby supporting more effective and interpretable decision-making.

$$\text{Minimize Cost}_{normalized} = TOC + (C_{TCE} TCE) + (C_{EP} EP) + PNF. \tag{4.21}$$

Subjected to the power balance, the limit constraints of each conversion device, and the pressure of the HS tank constraints in Eq. (4.4) – (4.11). The cost parameters presented in Table 4.2 have been standardized for consistency across objectives. The carbon cost rate was converted from THB per ton to THB per kilogram, while the peak demand charge was adjusted from a monthly rate to a daily rate by dividing by 30 days/month. These cost coefficients serve as weighting factors in the

multi-objective optimization, representing the relative priority assigned to each objective function.

Table 4.2 The cost parameters each objective into monetary units (Provincial Electricity Authority, 2023; Reuters, 2025).

Objective	*Unit*	*Cost parameter*	*Value*	*Description*
TOC	THB	-	-	Already expressed in monetary units
TCE	$kgCO_2$	Carbon cost rate (C_{TCE})	0.2 THB/ $kgCO_2$	Cost of carbon emissions per $kgCO_2$
EP	kW	Peak demand charge (C_{EP})	7 THB/ kW/day	Cost associated with peak electricity demand

4.5 Simulation Results

4.5.1 FMOO-Based OMES-WSPHS Optimization for Each Objectives

To construct the FSMF, the optimal scheduling pattern of HS is determined using PSO, while the scheduling of electricity and NG is optimized using LP. For multi-objective considerations, a satisfaction function must be developed to facilitate the fuzzy decision-making process, ultimately leading to a balanced or compromise solution.

The first objective focuses on minimizing the TOC, as evaluated in Chapter 3, Section 3.4.2. Therefore, Case V, as part of the case study, examines OMES-WSPHS solution for TOC minimization. The decision variables, including the scheduled HS operation and electricity-NG operation, are defined as a pattern for TOC minimization as illustrated in Fig. 4.7.

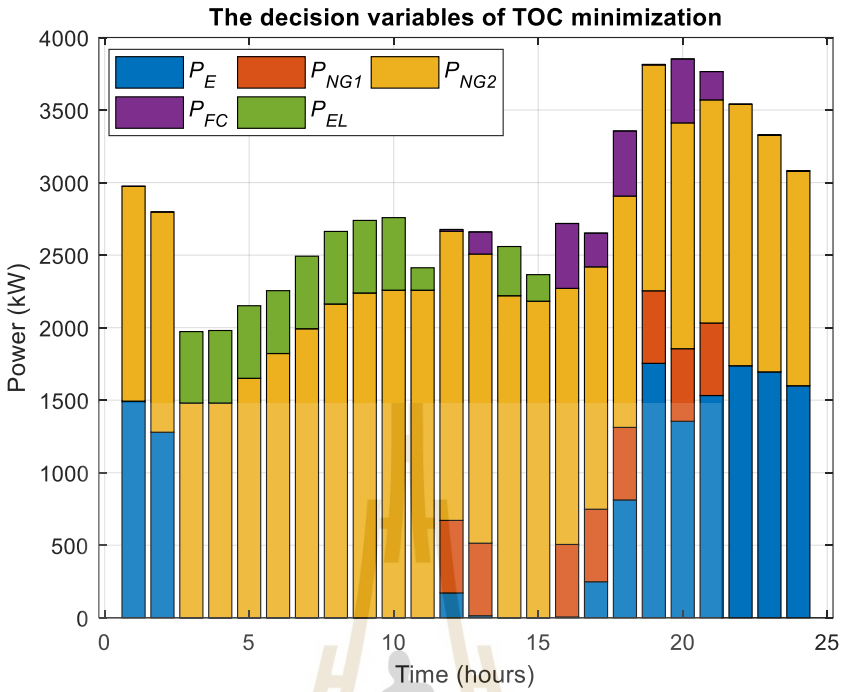

Figure 4.7 The decision variables of TOC minimization

The second objective focuses on minimizing TCE, as calculated in Eq. (4.12). The optimal solution of OMES-WSPHS for TCE minimization is illustrated in Fig. 4.8, where Fig. 4.8(a) presents the power scheduling obtained when considering TCE as the objective, and Fig. 4.8(b) shows the convergence of the solution under TCE minimization. To ensure the best and most reliable result, the optimization process for the second objective function is executed 30 trials, with the results shown in Fig. 4.8(c). Since the optimal solution for the second objective function has been determined, the decision variables scheduling pattern for TCE minimization can be illustrated in Fig. 4.9.

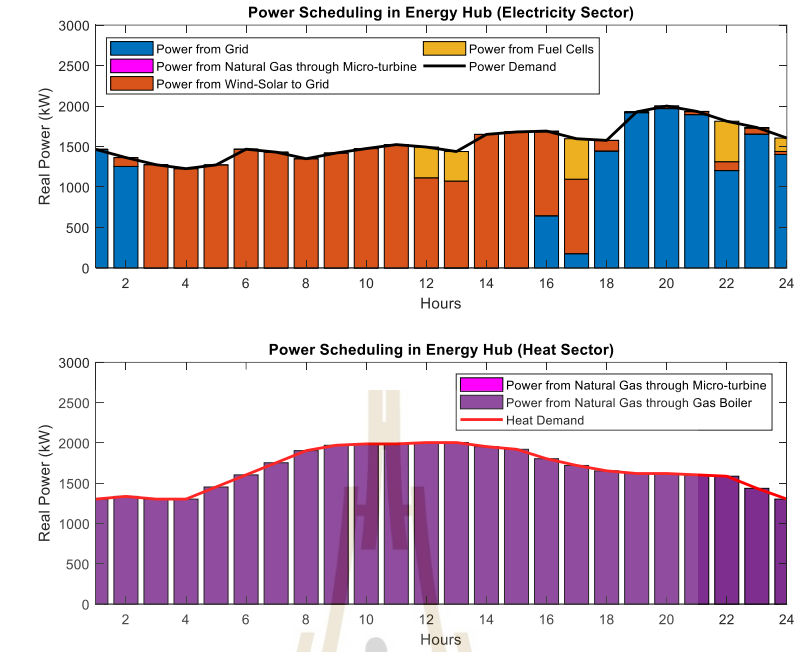

(a)

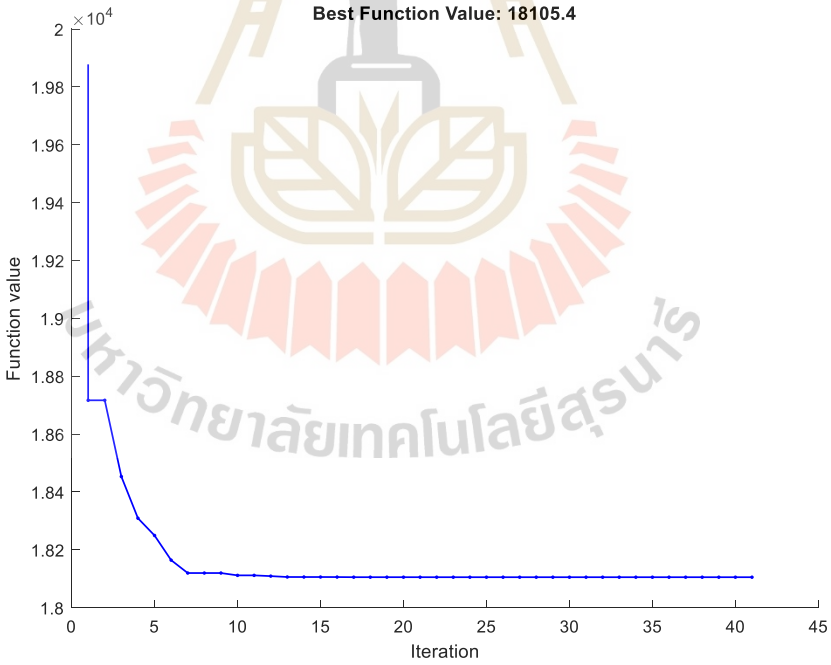

(b)

Figure 4.8 The optimal solution of OMES-WSPHS for TCE minimization (a) the power scheduling, (b) the convergence of the solution, and (c) The fitness results with 30 trials

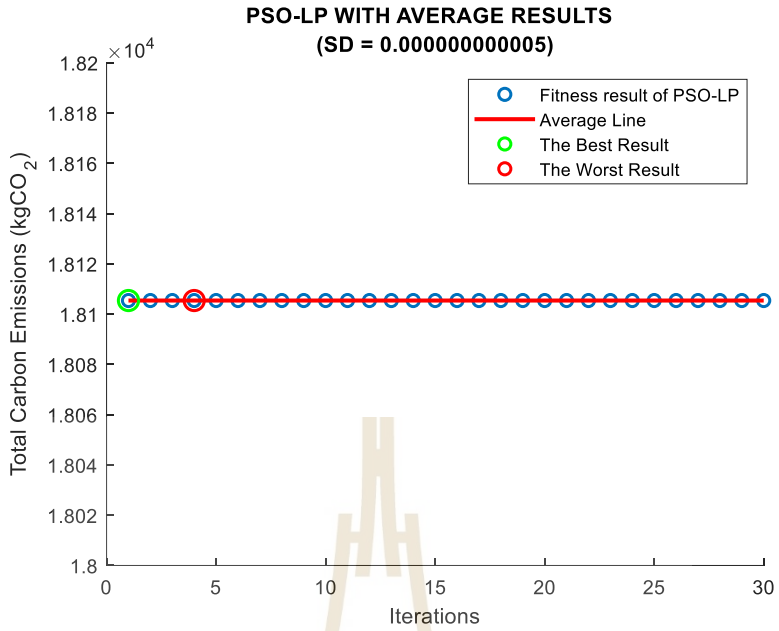

(c)

Figure 4.8 The optimal solution of OMES-WSPHS for TCE minimization (a) the power scheduling, (b) the convergence of the solution, and (c) The fitness results with 30 trials (Continued)

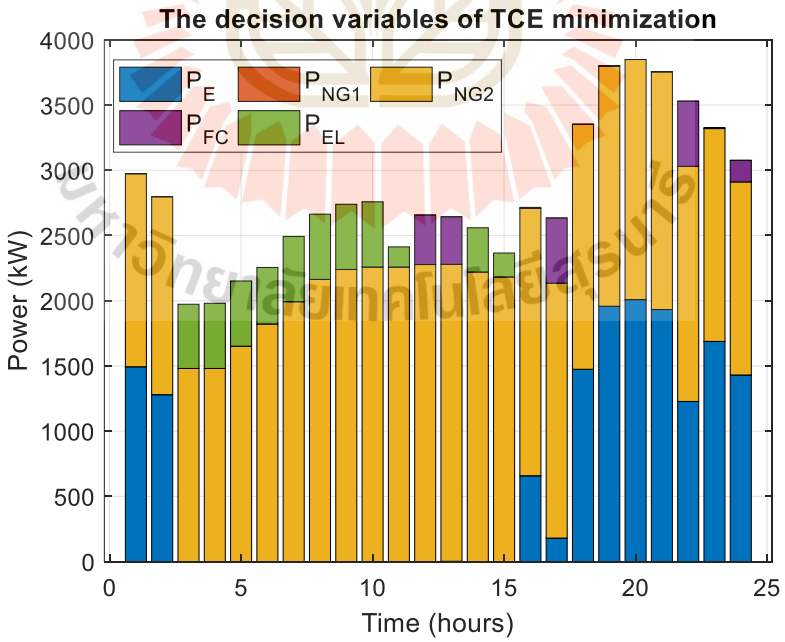

Figure 4.9 The decision variables of TCE minimization

The third objective focuses on minimizing EP, as calculated in Eq. (4.13). The optimal solution of OMES-WSPHS for EP minimization is illustrated in Fig. 4.10, where Fig. 4.10(a) presents the power scheduling when considering EP as the objective, and Fig. 4.10(b) shows the convergence of the solution under EP minimization. Similar to the second objective, the optimization process for the third objective function is executed 30 trials to ensure the best and most reliable results, with the results shown in Fig. 4.10(c). Once the optimal solution for EP minimization has been determined, the decision variables scheduling pattern for EP minimization can be illustrated in Fig. 4.11.

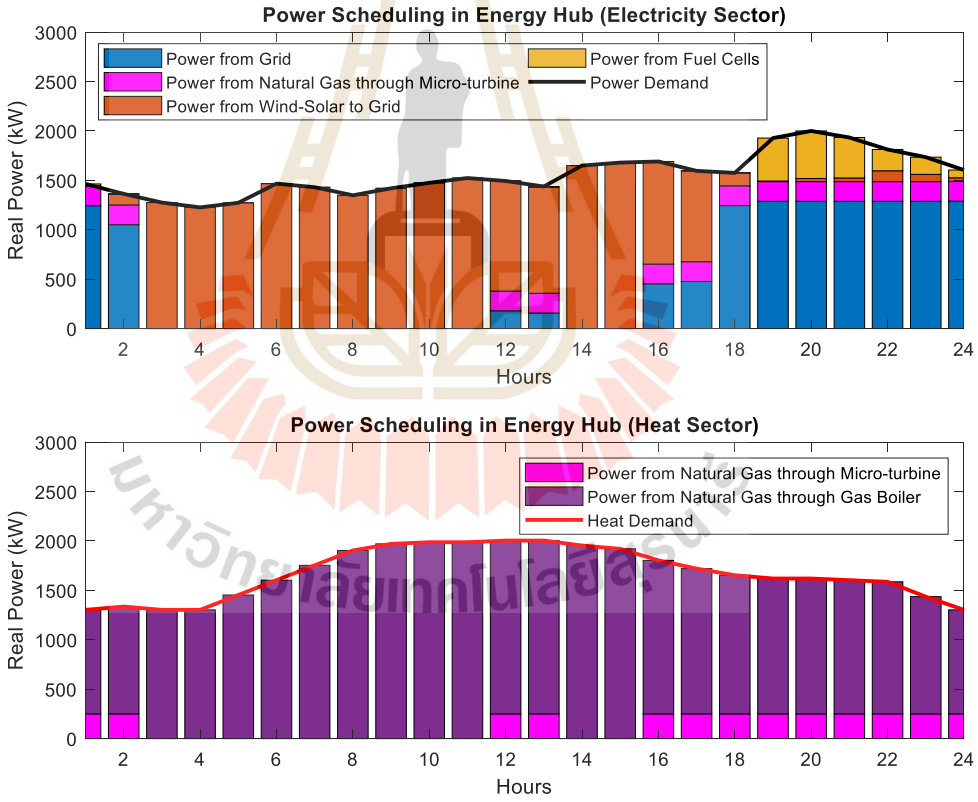

(a)

Figure 4.10 The optimal solution of OMES-WSPHS for EP minimization (a) the power scheduling, (b) the convergence of the solution, and (c) The fitness results with 30 trials

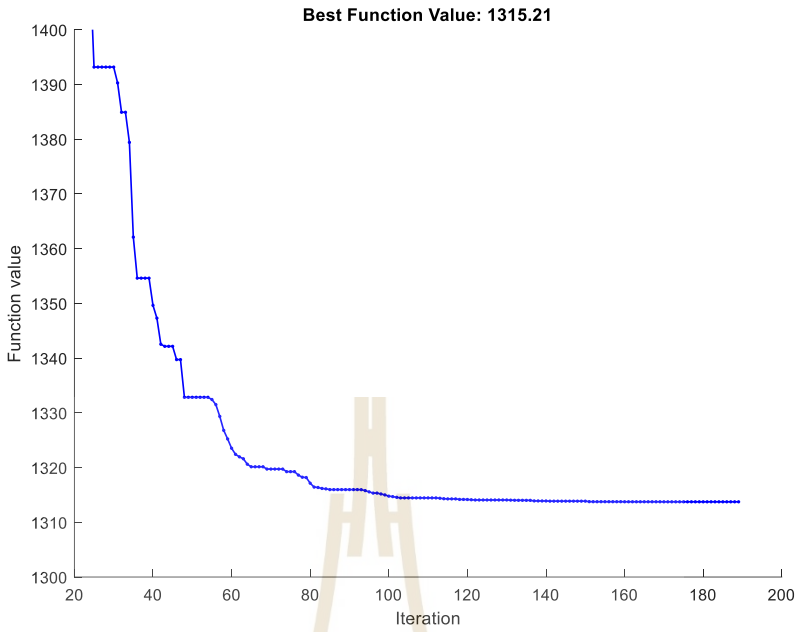

(b)

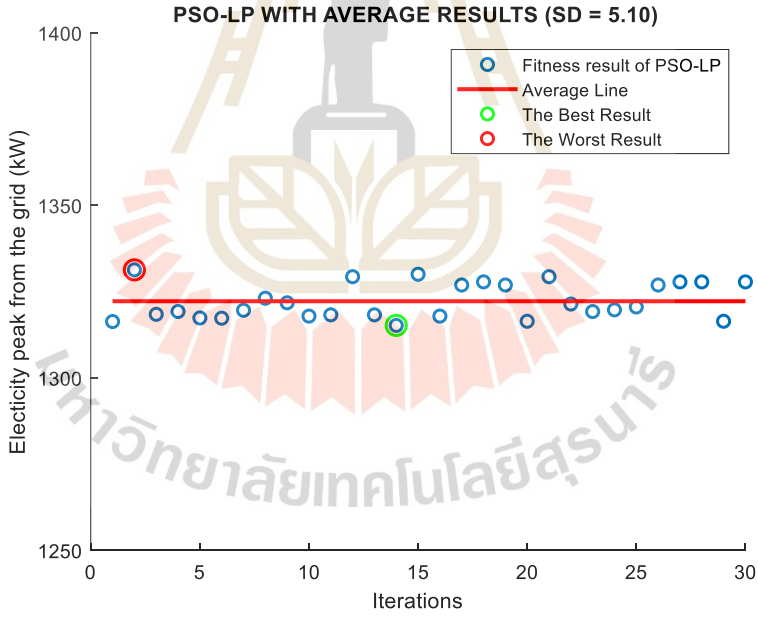

(c)

Figure 4.10 The optimal solution of OMES-WSPHS for EP minimization (a) the power scheduling, (b) the convergence of the solution, and (c) The fitness results with 30 trials (Continued)

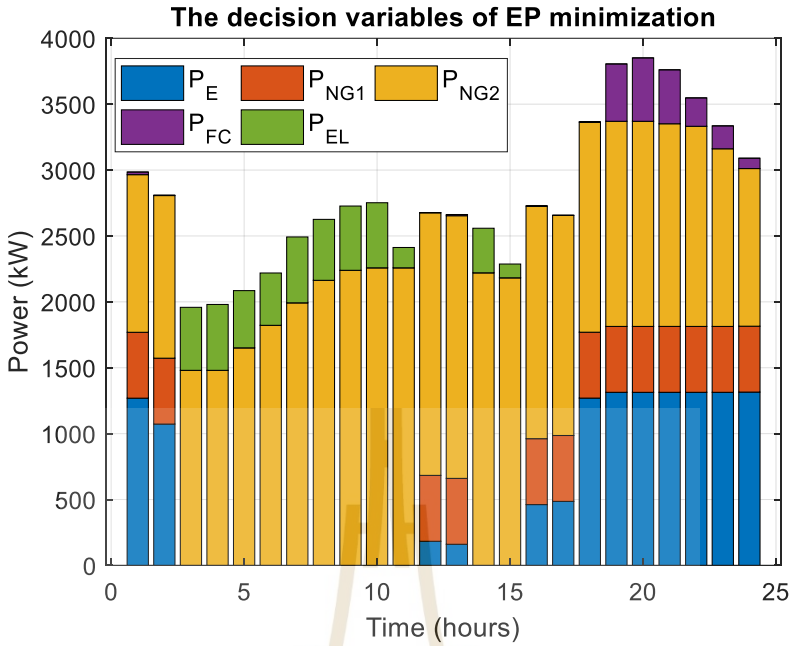

Figure 4.11 The decision variables of EP minimization

To effectively balance these objectives, FSMF is constructed to quantify the degree of satisfaction for each solution. This function assigns membership values between 0 and 1, representing the desirability of different scheduling patterns. By integrating this function into the decision-making framework, a compromise solution that considers all objectives can be achieved. The systematic approach involves optimizing each objective separately, normalizing the results for comparability, defining a fuzzy membership function for each objective follows the Eq. (4.18) – (4.20) respectively, and aggregating the satisfaction levels to determine an optimal scheduling pattern that balances TOC, TCE, and EP. This study defines the A scheduling pattern as the pattern for TOC minimization, the B scheduling pattern as the pattern for TCE minimization, and the C scheduling pattern as the pattern for EP minimization. By utilizing all three patterns to evaluate the objectives, the minimum and maximum values for each objective can be determined as shown in Table 4.3, which then allows for the creation of a FSMF to aid in the decision-making process. Each FSMF in is illustrated in 4.12 (a) TOC minimization, (b) TCE minimization, and (c) EP minimization.

Where the green highlight indicates the minimum value of each objective, while the orange highlight also represents the maximum value of each objective.

Table 4.3 The scheduling pattern for TOC, TCE, and EP

Objectives / *Pattern of Scheduling*	*TOC* (THB)	*TCE* ($kgCO_2$)	*EP* (kW)
A (min TOC as objective)	239,772	18,442.1	1,753.96
B (min TCE as objective)	242,935	18,105.4	2,008.61
C (min EP as objective)	243,241	18,717.1	1,315.21

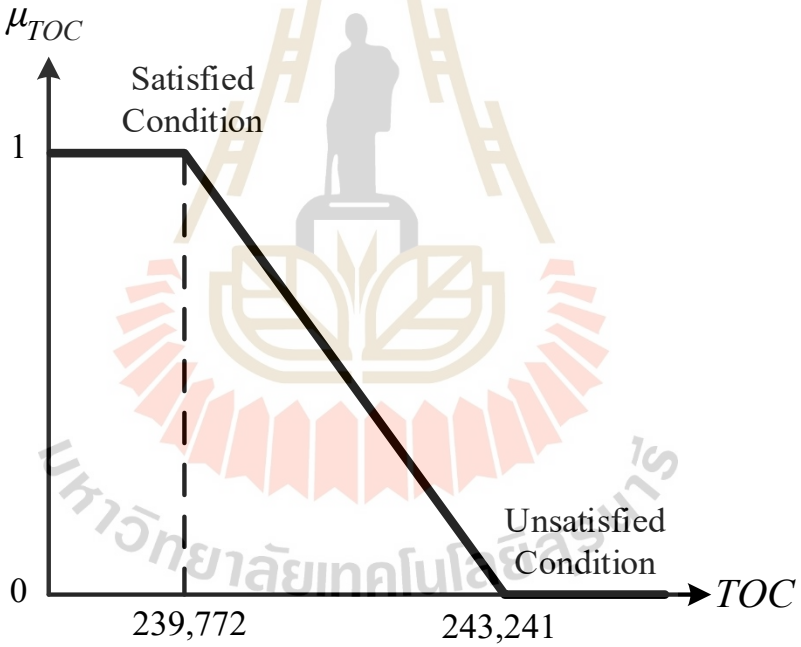

(a)

Figure 4.12 Each FSMF (a) TOC minimization, (b) TCE minimization, and (c) EP minimization

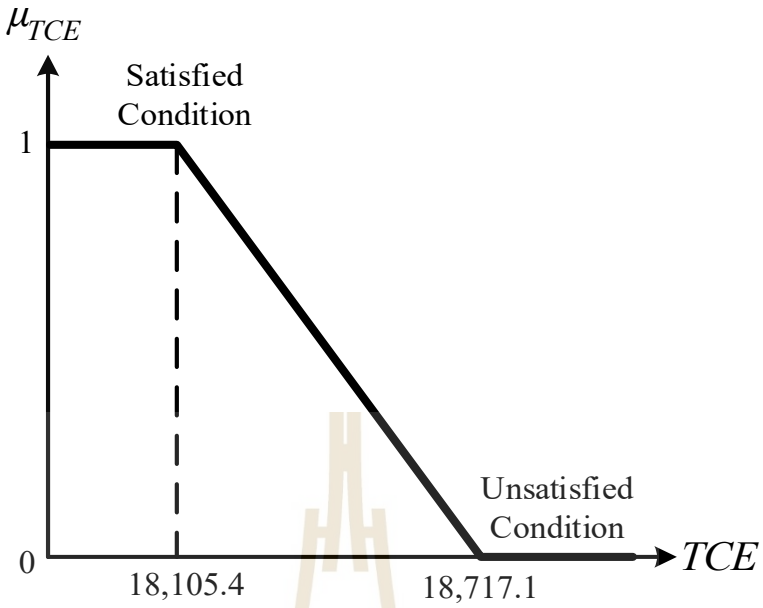

(b)

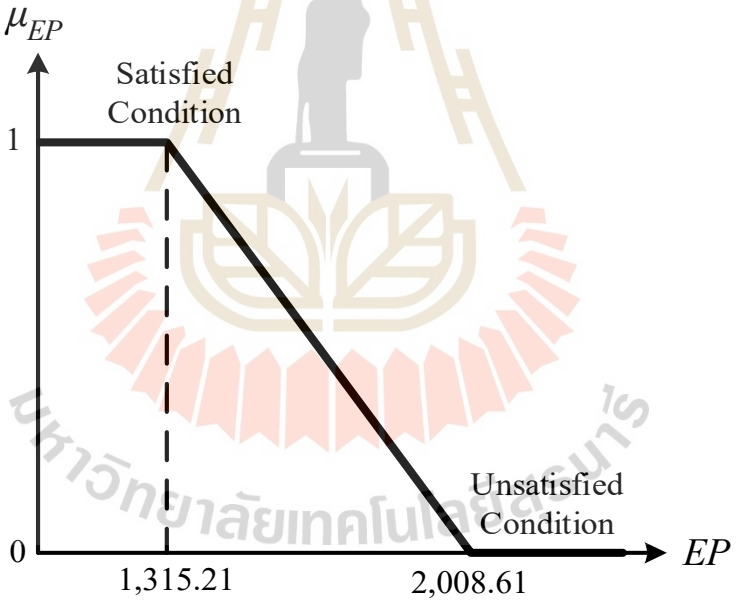

(c)

Figure 4.12 Each FSMF (a) TOC minimization, (b) TCE minimization, and (c) EP minimization (Continued)

4.5.2 FMOO-Based OMES-WSPHS Optimization for Total FSMF

According to Section 4.5.1, FSMF is individually defined for each objective. Consequently, the total FSMF represents overall satisfaction by capturing the maximum satisfaction among the minimum satisfaction levels of the three combined objective functions. The maximin principle is applied to maximize the minimum outcome among the three objectives, ensuring that the worst-case scenario is as favorable as possible. This approach guarantees a balanced and compromised solution that considers all objectives. By maximizing FSMF, the scheduling pattern of HS and the electricity-NG dispatch can be determined for the optimal compromise solution. The total FSMF solution is illustrated through the convergence plot in Fig. 4.13, while Fig. 4.14 presents the fitness total FSMF results over 30 trials.

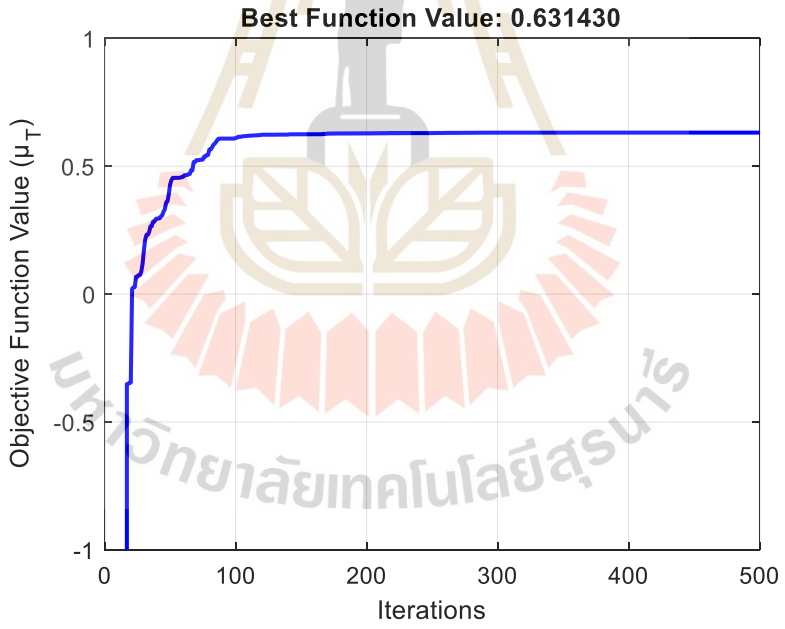

Figure 4.13 The convergence plot of the total FSMF solution

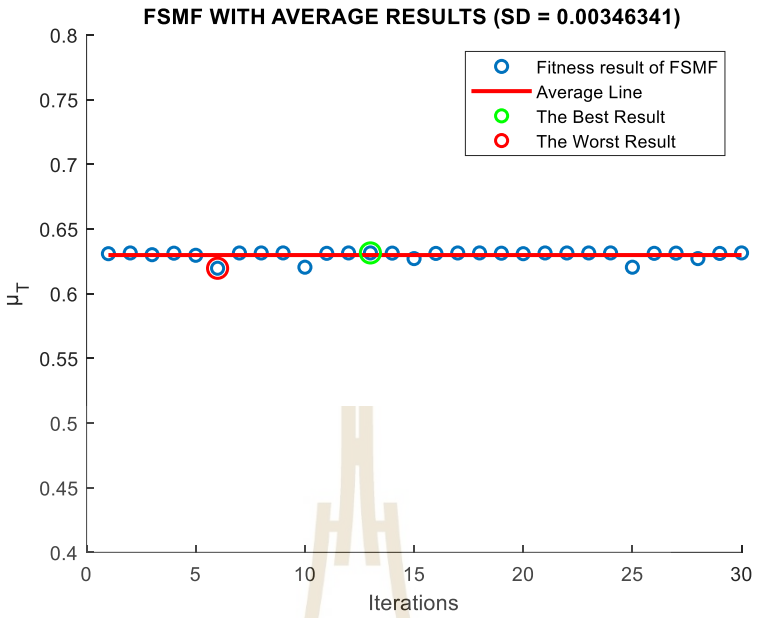

Figure 4.14 The fitness total FSMF results with 30 trials

For this proposed procedure, Fig. 4.15 illustrates the power scheduling for each energy sector which (a) electricity and (b) heat, ensuring a balanced trade-off among multiple objectives. In the electricity sector (Fig. 4.15 (a)), the microturbine operates mainly during 12:00–2:00 p.m. and 6:00–10:00 p.m., with fuel cells contributing intermittently in the same periods. In the heat sector (Fig. 4.15 (b)), heat demand is primarily met by a gas boiler, while the microturbine provides additional heat during 12:00–2:00 p.m. and 6:00–10:00 p.m. The HS scheduling and state of the tank can be demonstrated in Fig. 4.16 (a) and (b), respectively. For each objective function, the best and worst values are determined based on the optimization goal. For FSMF, the best value is the maximum, as a higher fuzzy satisfaction level indicates a more optimal solution, while the worst value is the minimum. Conversely, for TOC, TCE, and EP, the best values correspond to the minimum, as reducing total operating costs, total carbon emissions, and electricity peaks is desirable. In contrast, the worst values for these objectives are the maximum, as they represent higher costs, emissions, and peak loads, which are less favorable. These results highlight the trade-offs between

different objectives in MES-WSPHS optimal scheduling. Table 4.4 contains the results which show average value, best value, and worst value of FSMF, TOC, TCE, and EP.

Table 4.4 The results of statistics data for FSMF, TOC, TCE, and EP.

	BEST	AVERAGE	WORST
TOC	241,049.03	241,114.21	242,508.97
TCE	18,317.69	18,331.56	18,358.05
EP	1,570.8	1,579.3	1,731.5
μ_T	0.6314	0.6298	0.6196

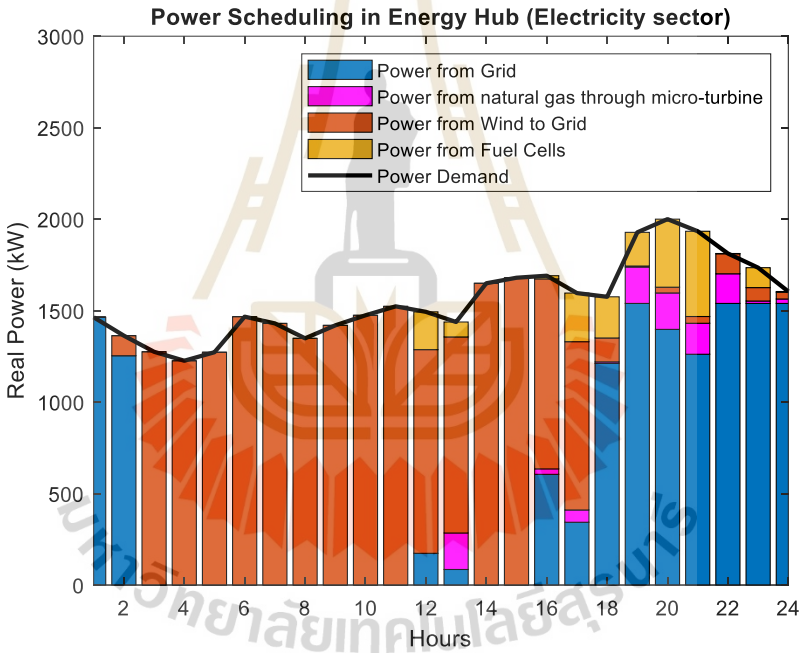

(a)

Figure 4.15 The total FSMF maximization for the power scheduling (a) electricity and (b) heat

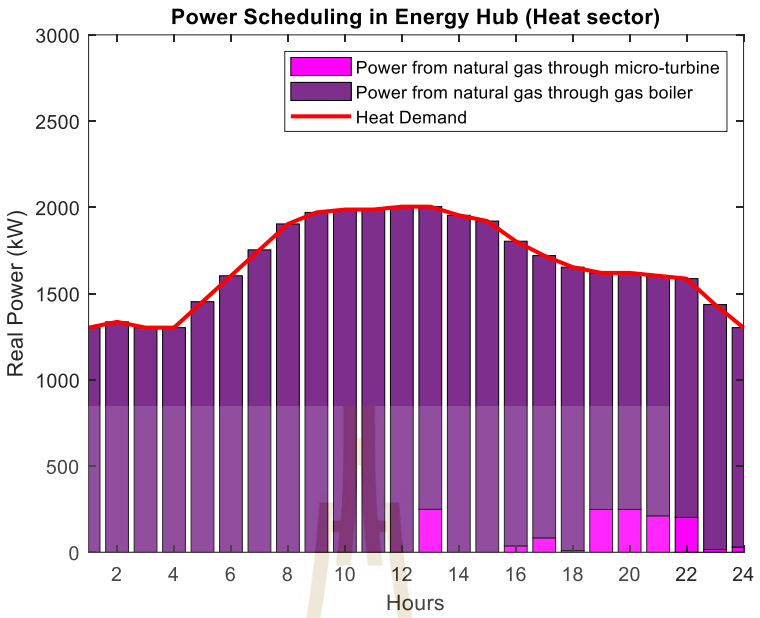

(b)

Figure 4.15 The total FSMF maximization for the power scheduling (a) electricity and (b) heat (Continued)

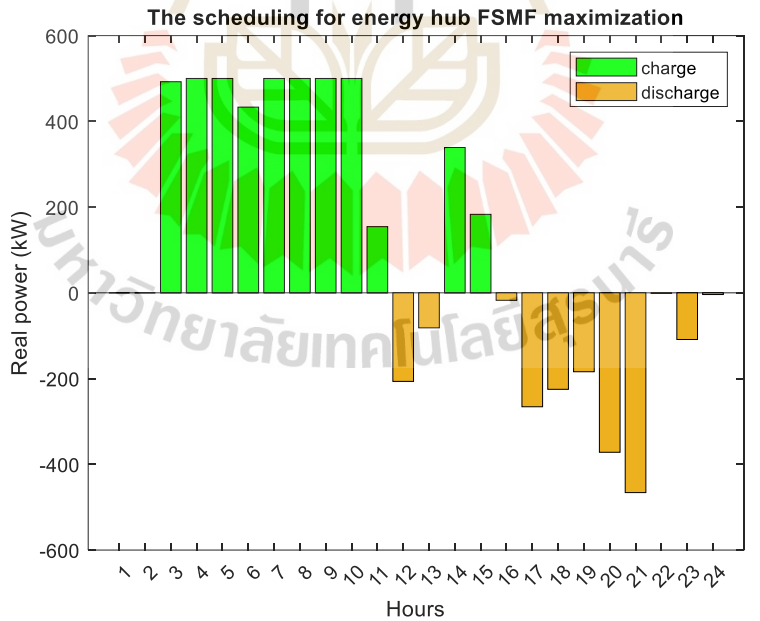

(a)

Figure 4.16 The total FSMF maximization for (a) The HS scheduling and (b) state of the tank

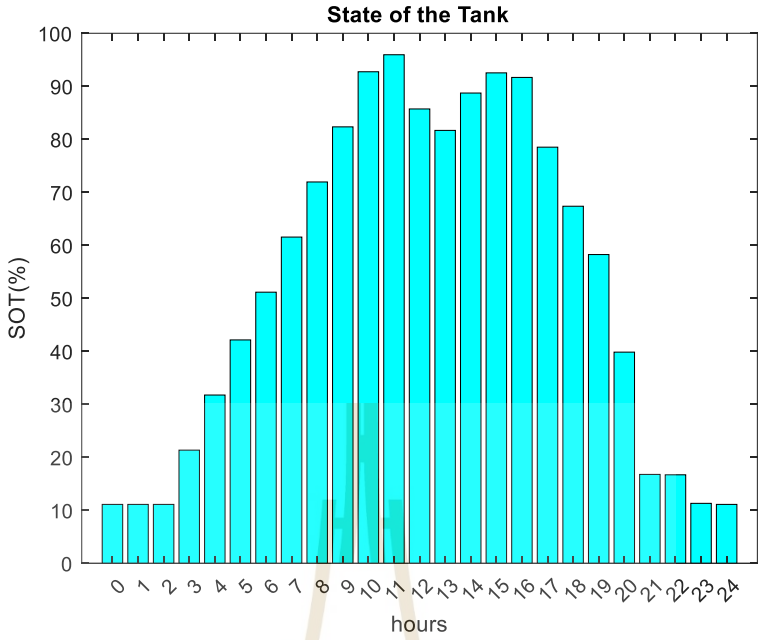

(b)

Figure 4.16 The total FSMF maximization for (a) The HS scheduling and (b) state of the tank (Continued)

4.5.3 WSMO vs. FMOO Optimization in OMES-WSPHS

This section demonstrates the effectiveness of the WSMO method in identifying alternative solutions for the multi-objective optimization problem. Unlike the FMOO approach, WSMO provides a more straightforward mechanism by allowing decision-makers to assign weights to each objective based on their relative importance. To ensure that can consider all objectives with different units, normalization is required. Accordingly, in this study, all objectives are converted into cost-equivalent units, as described in Eq. (4.21). The performance of WSMO is illustrated in Fig. 4.17, which shows the power scheduling across each energy sector while maintaining the power balance constraint. Complementing this, Fig. 4.18 presents the scheduling of HS along with the corresponding SOT. Additionally, Fig. 4.19 displays the convergence behavior of the WSMO algorithm, further confirming the stability of the obtained results.

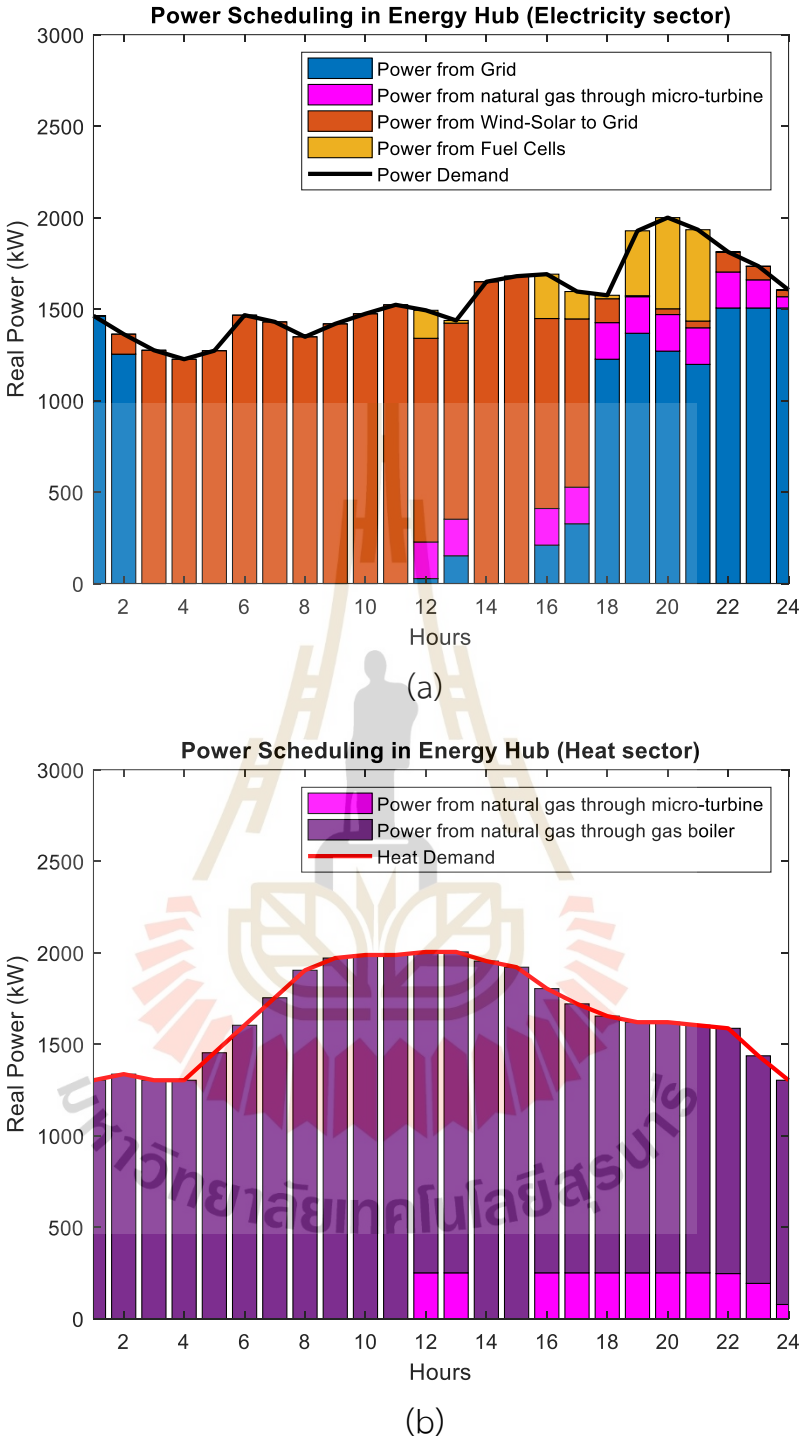

Figure 4.17 The WSMO performance for (a) electricity sector (b) heat sector

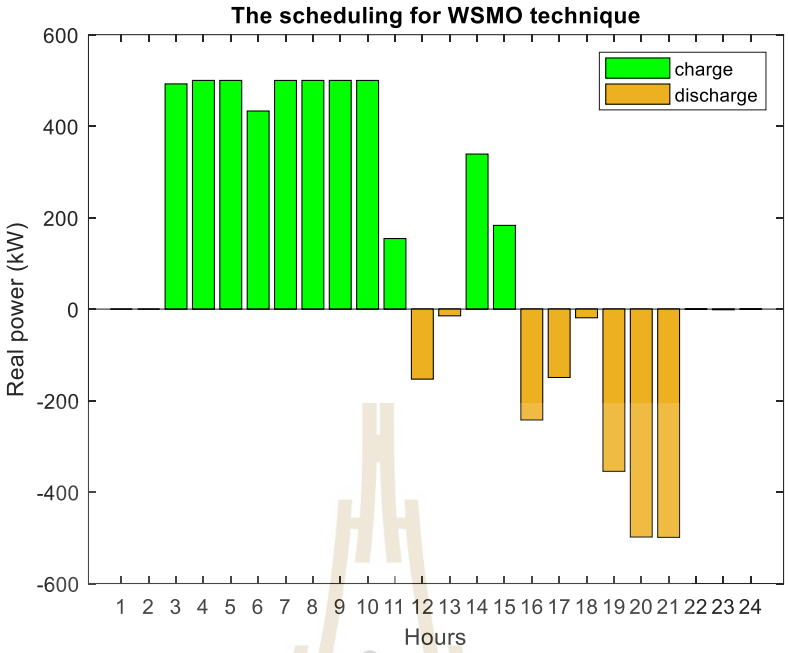

(a)

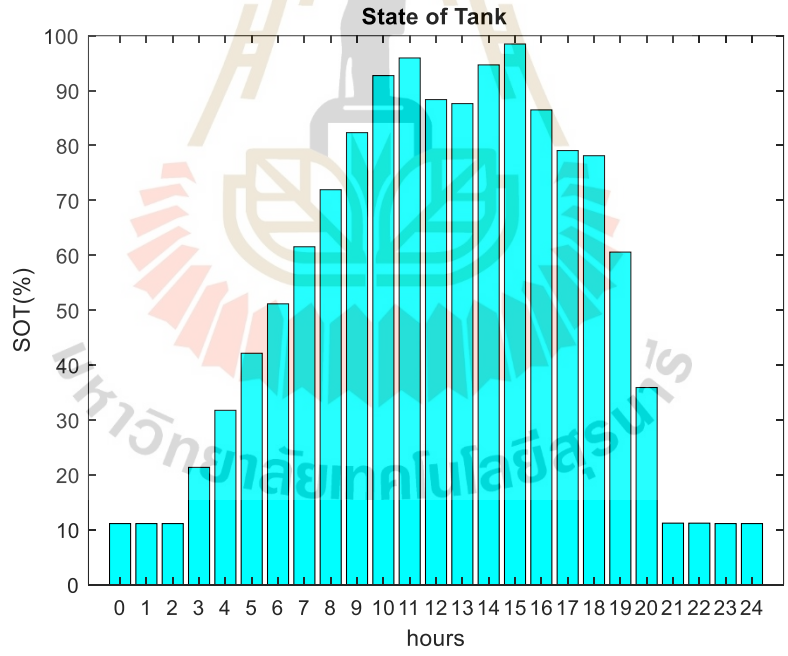

(b)

Figure 4.18 The WSMO performance for (a) The HS scheduling and (b) SOT

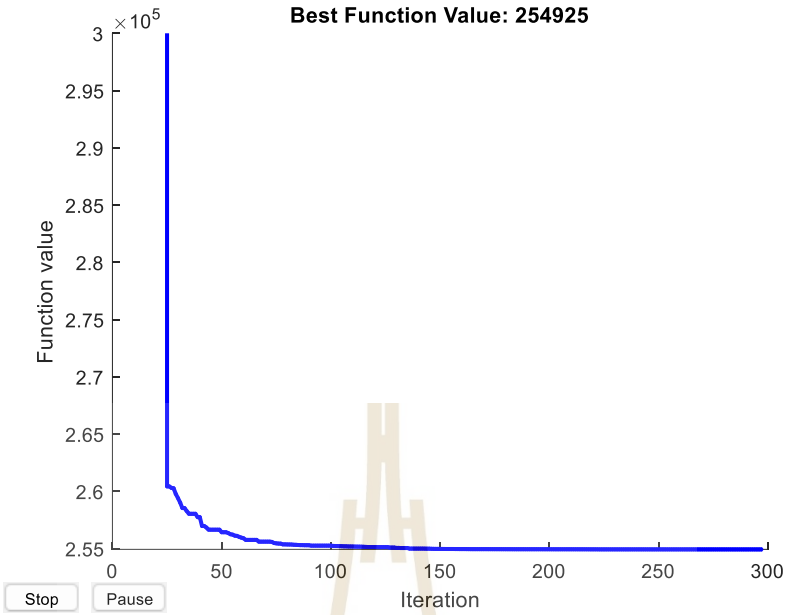

Figure 4.19 The convergence plot for WSMO technique

Table 4.5 A summary of the improvements achieved between WSMO and FMOO

Method	Objective functions		
	TOC	TCE	EP
WSMO	240,467.46	18,528	1,536.9
FMOO	241,049.03	18,317.69	1,570.8
Percentage Difference (%)	0.24%	1.13%	2.2%

Within the OMES-WSPHS framework, WSMO successfully generates a set of compromise solutions. However, when compared to FMOO, the FMOO approach proposes enhanced outcomes in certain objectives due to its ability to better balance competing trade-offs through fuzzy decision-making. Therefore, although WSMO achieves slightly better results in terms of TOC and EP, FMOO offers a more balanced compromise by significantly reducing carbon emissions while only slightly increasing cost and peak load. This highlights FMOO's superior capacity for handling trade-offs in

multi-objective scheduling problems under the OMES-WSPHS framework. A summary of the improvements achieved by each method is provided in Table 4.5.

4.6 Chapter Summary

This chapter introduced the FMOO framework for the OMES-WSPHS, considering three key objectives including TOC, TCE, and EP minimization. The optimization process for single objective is conducted using a PSO-LP approach, and the FMOO technique is employed to evaluate trade-offs among competing objectives. The simulation results demonstrated that the proposed methodology effectively balances cost, environmental impact, and peak energy from grid generation. By constructing FSMF for each objective, a systematic decision-making approach is implemented to determine an optimal scheduling pattern that maximizes overall system performance. The findings highlight the effectiveness of fuzzy optimization in handling multi-objective problems within energy systems, ensuring an optimal compromise solution that enhances system efficiency and sustainability. Compared to the WSMO method, the FMOO approach provides more balanced and adaptable solutions by eliminating the bias introduced by predefined weighting factors. Instead, it evaluates the relative satisfaction levels of each objective, enabling the system to operate in a more compromise-oriented and practical manner, particularly under conflicting operational conditions. The results indicate that FMOO achieves a superior balance across all objectives. While TOC and EP exhibit slight increases, these changes occur as a trade-off to significantly reduce the conflicting objective—TCE. Therefore, from the perspective of multi-objective compromise, FMOO demonstrates a more effective and harmonious performance.

CHAPTER V

UNCERTAINTY MODELING AND STOCHASTIC ANALYSIS FOR OMES-WSPHS INTEGRATION

5.1 General Introduction

In this chapter, the OMES-WSPHS integration is utilized as a stochastic analysis model to account for uncertainty variables, including fluctuations in weather modeled using Weibull distribution to represent RE generation and variations in end-user behavior to model multi-energy demand. The proposed approach minimizes TOC while ensuring system reliability and operational feasibility under uncertain conditions. The methodology employs a stochastic optimization process, leveraging MCS to handle uncertainties associated with renewable energy sources and energy demand variations. This chapter presents the performance evaluation of the proposed method and its effectiveness in achieving an optimal scheduling strategy for MES.

5.2 Problem Formulation

The mathematical formulation remains consistent with the previous chapter, ensuring that the optimization framework aligns with the problem structure in Chapter 3. Therefore, the objective function and constraints are retained as follows: Refer to Equations (3.21)–(3.31).

5.2.1 Uncertainty Variable Formulation

This section identifies the uncertainty variables considered in OMES-WSPHS integration, including wind speed, solar irradiance, electricity load, and heat load. It also outlines the process of extracting historical data to generate uncertainty

data sets for solar and wind. In contrast, due to the lack of historical data, the uncertainty in electricity and heat load is modeled using percentage-based standard deviation assumptions. To formulate the probabilistic wind speed and solar irradiance model, the historical annual data need to extracted hour-by-hour in for reflects the fluctuation in that hour (Chayakulkheeree, 2013). Figure 5.1 shows the probabilistic wind speed and solar irradiance model preparation.

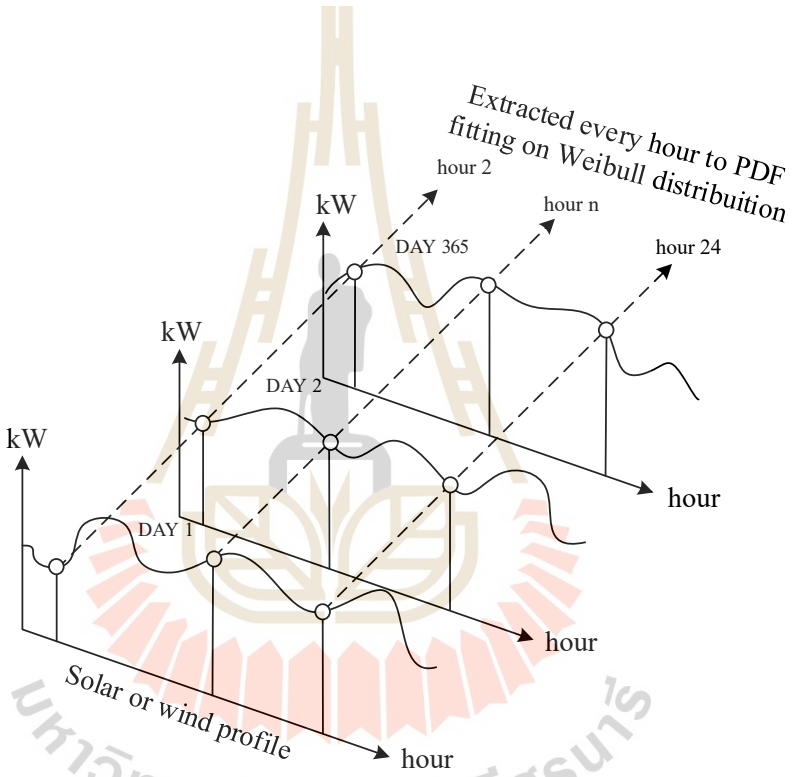

Figure 5.1 The probabilistic wind speed and solar irradiance model preparation, adapted from Chayakulkheeree (2013)

The historical annual data of wind speed and solar irradiance are analyzed to determine their mean and variability. The mean value and its range (mean – SD to mean + SD) for solar irradiance are presented in Fig. 5.2 (subplot 1), while the corresponding power output from PVPs is shown in Fig. 5.2 (subplot 2). Similarly, the mean and its range for wind speed are illustrated in Fig. 5.3 (subplot 1), with the power

output from WTs displayed in Fig. 5.3 (subplot 2). For both power output, using the power conversion equations from Chapter 3 (Eq. 3.3–3.5). Figures 5.4 and 5.5 present box plots to illustrate the statistical distribution of data for solar energy and wind energy, respectively. The construction of model the variability of wind speed and solar irradiance, the Weibull distribution is fitted to the data. The PDF of the solar irradiance and wind speed can be modeled in Weibull distribution as shown in Eq. (5.1) and Eq. (5.2), respectively. The key parameters for this distribution are the shape and scale factors, which vary hourly to account for fluctuations. The corresponding shape and scale values for each hour are listed in Table 5.1. Using these parameters, random values are generated based on the Weibull distribution.

$$f_{SI}(SI) = \frac{b_{SI}}{a_{SI}}\left(\frac{SI}{a_{SI}}\right)^{b_{SI}-1} e^{-\left(\frac{SI}{a_{SI}}\right)^{b_{SI}}}, \tag{5.1}$$

$$f_{v_{WTs}}(v_{WTs}) = \frac{b_{v_{WTs}}}{a_{v_{WTs}}}\left(\frac{v_{WTs}}{a_{v_{WTs}}}\right)^{b_{v_{WTs}}-1} e^{-\left(\frac{v_{WT}}{a_{WT}}\right)^{b\,v_{WTs}}}. \tag{5.2}$$

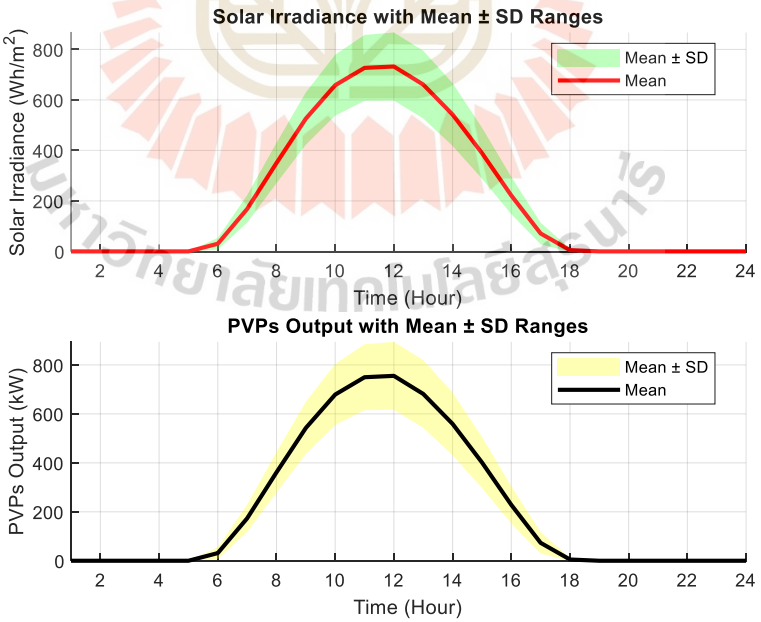

Figure 5.2 Mean, variability (Mean ± SD) of solar irradiance, and power output from PVPs

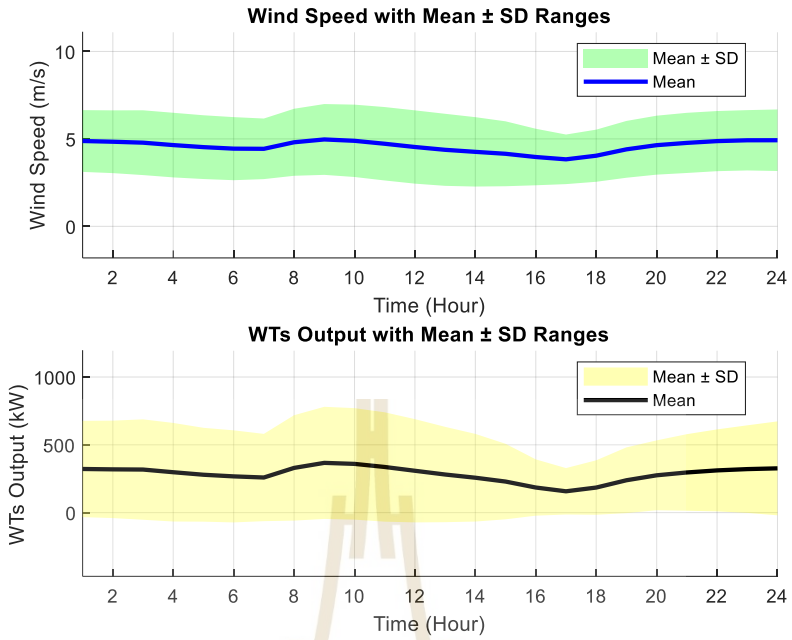

Figure 5.3 Mean, variability (Mean ± SD) of wind speed, and power output from WTs

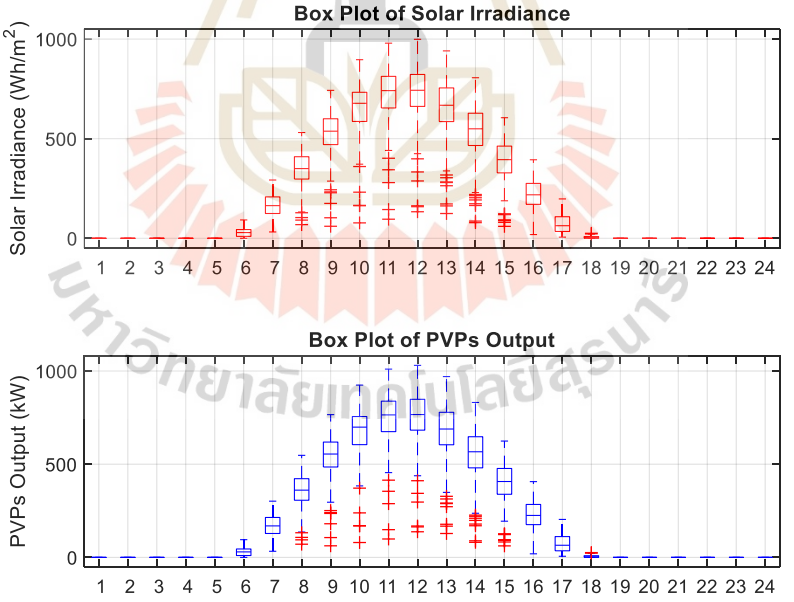

Figure 5.4 The box plots of solar irradiance and power output from PVPs

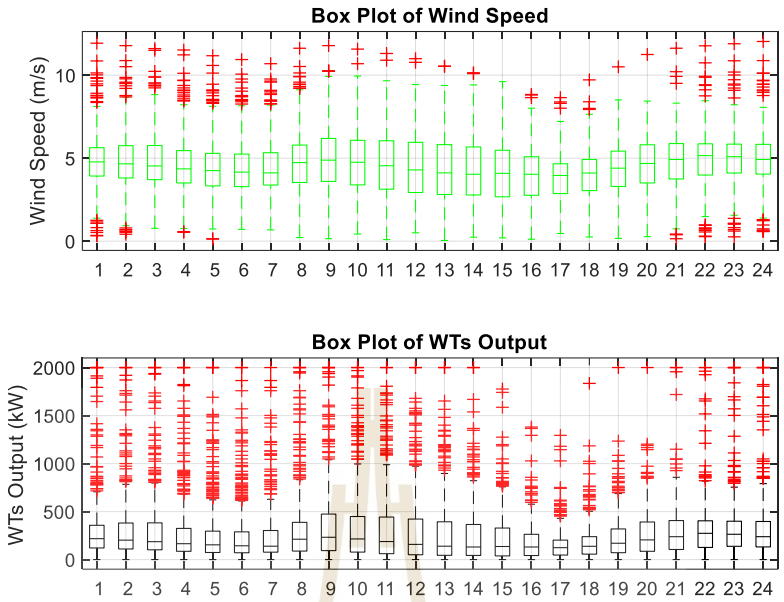

Figure 5.5 The box plots of wind speed and power output from WTs

Table 5.1 The corresponding shape and scale values of wind and solar for each hour

Hour	Solar irradiance (Wh/m^2)		Wind speed (m/s)	
	Shape (*a*)	Scale (*b*)	Shape (*a*)	Scale (*b*)
1	0	0	2.899	5.47
2	0	0	2.83	5.411
3	0	0	2.729	5.367
4	0	0	2.656	5.223
5	0	0	2.611	5.088
6	1.574	37.981	2.616	5.004
7	3.417	187.173	2.708	4.98
8	5.008	381.229	2.662	5.401
9	6.103	566.063	2.621	5.585
10	6.673	704.946	2.528	5.506
11	6.682	778.166	2.388	5.322
12	6.51	784.897	2.306	5.124

Table 5.1 The corresponding shape and scale values of wind and solar for each hour (Continued)

Hour	Solar irradiance (Wh/m^2)		Wind speed (m/s)	
	Shape (*a*)	Scale (*b*)	Shape (*a*)	Scale (*b*)
13	5.87	712.703	2.225	4.928
14	5.142	588.970	2.278	4.806
15	4.464	426.838	2.386	4.678
16	3.335	246.762	2.643	4.454
17	1.727	79.791	2.929	4.287
18	1.785	10.216	2.924	4.518
19	0	0	2.943	4.927
20	0	0	3.004	5.184
21	0	0	2.989	5.316
22	0	0	3.042	5.425
23	0	0	3.042	5.482
24	0	0	2.96	5.493

Electricity and heat loads can be modeled using a normal distribution PDF, as this approach effectively captures the typical energy consumption patterns observed in industrial applications. The PDF representing the normal distribution of electricity and heat loads are given in Eq. (5.3) and (5.4), respectively.

$$f_{L_E}(L_E) = \frac{1}{\sqrt{(2\pi)\sigma_{L_E}}} \exp\left(-\frac{(L_E - M_{L_E})^2}{2\sigma_{L_E}} \right), \tag{5.3}$$

$$f_{L_H}(L_H) = \frac{1}{\sqrt{(2\pi)\sigma_{L_H}}} \exp\left(-\frac{(L_H - M_{L_H})^2}{2\sigma_{L_H}} \right). \tag{5.4}$$

In this study, due to the absence of historical data, a percentage-based standard deviation assumption is adopted. Specifically, the mean values of electricity and heat load data are defined in Chapter 3, as shown in Fig. 3.4. The standard deviation is set at 2% of the mean value for each energy demand. The electricity and

heat loads are generated using the normal distribution model, their mean values and corresponding ranges (mean ± SD, mean ± 2SD, and ± 3SD) are illustrated in Fig. 5.6, where (a) represents electricity load and (b) represents heat load. Finally, the box plot for illustration of the statistical distribution of data for multi-energy loads can be shown in Fig. 5.7.

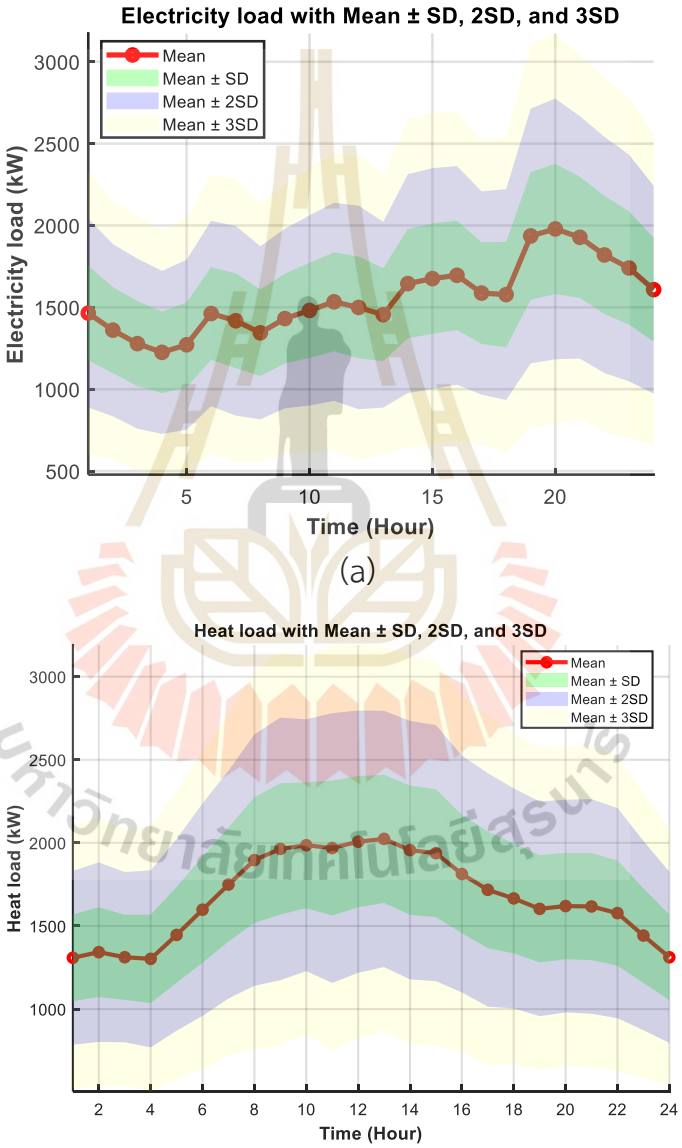

Figure 5.6 The mean values and corresponding ranges (mean ± SD, mean ± 2SD, and ± 3SD) for (a) electricity load and (b) heat load

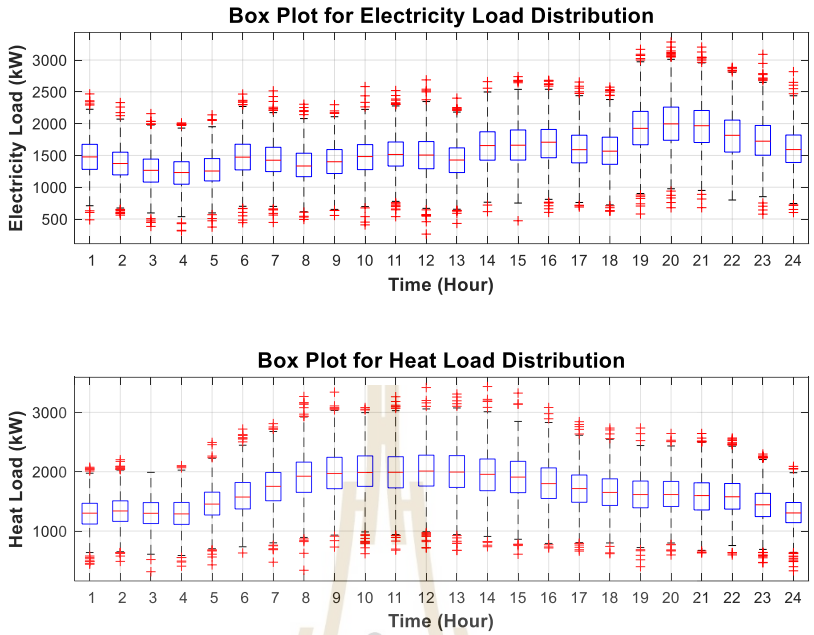

Figure 5.7 The box plots of electricity load and heat load

5.2.2 Probabilistic Technique Based on MCS

MCS has become a fundamental technique for modeling uncertainty in modern power systems. It is particularly valuable for its ability to handle high-dimensional and nonlinear problems, which are commonly encountered in integrated energy systems with renewable energy sources. These systems often exhibit inherent variability due to the intermittent nature of renewable resources such as wind and solar power. The core principle of MCS involves performing a large number of simulations based on random sampling from probability distributions that describe the behavior of uncertain input variables (Metropolis & and Ulam, 1949). In probabilistic modeling of power and multi-energy systems, uncertain variables such as RE generation, load demand, and electricity market prices are typically represented using probability distributions derived from historical data. These distributions are selected to best reflect the statistical characteristics and variability of each parameter. Common choices include normal, log-normal, Weibull, beta, and gamma distributions,

depending on the data properties. MCS utilizes these distributions to generate numerous random scenarios, enabling a comprehensive evaluation of system performance under uncertainty without relying on overly simplified assumptions. This approach provides system planners with the ability to account for a wide range of possible outcomes and make more informed and flexible decisions.

Each scenario generated by MCS represents a possible state of the system under a specific realization of uncertainty. These scenarios are processed through optimization models or system simulators to determine corresponding outputs, such as total operating cost, carbon emissions, reliability indices, or voltage stability margins. Statistical analysis of the results provides valuable insights into how uncertainties impact system performance. By integrating MCS into the modeling framework, the proposed approach enhances the robustness of scheduling decisions and allows system operators to prepare for a wide spectrum of potential operating conditions. This methodology not only supports risk-aware planning but also strengthens the flexibility and resilience of future intelligent energy systems.

5.3 Stochastic Analysis for OMES-WSPHS Using MCS

In this section, MCS is applied to evaluate the impact of uncertainty in the OMES-WSPHS. Given the stochastic nature of wind and solar power generation, electricity and heat demand, and HS scheduling, MCS is utilized to assess system performance under various realizations of these uncertainties. The process begins by defining probability distributions for key uncertain parameters, such as wind and solar power fluctuations modeled using a Weibull distribution and electricity and heat demand variations modeled using a normal distribution. Random samples are then generated based on these distributions, and each sampled scenario is used to solve the OMES-WSPHS optimization problem. In this study, the MCS is set to run for 500 iterations to ensure sufficient statistical representation of uncertainties. After completing the final iterations, it is necessary to verify the convergence of the

cumulative mean. The error of the cumulative mean can be determined based on the percentage calculation of the previous final iteration and the final iteration. If the resulting error is less than 1%, it indicates that the solution has successfully converged. A flowchart illustrating the MCS procedure for OMES-WSPHS is presented in Fig. 5.8.

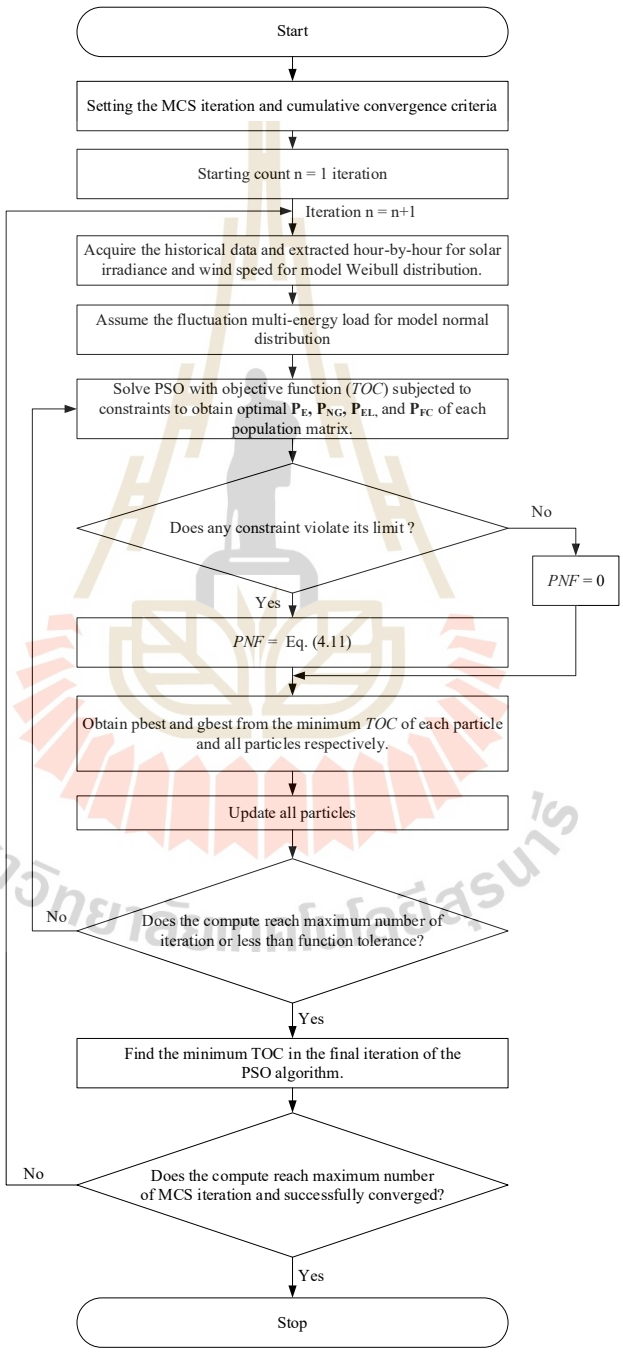

Figure 5.8 The flow chart of MCS procedure for OMES-WSPHS

The randomly sampled solar irradiance values are illustrated in Fig. 5.9, while the wind speed values are depicted in Fig. 5.10, leading to the corresponding electrical power output shown in Fig. 5.11. Additionally, both energy loads incorporate the uncertainty data from Fig. 5.6. Ultimately, all uncertainty parameters are considered as variable power generation inputs for determining the probabilistic solution. The results from multiple iterations are collected and analyzed using statistical measures, offering valuable insights into the feasibility of multi-energy scheduling under uncertainty.

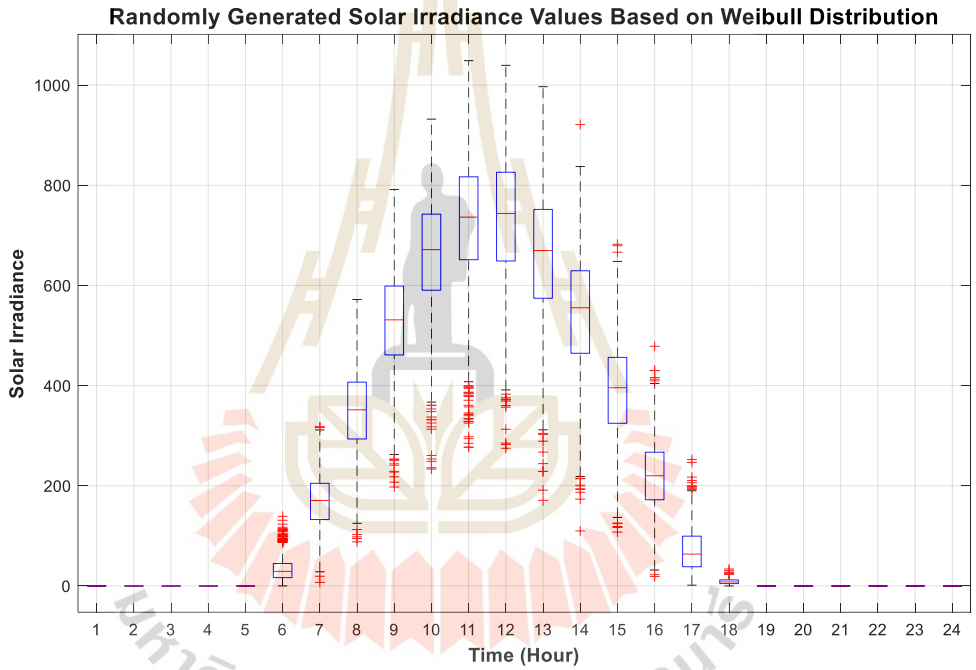

Figure 5.9 The box plot of Randomly generated solar irradiance values based on the Weibull distribution

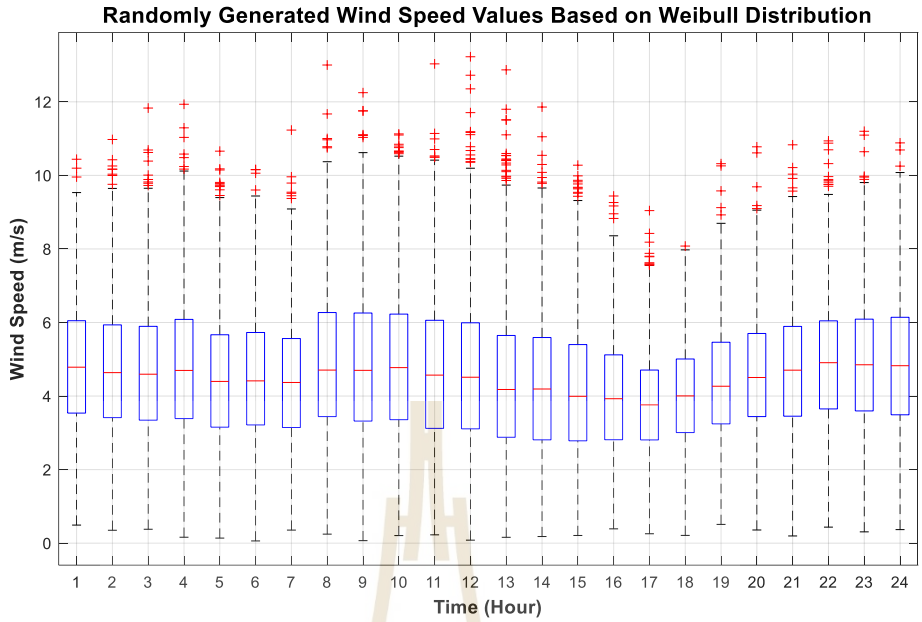

Figure 5.10 The box plot of Randomly generated wind speed values based on the Weibull distribution

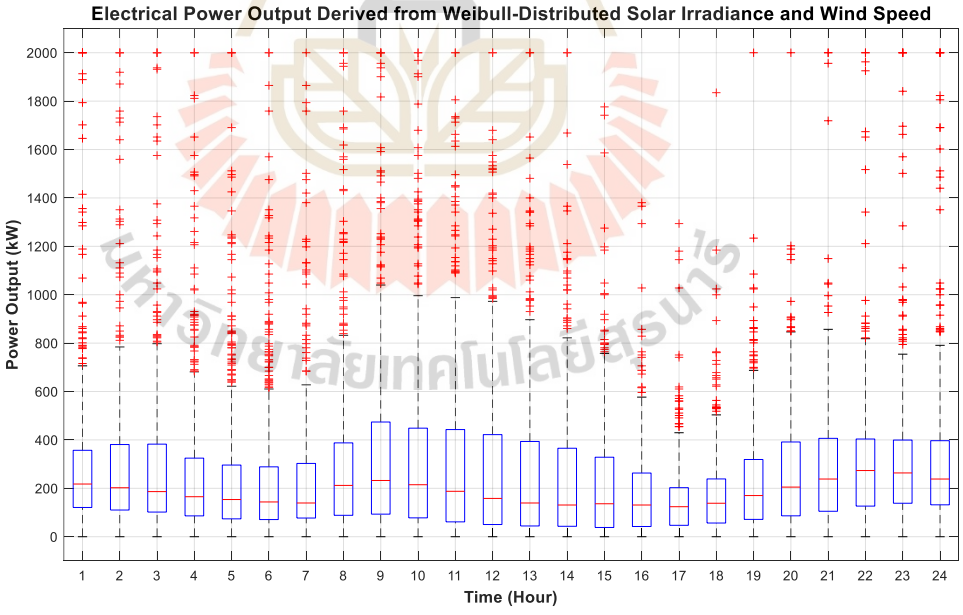

Figure 5.11 The box plot of electrical power output derived from Weibull-distributed solar irradiance and wind speed

5.4 Simulation Results

The cumulative mean of TOC over 500 iterations, as shown in Fig. 5.12, demonstrates the convergence behavior of the stochastic optimization process, specifically MCS. The results indicate a rapid initial decline in TOC, followed by stabilization after approximately 150 iterations. Beyond 300 iterations, TOC remains steady. Notably, when MCS reaches 500 iterations, the cumulative mean error defined as the difference between the previous final iteration and the final iteration falls to 0.0019%, below the 1% threshold, confirming that additional calculations are unnecessary. This demonstrates that the stochastic modeling approach handles uncertainty within the OMES-WSPHS integration. Consequently, the proposed framework minimizes operational costs while maintaining stability under uncertain conditions.

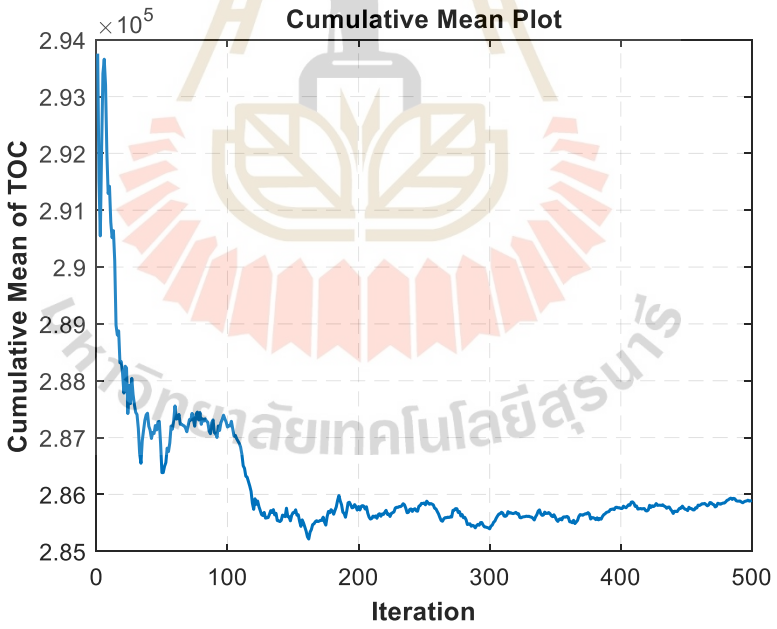

Figure 5.12 The cumulative convergence plot of MCS for TOC

In the MCS procedure, the probabilistic variables include power from solar and wind, as well as electricity and heat load. All probabilistic variables simultaneously

influence the results, making *TOC*, P_E, P_{NG}, P_{FC}, and P_{EL} probabilistic as well. The histogram plot and PDF fitting of TOC are illustrated in Fig. 5.13, with two fitted distributions: normal and Weibull. In this study, the normal distribution is found to be more optimal than the Weibull distribution, as indicated by the log-likelihood value, which has the smallest negative value—determining the best-fitting PDF for this data. The log-likelihood values of both distributions are presented in Table 5.2. Furthermore, the stochastic nature of the analysis introduces additional variability in TOC compared to the deterministic case. Due to the inherent uncertainties in renewable energy generation and demand variations, the probabilistic approach results in a higher TOC than a deterministic model, where all parameters are assumed to be known and fixed. This increase in TOC reflects the cost of accounting for uncertainties and ensuring system reliability under variable operating conditions.

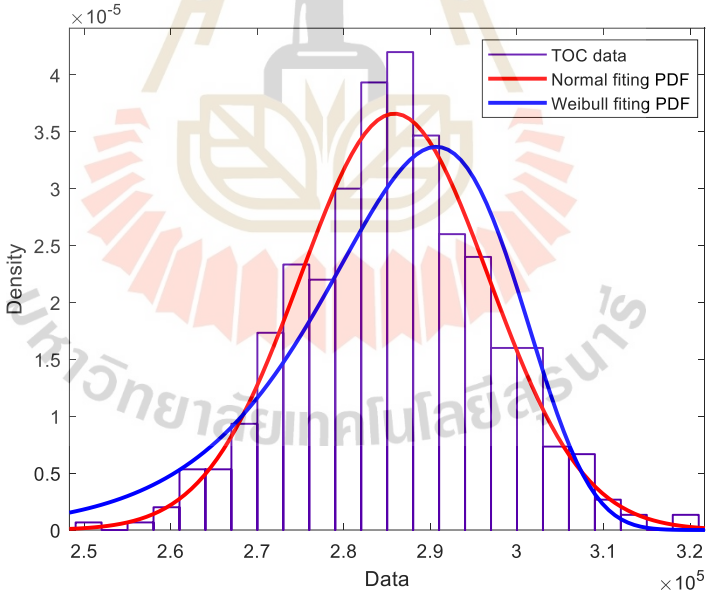

Figure 5.13 The PDF of TOC data

Table 5.2 The TOC log-likelihood of both distribution

Distribution	Normal	Weibull
Log-likelihood	-5,357.38	-5,392.97

The power scheduling results, including power from the grid and NG, are illustrated in Figs. 5.14 and 5.15. Since the data incorporates hourly uncertainties, a box plot should be used for visualization to effectively represent the range of data for each hour. Figures 5.16 and 5.17 illustrate the scheduling of HS under uncertainty conditions. The results highlight variations in power dispatch from EL and FC across different simulation iterations and hours. Additionally, the details of all discussed variables such as power scheduling from electricity, NG, and HS are provided in Appendix B.

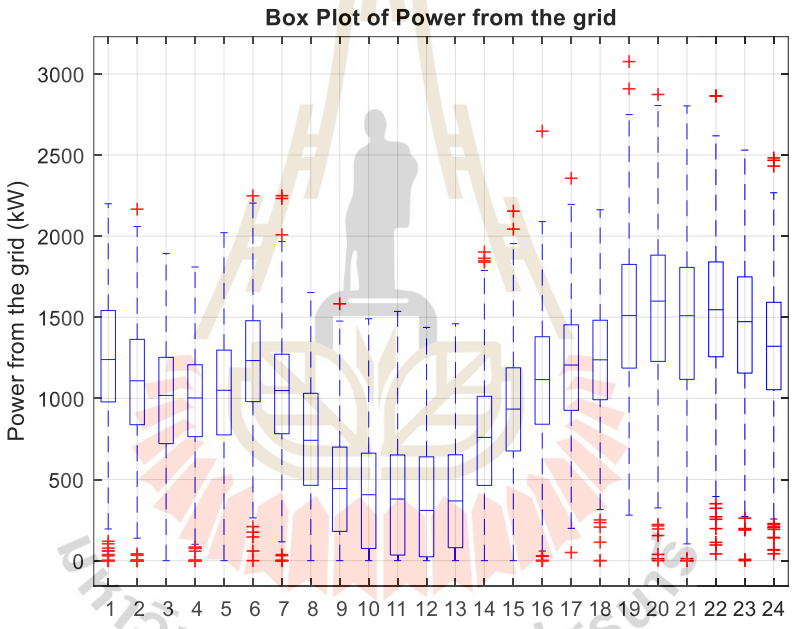

Figure 5.14 The box plot of P_E scheduling solution

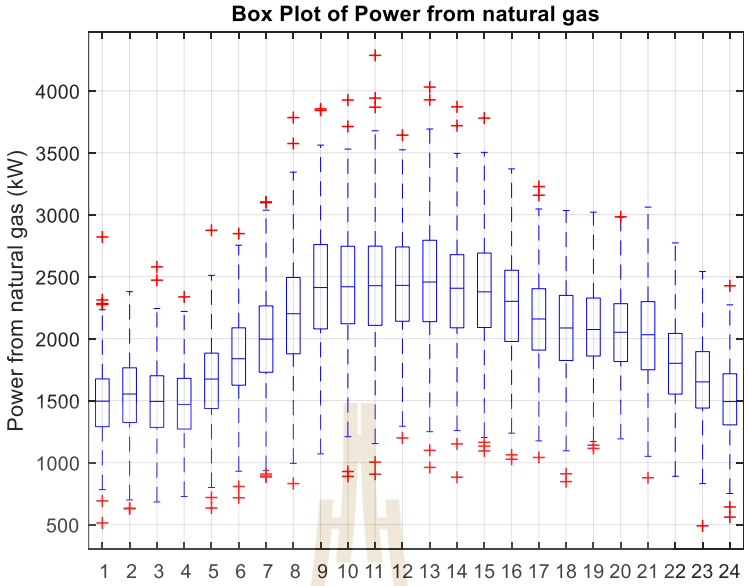

Figure 5.15 The box plot of P_{NG} scheduling solution

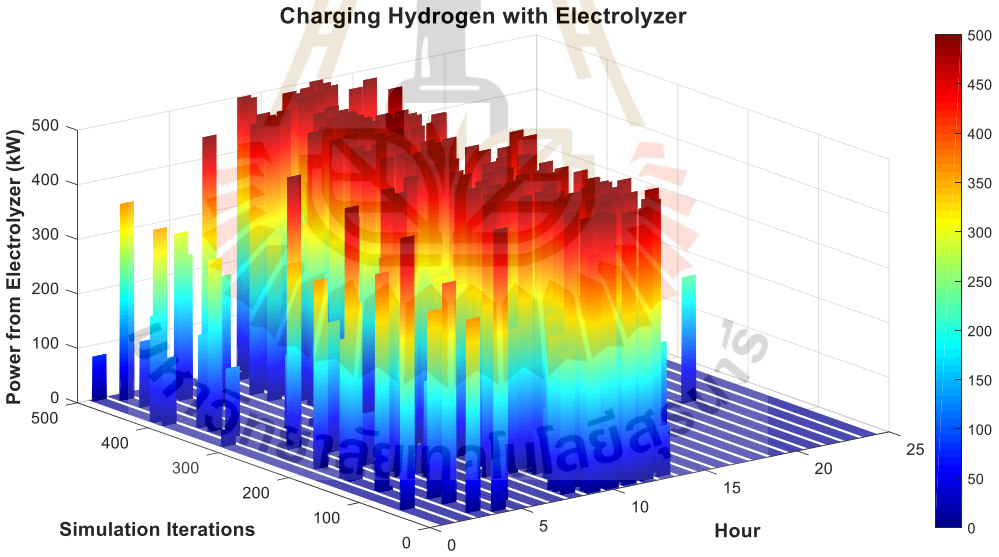

Figure 5.16 The 3D plot of P_{EL} scheduling solution

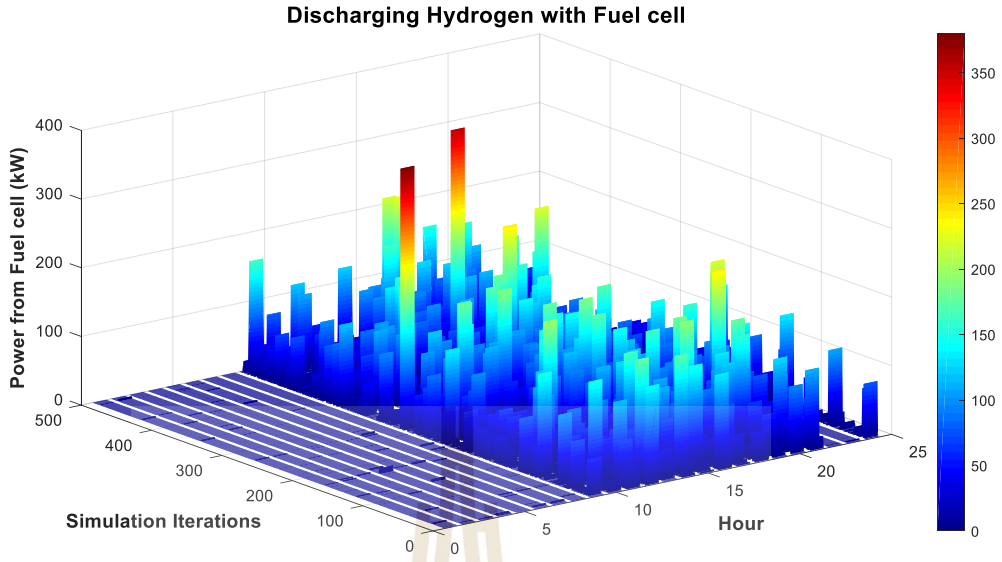

Figure 5.17 The 3D plot of P_{FC} scheduling solution

In Fig. 5.16, the 3D plot of P_{EL} scheduling reveals that the EL operates at higher power levels primarily from the morning to the afternoon. This scheduling pattern is influenced by the availability of surplus RE, particularly wind-solar power, which is more abundant during these hours. EL scheduling tends to reach near-rated power levels, indicating that the system maximizes hydrogen production when excess energy is available. This approach ensures efficient energy utilization and prepares sufficient hydrogen storage for later use. The scheduling also exhibits some variations due to uncertainty, but the general trend remains consistent, favoring high-power operations during periods of high RE generation. On the other hand, Fig. 5.17 illustrates the P_{FC} scheduling, which exhibits a different pattern compared to EL. The FC operates more frequently in the afternoon and night, aligning with periods when electricity demand is higher, and EL does not generate power. Unlike EL, FC does not operate at high power levels but instead follows a strategy of frequent scheduling with relatively low power output. This scheduling behavior ensures a steady supply of electricity from HS while preventing excessive depletion of stored hydrogen. The contrast between P_{EL} and P_{FC} scheduling highlights the coordinated operation of HS, where hydrogen is

efficiently produced and stored during high renewable generation hours and subsequently utilized in a controlled manner to balance the power demand in later hours.

5.5 Chapter Summary

The chapter presents an optimization framework that minimizes TOC and ensures system stability under uncertainty. The integration of WSPHS improves MES performance by efficiently using wind-solar energy and optimizing HS scheduling. The convergence analysis using MCS confirms the approach's robustness, with the final cumulative mean error falling below the 1% threshold. The study emphasizes the importance of stochastic modeling in RE generation and multi-energy demand. This result demonstrates an increase of TOC from the deterministic case, which indicates that the uncertainty influences the objective function. However, the most suitable PDF fitting for TOC in this work is normal distribution due to a lower log-likelihood.

CHAPTER VI

CONCLUSION

This thesis has proposed the OMES-WSPHS integration under various conditions. The first study focuses on minimizing TOC using two pricing mechanisms: TOU scheme and RTP scheme. In the TOU cases, different case studies are analyzed to assess TOC reduction when multi-energy sources are coordinated effectively. Additionally, the PSO-LP algorithm is proposed to optimize the scheduling problem. A comparative analysis between conventional PSO and PSO-LP reveals that PSO-LP achieves a near-global optimal TOC more effectively than conventional PSO. However, PSO performs better in terms of computational runtime, making both methods suitable for daily scheduling applications. The results highlight the benefits of multi-energy coordination and the integration of high penetration RE in achieving an optimal TOC.

For multi-objective optimization, the FMOO method is employed for OMES-WSPHS integration. The objective functions include TOC, TCE, and EP minimization. FMOO addresses this multi-objective problem by constructing FSMF using PSO-LP to obtain optimal single-objective solutions. Subsequently, PSO is utilized to maximize FSMF, ensuring a balanced trade-off among the conflicting objectives. The results demonstrate a compromise solution among TOC, TCE, and EP, leading to an effective balance between economic cost, environmental impact, and grid electricity demand reduction. For comparison, WSMO is also considered, providing an alternative compromise solution based on assigned weightings of the objectives. However, the FMOO approach enables a more flexible and informed decision-making process by considering the satisfaction levels of all objective functions simultaneously, leading to a compromise solution that avoids favoring any single objective too heavily.

The stochastic analysis of OMES-WSPHS integration examines probabilistic scheduling under uncertain conditions for TOC minimization. MCS is employed to evaluate the fluctuations in RE generation and energy loads, requiring multiple iterations to generate probabilistic results. The stochastic model considers four uncertain input variables, leading to four uncertain decision variables and one uncertain objective function. The results indicate an increase in TOC compared to the deterministic case, emphasizing the impact of uncertainty on the objective function. Among the probability distributions tested, the normal distribution is found to be the best fit for TOC in this study, as evidenced by a small negative log-likelihood value compared to Weibull distribution.

Overall, this study provides a comprehensive approach to optimize scheduling with MES-WSPHS integration model. The findings confirm that can improve cost-effectiveness while reducing environmental impact and peak electricity demand. The proposed PSO-LP algorithm successfully enhances scheduling efficiency, and the FMOO approach effectively balances conflicting objectives. Furthermore, stochastic analysis highlights the influence of uncertainty on TOC, reinforcing the need for probabilistic methods in energy system modeling. Future work may explore more advanced optimization techniques, expand uncertainty modeling, or extend the proposed framework to larger-scale multi-energy systems.

REFERENCES

Anna Sandhaas, H. K., César De Jesús, Niklas Hartmann. *Generation of Industrial Electricity and Heat Demand Profiles for Energy System Analysis* Proceedings of the IAEE International Conference,

Cau, G., Cocco, D., Petrollese, M., Knudsen Kær, S., & Milan, C. (2014, 2014/11/01/). Energy management strategy based on short-term generation scheduling for a renewable microgrid using a hydrogen storage system. *Energy Conversion and Management, 87*, 820-831. https://doi.org/https://doi.org/10.1016/j.enconman.2014.07.078

Chayakulkheeree, K. (2013, 2013/02/01). Probabilistic Optimal Power Flow with Weibull Probability Distribution Function of System Loading Using Percentiles Estimation. *Electric Power Components and Systems, 41*(3), 252-270. https://doi.org/10.1080/15325008.2012.742941

Chen, X., Cao, W., & Xing, L. (2019). GA Optimization Method for a Multi-Vector Energy System Incorporating Wind, Hydrogen, and Fuel Cells for Rural Village Applications. *Applied Sciences, 9*(17).

Chen, X., Wu, Q., & Zhang, J. (2019, 8-10 Nov. 2019). Optimal Control for a Wind-Hydrogen-Fuel Cell Multi-Vector Energy System. 2019 IEEE 3rd Conference on Energy Internet and Energy System Integration (EI2),

D'Silva, A. (2024). *Harnessing nature's power for clean hydrogen production*. AquaUniversity. Retrieved May 3, 2025 from https://algaeforbiofuels.com/powering-the-future-green-hydrogen-electrolyzers-fueled-by-solar-and-wind-energy/

Dash, S. K., Chakraborty, S., & Elangovan, D. (2023). A Brief Review of Hydrogen Production Methods and Their Challenges. *Energies, 16*(3).

Dechjinda, S., & Chayakulkheeree, K. (2024, 6-8 March 2024). Optimal Daily Scheduling of Hybrid Wind-Hydrogen Storage using Particle Swarm Optimization. 2024 12th International Electrical Engineering Congress (iEECON),

Energy Policy and Planning Office. (2023). *Thailand energy situation 2023*. Ministry of Energy, Thailand. https://www.eppo.go.th

Farah, A., Hassan, H., M. Abdelshafy, A., & M. Mohamed, A. (2020). Optimal Scheduling of Hybrid Multi-Carrier System Feeding Electrical/Thermal Load Based on Particle Swarm Algorithm. *Sustainability, 12*(11).

Geidl, M., Koeppel, G., Favre-Perrod, P., Klöckl, B., Andersson, G., & Fröhlich, K. (2007, 04/01). The energy hub-A powerful concept for future energy systems. *Third Annual Carnegie Mellon Conference on the Electricity Industry*, 13-14.

Geng, W., & Jia, L. (2020, 12-14 Sept. 2020). Hybrid Genetic Particle Swarm Optimization Based Economical Operation of Energy Hub. 2020 5th International Conference on Power and Renewable Energy (ICPRE),

Ha, T., Xue, Y., Lin, K., Zhang, Y., Thang, V. V., & Nguyen, T. (2022). Optimal Operation of Energy Hub Based Micro-energy Network with Integration of Renewables and Energy Storages. *Journal of Modern Power Systems and Clean Energy, 10*(1), 100-108. https://doi.org/10.35833/MPCE.2020.000186

Ha, T., Zhang, Y., Thang, V. V., & Huang, J. (2017). Energy hub modeling to minimize residential energy costs considering solar energy and BESS. *Journal of Modern Power Systems and Clean Energy, 5*(3), 389-399. https://doi.org/10.1007/s40565-017-0281-4

Hassan, A., Al-Awami, A. T., Muqbel, A. M., & Fouad, W. A. (2023, 3-6 Dec. 2023). Optimal Day-ahead Management of a Hydrogen-based Energy Hub Considering Different

Electrolyzer Technologies. 2023 IEEE International Conference on Energy Technologies for Future Grids (ETFG),

Honarmand, H. A., Ghaderi Shamim, A., & Meyar-Naimi, H. (2021, 2021/12/01/). A robust optimization framework for energy hub operation considering different time resolutions: A real case study. *Sustainable Energy, Grids and Networks, 28*, 100526. https://doi.org/https://doi.org/10.1016/j.segan.2021.100526

Ikuerowo, T., Bade, S. O., Akinmoladun, A., & Oni, B. A. (2024, 2024/07/26/). The integration of wind and solar power to water electrolyzer for green hydrogen production. *International Journal of Hydrogen Energy, 76*, 75-96. https://doi.org/https://doi.org/10.1016/j.ijhydene.2024.02.139

Imeni, M. L., & Ghazizadeh, M. S. (2023, 8-9 Feb. 2023). Pave the Way for Hydrogen-Ready Smart Energy Hubs in Deep Renewable Energy System. 2023 8th International Conference on Technology and Energy Management (ICTEM),

Imeni, M. L., Ghazizadeh, M. S., Lasemi, M. A., & Yang, Z. (2023). Optimal Scheduling of a Hydrogen-Based Energy Hub Considering a Stochastic Multi-Attribute Decision-Making Approach. *Energies, 16*(2).

Javadi, M. S., Anvari-Moghaddam, A., & Guerrero, J. M. (2017, 6-9 June 2017). Optimal scheduling of a multi-carrier energy hub supplemented by battery energy storage systems. 2017 IEEE International Conference on Environment and Electrical Engineering and 2017 IEEE Industrial and Commercial Power Systems Europe (EEEIC / I&CPS Europe),

Kennedy, J., & Eberhart, R. (1995, 27 Nov.-1 Dec. 1995). Particle swarm optimization. Proceedings of ICNN'95 - International Conference on Neural Networks,

Kholardi, F., Assili, M., Lasemi, M. A., & Hajizadeh, A. (2018, 10-12 Sept. 2018). Optimal Management of Energy Hub with Considering Hydrogen Network. 2018 International Conference on Smart Energy Systems and Technologies (SEST),

Liu, J., Sun, P., Yu, Y., Dong, S., Wang, K., & Yang, J. (2021, 9-11 Oct. 2021). Optimal Scheduling Considering Different Energy Hub Model of Integrated Energy System. 2021 IEEE 4th International Conference on Renewable Energy and Power Engineering (REPE),

Ma, R., Deng, J., Li, H., & Qin, J. (2017, 26-28 Nov. 2017). Improved particle swarm optimization algorithm to multi-objective optimization energy hub model with P2G and energy storage. 2017 IEEE Conference on Energy Internet and Energy System Integration (EI2),

Manwell, J., McGowan, J., & Rogers, A. L. (2002). *Wind Energy Explained: Theory, Design and Application*. https://doi.org/10.1002/0470846127

Metropolis, N., & and Ulam, S. (1949, 1949/09/01). The Monte Carlo Method. *Journal of the American Statistical Association, 44*(247), 335-341. https://doi.org/10.1080/01621459.1949.10483310

Ministry of Energy. (2019). *Power Development Plan (2018)*. MOE. Retrieved April 2019 from https://www.eppo.go.th/images/POLICY/PDF/PDP2018.pdf

Ministry of Energy. (2020). *Alternative Energy Development Plan (2018)*. MOE. Retrieved October 2020 from https://policy.asiapacificenergy.org/sites/default/files/Alternative%20Energy%20Development%20Plan%202018-2037%20%28AEDP%202018%29%28TH%29.pdf

Mohammadi, M., Noorollahi, Y., Mohammadi-ivatloo, B., Yousefi, H., & Jalilinasrabady, S. (2017, 06/03). Optimal Scheduling of Energy Hubs in the Presence of Uncertainty-A Review. *Journal of Energy Management and Technology, 1*, 1-17. https://doi.org/10.22109/JEMT.2017.49432

Mousavi, M., Celli, G., & Pilo, F. (2022, 17-19 Oct. 2022). Multi-objective Scheduling of an Energy Hub in a Multi-energy System Using Genetic Algorithm. 2022 2nd

International Conference on Energy Transition in the Mediterranean Area (SyNERGY MED),

Osman, A. I., Mehta, N., Elgarahy, A. M., Hefny, M., Al-Hinai, A., Al-Muhtaseb, A. a. H., & Rooney, D. W. (2022, 2022/02/01). Hydrogen production, storage, utilisation and environmental impacts: a review. *Environmental Chemistry Letters, 20*(1), 153-188. https://doi.org/10.1007/s10311-021-01322-8

Ould Amrouche, S., Rekioua, D., Rekioua, T., & Bacha, S. (2016, 2016/12/07/). Overview of energy storage in renewable energy systems. *International Journal of Hydrogen Energy, 41*(45), 20914-20927. https://doi.org/https://doi.org/10.1016/j.ijhydene.2016.06.243

Piawises, W., & Chayakulkheeree, K. (2024, 6-8 March 2024). Smart Home Energy Management Algorithm for TOU-Based Demand Response. 2024 12th International Electrical Engineering Congress (iEECON),

Provincial Electricity Authority. (2023). *Electricity tariffs (May 2023)*. P. E. Authority. https://www.pea.co.th/sites/default/files/documents/tariff/EN_Electricity_Tariffs_May_2023.pdf

Qadrdan, M., Abeysekera, M., Chaudry, M., Wu, J., & Jenkins, N. (2015, 2015/05/11/). Role of power-to-gas in an integrated gas and electricity system in Great Britain. *International Journal of Hydrogen Energy, 40*(17), 5763-5775. https://doi.org/https://doi.org/10.1016/j.ijhydene.2015.03.004

Ranjbarzadeh, H., Tafreshi, S. M. M., Ali, M. H., Kouzani, A. Z., & Khoo, S. (2022). A Probabilistic Model for Minimization of Solar Energy Operation Costs as Well as CO2 Emissions in a Multi-Carrier Microgrid (MCMG). *Energies, 15*(9), 3088. https://www.mdpi.com/1996-1073/15/9/3088

Reuters. (2025). *Thai cabinet approves collection of carbon tax*. Reuters. Retrieved January 21 from https://www.reuters.com/sustainability/thai-cabinet-approves-collection-carbon-tax-2025-01-21/

Shatnawi, M., Qaydi, N. A., Aljaberi, N., & Aljaberi, M. (2018). Hydrogen-Based Energy Storage Systems: A Review. *2018 7th International Conference on Renewable Energy Research and Applications (ICRERA)*, 697-700.

Son, Y. G., Oh, B. C., Acquah, M. A., Fan, R., Kim, D. M., & Kim, S. Y. (2021). Multi Energy System With an Associated Energy Hub: A Review. *IEEE Access, 9*, 127753-127766. https://doi.org/10.1109/ACCESS.2021.3108142

Thailand Greenhouse Gas Management Organization (Public Organization). (2022). *Emission Factors for Carbon Footprint Calculation*. https://thaicarbonlabel.tgo.or.th/index.php?lang=EN&mod=YjNKbllXNXBlbUYwYVc5dVgyVnRhWE56YVc5dQ&utm

Thang, V. V., Ha, T., Li, Q., & Zhang, Y. (2022, 2022/10/01/). Stochastic optimization in multi-energy hub system operation considering solar energy resource and demand response. *International Journal of Electrical Power & Energy Systems, 141*, 108132. https://doi.org/https://doi.org/10.1016/j.ijepes.2022.108132

Thanh-tung, H., Yong-jun, Z., Jian-ang, H., & Thang, V. V. (2016, 21-23 Oct. 2016). Energy Hub modeling for minimal energy usage cost in residential areas. 2016 IEEE International Conference on Power and Renewable Energy (ICPRE),

Timothée, C., Perera, A. T. D., Scartezzini, J.-L., & Mauree, D. (2017, 2017/12/01/). Optimum dispatch of a multi-storage and multi-energy hub with demand response and restricted grid interactions. *Energy Procedia, 142*, 2864-2869. https://doi.org/https://doi.org/10.1016/j.egypro.2017.12.434

Wang, L. (2023). Optimal Scheduling Strategy for Multi-Energy Microgrid Considering Integrated Demand Response. *Energies, 16*(12).

Wood, A. J., Wollenberg, B. F., & Sheblé, G. B. (2013). *Power generation, operation, and control*. John wiley & sons.

Xu, F., Li, X., & Jin, C. (2024). A multi-objective operation optimization model for the electro-thermal integrated energy systems considering power to gas and multi-

type demand response. *Journal of Renewable and Sustainable Energy, 16*(4). https://doi.org/10.1063/5.0217570

Yammani, C., Maheswarapu, S., & Kumari, M. (2012, 08/31). Optimal Placement of Multi DGs in Distribution System with Considering the DG Bus Available Limits. *Energy and Power, 2*, 18-23. https://doi.org/10.5923/j.ep.20120201.03

Zhang, W., Han, D., Sun, W., Li, H., Tan, Y., Yan, Z., & Dong, X. (2017, 26-28 Nov. 2017). Optimal operation of wind-solar-hydrogen storage system based on energy hub. 2017 IEEE Conference on Energy Internet and Energy System Integration (EI2),

Zidan, A., & Gabbar, H. A. (2016, 21-24 Aug. 2016). Optimal scheduling of energy hubs in interconnected multi energy systems. 2016 IEEE Smart Energy Grid Engineering (SEGE),

APPENDIX

APPENDIX A

Every energy profile for used in deterministic studies

Table A.1 Electricity load profile (Base load 2 MW)

Hour	Load (p.u.)	Hour	Load (p.u.)	Hour	Load (p.u.)
1	0.732	9	0.710	17	0.798
2	0.682	10	0.737	18	0.788
3	0.638	11	0.762	19	0.964
4	0.613	12	0.747	20	1
5	0.636	13	0.719	21	0.967
6	0.733	14	0.825	22	0.906
7	0.715	15	0.840	23	0.867
8	0.674	16	0.845	24	0.802

Table A.2 Heat load profile (Base load 2 MW)

Hour	Load (p.u.)	Hour	Load (p.u.)	Hour	Load (p.u.)
1	0.650	9	0.983	17	0.858
2	0.667	10	0.992	18	0.825
3	0.650	11	0.992	19	0.808
4	0.650	12	1	20	0.808
5	0.725	13	1	21	0.800
6	0.800	14	0.975	22	0.797
7	0.875	15	0.958	23	0.717
8	0.950	16	0.900	24	0.650

Table A.3 Solar power profile

Hour	Generation (kW)	Hour	Generation (kW)	Hour	Generation (kW)
1	0	9	484.224	17	369.615
2	0	10	696.251	18	137.531
3	0	11	868.164	19	5.730
4	0	12	999.965	20	0
5	0	13	999.965	21	0
6	0	14	939.795	22	0
7	34.383	15	787.938	23	0
8	243.544	16	598.833	24	0

Table A.4 Wind power profile

Hour	Generation (kW)	Hour	Generation (kW)	Hour	Generation (kW)
1	0	9	2000	17	469.543
2	109.424	10	2000	18	568.678
3	1860.538	11	852.158	19	0
4	2000	12	163.339	20	0
5	2000	13	121.572	21	31.561
6	2000	14	1103.843	22	36.961
7	2000	15	1131.437	23	109.425
8	2000	16	469.543	24	73.306

APPENDIX B

Hourly probabilistic scheduling results

(Graphical Data visualization)

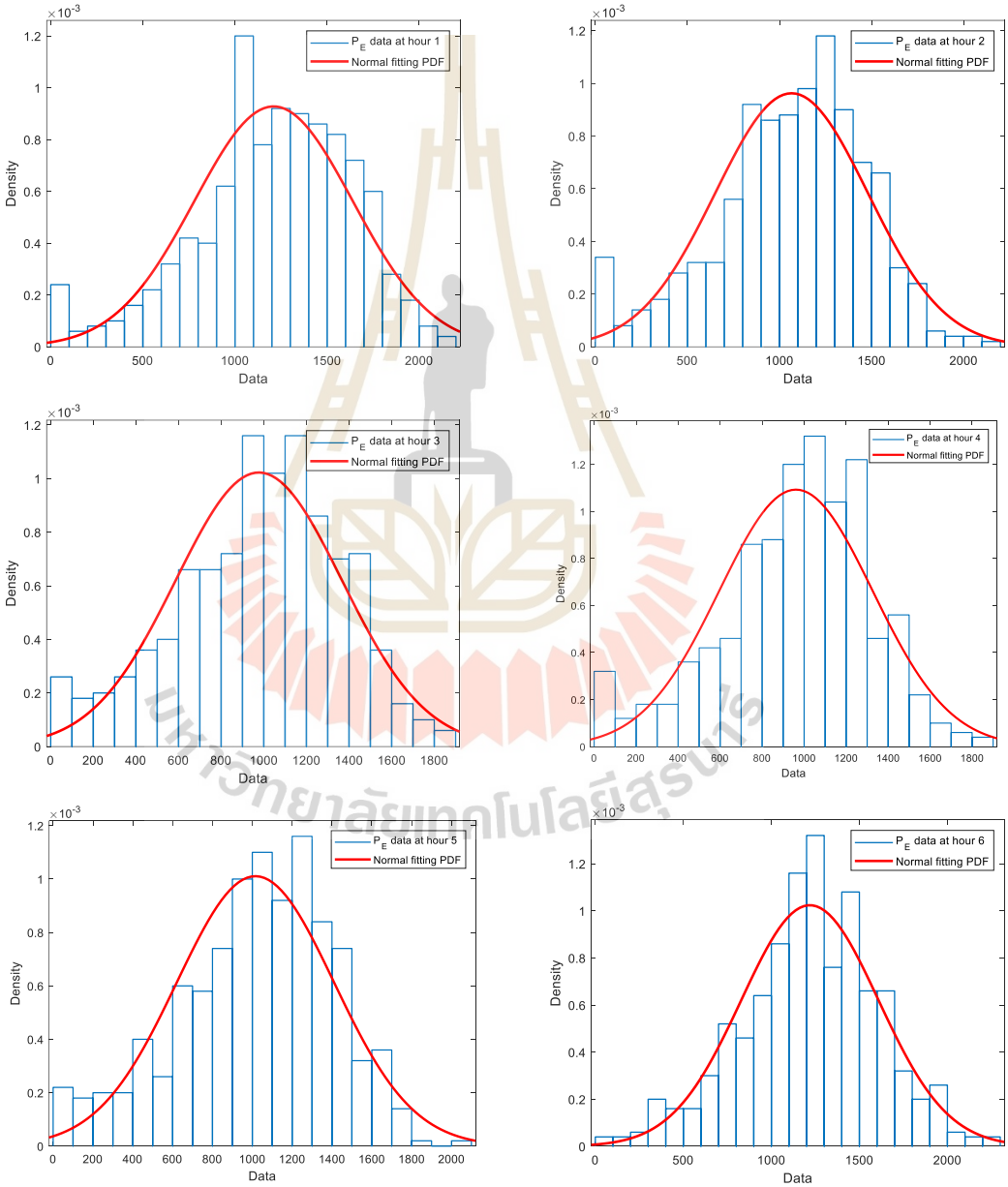

Figure B.1 The PDF of P_E scheduling in operating hours

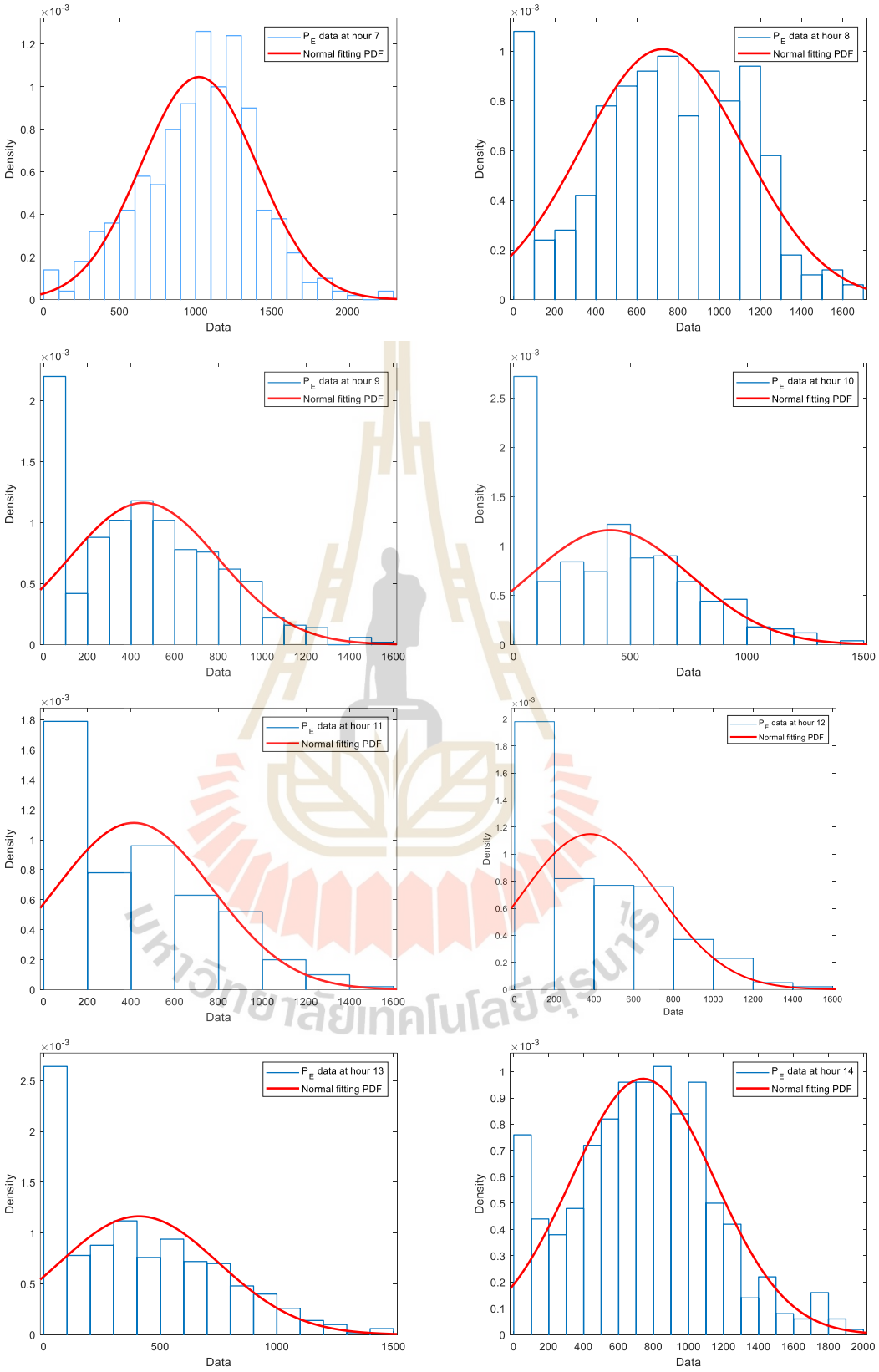

Figure B.1 The PDF of P_E scheduling in operating hours (Continued)

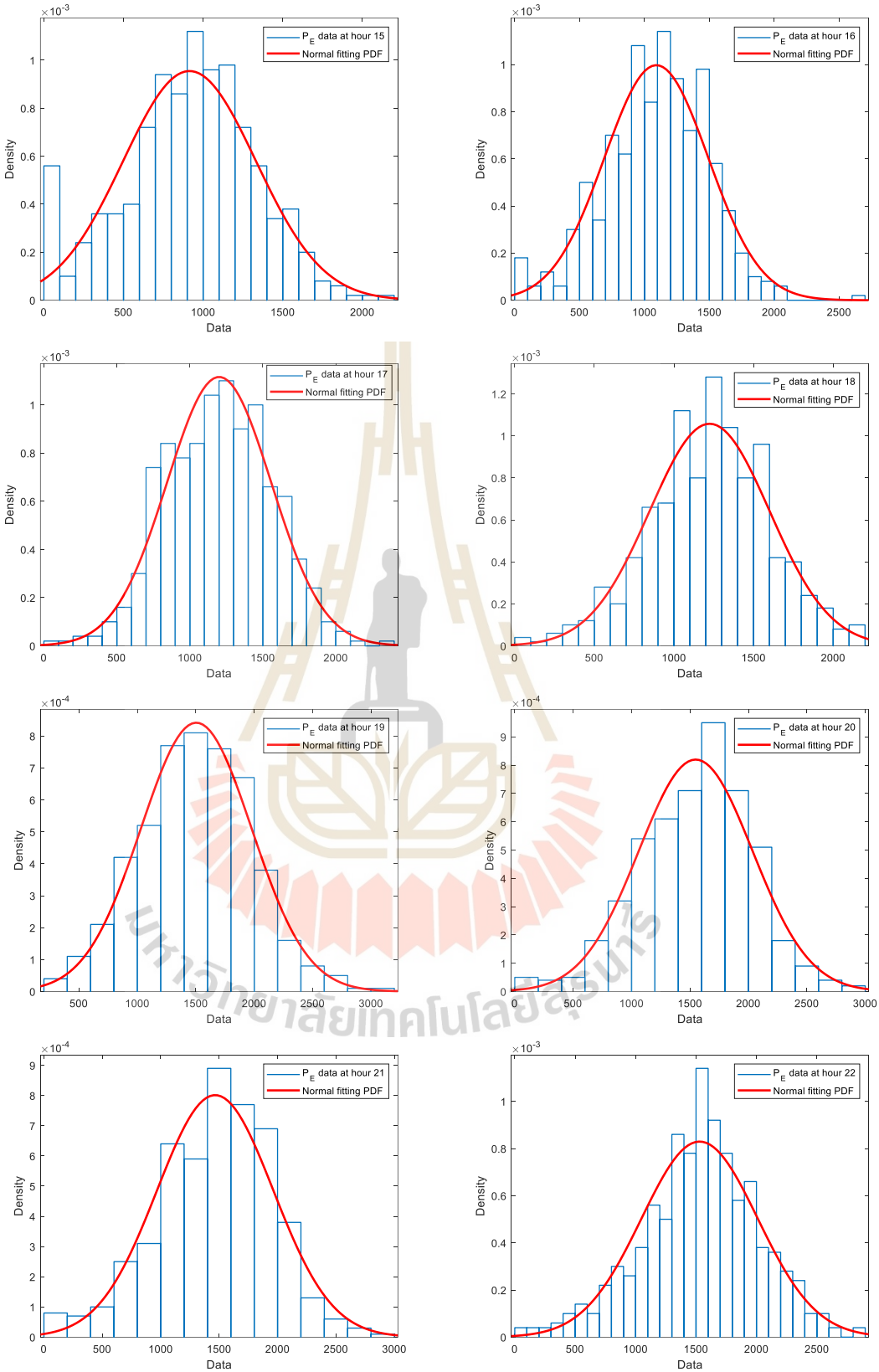

Figure B.1 The PDF of P_E scheduling in operating hours (Continued)

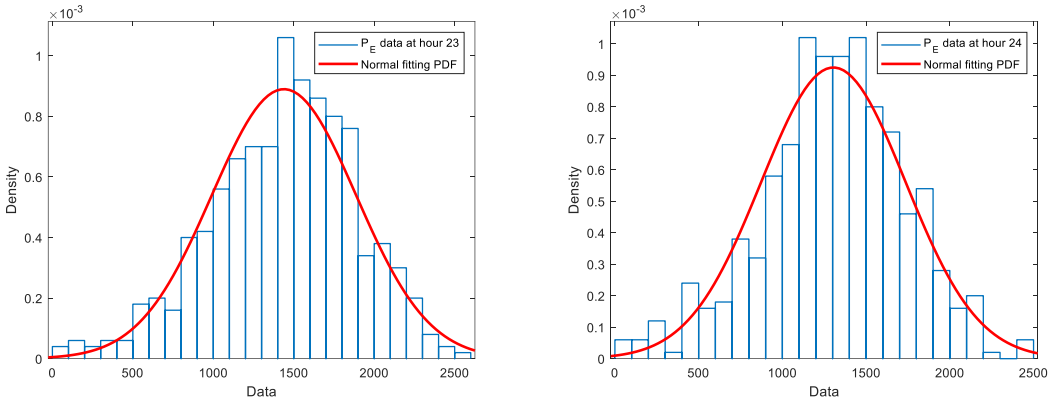

Figure B.1 The PDF of P_E scheduling in operating hours (Continued)

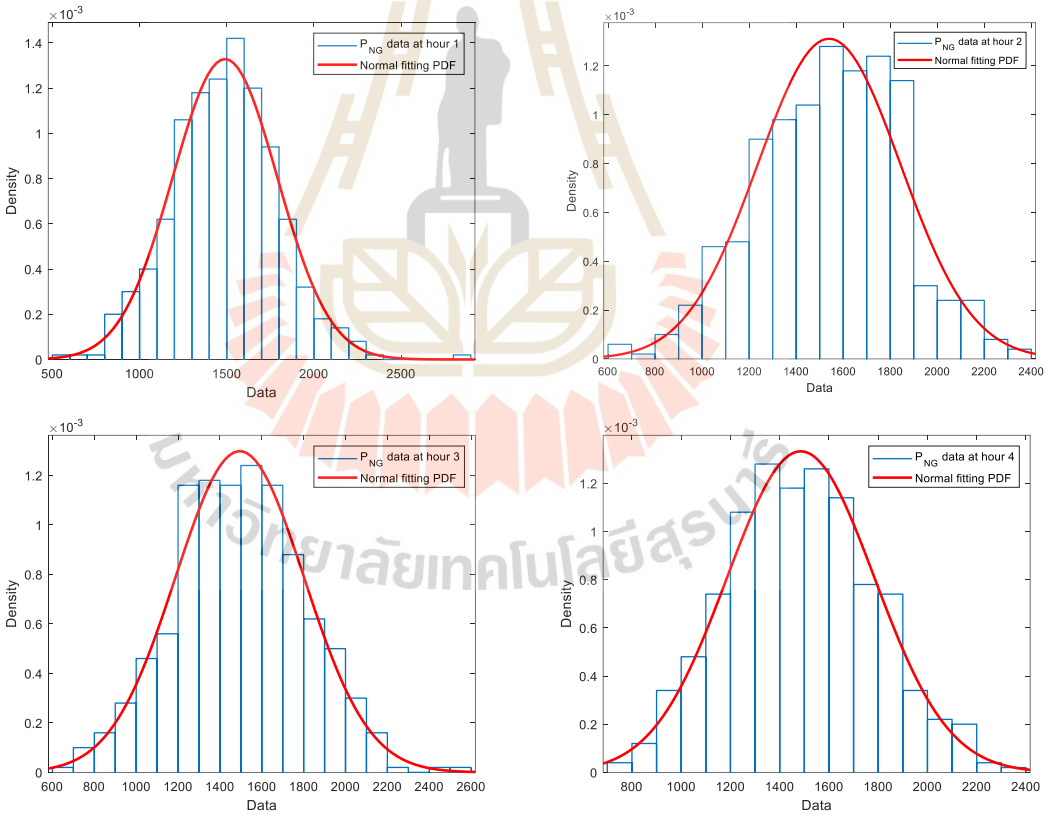

Figure B.2 The PDF of P_{NG} scheduling in operating hours

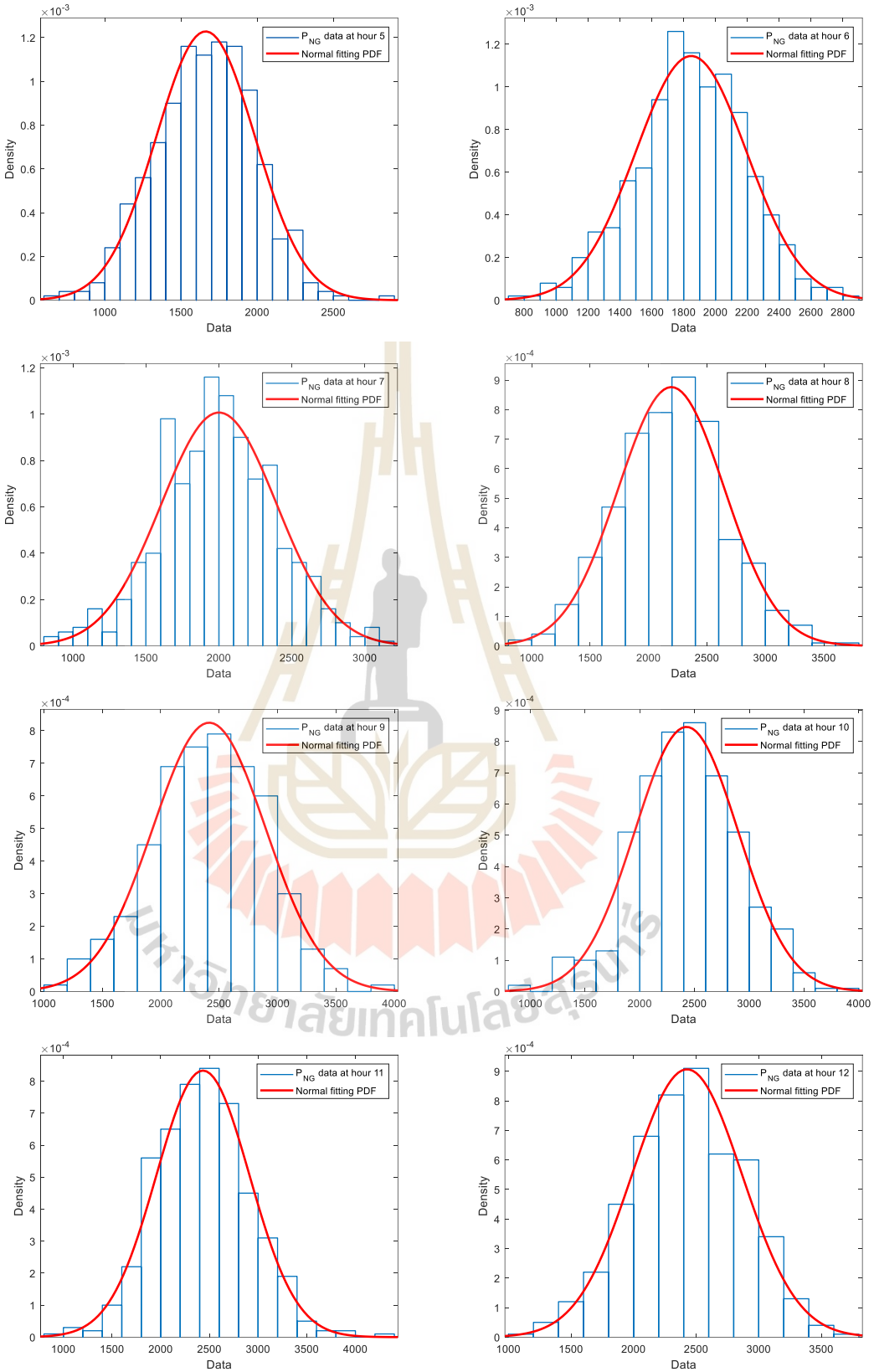

Figure B.2 The PDF of P_{NG} scheduling in operating hours (Continued)

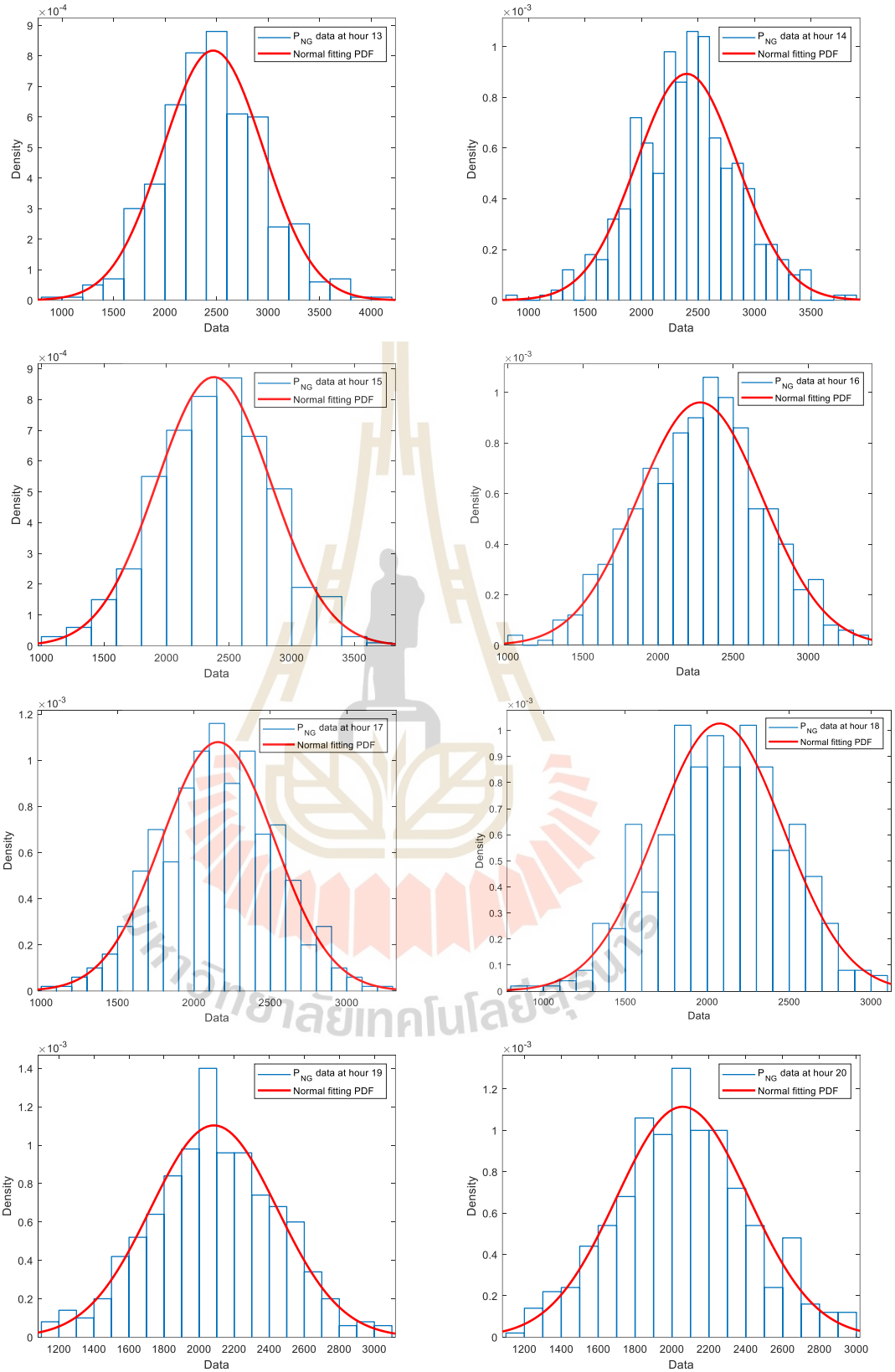

Figure B.2 The PDF of P_{NG} scheduling in operating hours (Continued)

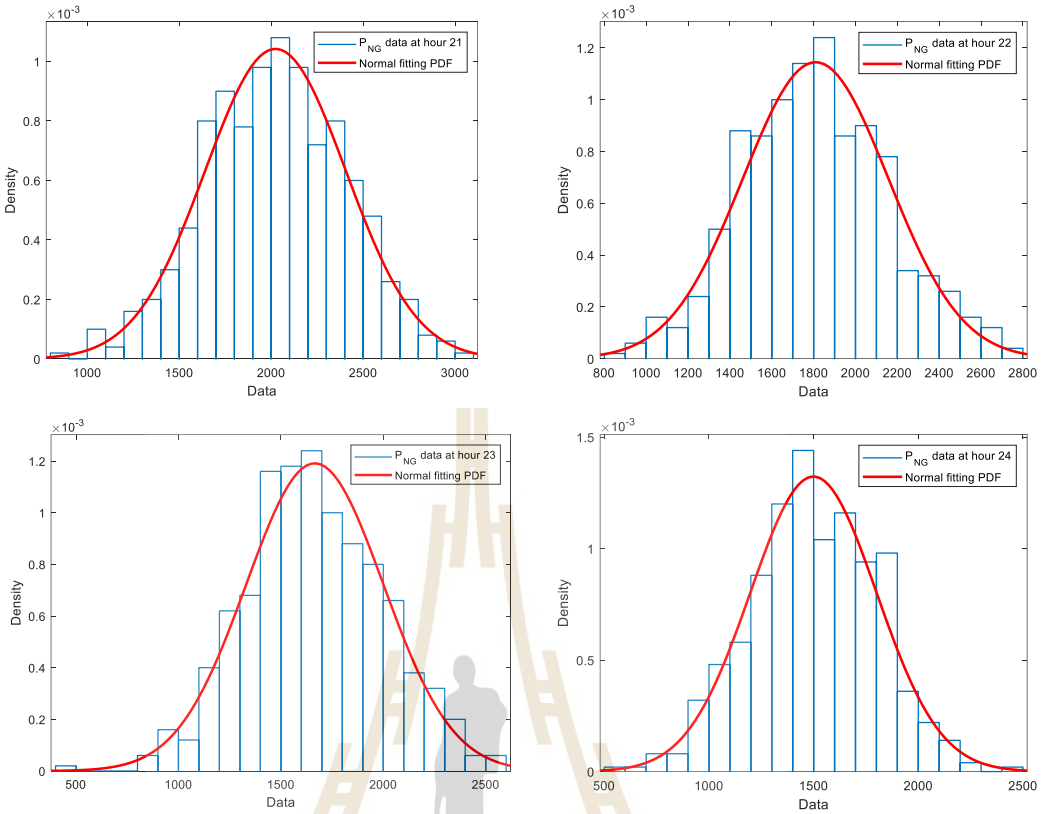

Figure B.2 The PDF of P_{NG} scheduling in operating hours (Continued)

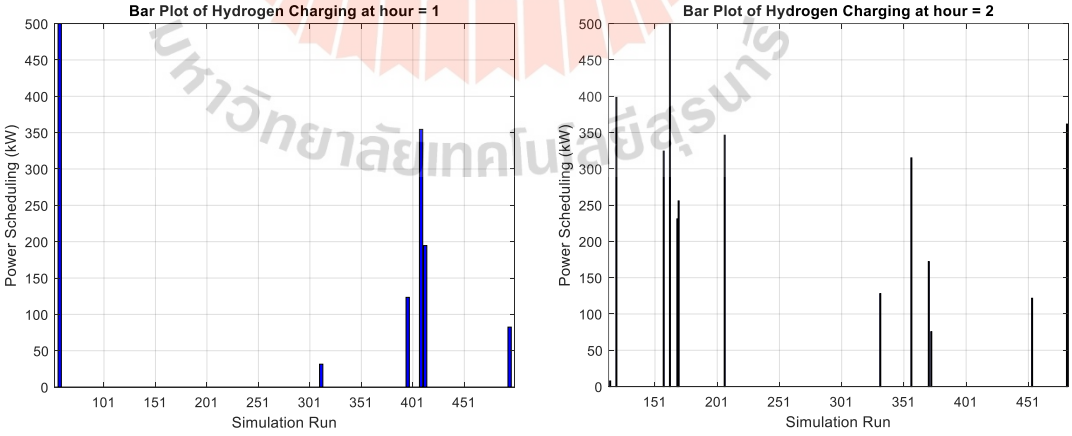

Figure B.3 The bar plot of P_{EL} which is hydrogen charging in operating hours

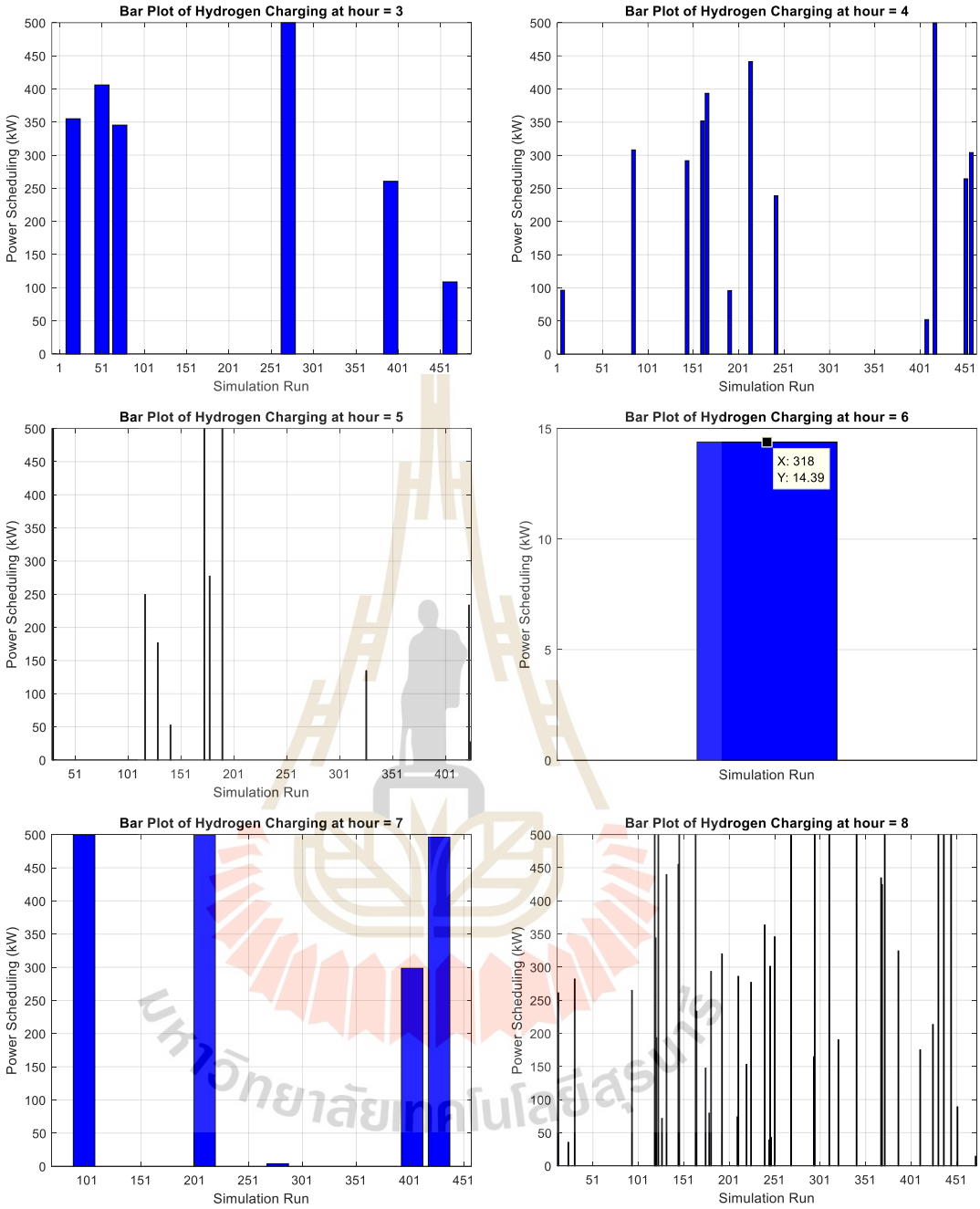

Figure B.3 The bar plot of P_{EL} which is hydrogen charging in operating hours (Continued)

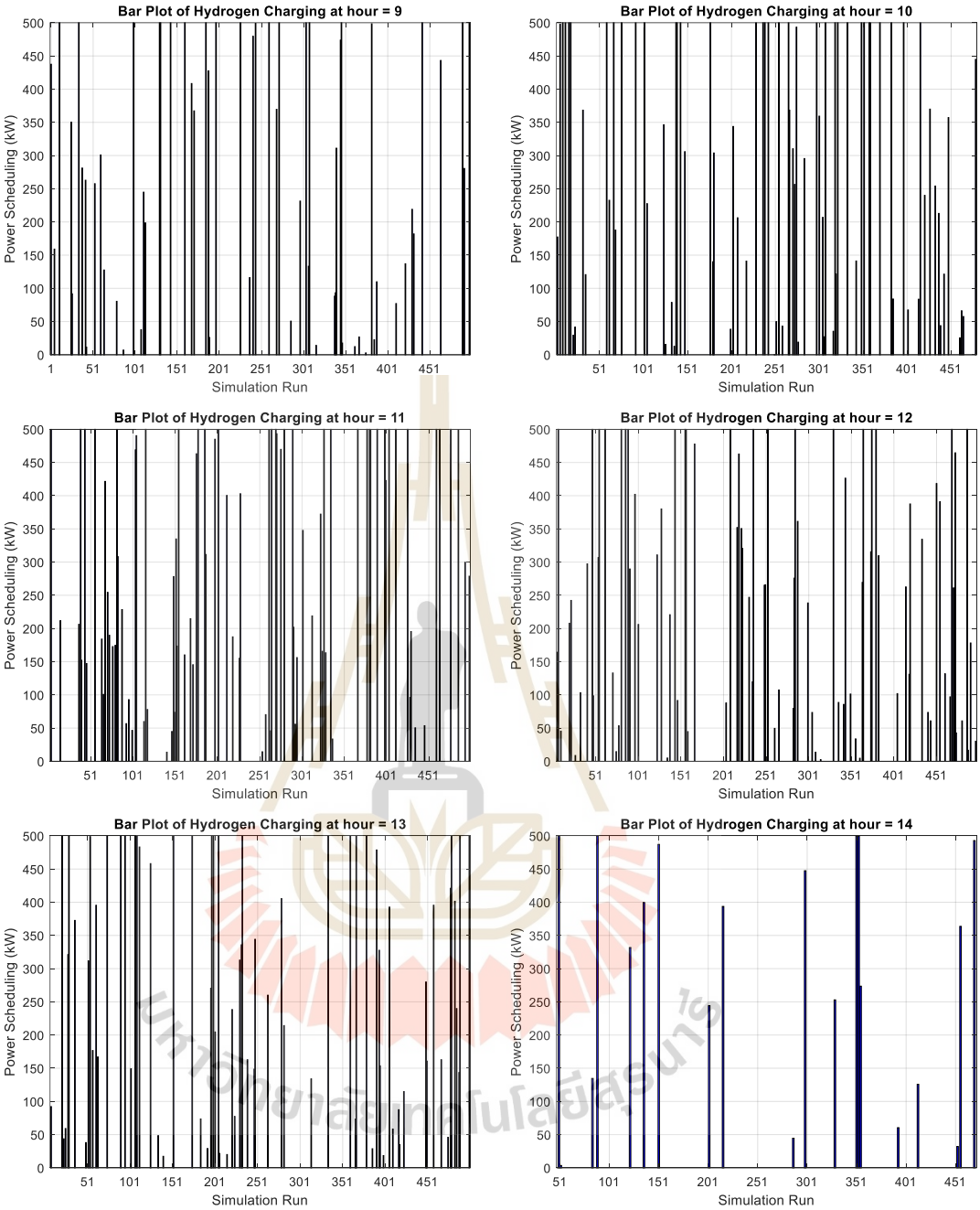

Figure B.3 The bar plot of P_{EL} which is hydrogen charging in operating hours (Continued)

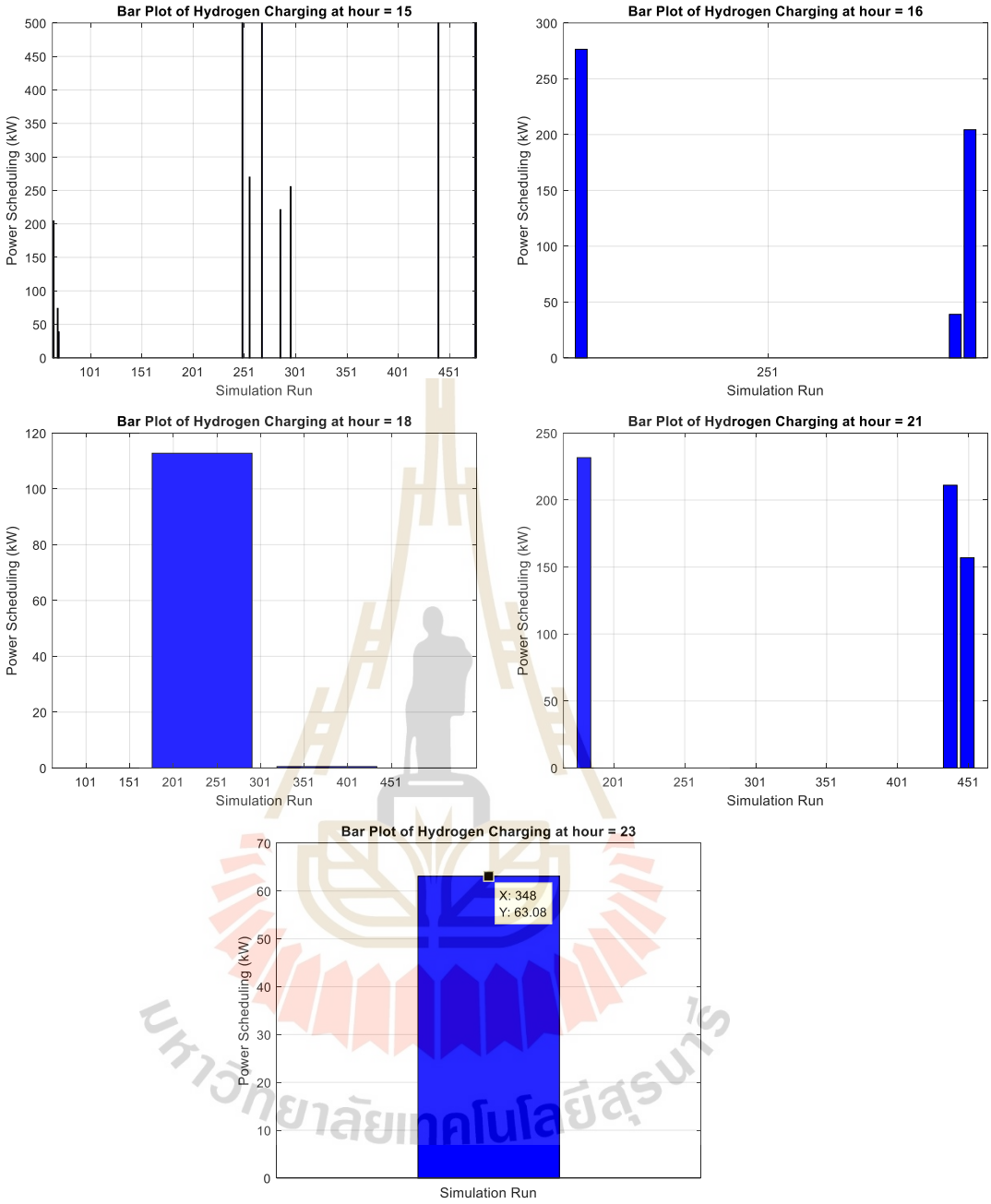

Figure B.3 The bar plot of P_{EL} which is hydrogen charging in operating hours (Continued)

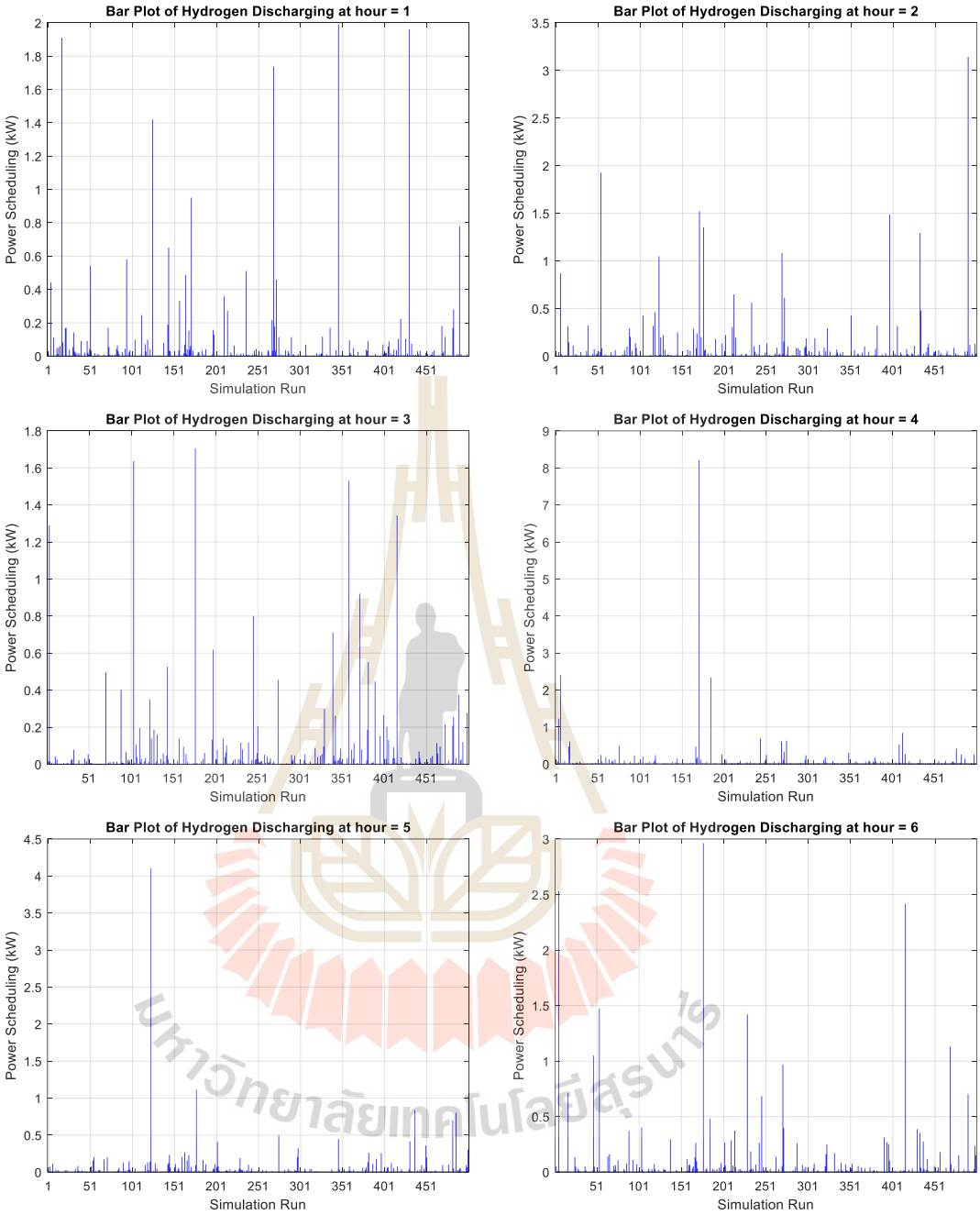

Figure B.4 The bar plot of P_{FC} which is hydrogen discharging in operating hours

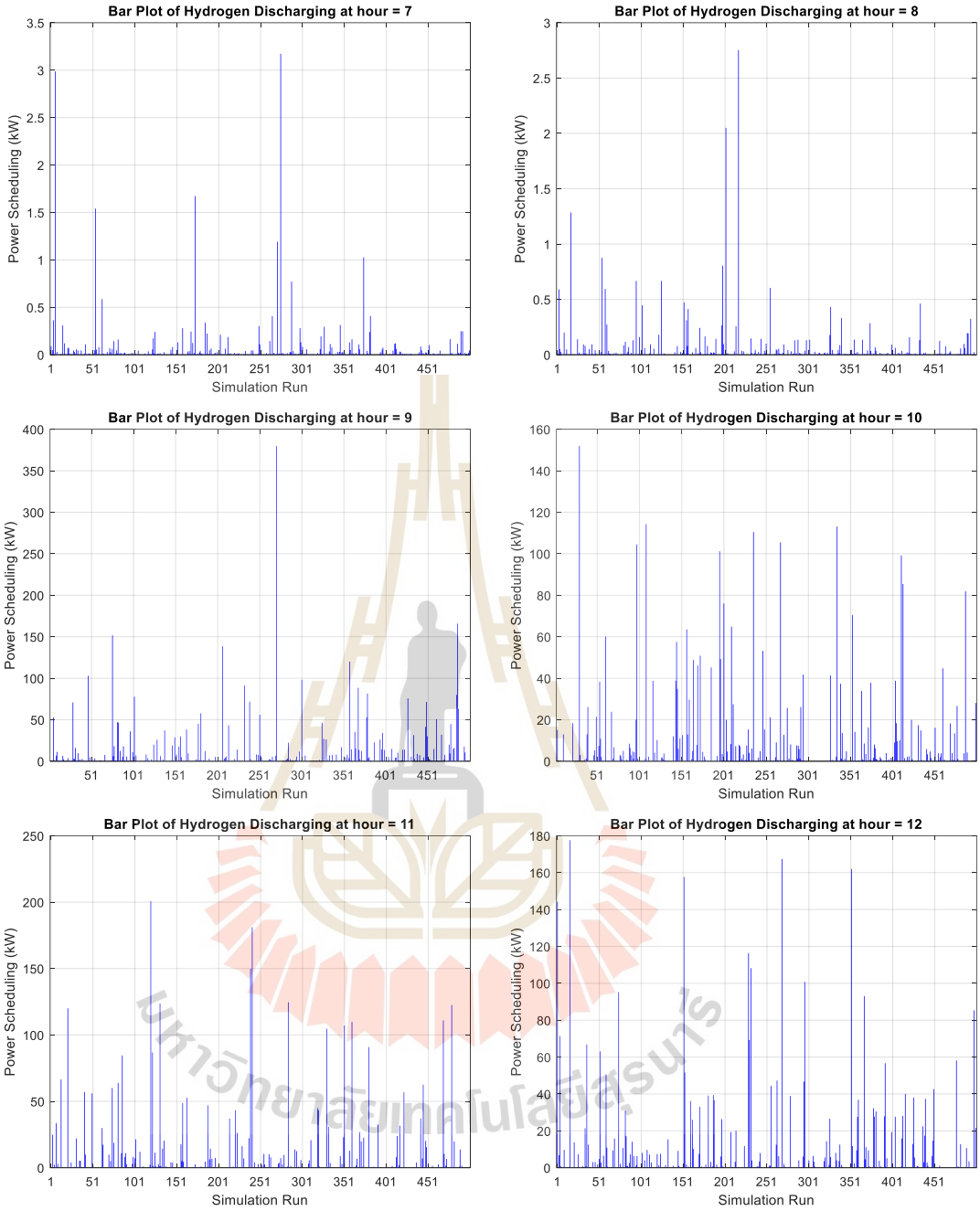

Figure B.4 The bar plot of P_{FC} which is hydrogen discharging in operating hours (Continued)

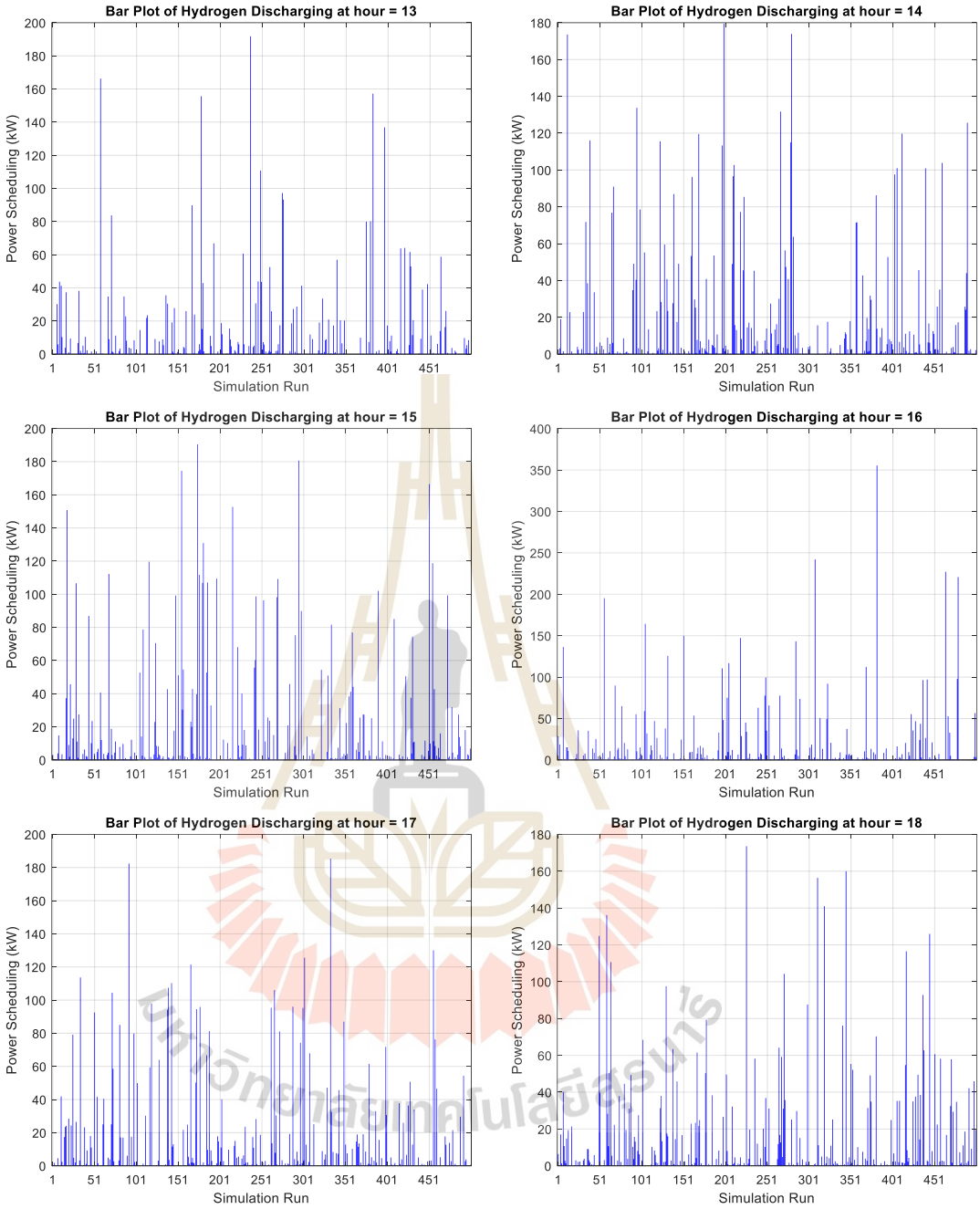

Figure B.4 The bar plot of P_{FC} which is hydrogen discharging in operating hours (Continued)

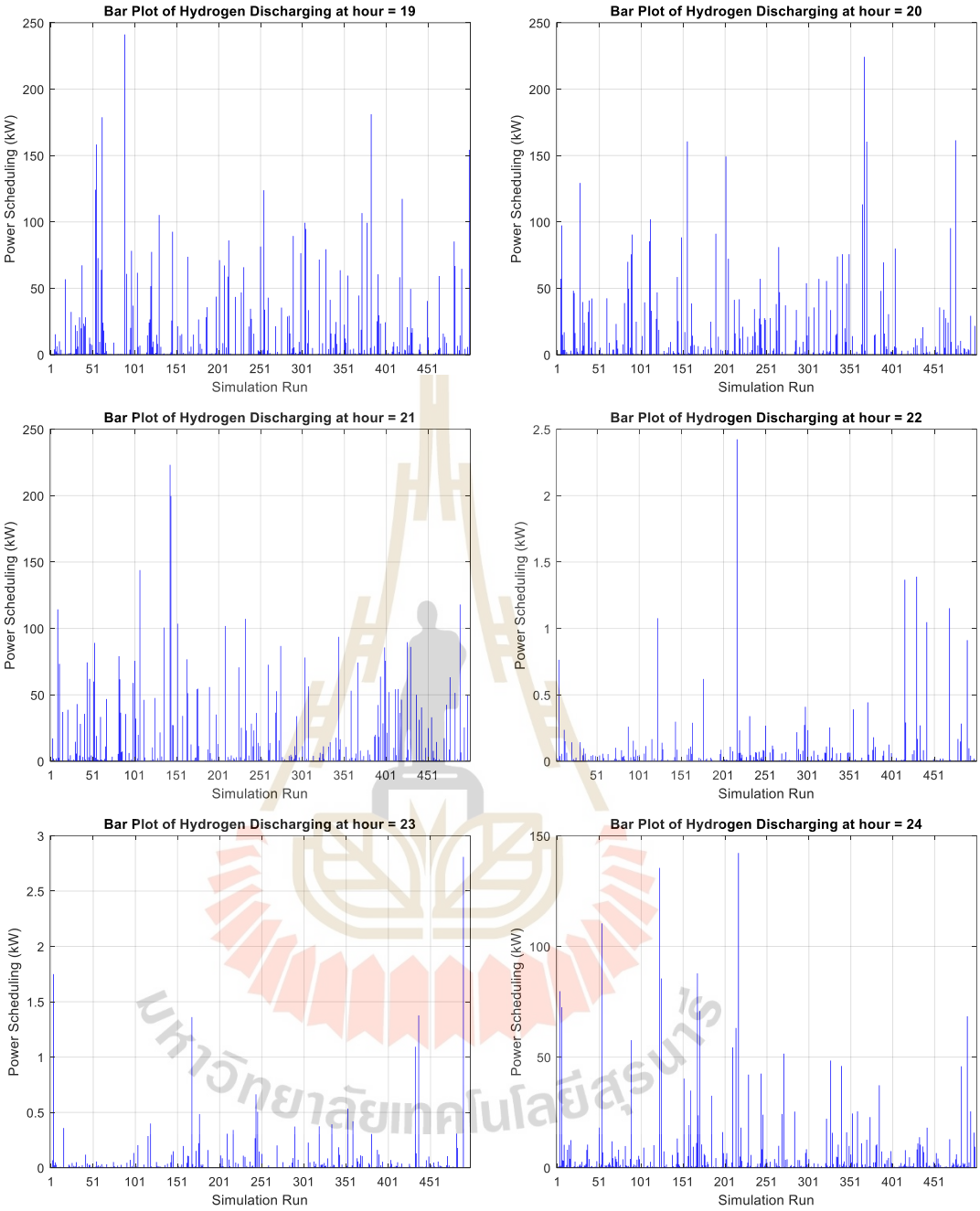

Figure B.4 The bar plot of P_{FC} which is hydrogen discharging in operating hours (Continued)

APPENDIX C

Detailed Simulation Results for Varying Initial Pressure in Case V under TOU Tariffs Considerations

This appendix presents the simulation results for various initial pressure values tested under OMES-WSPHS model with TOU tariffs in Case V. The results provide insights into how different initial pressure values impact system performance, as objective function in TOC. The data are organized as follows:

Table C.1 Simulation results for 40 bar Initial pressure

Energy scheduling	Energy (kWh)	Costs	TOC
Electricity	13,698.62	51,399.14	240,717.78
NG	47,329.66	189,318.64	
HS	6,531.35	-	

Table C.2 Simulation results for 60 bar Initial pressure

Energy scheduling	Energy (kWh)	Costs	TOC
Electricity	13,697.84	52,543.83	241,862.47
NG	47,329.66	189,318.64	
HS	6,533.94	-	

Table C.3 Simulation results for 80 bar Initial pressure

Energy scheduling	Energy (kWh)	Costs	TOC
Electricity	14,019.32	54,880.09	244,113.58
NG	47,308.37	189,233.49	
HS	5,535.44	-	

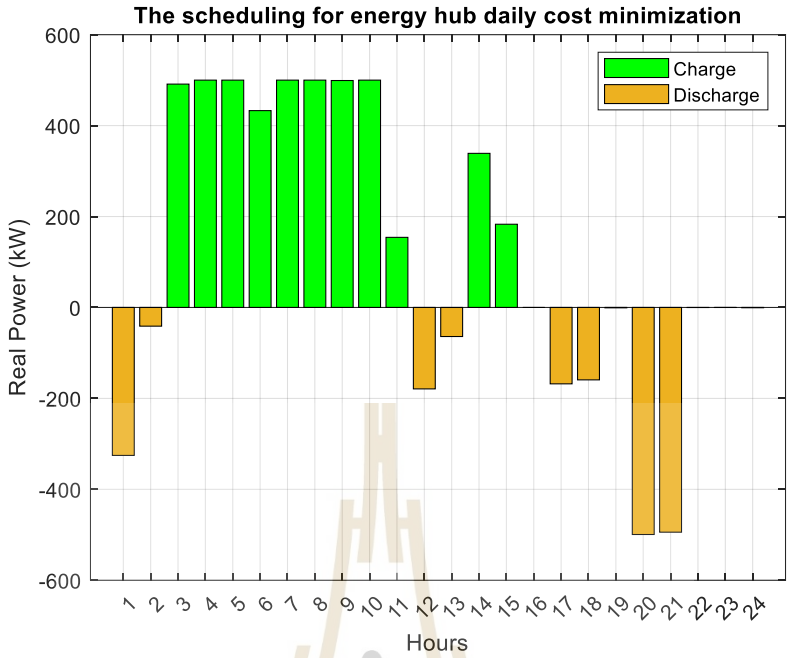

(a)

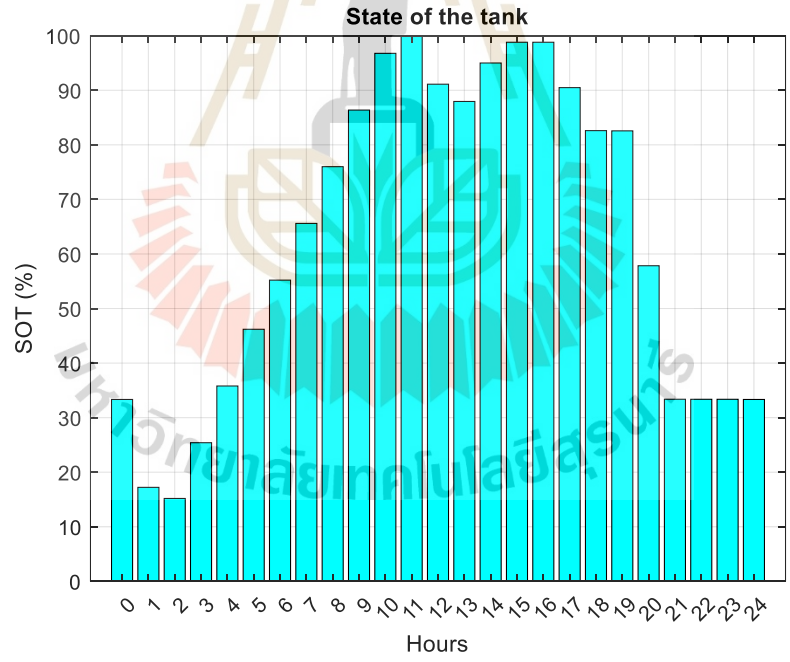

(b)

Figure C.1 (a) HS scheduling for 24 hours and (b) SOT 40 bar Initial pressure

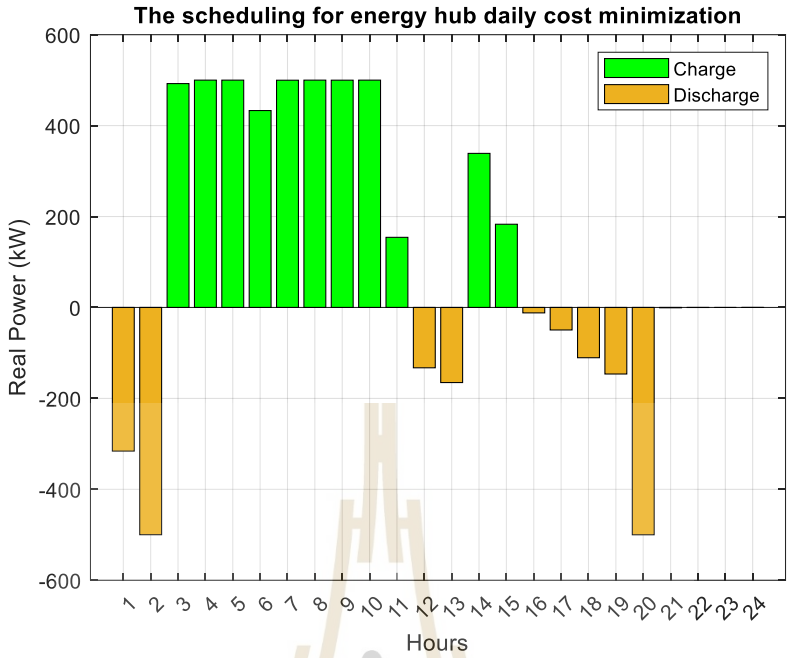

(a)

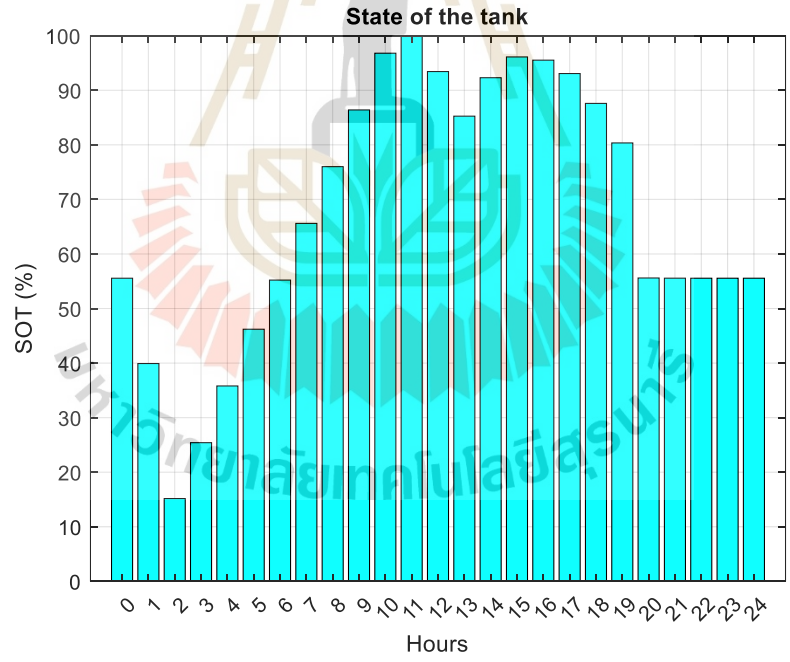

(b)

Figure C.2 (a) HS scheduling for 24 hours and (b) SOT for 60 bar Initial pressure

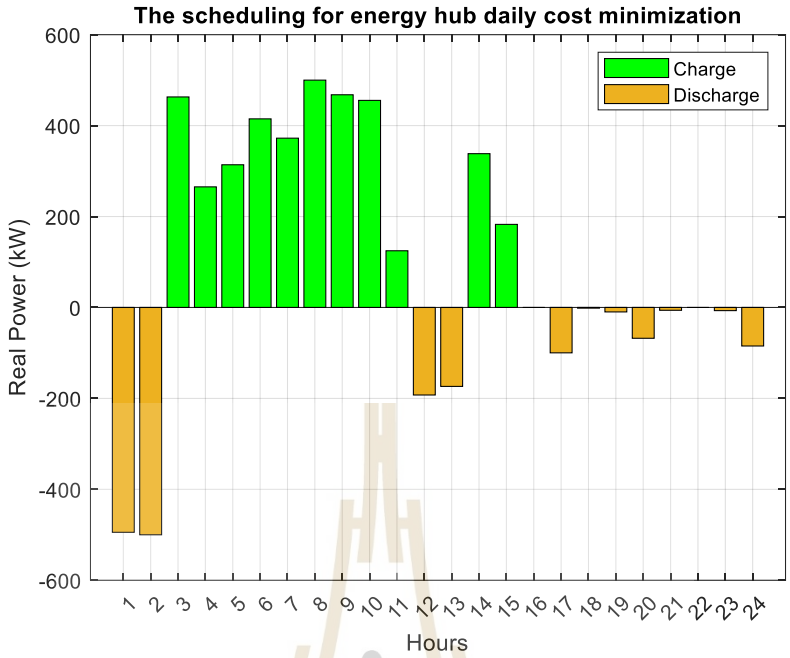

(a)

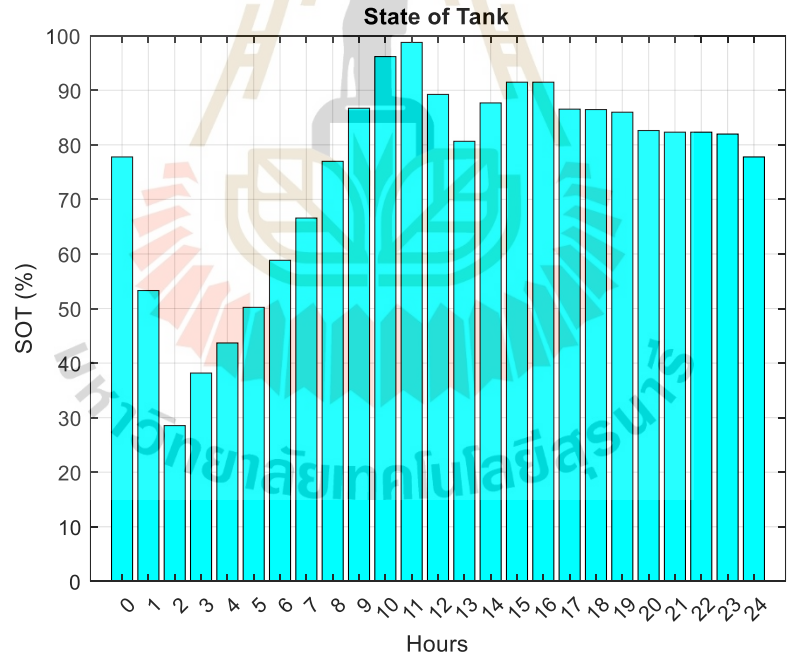

(b)

Figure C.3 (a) HS scheduling for 24 hours and (b) SOT for 80 bar Initial pressure

APPENDIX D

List of publications

S. Dechjinda and K. Chayakulkheeree (2024), Optimal Daily Scheduling of Hybrid Wind-Hydrogen Storage using Particle Swarm Optimization, 2024 International Electrical Engineering Congress (iEECON2024), Pattaya, Thailand.

S. Dechjinda and K. Chayakulkheeree (2024), Optimal scheduling of multi-energy systems with wind-solar power and hydrogen storage integration., GMSARN International Journal.

2024 International Electrical Engineering Congress (iEECON 2024)
March 6-8, 2024, Pattaya Chonburi, THAILAND

Optimal Daily Scheduling of Hybrid Wind-Hydrogen Storage Using Particle Swarm Optimization

Suttipong Dechjinda **Keerati Chayakulkheeree**

School of Electrical Engineering
Institute of Engineering, Suranaree University of Technology
Nakhonratchasima, Thailand
E-mail: suttipong.dechjinda@gmail.com, keerati.ch@sut.ac.th

***Abstract*— This paper proposes a particle swarm optimization-based optimal daily scheduling (PSO-ODS) for hybrid wind-hydrogen storage (HWHS). Minimizing daily energy loss (DL) is the main goal of the presented method. The approaches of PSO-ODS for HWHS were inspected with the modified IEEE 33-bus system with HWHS integration using load and wind profiles of Thailand. The studies are separated into two cases, which are the wind-integrated system with and without hydrogen storage optimal scheduling. The proposed approach can effectively decrease DL for the HWHS integrated distribution system, as indicated by the simulation results.**

Keywords— optimal daily scheduling, hydrogen storage, particle swarm optimization, wind energy.

NOMENCLATURE

ch	:	The matrix of charging of hydrogen storage.
dch	:	The matrix of discharging of hydrogen storage.
NB	:	The total number of buses.
NT	:	The total number of wind turbines.
PN	:	The penalty functions.
P_{EL}	:	The power of electrolyzer (kW).
$P_{EL,rated}$	:	The rated power of electrolyzer (kW).
P_{FC}	:	The power of fuel cell (kW).
$P_{FC,rated}$	:	The rated power of fuel cell (kW).
η_{EL}	:	The efficiency of electrolyzer (%).
η_{FC}	:	The efficiency of fuel cell (%).
E_{tank}	:	The energy of the hydrogen tank (kWh).
$E_{tank,rated}$	:	The rated energy of the hydrogen tank (kWh).
$P_{loss,h}$	:	The hourly power loss (kW).
DL	:	The daily energy loss (kWh).
$P_{w,h}$	:	The hourly wind power output (kW).
$P_{w,rated}$	:	The rated wind turbine (kW).
$P_{wpp,h}$	:	The hourly power output of wind power plants (kW).
V_i	:	The voltage of bus i (p.u.).
v_h	:	The wind velocity per hour (m/s).
$v_{w,rated}$	:	The rated wind velocity (m/s).
$v_{cut\text{-}in}$	:	The wind velocity specification allows the wind turbine to generate power (m/s).
$v_{cut\text{-}off}$	:	The wind speed specification allows the wind turbine to halt generating power (m/s).
G_{ij}	:	The line's conductance across buses i and j for $i \neq j$ (S).
δ_i	:	The angle bus voltage i (radian).

I. INTRODUCTION

Nowadays, energy from renewable sources is facing a significant challenge due to its inherent instability. The discontinuous pattern of renewable resources is one of their primary drawbacks, with most sources being unavailable for consistent utilization. For instance, wind power experiences fluctuations in wind speed, leading to unpredictable energy generation [1]. Although wind energy presently has the most developed technology, the most favorable large-scale improvement circumstances, and the most promising commercial growth tendency among renewable energy sources, its instability and unpredictability provide significant challenges to the power grid's ability to operate safely and steadily. A significant amount of wind energy is wasted when it is required to give up the wind in order to protect the power system, particularly when peak shaving is challenging [2]. Consequently, the significance of implementing energy storage systems grows as the amount of power produced from renewable resources rises [1-2]. There are several approaches to storing energy. One of the most modern technologies for storing surplus energy generated during off-peak hours is the retention of hydrogen. that has been stored can then be used to generate energy at peak times [3].

Hydrogen energy storage system (HESS) is a potential option for decarbonizing energy systems since it can produce electricity by using carbon-neutral renewable energy resources. When employed as an energy source, hydrogen exhibits the advantage of emitting no CO_2, making it an environmentally friendly alternative. Therefore, hydrogen energy storage is suitable for storing secondary energy. However, the challenge with hydrogen production from renewable sources is the low overall efficiency of energy conversion results in considerable energy and monetary losses [4-5].

As a result, much research related to hybrid wind-hydrogen system (HWHS) scheduling has been proposed. Hong et al. [2] investigated the optimal scheduling approach for the HWHS system while taking wind power efficiency into consideration. The artificial bee colony technique was utilized to tackle the problem of hydrogen production, increasing efficiency by 4.8%. O. Utomo et al. [4] discussed the optimal effective operations of a hydrogen storage and a fuel cell-connected energy system. The energy hub approach describes the system's mathematical structure. Meanwhile, linear programming is employed to lower total operating costs.

979-8-3503-8359-1/24/$31.00 ©2024 IEEE

G. He et al. [5] proposed an improved particle swarm optimization algorithm (IDW-PSO) that uses dynamic inertia weight adjustment to optimize the capacity configuration of a wind-solar hydrogen storage microgrid system. The approach improves optimization accuracy, lowers the probability of falling into the optimal location, and increases iteration performance.

There is plenty of knowledge and development needed for HWHS integration. Therefore, this paper proposes optimal daily scheduling (ODS) of HWHS to minimize daily energy loss (*DL*). The particle swarm optimization (PSO) is used to solve the proposed ODS for HWHS. To ascertain the validity and efficiency of the proposed approach, the modified IEEE 33-bus test system with HWHS is used as a case study.

The paper is structured in the following format. Section II addresses the HWHS modeling. The PSO-based ODS algorithm for resolving HWHS is presented in Section III. Section IV demonstrates and discusses the simulation results of the proposed PSO-ODS for HWHS using the modified IEEE 33-bus system. Finally, Section V provides the conclusion.

II. HWHS Modeling

For HWHS modeling, the wind power plant (WPP) and HESS are connected to a bus. While WPP generates the electricity, HESS schedules to eliminate wind power curtailment and regulate the power fluctuations. The model of the distribution system with HWHS is shown in Fig.1.

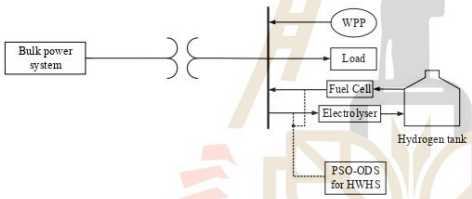

Fig. 1. The model of distribution system with HWHS.

A. Wind Power Modeling

A wind turbine will produce power when its velocity comes between the turbine's rated speed and the cut-in speed. If the velocity of the wind rises above the turbine's rated speed but falls below the cut-off speed, the output keeps the rated power constant. When the velocity of the wind surpasses the cut-off speed, the turbine is either halted to prevent the blades from rotating or pitched out of the wind.

A representation of the power performed from a wind turbine is (1) [6]:

$$P_{w,h}=\begin{cases}0 & \text{for} \quad 0<v_h\le v_{cut-in},\\ P_{w,rated}\times\left(\dfrac{v_h}{v_{w,rated}}\right)^3 & \text{for} \quad v_{cut-in}<v_h\le v_{w,rated},\\ P_{w,rated} & \text{for} \quad v_{w,rated}<v_h\le v_{cut-off},\\ 0 & \text{for} \quad v_h>v_{cut-off}.\end{cases} \tag{1}$$

The real power is injected into the load bus for peak shaving, whereas oscillation in wind speed affects the ability to cut peak during high demand times.

WPP consists of many wind turbines installed; the wind power of wind turbines in each hour is calculated from (1). When calculating the sum of wind power from all wind turbines, it is formulated as (2),

$$P_{wpp,h}=\sum_{i=1}^{NT}P_{w,i,h}. \tag{2}$$

B. HESS Modeling

Typically, the HESS consists of a pressurized gas tank, an electrolyzer, and fuel cells. The electrolyzer transforms electricity into a chemical substance in the shape of hydrogen when there is a surplus of power from the electricity. The hydrogen is stored to be used in a fuel cell, which uses oxygen from the air and hydrogen from the gaseous state for the generation of electricity. Long-term energy storage is possible when using hydrogen [7-8]. The efficiency models of HESS are given as (3) and (4).

$$P_{EL}=\eta_{EL}\times P_{wpp}, \tag{3}$$

$$P_{FC}=\eta_{FC}\times P_{EL}. \tag{4}$$

Fuel cells and the electrolyzer's efficiency are provided by [4]. HESS charging and discharging are carried out by the matrix, demonstrated in (5) and (6).

$$\mathbf{ch}=\left[P_{EL,1},\ldots,P_{EL,h},\ldots,P_{EL,24}\right],$$
$$\text{for } h=1,2,3,\ldots,24, \tag{5}$$

$$\mathbf{dch}=\left[P_{FC,1},\ldots,P_{FC,h},\ldots,P_{FC,24}\right],$$
$$\text{for } h=1,2,3,\ldots,24. \tag{6}$$

III. PSO-Based ODS Algorithm

PSO is a swarm intelligence technique for nonlinear function optimization. The idea is to simulate the actions associated with a swarm of particles, each of which could provide a potential solution for the optimization problem. The particles traverse a search space, repositioning themselves in both the swarms and their own best-known placements. The objective is to iteratively update the particle locations to find the best solution [9].

A. Objective Function

Our suggested approach in this work is to minimize *DL* considering the penalty function for constraints violation, which can be represented as (7),

$$\text{minimize} \quad DL=\sum_{h=1}^{24}P_{loss,h}+PN. \tag{7}$$

When calculating $P_{loss,h}$, the process involves determining the value through power flow calculations represented as (8),

$$P_{loss,h}=\sum_{i=1}^{NB}\sum_{\substack{j=1\\ j\neq i}}^{NB}G_{ij}\left[(V_{i,h})^2+(V_{j,h})^2-2V_{i,h}V_{j,h}\cos(\delta_{i,h}-\delta_{j,h})\right],$$
$$\text{for } i,j=1,2,3,\ldots,\text{NB}, h=1,2,3,\ldots,24. \tag{8}$$

The constraints for HESS limitations are,

$$P_{FC,\min} < P_{FC} < P_{FC,rated}, \quad (9)$$

$$P_{EL,\min} < P_{EL} < P_{EL,rated}, \text{ and} \quad (10)$$

$$E_{tank,\min} < E_{tank} < E_{tank,rated}. \quad (11)$$

In the first step, the storage level is determined by a value that relies on the lowest and highest storage capacity. Mathematically, the associated storage levels for the following time intervals have been defined as follows:

$$E_{tank,h} = E_{tank,h-1} + \mathbf{ch}(h) - \mathbf{dch}(h). \quad (12)$$

The scheduling of **ch** and **dch** in (5) and (6) is obtained by PSO. The matrix **ch** and **dch** are used for acquiring *DL* in (7); the scheduling was updated by the PSO. The objective function is to minimize *DL*, which is obtained by load flow analysis. The term "gbest" refers to the minimum value of *DL* among all particles, whereas "pbest" denotes the minimum *DL* of an individual particle [10]. The PSO-based ODS algorithms are illustrated in Figure 2.

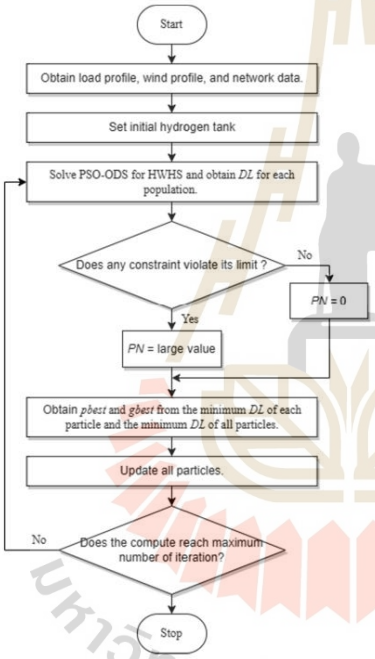

Fig. 2. The flow chart of the PSO-ODS for HWHS.

IV. Result And Disscusion

In this paper, two system case studies are investigated, including:

Case I: IEEE 33-bus system with WPP integrated.

Case II: IEEE 33-bus system with PSO-based ODS for HWHS.

The load profile of the northeastern region of Thailand and the wind speed profile from the Thai Meteorological Department are used, as observed in Figs.3 and 4. The reduction in *DL* between Case I and Case II is observed for comparison.

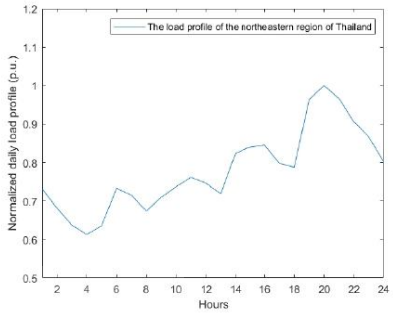

Fig. 3. The load profile of the northeastern region of Thailand

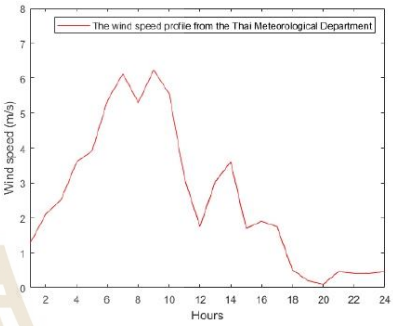

Fig. 4. The wind speed profile from the Thai Meteorological Department

A. IEEE 33-bus with WPP integrated

In this case, WPP connects to bus no. 26 [6] of the IEEE 33-bus radial distribution test system [11]. The number of wind turbines is 25. The system is modified as shown in Fig. 5.

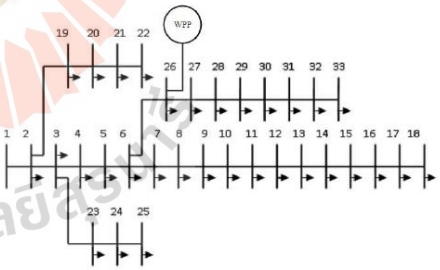

Fig. 5. The modified IEEE 33-bus radial distribution test system with WPP.

TABLE I. SPECIFICATION OF EWT DW 52-500 KW [12]

Parameters	Values
$P_{w,rated}$	500 kW
$v_{cut\text{-}in}$	3 m/s
$v_{w,rated}$	10 m/s
$v_{cut\text{-}off}$	25 m/s

2024 International Electrical Engineering Congress (iEECON 2024)
March 6-8, 2024, Pattaya Chonburi, THAILAND

The practical specifications of the EWT DW 52–500 kW wind turbine are used to simulate fluctuations in output power with wind speed [11–13]. The WPP is located at bus number 26 [6]. The specification of each wind turbine is given in Table I [12].

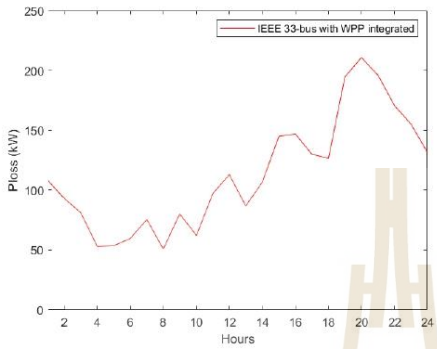

Fig. 6. The hourly power loss of IEEE 33-bus with WPP integrated.

Figure 6 displays the power loss for each hour of the modified IEEE 33-bus system with WPP integrated. WPP has an abundance of wind power during off-peak load times. Nevertheless, there is a shortage of wind during peak demand periods, which indicates that no real power from WPP can be injected into the system, leading to high power loss during peak hours. The result shows that *DL* in Case I is 2,727 kWh.

B. IEEE 33-bus system with PSO base ODS for HWHS.

In this case, HWHS connects to bus no. 26 of the IEEE 33-bus radial distribution test system [11]. Incorporating HESS into the structure provides a solution to wind fluctuation and uncertainty. Using HESS to minimize *DL* is the primary goal of this effort. In the simulation, the initial quantity of hydrogen is 20% of the tank's capacity. The system is modified as shown in Fig. 7. In each trial, the particle size is set at 100 particles, and the running iteration is 100 iterations. The convergence curve for *DL* solution is displayed in Fig 8.

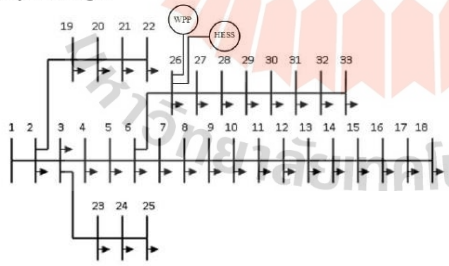

Fig. 7. The modified IEEE 33-bus radial distribution test system with HWHS.

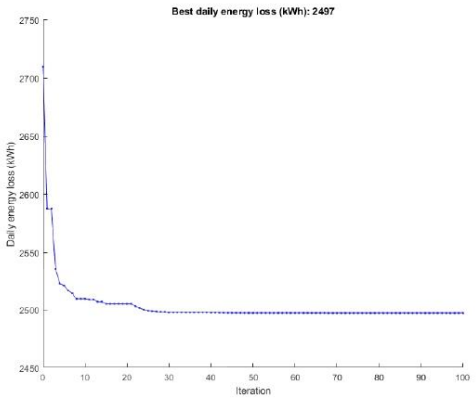

Fig. 8. The convergence of *DL* solution.

Figure 9. and Table II illustrate the outputs from 30 trials of Case II. The best and worst solutions are 2497.0002 kWh and 2497.0333 kWh, respectively. The average from 30 trials from Case II is 2497.0049 kWh. The solutions with 30 trials showed that the *DL* solutions are clustered. Therefore, the proposed tecnique is shown to be dependable and potentially find the optimal solution.

TABLE II. THE LOWEST, AVERAGE, AND HIGHEST *DL* FROM 30 TRIAL SOLUTIONS OF PSO-ODS FOR HWHS

	PSO-ODS FOR HWHS		
The daily energy loss (kWh)	***Lowest***	***Avg.***	***Highest***
	2497.0002	2497.0049	2497.0333

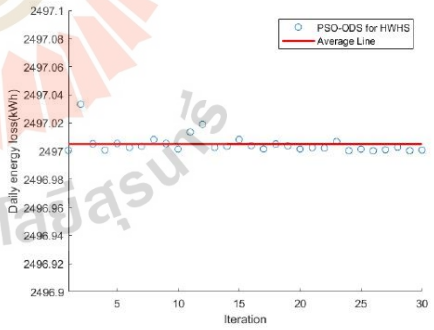

Fig. 9. The solution with 30 trials of PSO-ODS for HWHS.

The optimal scheduling of HESS is shown in Fig. 10. The scheduling is managed by the PSO algorithm to minimize energy losses. The HESS charges when $P_{wpp,h}$ is high, and in this interval is off-peak load time and discharging when peak

load time. The comparison results between Case I and Case II are shown in Fig. 11. As illustrated in Figs. 10 and 11, by using the proposed method, the HESS discharges between 3:00 p.m. and 12:00 a.m., which is the peak period. The HESS charges between 4:00 a.m. and 11:00 a.m. and between 1:00 p.m. and 2:00 p.m., which is the light load period. At 1:00 a.m. and 12:00 p.m., the HESS discharges power due to a shortage of wind power generation. This results in a significant decrease in real power loss.

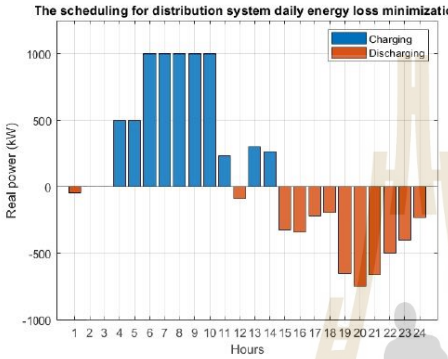

Fig. 10. The scheduling for distribution system *DL* minimization.

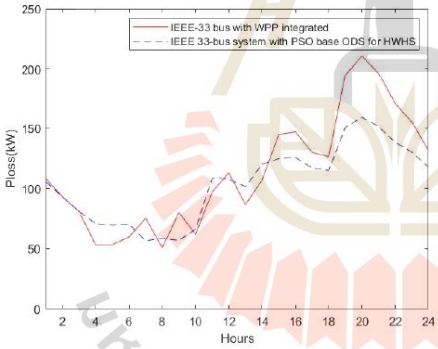

Fig. 11. The comparison of power loss between IEEE 33-bus with WPP integrated and IEEE 33-bus with PSO-ODS for HWHS.

The HESS parameters used in the simulations in Case II are shown in Table III.

TABLE III. THE PARAMETERS OF HESS ARE USED IN CASE II

Parameters	Values
$P_{FC,rated}$	1000 kW
$P_{EL,rated}$	1000 kW
$E_{tank,rated}$	10000 kWh

V. CONCLUSION

In this paper, the ODS using PSO for HWHS to minimize *DL* is proposed. The proposed approach was assessed using an IEEE 33-bus radial distribution test system utilizing the load profile of the northeastern region of Thailand and the wind speed profile of the Thai Meteorological Department. The system case studies are separated into two cases. The case where HWHS is integrated into the system illustrates that there is energy arbitrage using HESS to discharge the real power into the system when the system has peak load time and charging during times of light load, and wind power is plentiful. The result showed that the proposed method can effectively minimize *DL* and efficiently utilize the HWHS.

ACKNOWLEDGMENT

We extend our sincere appreciation to Suranaree University of Technology, Thailand, for their scholarship and facilities provided throughout this research endeavor. Their invaluable support greatly influenced the successful culmination of this study.

REFERENCES

[1] M. Shatnawi, N. A. Qaydi, N. Aljaberi and M. Aljaberi, "Hydrogen-Based Energy Storage Systems: A Review," 2018 7th International Conference on Renewable Energy Research and Applications (ICRERA), Paris, France, 2018, pp. 697-700, doi: 10.1109/ICRERA.2018.8566903.

[2] Z. Hong, Z. Wei, and X. Han, "Optimization scheduling control strategy of wind-hydrogen system considering hydrogen production efficiency," *Journal of Energy Storage*, vol. 47, p. 103609, Mar. 2022, doi: 10.1016/j.est.2021.103609.

[3] L. Valverde, F. J. P. Lucena, J. Guerra, and F. Rosa, "Definition, analysis and experimental investigation of operation modes in hydrogen-renewable-based power plants incorporating hybrid energy storage," *Energy Conversion and Management*, vol. 113, pp. 290–311, Apr. 2016, doi: 10.1016/j.enconman.2016.01.036.

[4] O. Utomo, M. Abeysekera, and C. E. Ugalde-Loo, "Optimal operation of a hydrogen storage and fuel cell coupled integrated energy system," *Sustainability*, vol. 13, no. 6, p. 3525, Mar. 2021, doi: 10.3390/su13063525.

[5] G. He, Z. Wang, H. Ma, and X. Zhou, "Optimal capacity configuration of Wind–Solar hydrogen storage microgrid based on IDW-PSO," Batteries, vol. 9, no. 8, p. 410, Aug. 2023, doi: 10.3390/batteries9080410.

[6] S. Paul, H. Karbouj and Z. H. Rather, "Optimal Placement of Wind Power Plant in a Radial Distribution Network Considering Plant Reliability," 2018 International Conference on Power System Technology (POWERCON), Guangzhou, China, 2018, pp. 2021-2026, doi: 10.1109/POWERCON.2018.8601946.

[7] H. Eskandari, M. Kiani, M. Zadehbagheri, and T. Niknam, "Optimal scheduling of storage device, renewable resources and hydrogen storage in combined heat and power microgrids in the presence plug-in hybrid electric vehicles and their charging demand," Journal of Energy Storage, vol. 50, p. 104558, Jun. 2022, doi: 10.1016/j.est.2022.104558.

[8] S. O. Amrouche, D. Rekioua and T. Rekioua, "Overview of energy storage in renewable energy systems," 2015 3rd International Renewable and Sustainable Energy Conference (IRSEC), Marrakech, Morocco, 2015, pp. 1-6, doi: 10.1109/IRSEC.2015.7454988.

[9] J. Kennedy and R. Eberhart, "Particle swarm optimization," Proceedings of ICNN'95 - International Conference on Neural Networks, Perth, WA, Australia, 1995, pp. 1942-1948 vol.4, doi: 10.1109/ICNN.1995.488968.

[10] K.Kaiyawong and K.Chayakulkheeree, "Coordinated optimal placement of energy storage system and capacitor bank considering optimal energy storage scheduling for distribution system using Mixed-Integer Particle swarm optimization," International Journal of Intelligent Engineering and Systems, vol. 15, no. 2, pp. 329–337, Apr. 2022, doi: 10.22266/ijies2022.0430.30.

[11] P. S. Meera and S. Hemamalini, "Optimal Siting of Distributed Generators in a Distribution Network using Artificial Immune System," International Journal of Electrical and Computer Engineering, vol. 7, no. 2, p. 641, Apr. 2017, doi: 10.11591/ijece.v7i2.pp641-649.

[12] EWT, "Wind turbines," *EWT*, Dec. 18, 2018. https://ewtdirectwind.com/turbines/

[13] E. Beshr, H. A. Abdelghany, and M. Eteiba, "Novel optimization technique of isolated microgrid with hydrogen energy storage," *PLOS ONE*, vol. 13, no. 2, p. e0193224, Feb. 2018, doi: 10.1371/journal.pone.0193224.

Optimal scheduling of multi-energy systems with wind-solar power and hydrogen storage integration

Suttipong Dechjinda[1], Keerati Chayakulkheeree [1,*]

ARTICLE INFO

Article history:
Received:
Revised:
Accepted:

Keywords:
Optimal scheduling
Multi-energy systems
Hydrogen storage
Energy hubs
Wind-solar power

ABSTRACT

This paper presents an optimization framework for scheduling a grid-connected multi-energy system that converts electricity from the power grid and natural gas to electricity and heat consumption, integrating wind-solar power and hydrogen storage. The study aims to develop a model that efficiently schedules energy usage while accounting for excess wind-solar power utilization, storage capabilities, and hydrogen scheduling. By incorporating dynamic pricing mechanisms, such as real-time pricing, and a stochastic model to address load fluctuations during peak periods, the proposed method provides a more realistic and adaptive approach to energy management. A combination of linear programming (LP) and particle swarm optimization (PSO) is employed to balance supply demand and minimize total operating costs. The results demonstrate significant improvements in coordinated operation efficiency and cost savings under various scenarios. Additionally, although the proposed technique demonstrates faster convergence, it requires longer runtime computation while delivering a more near-optimal global solution compared to conventional PSO. This framework offers a solution for enhancing efficiency, cost reduction, and operational flexibility of multi-energy systems, paving the way for a more sustainable and economically viable energy future.

1. INTRODUCTION

In the modern era, the incorporation of several different energy systems that are composed of many energy carriers is paving the way for a more sustainable future [1]. One of the most significant characteristics of this system is that it has multiple energy carriers, not only electricity. Synergies among different types of energy are seen to provide a substantial capability for system development [2, 3]. In addition to the possibilities of modern technology, state-of-the-art, emerging, and upcoming energy technologies, such as fuel cell (FC), are considered [4]. The multi-energy system (MES) is the solution to decrease the operating cost and promote carbon neutrality. The energy hub (EH) concept is used to consider efficiently supplying energy in each section using many kinds of energy. The EH infrastructure was first discovered in [2], and the basic concept of an EH is shown in Fig. 1. However, this concept will achieve the main goal of industrial, commercial, and residential consumers emphasizing how to minimize total operating costs (TOC) [5].

The trending technology in the MES with the EH model is combined heat and power (CHP) such as micro-turbine (MT) can dispatch two energies consisting of heat and electricity energy, power-to-gas (PtG) such as electricity energy to hydrogen gas, and gas-to-power (GtP) such as hydrogen gas to electricity energy [6, 7]. In this framework, PtG technology converts renewable energy (RE) to hydrogen gas by electrolyzer (EL). When RE generates excess energy, it can be utilized, stored, or distributed when it is synergized with a system called "Hydrogen Storage (HS)". GtP technology converts hydrogen gas to electricity energy via FC in HS. CHP technology dispatches electricity and heat demand by fueling natural gas (NG) [8, 9].

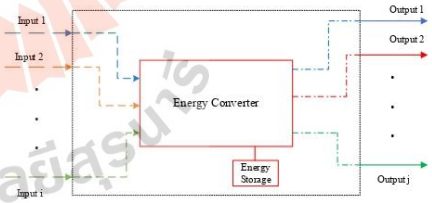

Fig. 1. The basic concept of an EH

Hydrogen production is defined in various color codes depending on the manufacturing process and cleanliness. It can be categorized into five colors: grey, brown, blue, turquoise, and green hydrogen [10]. Grey hydrogen is

[1]*School of Electrical Engineering, Suranaree University of Technology, Nakhonratchasima, 30000, Thailand.*
**Corresponding author:* Keerati Chayakulkheeree; Email: keerati.ch@sut.ac.th

produced from fossil fuels such as NG through steam reforming, emitting around 10 tons of CO_2 during the process [10, 11]. It's commonly used in petroleum-based chemicals and ammonia production. Brown hydrogen, derived from coal gasification, also releases significant CO_2. Blue hydrogen mitigates these emissions by employing carbon capture and storage. Turquoise hydrogen, generated via methane pyrolysis, produces solid carbon soot instead of CO_2. Green hydrogen, the cleanest, is produced using RE sources, such as wind or solar but faces challenges related to system efficiency and energy intermittent. Integrating HS can address these challenges [10]–[13].

Consequently, a significant amount of research has been proposed on MES with the EH model. Thanh-tung et al. [9] proposed a model of residential area load including electricity and heat from dispatching a multi-energy source (electricity and NG). Using mixed integer programming (MIP) based-general algebraic modeling system (GAMS) software to minimize the energy usage cost. The optimal results show that off-peak energy demand is primarily supplied by the grid, while normal and peak-hour demand is partially met by converting energy from NG to electricity, reducing system peaks, and lowering customer costs. The integration of multiple energy types improves electricity supply reliability. Then, Ha et al. [14] presented an integrating battery energy storage systems (BESS), photovoltaic panels (PVP), and solar energy model for residential areas. The case study is divided into four scenarios, each comprising variations such as with or without BESS and PV systems. The energy usage cost minimization using MIP-GAMS illustrates that the result in each case is decreasing. When PVP and BESS are integrated, the TOC is lowest. Moreover, Liu et al. [15] studied an EH model in different energy integrated. The study separated three kinds of EH cases to assess how different combinations of energy equipment. The components of EH include a boiler, cogeneration unit, chiller boiler, electric heat pump, and energy storage to dispatch electricity, heat, and cooling demand from electricity and NG as a source. The optimization process aims to minimize the TOC of the energy system, ensuring efficient energy utilization and balancing between different energy sources. The result shows that the optimal EH configuration is the most collaborative of energy. It can significantly reduce energy costs by coupling electricity, gas, and heat networks while optimizing the use of equipment like CHP and heat pumps. Additionally, Javadi et al. [16] focused on BESS integration to enhance the operational efficiency of a multi-carrier EH through optimal scheduling. The EH consists of various components, including micro-combined heat, electric heat pumps, boilers, absorption chillers, and battery storage with the energy management problem modeled using mixed-integer nonlinear programming (MINLP). The optimization aims to reduce costs and improve battery life by considering energy prices and battery state of charge. Simulation results highlight the importance of optimizing energy storage, leading to lower operational costs, better load management, and improved system reliability. Also, Geng and Jia [17] proposed a hybrid genetic algorithm and particle swarm optimization (GA-PSO) strategy, which combines PSO with GA to solve the optimal operation of EH. The EH model is comprised of electricity storage and heat storage coordinated with a gas turbine, gas boiler, electric chiller, and absorption chiller to dispatch electricity, heat, and cooling demand. When comparing a proposed algorithm GA-PSO with the conventional PSO, the results emphasize that GA-PSO significantly enhances convergence capability while also demonstrating a better economy in optimizing EH operations. In addition, Wang [18] proposed the strategy of optimal scheduling for multi-energy microgrids that integrates electricity and thermal energy sources, considering demand response and BESS integration. Using MILP solved by CPLEX, the study simulates the operation of a grid-connected microgrid consisting of FC, wind turbines (WTs), PVP, and thermal storage. Three different energy dispatch schemes are tested, with the third scheme incorporating demand responses showing the best results. This scheme not only reduces operational costs but also turns grid interactions into profit opportunities by smoothing energy demand and optimizing the use of RE and storage. The research demonstrates how integrating demand responses can enhance system flexibility, lower costs, and promote sustainable energy use. Furthermore, Timothée et al. [19] investigated the optimal dispatch of a multi-storage and multi-energy hub, integrating PVP, WTs, boilers, internal combustion generators, and cogeneration plants, alongside both heat and electricity storage systems. The study employed an evolutionary algorithm (EA) for optimization and compared the results with PSO. Results highlighted the volatility in dispatch strategies, which could be mitigated by increasing battery storage capacity. The results indicate that both the battery and internal combustion generators are utilized to meet peak power demand and export electricity to the grid when prices are elevated. In terms of heat demand, the boiler operates at full capacity, with the cogeneration plants unit contributing a smaller portion of the heat supply compared to the boiler. The research emphasizes the importance of optimizing EH to manage demand, renewable variability, and grid interactions, ensuring cost-effective and efficient energy distribution.

As a result, infrastructure MES with EH necessitates a significant amount of research and development [20]–[24]. This paper proposes a multi-energy system with wind-solar power and hydrogen storage (MES-WSPHS), incorporating energy management strategies for dispatching electricity and heat demands. The framework accounts for electricity tariffs based on time-of-use (TOU) and a constant NG

price, while also evaluating the impact of dynamic pricing models, such as real-time pricing (RTP). In the proposed method, a hybrid particle swarm optimization and linear programming (PSO-LP) approach. The MES includes electricity from the power grid and NG is optimally scheduled by LP, on an hourly basis. Meanwhile, the integrated wind-solar power and HS system are optimally scheduled by PSO daily. At peak load times, Monte Carlo simulation (MCS) is used to assess the fluctuations in demand, providing a more practical analysis. Additionally, this framework addresses a research gap by proposing an EH model that fully integrates green hydrogen production from HS and utilizes PSO-LP which is a combination of metaheuristic algorithm and deterministic optimization techniques for finding the best solution.

Table 1. Research gap analysis

Works	Interconnect multi-energy				Algorithm					Type of H_2		Objective
					MIP							
	Electricity	NG	WTs- PVP	H_2	MLP	MINLP	PSO	GA	EA	Grey	Green	
[9]	✓	✓			✓							TOC
[14]	✓	✓			✓							
[15]	✓	✓			✓							
[16]	✓	✓				✓						
[17]	✓	✓					✓	✓				
[18]	✓	✓	✓		✓							
[19]	✓	✓	✓				✓		✓			
This work	✓	✓	✓	✓	✓ (LP)		✓				✓	

The rest of the paper is organized as follows: Section II delves into system modeling and its principal components, providing detailed mathematical modeling of MES-WSPHS, WTs, and PVP, which are a renewable resource, conversion technologies, and HS mechanisms. Section III details the PSO-LP techniques used to optimize scheduling with a focus on minimizing TOC and a load stochastic model at peak spot time is proposed. Section IV presents case-based scenario studies and simulations to evaluate the effectiveness of the proposed methods. Including simulation when using RTP to reflect practical market conditions. The stochastic model with MCS is utilized to demonstrate when the demands have a fluctuation condition [25]. Finally, Section V provides a comprehensive summary of the key findings, highlighting the most significant insights drawn from the analysis.

2. SYSTEM MODELLING

2.1. MES-WSPHS

For system modeling, the components of MES-WSPHS are shown in Fig. 2. The input part consists of an electricity grid and NG to dispatch energy to the output which is electricity and heat demands. The conversion technology, which is the center of EH includes a transformer (TR), gas boiler (GB), MT, WTs, and PVP. With HS, the excessive RE can be converted to hydrogen and stored for utilization at the proper period. As a result, the resources can be coordinately utilized, leading to higher overall efficiency. In Fig. 2, electricity (P_E) and NG (P_{NG}) serve as the primary input power for the system and must supply the required electricity demand (L_E) and heat demand (L_H), respectively [5]. Conversion efficiency is considered and can be mathematically expressed as shown in (1).

$$\begin{bmatrix} L_E \\ L_H \end{bmatrix} = \begin{bmatrix} \eta_{TR} & \eta_{MT}^{E} & 0 \\ 0 & \eta_{MT}^{H} & \eta_{GB} \end{bmatrix} \begin{bmatrix} P_E \\ P_{NG}^{1} \\ P_{NG}^{2} \end{bmatrix} + \begin{bmatrix} P_{WPS} + P_{FC} \\ 0 \end{bmatrix}. \quad (1)$$

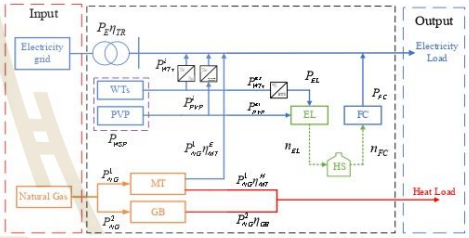

Fig. 2. The components of MES with EH model

2.2. WTs and PVP modeling

In a wind speed profile, the wind speed must be evaluated at a height corresponding to the turbine's cross-sectional area. Therefore, equation (2) illustrates a calculation for estimating wind speed at this altitude based on the power law theory [26].

$$\frac{v_{WT}(h)}{v_{WT\_r}(h)} = \left(\frac{z}{z_r}\right)^{\alpha}. \quad (2)$$

A wind turbine generates electricity when the wind speed is above the cut-in speed or below the cut-off speed, otherwise the turbine produces no power. The power output increases with the cube of the wind speed divided by the rated wind speed when the wind speed is between the cut-in speed and the rated wind speed. Once the wind speed reaches the rated level, the turbine generates a constant rated power until the cut-off speed is reached. Above the cut-off speed condition, it is shut down to prevent damage. A wind turbine power output can be expressed (3) [27]:

$$P_{WT}(h)=\begin{cases}0 & \text{for } 0<v_{WT}(h)<v_{cut-in},\\ P_{WT,rated}\times\left(\dfrac{v_{WT}(h)}{v_{WT,rated}}\right) & \text{for } v_{cut-in}<v_{WT}(h)<v_{WT,rated},\\ P_{WT,rated} & \text{for } v_{WT,rated}<v_{WT}(h)<v_{cut-off},\\ 0 & \text{for } v_{WT}(h)<v_{cut-off}.\end{cases} \quad (3)$$

The total wind power per hour from (3), can be determined as the sum of each wind turbine, which can be modeled in (4).

$$P_{WTs}(h)=\sum_{k=1}^{NT}P_{WT,k}(h). \quad (4)$$

The PVP can be modeled as (5) which considers solar energy convert into electrical energy. The output is DC power and needs to be converted into AC power through an inverter [28].

$$P_{PVP}(h)=A\times\beta\times SI(h). \quad (5)$$

When the wind and solar power are excessed, it can be stored in the form of hydrogen. Therefore, the grid-injected wind and solar power at time h can be shown in (6)-(11).

$$P_{WTs}(h)=P^{i}_{WTs}(h)+P^{ex}_{WTs}(h), \quad (6)$$

$$P_{PVP}(h)=(P^{i}_{PVP}(h)\times\eta_{DC/AC})+P^{ex}_{PVP}(h), \quad (7)$$

$$P_{WSP}(h)=P_{WTs}(h)+P_{PVP}(h), \quad (8)$$

$$P^{ex}_{WSP}(h)=\begin{cases}0 & \text{if } P_{WSP}(\mathrm{h})\le \mathrm{L}_{E}(\mathrm{h})\\ P_{WSP}(h)-L_{E}(h) & \text{if } P_{WSP}(h)>L_{E}(h)\end{cases}, \quad (9)$$

$$P^{i}_{WSP}(h)=\begin{cases}P_{WSP} & if\ P_{WSP}(h)\le L_{E}(h)\\ L_{E}(h) & if\ P_{WSP}(h)>L_{E}(h)\end{cases}, \quad (10)$$

$$P_{EL}(h)=(P^{ex}_{WTs}(h)\times\eta_{AC/DC})+P^{ex}_{PVP}(h). \quad (11)$$

2.3. Conversion technologies

The conversion devices are TR, GB, and MT. In the electrical energy sector, TR is used to convert the grid voltage to the load. The TR efficiency model can be expressed as (12) when electricity flows through the TR to supply loads.

$$P_{TR}=P_{E}\eta_{TR}. \quad (12)$$

In the NG energy sector, GB and MT are employed to convert NG to power [9, 14]. The efficiencies of the GB and MT are utilized to determine the load supply from NG formed as in (13) and (14). When considering NG cost, the power from NG can be defined as (15).

$$P_{GB}=P^{2}_{NG}\eta_{GB}, \quad (13)$$

$$P^{E,H}_{MT}=\begin{cases}P^{1}_{NG}\eta^{E}_{MT}; \text{ for electricity output}\\ P^{1}_{NG}\eta^{H}_{MT}; \text{ for heat output}\end{cases}, \quad (14)$$

$$P_{NG}=P^{1}_{NG}+P^{2}_{NG}. \quad (15)$$

2.4. HS mechanism

HS has gained considerable attention in recent studies and research efforts. In these systems, hydrogen is produced by EL when the power generated by WTs and PVP exceeds the power demand and is stored as a chemical substance. This stored hydrogen can later be used in the FC, where it reacts with oxygen from the air to generate electricity in its gaseous state. HS enables long-term energy retention, as highlighted in [29]. By applying Faraday's law, the molar flow rate of hydrogen is produced by the EL. The FC turns hydrogen into electricity, and hydrogen consumption is directly proportional to its power output [1, 30]. The molar flow of EL and FC can be described as a function in (16) and (17), respectively.

$$n_{H_2,EL}=\frac{\eta_{EL}P_{EL}}{LHV_{H2}}, \quad (16)$$

$$n_{H_2,FC}=\frac{P_{FC}}{\eta_{FC}LHV_{H2}}. \quad (17)$$

In the operation of HS, FC and EL cannot be operated simultaneously. Therefore, Y_{EL} and Y_{FC} representing binary numbers (0,1) are introduced for FC and EL operating conditions as shown in (18) [1, 30].

$$Y_{EL}=\begin{cases}1 & \text{when } Y_{FC}=0\\ 0 & \text{when } Y_{FC}=1\end{cases}. \quad (18)$$

A key control variable in the HS system is the hydrogen tank pressure at each hour. The tank pressure reflects the amount of hydrogen contained in the storage vessels and molar flow from (16) and (17) are used to calculate the pressure at each hour. The pressure calculation for the hour h is dependent on the previous time step, as shown in (19) [1, 30].

$$p_{\text{tank}}(h)=p_{\text{tank}}(h-1)+\left(\frac{\Re T_{H_2}}{V_{H_2}}n_{H_2,EL}(h)-n_{H_2,FC}(h)\right). \quad (19)$$

3. PROBLEM FORMULATION

3.1. Objective function

The proposed method uses the PSO-LP technique to find the optimal scheduling of MES-WSPHS. The multiple energy deliveries are formed as variables on an hourly basis, to find the optimal solution for the system that makes it the minimum operating cost. The analysis considers the TOU tariff and RTP as separate factors throughout the day. Therefore, the objective function is to minimize total operating costs while accounting for the TOU tariff and RTP independently, with a penalty function incorporated to address any constraints violations, as shown in (20).

$$\text{Minimize TOC}=\sum_{h=1}^{24}(C_{E}(h)P_{E}(h)+C_{NG}(h)P_{NG}(h))+PNF. \quad (20)$$

Subjected to the power balance constraints in (21)-(22),

$$L_E(h) - P_{FC}(h) - P^i_{WSP}(h) = P_{TR}(h), \quad (21)$$

$$L_H(h) = P_{GB}(h) + P^H_{MT}(h), \quad (22)$$

and the limit constraints of each conversion device as demonstrated by (23)-(28),

$$0 \le P_{TR}(h) \le P_{TR,rated}, \quad (23)$$

$$0 \le P^{E,H}_{MT}(h) \le P^{E,H}_{MT,rated}, \quad (24)$$

$$0 \le P_{GB}(h) \le P_{GB,rated}, \quad (25)$$

$$0 \le Y_{EL} P_{EL}(h) \le P_{EL,rated}, \quad (26)$$

$$0 \le Y_{FC} P_{FC}(h) \le P_{FC,rated}, \text{ and} \quad (27)$$

$$p_{\text{tank,min}} \le p_{\text{tank}}(h) \le p_{\text{tank,rated}}. \quad (28)$$

In this paper, the initial pressure which is indicated in the content of the HS tank is set to the final pressure when the day is over, as shown in (29),

$$p_{\text{tank}}(h = \text{initial}) = p_{\text{tank}}(h = 24). \quad (29)$$

In addition, penalty function terms can handle some constraints, which can't define a lower and upper boundary such as (25) and (26). The penalty function can be defined as a Karush–Kuhn–Tucker condition (KKT) in (30)

$$PNF = \lambda_1[(p_{\text{tank}}(h) - p_{\text{tank,min}})^2 + (p_{\text{tank}}(h) - p_{\text{tank,rated}})^2] + \lambda_2[(p_{\text{tank}}(h = 24) - p_{\text{tank}}(h = initial)]^2. \quad (30)$$

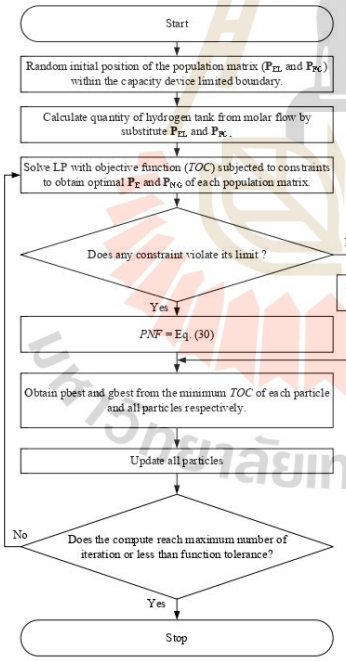

Fig. 3. The workflow of the PSO-LP technique under TOC

The operation of this work procedure, which involves calculating the objective function while handling constraints, follows the workflow depicted in Fig. 3

3.2. PSO-LP technique

The HS scheduling is a continuous variable (P_{EL} and P_{FC}), while the relation of power from the grid and NG (P_E and P_{NG}) can be formed as a linear problem. Therefore, we modify the mathematical formulation of the problem to account for utilizing a heuristic algorithm in the main loop and utilizing a deterministic algorithm in the subroutines. LP will optimize the problem in subroutines. Then, the main loop will be optimized by PSO. The overview concept of hybrid PSO-LP is shown in Fig. 4. The hybrid PSO-LP technique is an enhanced version of the traditional PSO algorithm, designed to be more efficient. The PSO is used for searching for optimal HS scheduling incorporating the optimal condition of electricity from the power grid and NG, under wind and solar power, electricity load, and heating load conditions.

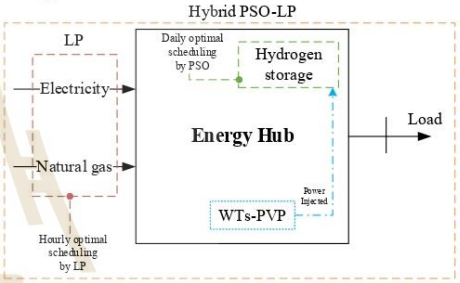

Fig. 4. The overview of hybrid PSO-LP

The PSO algorithm is a stochastic optimization technique inspired by the collective behavior of bird flocks and their emergent dynamics. In PSO, a population of potential solutions, referred to as particles, is used to search for the optimal result. This population is called a swarm, and each particle represents a possible solution. The algorithm begins by randomly assigning positions to the particles within the search space. These particles then update their positions in successive iterations, adjusting based on their velocities. Each particle keeps track of its best position, referred to as *pbest(i,h)*, and updates its velocity based on that. Particles also communicate with one another to adjust their movement. If a particle finds a solution better than its previous *pbest*, the value is replaced. Among the entire population, the best solution found is called the global best (*gbest*). In this paper, the population is formulated as follows (31) [31]:

$$\mathbf{P}_{\mathbf{EL,FC}} = [P_{EL,FC}(1), P_{EL,FC}(2), ..., P_{EL,FC}(h), ..., P_{EL,FC}(24)]. \quad (31)$$

The matrix in (31) will solve the individual objective function simultaneously. Then this matrix is used to update

each particle's velocity as displayed in (32), and the next step of the matrix is updated by velocity as shown in (33) [31].

$$v(i,h+1) = wv(i,h) + c_1 rand_1(pbest(i,h) - \mathbf{P}_{EL,FC}(i,h)) + c_2 rand_2(gbest(i,h) - \mathbf{P}_{EL,FC}(i,h)), \quad (32)$$

$$\mathbf{P}_{EL,FC}(i,h+1) = \mathbf{P}_{EL,FC}(i,h) + v(i,h+1). \quad (33)$$

3.3. Stochastic load model

In practical terms, electricity and heat loads fluctuate based on user activity. Consequently, at the peak electricity and heat loads can be probabilistically modeled using a normal distribution. The normal distribution is a widely utilized probability density function (PDF) that represents continuous random variables with a characteristic bell-shaped curve. The PDF of the normal distribution is given by [32]:

$$f_{L_E}(L_E) = \frac{1}{\sqrt{(2\pi)\sigma_{L_E}}} \exp\left(-\frac{(L_E - \mu_{L_E})^2}{2\sigma_{L_E}}\right), \quad (34)$$

$$f_{L_H}(L_H) = \frac{1}{\sqrt{(2\pi)\sigma_{L_H}}} \exp\left(-\frac{(L_H - \mu_{L_H})^2}{2\sigma_{L_H}}\right). \quad (35)$$

4. RESULTS AND DISCUSSION

This section presents the data and simulation results for four case studies. MATLAB programming is used to develop an optimal daily scheduling algorithm for the proposed MES-WSPHS. Each case represents a distinct scenario, such as the inclusion of HS and coordination between electricity and NG systems. Different scheduling scenarios are analyzed.

4.1. Data acquired and assumptions

To evaluate the performance and feasibility of the MES-WSPHS configuration, it is essential to analyze the efficiency and capabilities of its individual components as shown in Table 2 [8, 20]. The electricity load profile utilized in this study was obtained from a typical summer day in the northeastern region of Thailand, with a peak load defined at 2 MW [27] as shown in Fig. 5(a). The heat load profile was acquired from [33] as illustrated in Fig. 5(b). The wind and solar profile were derived from data collected on a summer day in Pakchong, Thailand [27] .

This study examines a wind power system with four turbines rated at 500 kW each (NT = 4), as shown in Fig. 6. Subplots 1 and 2 in Fig. 6 illustrate wind speed conversion to power. Hourly solar irradiance and PVP output are shown in Fig. 7, subplots 1 and 2, respectively. Fig. 8 highlights excess wind and solar power over demand. Electricity costs follow TOU tariffs [34], while NG prices remain constant. Furthermore, RTP, which reflects dynamic price adjustments, both are described in Fig. 9

Table 2. The efficiency and rated device of each component

List	Component	Efficiency	Rated
No.1	Transformer	98%	2500 kVA
No.2	Electrolyzer	70%	500 kW
No.3	Fuel cell	60%	500 kW
No.4	Micro-turbine	40%, 50%	500 kW
No.5	Gas boiler	88%	1600 kW
No.6	Converter	95%	-
No.7	Pressure tank	-	100 bar

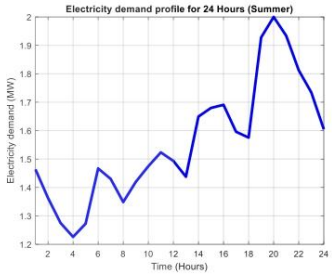

(a)

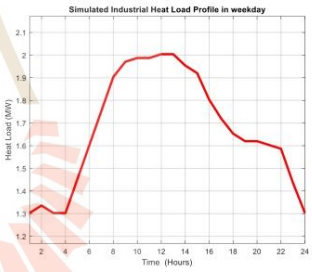

(b)

Fig. 5. The load profile (a) electricity (b) heat

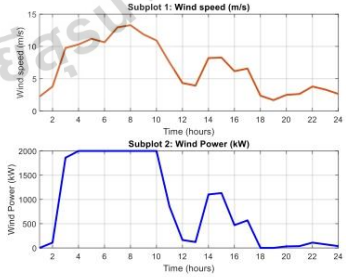

Fig. 6. The wind profile

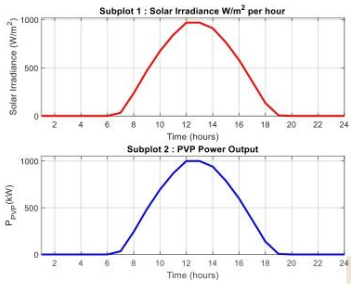

Fig. 7. The solar profile

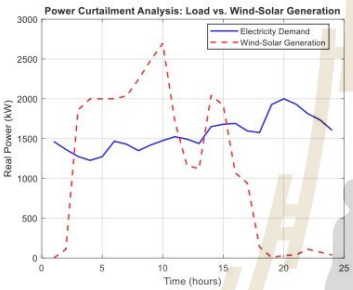

Fig. 8. The excess wind-solar generation

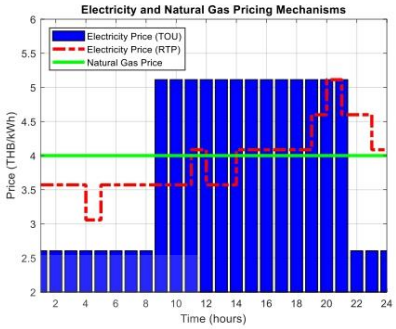

Fig. 9. The electricity and natural gas pricing mechanism

4.2. The simulation results

The case studies, illustrated in Fig. 10, are divided into four scenarios for analysis, as follows:

Case I: MES-WSP without HS, operating with uncoordinated electricity and NG under TOU tariffs.

Case II: MES-WSP with HS, but without coordinated operations between electricity and NG, under TOU tariffs.

Case III: MES-WSP with coordinated operations between electricity and NG, but without HS, under TOU tariffs.

Case IV: MES-WSP with HS and coordinated electricity and NG operations, under TOU tariffs.

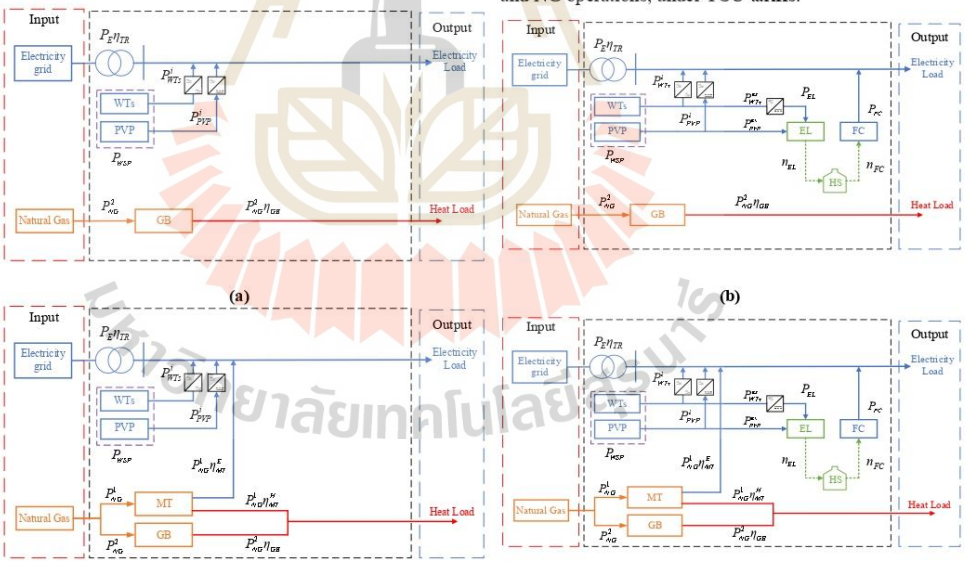

Fig. 10. Illustration of each case study (a) Case I, (b) Case II, (c) Case III, and (d) Case IV

In each case, the scheduling of energy proportions varies depending on the scenario. For cases without HS, only LP is employed to find the solution since there are no variables for the FC and EL. However, in scenarios incorporating HS, a hybrid PSO-LP method is utilized. This approach first optimizes the operation of the fuel cell and EL using PSO, and the results are subsequently processed using LP. The scheduled energy output for each component, as well as the costs associated with each energy sector, are summarized in Table 3. Furthermore, since HS is considered in Cases II and IV, with PSO-LP employed to derive the solutions, Figs. 11 to 16 provide detailed insights into the power balance, optimization algorithm, and the impact of HS on the proposed system. The figures are organized by case: (a) Case II and (b) Case IV, and they highlight the effectiveness of the proposed optimization in achieving optimal solutions. While demonstrating the role of HS integration with and without coordinated operation of NG-electricity to balance multiple types of energy with energy demand. However, in case of MT integration, more power loss occurs from operation efficiency than without MT integration but helps to significantly reduce TOC.

Table 3 Summary of power scheduling and energy costs for each sector

Case	Energy scheduling (kWh)									Operation costs (THB)		
	Energy through components					Demand-side				Electricity	NG	Total
	TR	MT	WSP	FC	GB	Gen	Used	Loss	Curtailed			
1	16,956	-	27,835	-	40,130	90,382	77,530	5,818	7,034	68,887	182,410	251,297
2	15,024	-		1,933		84,996		5,779	1,687	61,711	182,410	244,121
3	15,356	3,600		-	38,130	90,679		5,913	7,236	60,538	189,319	249,857
4	13,424	3,600		1,933		85,090		5,873	1,687	50,453	189,319	239,772

Various energy sources are utilized to meet output demands through multiple energy scheduling in the EH. In Table 3, Case I represents no cooperation between electricity and NG systems, where each sector operates independently, focusing solely on its efficiency. Conversely, Case III involves coordinated operation between electricity and NG, with NG being used to dispatch the electricity load via MT to reduce electricity consumption. Excess wind and solar power, as shown in Fig. 8, is not utilized, resulting in no additional energy savings.

Case II integrates HS without coordination with the electricity and NG systems, whereas Cases IV incorporates both HS and coordinated operation, referred to as MES-WSPHS. This significantly enhances energy management strategy since HS stores excess wind and solar energy, which is then discharged at other times. The power balance in each energy sector is depicted in Fig. 11(a) and 11(b) for electricity and in Figs. 12(a) and 12(b) for heat. Both Figs 11 and 12 focus exclusively on cases involving HS integration.

The energy flow through the MT, which operates in Cases III and IV produces both electricity and heat. In Case III and Case IV, the MT is scheduled to operate from 12 a.m. to 9 p.m. During these periods, NG costs are lower than the peak electricity costs in TOU tariffs. However, when energy generation is sufficient to meet demand, the MT does not operate in that hour. Figs 11(b) and 12(b) show the NG through MT do not operate at 2 p.m. and 3 p.m.

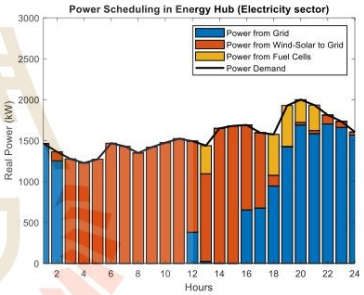

(a)

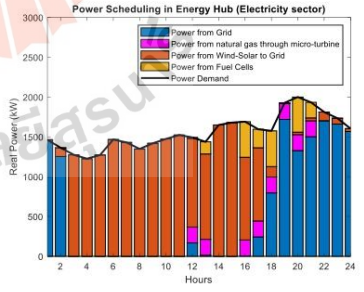

(b)

Fig. 11. Power scheduling in EH (electricity sector) (a) Case II and (b) Case IV

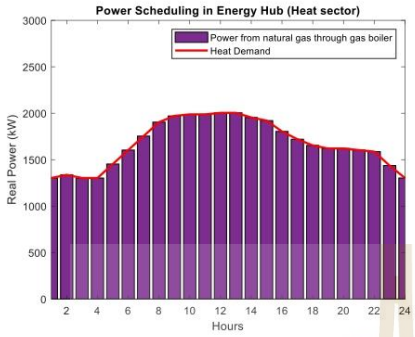

(a)

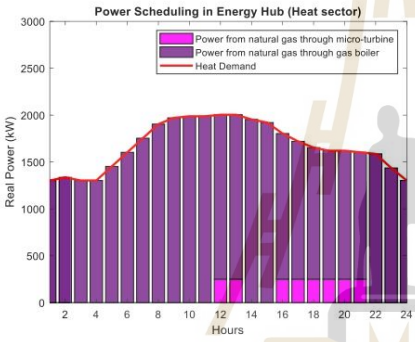

(b)

Fig. 12. Power scheduling in EH (heat sector) (a) Case II and (b) Case IV

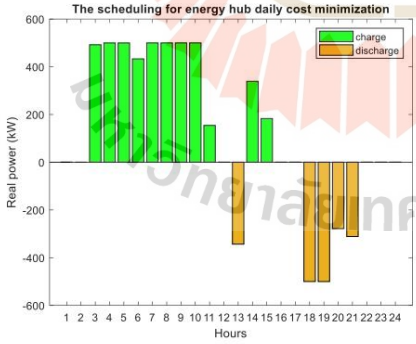

(a)

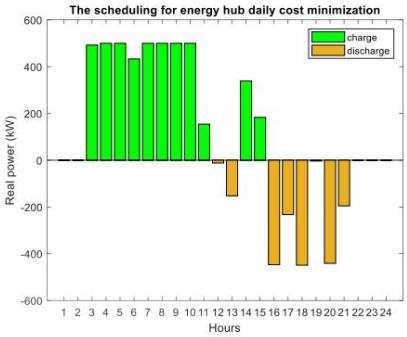

(b)

Fig. 13. HS scheduling for 24 hours ((a) Case II and (b) Case IV

Case II and Case IV with HS integration, EL turns an excess wind and solar power from 3 a.m. to 11 a.m. and 2 p.m. to 3 p.m. to HS. Then FC turns hydrogen into electricity to reduce electricity from the grid, the schedule of HS operation varies from case to case. Case II and Case IV have different patterns of FC scheduling. However, the power from FC operated is performing in the peak electricity costs period to reduce energy from the grid, resulting in a lower TOC and energy curtailment. The TOU tariff is utilized to define the objective, resulting in the FC operating as illustrated in Fig. 13 (a) Case II and (b) Case IV. In the study, the initial hydrogen tank pressure is set at 20 bar. During HS scheduling, the tank pressure is maintained within a range of no more than 100 bar and no less than 10 bar, which is defined in the state of the tank (SOT) is 100% and 0%, respectively. With the pressure at the final hour of the day equal to that of the initial hour. As shown in Fig. 14 (a) Case II and (b) Case IV, SOT is displayed as a percentage, representing the hydrogen energy storage model.

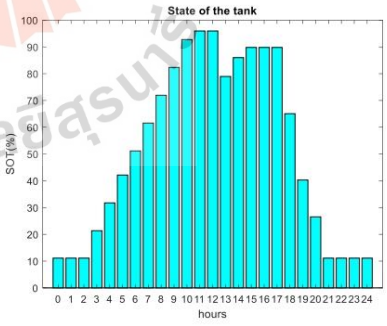

(a)

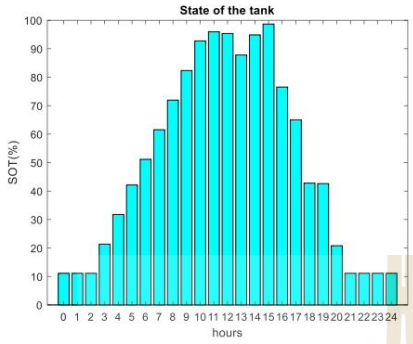

(b)

Fig. 14. State of the tank (%SOT) in HS
(a) Case II and (b) Case IV

Figure 15 (a), and (b) show the convergent PSO-LP solutions of Case II and Case IV, respectively. The best function value is TOC in both cases. Case II starts converging around 20 iterations and stops finding the optimal solution in 128 iterations. Case IV starts converging around 30 iterations and stops finding the optimal solution in 285 iterations. However, both cases can converge before the maximum iteration setting because the final solution is less than the function tolerance.

Figure 16 (a) and (b) demonstrate the results from 30 trials of Case II and Case IV which show the best, worst, and average lines of solutions, indicate that the fitness results of PSO-LP are clustered, with the standard derivations (SD) of 4.30 and 5.11, respectively. Therefore, the proposed method is demonstrated to be reliable and has the potential to find the optimal solutions.

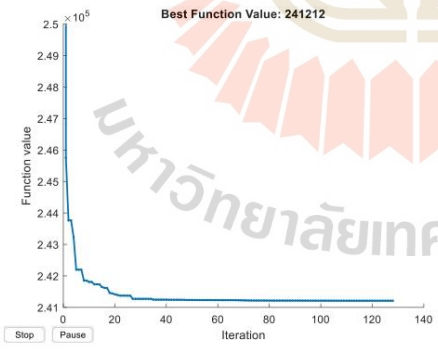

(a)

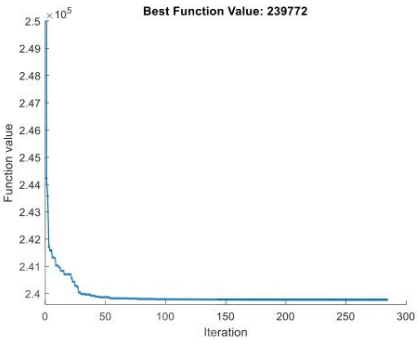

(b)

Fig. 15. The PSO-LP convergence plot
(a) Case II and (b) Case IV

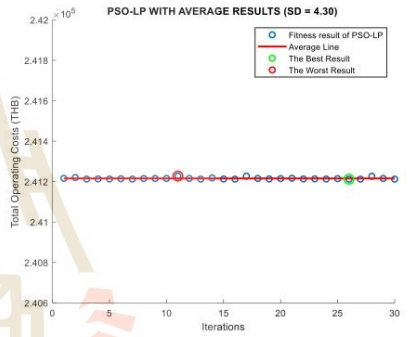

(a)

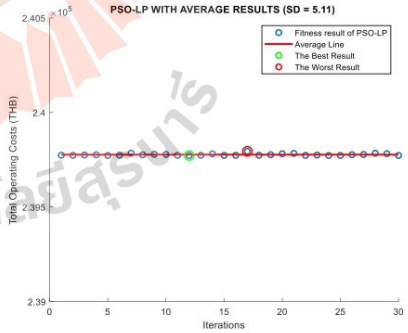

(b)

Fig. 16. The PSO-LP fitness results with 30 iterations
(a) Case II and (b) Case IV

4.3. MES-WSPHS with RTP mechanism

In this section, the impact of RTP on the operation of the MES-WSPHS is analyzed. The study investigates how dynamic electricity pricing influences the scheduling of various energy resources, ensuring cost-effective and efficient energy management. Fig. 17(a) and 17(b) illustrates the power scheduling for each energy sector. In the electricity sector, MT and HS are scheduled to operate between 7 p.m. and 10 p.m., that reflects the RTP mechanism indicates higher electricity prices during this period.

The integration of HS further enhances system flexibility, as depicted in Fig. 18(a), which illustrates the charge and discharge patterns of the HS system. It can be observed that hydrogen is primarily stored during low electricity price periods and discharged during peak price hours, aligning with the cost-minimization strategy. SOT is displayed in Fig. 18(b). The quantity of hydrogen in tank shows hydrogen reserves gradually increasing during the daytime and depleting as energy is discharged in the evening.

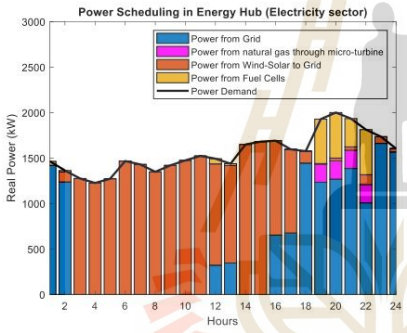

(a)

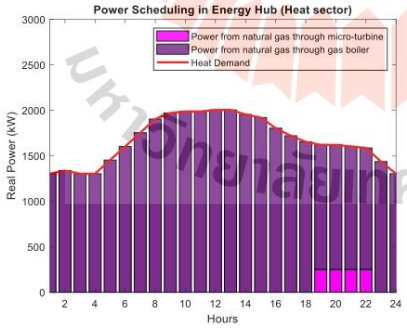

(b)

Fig. 17. Power scheduling in EH (a) electricity and (b) heat

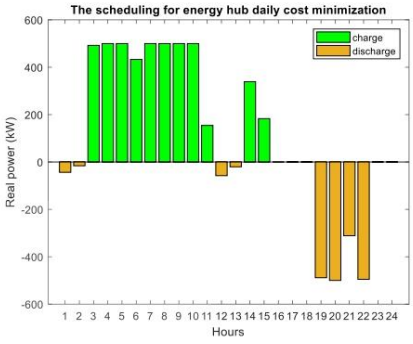

(a)

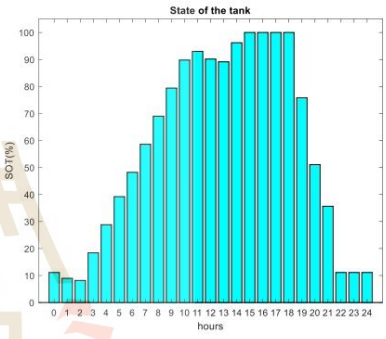

(b)

Fig. 18. (a) HS scheduling and (b) %SOT

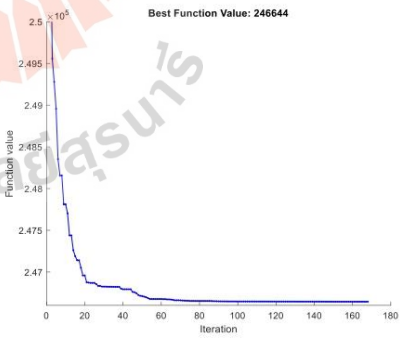

(a)

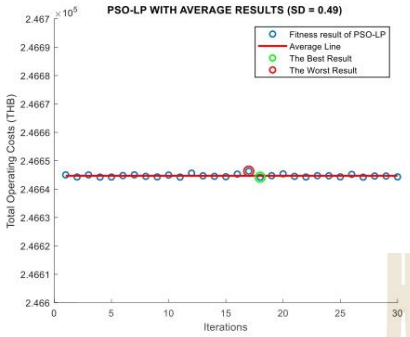

(b)

Fig.19. The PSO-LP (a) convergence plot and (b) fitness results with 30 iterations

Figure 19 (a) and (b) demonstrate the results from 30 trials of MES-WSPHS under RTP which show the best, worst, and average lines of solutions, indicate that the fitness results of PSO-LP are clustered, with the standard derivations (SD) of 0.49. This study is reliable and has the potential to find optimal solutions more than TOU tariff.

4.4. The comparison between PSO and PSO-LP

This section illustrates a different solution between the PSO and PSO-LP technique under the TOC as an objective function and demonstrated in Case IV. The aim is to highlight the performance of each approach that can minimize TOC effectively. To ensure a fair comparison between algorithms, the study established consistent parameters, as outlined in Table 4.

Table 4. The parameters of the PSO and PSO-LP settings

Variable	Settings
Swarm sizes	100
Iterations	500
Function Tolerance	$<10^{-6}$
w	[0.1,1.1]
c_1	1.49
c_2	1.49
$rand_1, rand_2$	[0,1]

Table 5. The runtime of the PSO and PSO-LP

Algorithm	Runtime (s)
PSO	611
PSO-LP	3,000

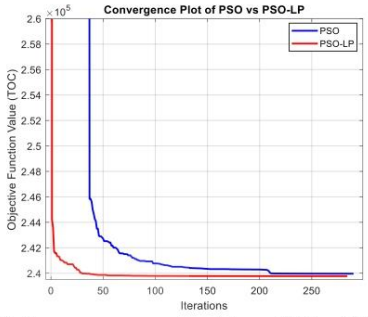

Fig. 20. Convergence comparison between PSO and PSO-LP

Figure 20 presents a comparison between PSO and PSO-LP, illustrating that both algorithms demonstrate similar convergence behavior. However, the proposed PSO-LP terminates the optimization process at 285 iterations, due to the predefined convergence criteria based on the tolerance between the current particle swarm and the previous swarm, with a function tolerance of less than 10^{-6}. This enables PSO-LP to achieve a near-optimal global solution. In contrast, PSO requires 291 iterations to terminate, taking slightly longer and failing to reach a near-optimal solution.

On the other hand, PSO-LP requires significant computational resources due to its two-step process: running PSO in the main loop and executing LP as a subroutine. This results in a longer runtime for PSO-LP compared to conventional PSO. Nevertheless, both algorithms are suitable for this problem, as the scheduling process must be completed within a day. The runtime details for this study are provided in Table 5.

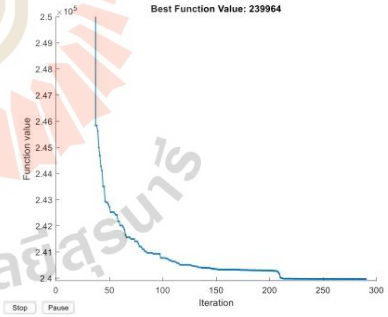

Fig. 21. The PSO convergence plot

The PSO convergence plot in Fig. 21 indicates a final TOC value of 239,964 THB, whereas the PSO-LP convergence plot in Fig. 15 (b) shows a final TOC value of 239,772 THB. This comparison highlights that PSO-LP achieves a more optimal solution than the conventional PSO algorithm.

4.5. MES-WSPHS with stochastic load model

The results of the Monte Carlo analysis demonstrate the effectiveness of the MES-WSPHS under varying stochastic load conditions at the peak time. Random load samples were generated until the tolerance criteria were satisfied, resulting in a probabilistic set of the load data. This dataset includes the mean value, standard deviation, and a fitting curve based on a normal distribution, allowing for an evaluation of the system's ability to adapt to uncertainty. Figure 22 shows the variability of the stochastic load at peak hour (one spotted), representing realistic fluctuations in demand. The peak electricity demand scenario represented by the stochastic load PDF for normal distribution is illustrated in Fig. 22. The parameter setting of MCS can be shown in Table 6.

Table 6. MCS parameters

Parameters	The mean value		The standard deviation	
	μ_E	μ_H	σ_E	σ_H
Values	$L_{E,\text{at E max}}$	$L_{H,\text{at E max}}$	$0.1\times\mu_E$	$0.1\times\mu_H$

When applying MCS to simulate the stochastic load model for determining the optimal scheduling of MES-WSPHS, the results, including TOC, electricity scheduling, and NG scheduling, are represented as PDF, as shown in Figs. 23 and 24. The convergence plot as shown in Fig 25 highlights the changes in the objective function with repeatability. The trend of the MCS procedure shows an increase as the number of iterations grows. Convergence analysis is essential for assessing the reliability of the proposed method and ensuring its ability to produce accuracy and uniform results.

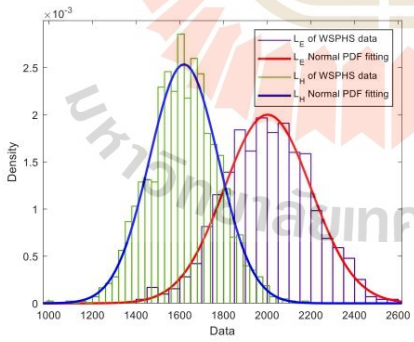

Fig. 22. Stochastic load PDF for MES-WSPHS at the peak electricity demand scenario

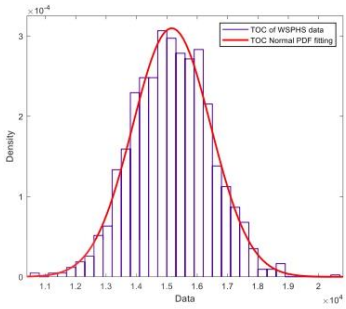

Fig. 23. Solution PDF for MES-WSPHS illustrates TOC at the peak electricity demand scenario

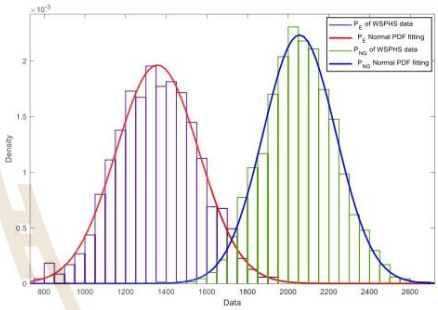

Fig. 24. Solution PDF for MES-WSPHS illustrates electricity and NG scheduling at the peak electricity demand scenario

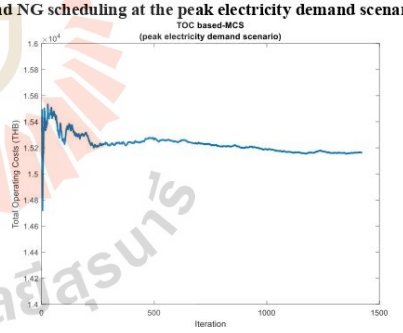

Fig. 25. The convergence plot TOC based-MCS at the peak electricity demand scenario

As a result, the proposed MES-WSPHS utilizes PSO-LP to determine the TOC minimization under TOU tariff and considers that, under probabilistic peak load conditions, the results can fit in a normal distribution perfectly. The mean value and the standard deviation of the normal distribution in each probabilistic variable follow in Table 7.

Table 7. The mean value and the standard deviation of the normal distribution

Parameters	The mean value (μ)	The standard deviation (σ)
L_E	2,001.95	199.356
L_H	1,619.01	157.347
P_E	1,357.02	203.425
P_{NG}	2,055.69	178.803
TOC	15,161.9	1,287.77

5. CONCLUSIONS

In this paper, the optimal scheduling of MES-WSPHS, using PSO-LP, to minimize TOC is proposed. The proposed approach was assessed using the MES with the EH model utilizing the electricity load profile of the northeastern region of Thailand, the wind speed and solar irradiance profile from one day in summer, and the heat load profile from the normalized profile of industry on weekdays. The study can be divided into four cases to thoroughly analyze the individual and combined impacts of HS and the coordination strategies between electricity and NG. The influence of RTP and the stochastic model is proposed to demonstrate a practical condition. Additionally, a comparison between conventional PSO and PSO-LP is discussed, highlighting that PSO-LP performs fast convergence and is more accurate than PSO under the same conditions. The results showed that the proposed method can effectively minimize TOC, enhance the economic operation of MES-WSPHS, and efficiently adapt to uncertainties and real-time price variations. The integration of RTP and stochastic modeling further emphasizes the robustness and practicality of the proposed approach in real-world scenarios.

ABBREVIATION

Variable

$\mathbf{P}$ = The matrix contains a scheduling variable.
η = Efficiency (%).
P = The power inputs or the power flow through the device (kW).
L = The power outputs or power demands (kW).
NT = The total number of wind turbines.
v = The velocity (m/s).
Y = The parameter indicates the operation state.
C = The cost of the energy input (THB/kWh).
PNF = The penalty functions.
λ = The Lagrange multiplier.
LHV = The low heat value (MJ/kmol).
$\Re$ = The gas constant (J/mol·K).
T = The mean temperature (K).
V = The volume (m^3).
p = The pressure (bar).
n = The molar flow (mol/s).
h = The times (hour).
z = The height (m).
α = The power law exponent.
A = Area of PVP installed (m^3).
β = PVP efficiency (%)
SI = Solar irradiance (W/m^2)
w = Inertia weight.
c = Learning factor.
$rand$ = A random number between 0 and 1.
$pbest$ = personal best.
$gbest$ = global best.
f = The probability density function.
σ = The standard deviation of the normal distribution.
μ = The mean value of the normal distribution.
SOT = The state of the tank (%).
TOC = The total operating costs (THB).

Subscript and Superscript

1 = The number which indicates the order.
2 = The number which indicates the order.
E = Electricity.
H = Heat.
NG = Natural gas.
H_2 = Hydrogen.
EL = Electrolyzer.
FC = Fuel cell.
MT = Micro-turbine.
TR = Transformer.
GB = Gas boiler.
WSP = Wind-solar power.
AC/DC = AC-to-DC converter.
DC/AC = DC-to-AC converter.
r = Reference.
WTs = Wind turbines.
i = Power injected into the grid.
ex = The excess power.
PVP = Photovoltaic panels.
tank = The storage of hydrogen.
$rated$ = The maximum limit.
min = The minimum limit.

ACKNOWLEDGEMENTS

We express our sincere gratitude to Suranaree University of Technology (SUT) for providing the essential resources and supportive environment that made this research possible.

REFERENCES

[1] M. L. Imeni; M. S. Ghazizadeh; M. A. Lasemi; and Z. Yang. 2023. Optimal Scheduling of a Hydrogen Based Energy Hub Considering a Stochastic Multi-Attribute Decision-Making Approach. Energies 16(2): 631.

[2] M. Geidl, G. Koeppel, P. Favre-Perrod, B. Klöckl, G. Andersson, and K. Fröhlich. 2007. The energy hub A powerful concept for future energy systems. Proceedings of the Third Annual Carnegie Mellon Conference on the Electricity Industry. Pittsburgh, PA, USA, 13–14 March. The Carnegie Mellon Electricity Industry Center.

[3] M. Geidl and G. Andersson. 2007. Optimal Power Flow of Multiple Energy Carriers. IEEE Transactions on Power Systems 22(1): 145-155.

[4] M. Lasemi and M. Ghazizadeh. 2023. Pave the Way for Hydrogen-Ready Smart Energy Hubs in Deep Renewable Energy System. Proceedings of the 2023 8th International Conference on Technology and Energy Management (ICTEM). Mazandaran, Babol, Iran, 8-9 February. IEEE Publisher.

[5] A. Zidan and H. A. Gabbar. 2016. Optimal scheduling of energy hubs in interconnected multi energy systems. Proceedings of the 2016 IEEE Smart Energy Grid Engineering (SEGE). Oshawa, ON, Canada, 21-24 August. IEEE Publisher.

[6] M. Qadrdan; M. Abeysekera; M. Chaudry; J. Wu; and N. Jenkins. 2015. Role of power-to-gas in an integrated gas and electricity system in Great Britain. International Journal of Hydrogen Energy 40(17): 5763-5775.

[7] N. C. Martin, F. V. Lith, and A. v. d. Molen. 2023. Remuneration and coordination aspects of flexibility by Power-to-Gas and Gas-to-Power technologies in distribution networks. Proceedings of the 27th International Conference on Electricity Distribution (CIRED 2023). Rome, Italy, 12-15 June. IET Publisher.

[8] T. Ha; Y. Xue; K. Lin; Y. Zhang; V. V. Thang; and T. Nguyen. 2022. Optimal Operation of Energy Hub Based Micro-energy Network with Integration of Renewables and Energy Storages. Journal of Modern Power Systems and Clean Energy 10(1): 100-108.

[9] H. Thanh-tung, Z. Yong-jun, H. Jian-ang, and V. V. Thang. 2016. Energy Hub modeling for minimal energy usage cost in residential areas. Proceedings of the 2016 IEEE International Conference on Power and Renewable Energy (ICPRE). Shanghai, China, 21-23 October. IEEE Publisher.

[10] A. I. Osman et al. 2022. Hydrogen production, storage, utilisation and environmental impacts: a review. Environmental Chemistry Letters 20(1): 153-188.

[11] M. Dvoynikov; G. Buslaev; A. Kunshin; D. Sidorov; A. Kraslawski; and M. Budovskaya. New Concepts of Hydrogen Production and Storage in Arctic Region. Resources 10(1): 3.

[12] A. b. Jumah. 2024. A comprehensive review of production, applications, and the path to a sustainable energy future with hydrogen. RSC Advances 14(36): 26400-26423.

[13] J. Zhang and J. Li. 2024. Revolution in Renewables: Integration of Green Hydrogen for a Sustainable Future. Energies 17(16): 4148.

[14] T. Ha; Y. Zhang; V. V. Thang; and J. Huang. 2017. Energy hub modeling to minimize residential energy costs considering solar energy and BESS. Journal of Modern Power Systems and Clean Energy 5(3): 389-399.

[15] J. Liu, P. Sun, Y. Yu, S. Dong, K. Wang, and J. Yang. 2021. Optimal Scheduling Considering Different Energy Hub Model of Integrated Energy System. Proceedings of the 2021 IEEE 4th International Conference on Renewable Energy and Power Engineering (REPE). Beijing, China, 9-11 October. IEEE Publisher.

[16] M. S. Javadi, A. Anvari-Moghaddam, and J. M. Guerrero. 2017. Optimal scheduling of a multi-carrier energy hub supplemented by battery energy storage systems. Proceedings of the 2017 IEEE International Conference on Environment and Electrical Engineering and 2017 IEEE Industrial and Commercial Power Systems Europe (EEEIC / I&CPS Europe). Milan, Italy, 6-9 June. IEEE Publisher.

[17] W. Geng and L. Jia. 2020. Hybrid Genetic Particle Swarm Optimization Based Economical Operation of Energy Hub. Proceedings of the 2020 5th International Conference on Power and Renewable Energy (ICPRE). Shanghai, China, 12-14 September. IEEE Publisher.

[18] L. Wang. 2023. Optimal Scheduling Strategy for Multi-Energy Microgrid Considering Integrated Demand Response. Energies 16(12): 4694.

[19] C. Timothée; A. T. D. Perera; J.-L. Scartezzini; and D. Mauree. 2017. Optimum dispatch of a multi storage and multi-energy hub with demand response and restricted grid interactions. Energy Procedia 142: 2864-2869.

[20] Y. G. Son; B. C. Oh; M. A. Acquah; R. Fan; D. M. Kim; and S. Y. Kim. 2021. Multi Energy System With an Associated Energy Hub: A Review. IEEE Access 9: 127753 – 127766.

[21] A. Shammary, A. A. Hafez, A. F. M. Ali, A. A. Mahmoud, M. I. Mohamed, and M. A. Merazy. 2022. Energy Hub Modeling and Operation, A Comprehensive Review. Proceedings of the 2022 23rd International Middle East Power Systems Conference (MEPCON). Cairo, Egypt, 13-15 December. IEEE Publisher.

[22] A. Maroufmashat; S. T. Taqvi; A. Miragha; M. Fowler; and A. Elkamel. 2019. Modeling and Optimization of Energy Hubs: A Comprehensive Review. Inventions 4(3): 50.

[23] T. Ding; W. Jia; M. Shahidehpour; O. Han; Y. Sun; and Z. Zhang. 2022. Review of Optimization Methods for Energy Hub Planning, Operation, Trading, and Control. IEEE Transactions on Sustainable Energy 13(3): 1802-1818.

[24] S. H. R. Hosseini; A. Allahham; S. L. Walker; and P. Taylor. 2020. Optimal planning and operation of multi-vector energy networks: A systematic review. Renewable and Sustainable Energy Reviews 133: 110216

[25] K. Rojanaworahiran and K. Chayakulkheeree. 2021. Probabilistic Optimal Power Flow Considering Load and Solar Power Uncertainties Using Particle Swarm Optimization. GMSARN International Journal 15(1): 37-43.

[26] J. Manwell; J. McGowan; and A. L. Rogers. 2002. Wind Energy Explained: Theory, Design and Application. Chichester: John Wiley & Sons.

[27] S. Dechjinda and K. Chayakulkheeree. 2024. Optimal Daily Scheduling of Hybrid Wind-Hydrogen Storage using Particle Swarm Optimization. Proceedings of the 2024 12th International Electrical Engineering Congress (iEECON). Pattaya, Thailand, 6-8 March. IEEE Publisher.

[28] C. Yammani; S. Maheswarapu; and M. Kumari. 2012. Optimal Placement of Multi DGs in Distribution System with Considering the DG Bus Available Limits. Energy and Power 2(1): 18-23.

[29] S. Ould Amrouche; D. Rekioua; T. Rekioua; and S. Bacha. 2016. Overview of energy storage in renewable energy systems. International Journal of Hydrogen Energy 41(45): 20914-20927.

[30] G. Cau; D. Cocco; M. Petrollese; S. Knudsen Kær; and C. Milan. 2014. Energy management strategy based on short-term generation scheduling for a renewable microgrid using a hydrogen storage system. Energy Conversion and Management 87: 820-831.

[31] J. Kennedy and R. Eberhart. 1995. Particle swarm optimization. Proceedings of the ICNN'95 - International Conference on Neural Networks. Perth, WA, Australia, 27 November – 1 December. IEEE Publisher.

[32] P. Muangkhiew and K. Chayakulkheeree. 2024. Probabilistic Fuzzy Multi-Objective Optimal Power Flow. GMSARN International Journal 18(2): 213-222.

[33] H. K. Anna Sandhaas, César De Jesús, and Niklas Hartmann. 2022. Generation of Industrial Electricity and Heat Demand Profiles for Energy System Analysis. Proceedings of the IAEE International Conference.

[34] W. Piawises and K. Chayakulkheeree. 2024. Smart Home Energy Management Algorithm for TOU Based Demand Response. Proceedings of the 2024 12th International Electrical Engineering Congress (iEECON). Pattaya, Thailand, 6-8 March. IEEE Publisher.

BIOGRAPHY

Suttipong Dejchinda is currently pursuing a Master of Engineering in Electrical Engineering at Suranaree University of Technology (SUT), where he previously earned his Bachelor of Engineering with first-class honors in 2022. His research focuses on the optimal scheduling of multi-energy systems, particularly the integration of wind-solar power and hydrogen storage. To enhance energy efficiency and reduce energy losses, he has developed optimization algorithms based on Particle Swarm Optimization (PSO). His research findings have been presented at the 12th International Electrical Engineering Congress (iEECON 2024) and accepted for publication in the GMSARN International Journal. In addition to his research, Suttipong has extensive teaching experience in electrical engineering. He has led laboratory courses covering fundamental topics such as diodes, rectifiers, Kirchhoff's laws, and motor and transformer applications. Furthermore, he has taught programming for electrical engineering applications, guiding students in Python-based circuit simulation and interface development. His teaching approach emphasizes both theoretical understanding and hands-on application, enabling students to effectively analyze and design electrical systems.

Suttipong's research interests in optimizing the operation of multi-energy systems, with a particular focus on renewable energy integration, hydrogen storage management, and energy efficiency improvement. His work explores advanced optimization techniques for scheduling energy resources to minimize costs, carbon emissions, and system losses. He is also interested in developing robust models for energy systems under uncertainty, ensuring stability and reliability in future smart grids. Through his research, he aims to contribute to the advancement of sustainable energy solutions and the transition toward low-carbon power systems.